Fault Detection and Isolation

for Railway Vehicle Suspensions

Xuejun Ding

Submitted in accordance with the requirements for the degree of
Doctor of Philosophy

The University of Leeds
School of Electronic and Electrical Engineering

December 2009

The candidate confirms that the work submitted is his own and that appropriate credit has been given where reference has been made to the work of others.

Acknowledgements

I would like to thank my supervisors, Dr. Li Zhang, for taking over the supervision of my writing up and for her whole hearted support.

Special thanks are due to my former supervisor, Prof. T X Mei, who has continuously encouraged me get deep into the research with his innovative advice, persistent help, his kindness and patience; as well as continued support after his move to Salford University.

Thanks go to Mrs. Margaret Wood and Dr. Paul A Cooke, who contributed a lot for refining my writing.

My thanks also go to my colleagues Yongji Zhou, Xuandi Zhao, Jianhua Yu and other friends for their valuable support and advice.

I would like to thank the School of Electronic and Electrical Engineering and the University for the International Award for supporting this research over the last three years.

Then I would like to express my gratitude to my parents and sister; they always love me, and encourage me unconditionally.

Last but not least thanks to my wife Wei Liu for her unfailing support in many ways. Without her love, her contribution and encouragement, this work would never have been completed. During my PhD program my son Haoyang Ding always made gave me much pleasure and pushed me to strive for future. I dedicate this thesis to them.

Abstract

The ability to detect and isolate component faults in a railway suspension system is important for improved train safety and maintenance. An undetected failure in the suspension systems can cause severe wheel-rail wear, reduce ride comfort, worsen passenger safety and increase unexpected maintenance costs. Existing fault detection methods are limited in several respects, such as effectiveness/sensitivity for fault detection, or robustness to external condition changes. This thesis investigates a model-less fault detection and isolation approach using cross correlation and/or relative variance techniques, developed to overcome these limitations.

This thesis treats a conventional bogie vehicle with a symmetrical structure. Excited by the track irregularities, the dynamics of the vehicle are studied under the normal conditions, with an emphasis on the vertical and related motions of the bogies and the carbody.

Two fault detection schemes employing data processing using data directly from measurement are discussed. One uses cross correlation evaluation of the basic bogie motions to detect component fault; the other takes advantage of the relationship between the relative variances of the suspension accelerations.

Finally, the fault isolation schemes are assessed based on the comparison of fault detection performances in different conditions. The proposed approach does not require detailed knowledge of the vehicle/bogie and external track irregularities. The effectiveness of the approach is verified by computer simulations in Matlab/Simulink.

Contents

Figures

Tables

Chapter 1
Introduction and Literature Review

1.1 Introduction

1.1.1 Background to the Study

Currently, there is a great interest in condition monitoring in vehicle systems. The main reasons for such an interest are two folds [1]. The first is to achieve the safety requirement. A failure of the suspension component cannot only increase the wear of wheels and rail, but also may affect system stability, reduce ride comfort and even endanger passenger safety in extreme cases. Detection of component failures at the earliest opportunity prevents further deterioration in vehicle performance and enhances vehicle safety and reliability. The second is to reduce the maintenance cost. Early detection of incipient component faults is helpful in reducing costs and preventing them turning into a more serious and/or dangerous situation. As a result, maintenance in the future may be carried out on demand to replace scheduled maintenance, which results in a substantial saving and significant reduction in the total life cycle costs. As the speed of railway travel becomes faster, the demand for stable and reliable suspension systems for high-speed trains is likely to increase in order to deliver a safe and comfortable passenger experience. To meet these requirements, Fault Detection and Isolation (FDI) systems, which help improve the railway vehicle operational performance, are expected on future rail vehicles.

Although other improvements such as modern control strategies in railway vehicles have been studied in depth, the development of fault detection and condition monitoring methods are still a relatively new subject [2] [3]. During the last three decades, a lot of FDI work has been carried out at a theoretical level, but only a limited number of applications were applied in the aircraft and automobile industries

[4][5][6][7]. Advanced condition monitoring in railway vehicles is however lagging behind, where some possibilities are being recommended and a number of ideas proposed in recent publications. There is still a lack of practical applications, although a few theoretical model-based methods have been studied in the railway field [1] [8] [9] [10].

Typically, fault detection methods can be categorised into the qualitative discrimination or quantitative analytical approach, including time or frequency analysis, knowledge-based and model-based approaches [7] [11]. However, system disturbance and noises could distort the fault decision making process. The simplification or the linearization of non-linear systems used by some of the techniques could cause estimation errors. More essential work is yet to be done on the development of implementable systems and in particular on the improvement of the sensitivity and robustness of practical fault detection methods.

1.1.2 Aims and Objectives

The aim of this study is to develop a simple and effective approach to be used for FDI of railway vehicle suspension systems. The research intends to investigate and understand the generalised dynamic performance and interactions existing in the railway vehicle suspension system, by a combination of analytical formulation and numerical modelling. The study of the basic conventional railway bogie vehicle model is involved, the results from which can be applied to a range of applications in other railway vehicles. To achieve this aim, the specific objectives are as presented as follows:

- To fully understand the relevant mechanisms of the railway vehicle suspension systems, especially dynamic interactions between different motions in relation to component fault(s)

- To avoid the use of complex mathematical modelling, linearisation processes and data processing algorithms so that the proposed approach can be easily implemented

- To improve the sensitivity, accuracy and robustness of fault detection against system disturbances and external condition changes so that it can be conveniently tuned in practical applications

1.2 Literature Review

1.2.1 Condition Monitoring - the Concept

Condition monitoring technology is basically applicable to a system whose performance deteriorates with component failure, and aims to detect and isolate the failure at an incipient stage to prevent it causing serious malfunction [2] [12]. In many cases, only output signals can be collected or measured, therefore a signal based method may be applied. A common illustration of a railway vehicle condition monitoring scheme is shown in Figure 1.1. The inputs can be any system control inputs or track excitations; the plant/vehicle system generates the outputs which are measured by the mounted sensors; the disturbances are the environment or measurement noises which may affect the system, and the output measurements are then fed to the monitoring system. The condition monitoring system augments the physical system, monitoring system variations by historical data or on-line, and focusing on detecting and isolating the faulty component and processing the failure before it causes serious problems. This is the key role of a condition monitoring system [2] [6].

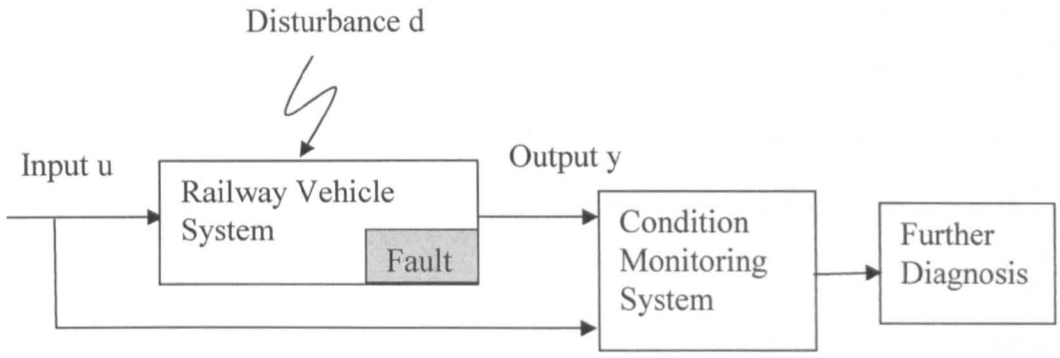

Figure 1.1 General condition monitoring or fault detection scheme for railway vehicle

1.2.2 Background and Applications in Vehicle Systems

Generally, the condition monitoring technology serves two fundamental functions: a) to detect faults and b) if possible, to isolate them. Before the 1980s, fault detection and isolation was highly dependent on the limits of computational power and the cost of hardware [13]. After the 1990s, there has been a gradual increase in academic research and applications in fault detection and isolation techniques including in the automobile industry [11] [14].

Based on the system output measurements, a lot of work has been undertaken in detecting faults, by exploring information contained in the measurements to indicate the failure of system components. Through a study of the profile of the measurements, several methods in detecting the failure have been presented according to their different data implementation techniques [14].

1.2.2.1 Direct Computation and Signal Processing Methods

Component faults tend to change the behaviour of a system and often affect the output of measured signals. The characteristics of the related changes can therefore be extracted and processed as a means for fault detection [7]. The use of filters is a convenient way to extract the fault-relevant signal characteristics from the

vibrational measurements, where the band-pass filter is popularly employed. Its principle is based on the phenomenon that the resonances of interest mostly occur in a specific frequency range, and in many cases the extracted information can be achieved by restricting the signals within a certain frequency bandwidth $\omega_{min} \leq \omega \leq \omega_{max}$. It allows the interested main frequencies and their amplitudes to be measured, which may be especially sensitive to some faults. The filter based methods are relatively straight forward to design and can be used for detecting a variety of faults. However, they can suffer from reliability problems with possibly a relatively large number of false alarms or missed detections. Innovative filter designs such as exponential weighted and the limited memory filters are sometimes used to obtain a faster response and more sensitive fault detection [13] [15] [16].

Besides the development of the filter approaches, some other time domain fault detection methods using direct computation are adopted in the dynamic systems, mainly based on vibrational analysis [14] [17]. The fundamental principle upon these vibrating structure based methods is that faults in a subsystem may cause behavioural discrepancies in their vibration responses. The goal of the FDI problem is to achieve the reliable detection of such discrepancies by the vibrant signal processing and reveal their association which is related to a specific fault. These time domain analysis are an important part of the FDI families, which deal with time series data or measured random signals using statistical tools (mean, peak etc) and analyse their observed behaviours. They are data-based rather than model-based although these data are obviously related to the physical system or models, which indicate an inverse-model analytical type [17].

The time domain statistical methods are widely used to investigate the random characteristics of a dynamic system. It is important to summarise the data obtained and be able to draw meaningful and useful features. The typical vibrational signals of dynamic systems include displacement, velocity and acceleration; they all deliver relevant information about the structural dynamics. For railway vehicle system,

acceleration is the most commonly used for fault detection analysis, as it can be easily measured by inertial sensors with acceptable accuracy [18] [19]. The simplest approach in the time domain is to measure the overall root mean square (RMS) level, i.e., the RMS value of the measured accelerations. This method has been applied with limited success for the fault detection of component fault [20], where the fault is detected by observing the changed RMS magnitude of the measured features of the dynamic systems, because the component damage or failure can cause relative changes in the level of acceleration outputs. However, the performance of this method can be affected by the external operational conditions such as rail track geometry and speed changes. A comparison of fault detection using the RMS method with the proposed approaches in this study is presented later in Chapter 4.

Other time domain analytical condition monitoring methods have been successfully used for industrial applications. A typical example is the Shock Pulse Method (SPM). This method simply detects the mechanical shock wave caused by the impact between two contacted systems. This can be as simple as 'listening' or 'feeling' symptoms but using sophisticated spectral analysis and instruments. The shock pulse method is widely applied in industrial environments such as rolling and vibrational systems. At the impact point, the acceleration of the impacted substance establishes a compressive wave radiating in all directions, and the magnitude of the wave is an indirect variable to the impact velocity. Following the impact, the deflection of the mass near the impact point deforms and the vibration occurs, the SPM evaluates and detects the magnitude of the resultant compression wavefront (the shock pulse) by a set of piezo-electric accelerometers. The contacted surfaces always have a certain degree of roughness, so when rolling occurs, the roughness will cause mechanical impact and thereby shock pulses are generated and measured. If the studied component is damaged or has a failure somewhere, the shock pulse may periodically increase to a large magnitude compared with that under the normal conditions. The periodic time interval of the increased shock pulse relies on the contacted rolling

velocity [21]. The shock pulse method is simple to implement, and may be suitable for rolling element fault detection such as railway wheels and axles.

The time domain methods in the FDI application offer a number of potential advantages in implementation and some are useful for the railway vehicle system. The merits mainly include: no requirement of physical models, inherent avoidance of uncertainty by statistical tools and explicit fault decision making. On the other hand, as the physical models are not employed, time domain methods may detect a fault only available to the specific physical systems themselves, their quantitative outcomes are unique and cannot be applied for other derivative systems although they could have the similar structures.

Another important direct measurement based FDI analysis is to use frequency domain methods. These methods could be a related frequency transformation from the time domain measurements, or a spectral analysis by estimation [6] [14] [22]. The most popular approach is spectral analysis using a Fast Fourier Transform (FFT) algorithm; it attempts to estimate the magnitude of change of frequency content for a selective set of system measurements. For example, a damper fault is common in the railway suspension system [9]. It has little effect on the change of the suspension natural frequency; however, it contributes to a reduced system damping ratio which increase the frequency content near the system natural frequencies and decrease the response at the high frequency ranges. As it is possible to estimate the natural frequency from the railway vehicle dynamics, the evaluation of the FFT spectral change near to the system natural frequency can be used as a potential method to detect the suspension damper fault.

Although it is simple to directly use a FFT algorithm to evaluate the spectral changes as an indicator of component fault, the feasibility of this method is still limited; the spillover and spectral leakage phenomena may affect the choice of extracted frequency, and distort the spectral magnitude which does not exactly appear as an

ideal peak if its frequency does not coincide with any $f_n=n/T$ (n integer). Some interpolation algorithm and window functions can be used to improve the accuracy of the spectral level, but it will increase the structure complexity and require more computation power.

Rather than comparing the frequency content via FFT algorithm, another useful condition monitoring technique in the frequency domain is to estimate the parameters of a signal by calculating their corresponding frequencies. This frequency-based spectral analysis approach is studied through a test rig for the purpose of detecting vehicle tire pressure loss [6] [23]. The test is processed with a quarter car mass-spring-damper model, and the vibration from the vehicle body is ignored because its frequency range is much lower than that from the wheel and axis vibrations. The wheel accelerations are used for this signal spectral analysis, and only the vertical wheel acceleration is measured for a simplified application. Based on an Auto-Regressive (AR) parameter estimation, the resonant frequency of the wheel is estimated from the vertical acceleration measurements. Theoretically, loss of air pressure will cause a lower estimated wheel resonant frequency. The tested tire pressure is initially set to 2.0 bar and then reduced to 1.5 bar, the estimated frequency is thereby reduced by about 0.7Hz compared with the higher tire pressure. When the air pressure is further reduced, the change in the level of the estimated frequency is enlarged. As a result, the difference of the wheel frequency indicates the fault condition of the tire, i.e., the loss of air pressure. This signal spectral analysis method is suitable for air leakage detection for the vehicle tire, but is not suitable for the detection of component failures in the suspensions.

The frequency domain method used in condition monitoring is explicit. In certain specific situations, it is still considered as a powerful condition monitoring analytical method. However it has two main drawbacks. One is the Fourier Transform is relatively time-consuming, which increases the complexity of the detection procedure. Another disadvantage comes from the impact changes in external

condition, which may affect the detection quality and result in inappropriate decision making. Furthermore, the frequency spectrum normally can often be overwhelmed by noises from measurement or corrupted from other system components. Therefore, it is difficult to get precise failure information by using conventional frequency analysis methods. In order to overcome the problems, recent advanced signal processing methods such as Wavelet analysis has been suggested to extract weak transient signals from which the normal FFT methods could be ineffective. [24][25].

According to [25], the Wavelet Transform (WT) is an analytical method in time-frequency domain which provides a signal analysis approach capable of detecting local faults in a dynamic vehicle system. A full automobile vehicle is studied, the suspension faults are assumed to occur as a result of the damage to shock absorbers (damper) and bushings. The performance of fault detection of spectral analysis using FFT is compared with that using WT. The FFT spectral analysis can detect the frequency content change but suffers from transient noises and exhibits an error in estimating contents near the natural frequency in fault conditions. However, the WT method can analyse the energy density distribution in different frequencies properly. By carefully selecting a mother wavelet with an appropriate scale factor in the frequency domain and the translation factor in the time domain, the distinction of the energy distribution can be largely optimised. The relatively maximum energy near the natural frequency is evaluated under the normal and fault conditions. The faults of the damper and bushing can be detected by comparing their corresponding energy amplitude changes, and transient phenomenon which often occurs in FFT analysis is greatly removed. The WT analysis has some advantages over the FFT algorithm. The WT processing time is shorter due to less computation as compared to that of the FFT algorithm, and the WT can improve accuracy by optimising the signal energy distribution and slightly resist the influence of noise by reducing transient phenomenon. However, the wavelet coefficient tuning can be complicated and needs to be frequently changed with different operational conditions [26].

1.2.2.2 Knowledge-based Methods

These methods are more suitable for nonlinear and high noise contaminated systems, and they are based on the observed analytical and heuristic signs and also the heuristic knowledge of the fault detection and isolation procedure [7]. For a knowledge-based fault diagnosis system, it is unnecessary to rely on statistical algorithms or to employ an analytical system model, as the approach is centred on the core information extracted from the dynamic system outputs. In this way, only qualitative or empirical systematic knowledge is used, and the measured outputs are normally formed as the signs of the fault-relevant knowledge in the process, mainly in a heuristic manner. Many current knowledge-based methods adopt fuzzy logic systems to map the inputs and measurements from a dynamic system. The signs formed from measurements may be indicated as binary values [0, 1] or treated as fuzzy sets to be considered in the fault detection and diagnosis analysis, and these data are used to set up a fault library upon which the FDI engine is based. By clustering the utilisation of fuzzy separation, the faulty area can be possibly identified [27]. Due to the development of Artificial Intelligence (AI) technology, some other AI design techniques for knowledge-based FDI scheme have also been studied. A recent trend comes with the application of neural networks as another important knowledge-based FDI technique, because of its flexibility due to the inherent training and learning abilities both for nonlinear and linear systems; and the discrimination between normal and abnormal cases being more straightforward to implement [28].

Without the need for a complex and accurate analytical model, these methods use data-driven and knowledge-based techniques to estimate the system dynamics and make performance assessments. The heuristic knowledge obtained from the training and learning process is of crucial importance. For a vehicle FDI system, the different fault conditions may give rise to different output patterns, where the typically defined normal and abnormal ones are included. Then one or more of the

knowledge-based methods are applied to analyse the heuristic symptom of system outputs, and the current pattern of system operation can then be directly classified after the mapping of these signals to the prior knowledge sets. In most cases, to begin with a knowledge-based expert system, a rule-based decision-making system is required for the training process. When there is no further knowledge ready for the relation of the chosen features and fault diagnosis process, a reference vector S_n is firstly pre-determined as the normal case. Then the measured output vectors S including all signs are determined experimentally for a certain fault F_j. By repeating this procedure in different circumstances, the relationships between the fault set F and system output vectors S are therefore learned. These relationships can form the basis of an explicit knowledge base. By comparing S with the normal reference S_n, any possible faults F are indicated.

Compared with the direct measurement and signal processing methods in time and/or frequency domains, one major advantage of the knowledge-based methods is their advanced capability in identifying system faults. On the other hand, the system process disturbance, measurement noise and other uncertainties from different operational conditions are often mixed with desired data in the training procedure, which may make the feature or pattern distort from expectation and hereby cause false or missed detection.

1.2.2.3 Model-based Methods

More recently, there have been a number of investigations into the use of model-based methods in fault detection for vehicle systems, as the modelling techniques and specific models for railway vehicle dynamic systems are well-developed [2] [11] [14]. Most model-based FDI techniques have been used for automobiles, including applications for actuators, suspension component fault detection and drive-by-wire systems which are summarised in [6] [7] [29]. There are also studies of the model-based FDI approaches for railway vehicles dynamics. For example, Li *et al.*

presented the parameter estimation methods for railway vehicle suspension damper fault detection [9] [30], Goda *et al.* proposed a Kalman-Bucy filter based approach for damper fault and conicity change of a railway vehicle bogie [1], and Hayash *et al.* explored the interacting multiple model (IMM) method for railway vehicle suspension and sensor failure detections [10] [31]. These methods all require a mathematical model generated from the real physical system. Assuming the mathematical model agrees well with the physical system, faults which change the process behaviour will mostly result in changes in the selected features. Based on the evaluation of the residuals, using a suitably chosen threshold, the failure can be indicated. The residuals can be generated by the difference between the output measurements and their corresponding estimations from the mathematical model. For a FDI system, the residual is a function of inputs and outputs of the monitored system, which is also independent of the normal operation state of the system [12]. They should be zero or their mean tends to zero if there are no faults in the physical system. The residuals will deviate from zero significantly when a fault occurs and this evaluation of the deviation away from zero can be used as an indicator of the fault [32].

Three basic methods are classified for the model-based methods:

(1) Parameter estimation;

(2) Parity equation;

(3) Observer and state estimation.

The parameter estimation techniques can be used in detecting faults resulting from component degradation. The estimation is directly associated with the system model and the measurable outputs, focusing on the investigation of system parameters. For this method, the residuals are the differences between the nominal system model parameters and their estimations. The comparison of relevant parameters between the mathematical model and the real one can indicate whether the studied

components are faulty, and the severity of the faults can be shown providing the model is sufficiently precise. An example of this method is given by [23] to study the performance of the hydraulic damper of a car. The designated fault is obtained on a test rig, which has been mounted with a continuously adjustable damper. The fault detection result is given by a recursive calculation based on an improved least square (LS) algorithm. The system dynamic equation is established by modelling the relationship between the force and velocity of the damper. The damping coefficient can be estimated by measuring the car body acceleration and the suspension deflection between the body and the wheels, and the relative velocity of the damper can be derived by differential equations. In this example, the actual damping coefficient of the damper is known in advance. By comparing the difference between the damping estimation and the real value, the fault (i.e., from the adjustment of the damper) is indicated, together with the approximate distorted damping value. This parameter estimation is advantageous in that most damper faults can be detected, but the high cost of a deflection sensor could affect practical applications.

Parameter estimation methods have also been studied for the railway vehicle suspension component FDI problem, as presented by Li *et al.* in [9] [30]. This project is focused on the fault detection and isolation in the railway vehicle/track interface. In their study a plan view model of a half railway vehicle is used in the simulation. This model is generated from a Coradia Class 175 railway vehicle, including the lateral and yaw motions of the wheelsets and the bogie, and the lateral DoFs for the carbody. By investigating the faults of the lateral damper and the anti-yaw damper in the secondary suspension system, two model-based parameter estimation methods were presented. The first method is performed with the Kalman filter estimation and the weighted sum square residual (WSSR) detection. The innovation from a Kalman filter is used as a residual signal for FDI analysis, where the residual is generated by the difference between the output measurement and its estimation. Component faults or changes in the dynamic system can be detected by a

statistical WSSR hypothesis test. Once a fault is detected, the innovations of the bogie yaw gyro and the vehicle body accelerometer data can be used for Power Spectrum Density (PSD) or RMS evaluation. The method has reasonable computational efficiency and rapid response to abrupt faults, which is especially suitable for the FDI of a hard component fault needing immediate attention. The second method is presented by the authors using Rao-Black Particle Filter (RBPF) based parameter estimation. This particle filter is a simulation-based method for the general non-linear non-Gaussian state estimation, focusing on the evaluation of the complete Probability Density Function (PDF) for these states. The RBPF is more comprehensive compared with the state estimation by the extended Kalman filter (EKF), as it only estimates the few central moments which are normally difficult to analyse due to nonlinearity, and the Kalman filter may be used for the augmented states estimation. Thus, the RBPF estimation is flexible as it can give a simple approximation to the required estimation without being restricted to any linearity and/or Gaussianity constraints to the railway vehicle model. The RBPF is shown to be particularly effective in detecting the soft faults with gradual nominal parametrical value changes. By comparing the two parameter estimation methods for the railway vehicle FDI problem, the authors state that the RBPF based parameter estimation method is more powerful, as it is easier to do analytical derivatives (such as Jacobians). This is particularly useful in the case when the systematic matrix of the estimated parameters is very complicated. However, a major disadvantage is that it has to estimate a larger dimension of states generated from the augmented model.

The parity equation method is another model-based FDI technique. It requires a fixed state model which is used as the reference for the system measurements. The parity equation traces the consistency of the mathematical equation with the measurements, where any inconsistency in the measurements is combined into an independent parity equation which gives a parity vector [6] [33] [34]. The sensitivity of a residual vector shows only its change related to a corresponding fault, which is

quite useful for the fault isolation scheme. The parity equation method is especially valuable for additive faults. An example is given for sensor fault detection in a car system [6]. Two kinds of faults are assumed to occur on an acceleration sensor. One is the offset fault which has a 3% increase of the maximum measurable range added to the normal measurement; the other is the gain error which gives 20% extra gain compared with the normal value. After the parity relation analysis, the faults are detected respectively by comparing the residual changes with the selective thresholds. The offset fault is indicated by a significant increase in the residual and the gain fault is detected by both a moderate residual change and a variance increase at the same time. The results also show that by establishing one parity space, the different sensor faults can be detected simultaneously in the same computational processing, together with their identification from their corresponding residual change characteristics. The parity equations do not need extra parameter measurements and require less computation than the parameter estimation. However it has some drawbacks, such as it cannot give as deep insight into the fault as the parameter estimation method, and it is more difficult to reduce the noise effects and to apply to a multiplicative component fault, which makes the parity equation difficult to use in railway applications [6].

The observer and state estimation method in FDI analysis is probably the most common approach among the model-based condition monitoring methods. The basic idea of the observer and state estimation method is to reconstruct measurable plant states and to generate residuals by comparing the estimated outputs with the real measurements. By introducing the state estimations and the output measurements, different fault schemes can be established for a FDI system. The most widely used state estimators are the Luenberger observer and the Kalman filter, which are used for deterministic and stochastic cases respectively [2] [35]. By employing a mathematical model, the observer and state estimation algorithm gives a prediction of current states which are normally difficult to measure. The estimated outputs are

then evaluated by manipulating the estimated states instead of those in the real physical plant. The residual is generated by comparing the measured output and the estimated output derived from a nominal model. The scheme of this method is shown in Figure 1.2.

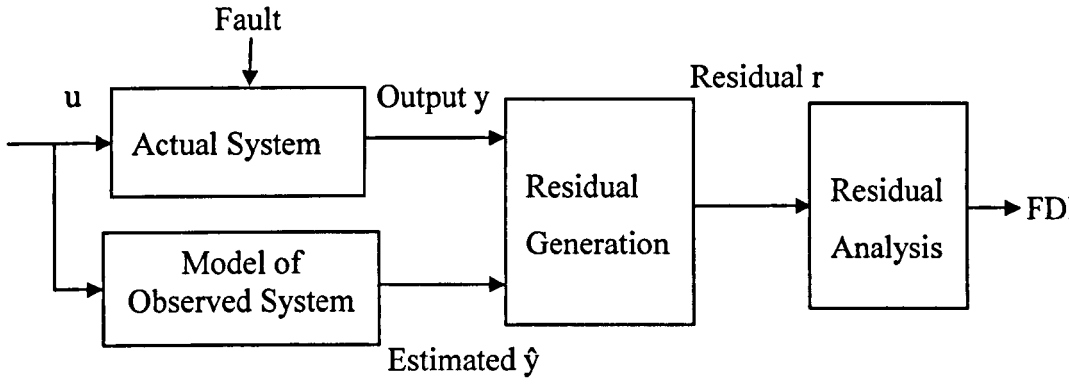

Figure 1.2 Fundamental FDI scheme using observer and state estimation

The observer and state estimation method is appropriate for faults associated with states which are difficult to measure, whereas the Kalman filter is the most often used estimation algorithm in solving the linear stochastic problem, as it is a powerful and effective estimation algorithm of past, present and future states [36] [37]. Many researchers use it in estimating implicit and complicated states of dynamic vehicle system [38], which also makes it a potential and useful approach in vehicle FDI problems. The Kalman filter is originally defined as the state estimator for the linear system, however most of the physical systems are more or less non-linear; therefore nonlinear state estimation is needed when linear estimation cannot give satisfactory performances. In this case, the Kalman filter can be extended for utilisation in a non-linear system, which is so the called Extended Kalman filter (EKF). The EKF is an applicable state estimation algorithm for nonlinear systems; however particular attention should be paid to the accuracy and stability of the Jacobian matrixes when the partial derivatives are employed in the linearisation procedure [39].

The use of EKF has been studied to detect fault in an underwater vehicle with actuator faults [40]. The fault detection problem is solved by evaluating any significant residual changes to the interested behaviours of the underwater vehicle outputs. Their results show that the EKF based estimation method is effective for left and right thrusters fault detection of the underwater vehicle, and the use of low-pass filter can greatly improve the detection quality.

The observer and state estimation fault detection method has also been studied for railway vehicle systems. Goda *et al.* give an application by using a Kalman-Bucy filter to detect the railway bogie faults and apply an isolation scheme to separate these faults [1]. This application shows the possibility of detecting suspension failure and conicity changes using state estimations from Kalman-Bucy filter. To simplify the Kalman filter based estimator design, a linearised plan-view railway vehicle model is developed. The model includes the lateral and yaw movements for the wheelsets and bogies. The lateral accelerations and yaw velocities are assumed to be measured by inertial sensors, with their associated measurement noises taken into account. One advantage of this method is that the Kalman-Bucy filter uses only few sensor measurements in estimating the states optimally [18]. The residual is generated by the difference between the real measurement and estimated output predicted by Kalman-Bucy filter. By checking the ongoing residual changes with an experimental threshold, the faults can be detected.

There is another model-based fault detection study using the interacting multiple model approach (IMM), which employs a number of dynamic models for fault detection in railway vehicle systems. The IMM method explores an estimation method using different dynamic railway vehicle models which cover typical failures in the system structure, parameters and sensors [10]. As railway vehicle dynamics is inherently interactive, this method can provide an effective way in detecting component failures. In [31], the IMM estimator is designed based on eight typical modes of a half vehicle model which include no failure, different level of spring and

damper failures in secondary suspension system and some sensor errors, where the mode probabilities and states of the studied measurements are estimated using Kalman filters. The calculation results show that different mode probabilities change with different kind/level of faults. Using IMM method, the faults can not only be detected but also identified by comparison with the predefined mode sets. However, this method may need to use a large number of models to get effective results in practical railway applications, which can lead to more a complicated analysis and also increase the computational burden and hardware cost.

1.2.3 Brief Summary

In summary, the above literature reviews have highlighted a number of issues in condition monitoring and FDI problems. Although the model-based FDI methods are becoming the fast increasing research topic in recent studies [41], the quality of the analytical model is critical for the attainable quality of the fault detection problem. A poor or imprecise model will lead to a false alarm or missed detection. It is inevitable that the more complex the system model and the more model-dependent the FDI technique, the more possibility that the detection will result in sensitivity problems. Recently the robustness issue has received considerable attention, especially in dealing with the decoupling of the disturbance and fault signals. For the unstructured uncertainty systems, it is difficult to optimise the separation of the disturbance decoupling and hard to distinguish the additive and multiplicative faults [3] [12] [32] [41]. On the other hand, the model-based methods are fundamentally applicable for linear systems, although they can be extended to the application of nonlinear processes by analytical derivation or linearisation. However, there are potential difficulties related to nonlinear properties in the linearisation process, and stability issue associated with the model-dependent fault diagnosis, which may lead to complicated solutions [35] [42].

A novel FDI proposal, which can effecyively overcome these shortcomings by carefully taking into account the specific structure and suspension component configuration for the railway vehicle system, is thereby studied.

1.3 Approaches and Ideas Presented in this Thesis

This thesis presents a novel approach which is quite simple but effective for the FDI problem in railway vehicle suspension systems. It is formed as a data processing method with emphasis on data comparison techniques, which requires little prior knowledge of the system model except some basic parameters such as vehicle travelling speed and the distance between suspensions. The proposed technique focuses on the comparison of dynamic behaviours between the two suspensions where identical components are normally used [43]. When there are no faults in the suspension system, it can be readily shown that some of the motions (e.g. bounce and pitch) of the bogie (and to a large extent the vertical movements at the leading and trailing suspensions) can be considered decoupled because of the symmetrical suspension configuration and that therefore there is little interaction between the two motions. However a component failure (e.g. a damper) in either suspension will introduce an imbalance into the system, with resulting in dynamic interactions between motions. Due to the overall damping loss, the dynamic interactions mainly bring two different interactive effects near the resonant natural frequency and frequencies beyond that. One is the increasing response around the system natural frequencies, and the other is the gain decrease along the higher frequency band, whereas the second effect is more dominant because the frequency band of the system response is much wider than the part near the natural frequency. The interactions caused by the unbalanced suspension parameters are exploited in the study and computed by cross correlation analysis as a measure of suspension conditions.

The proposed technique requires inertial measurements to be taken from the bounce, pitch and roll accelerations. To reveal any interactive change, the two measured accelerations are processed by computing their cross correlations, and by taking into account the time shift between the track inputs at the two chosen suspensions. As shown in the following chapters, the novel detection scheme is not only highly sensitive to component faults but also robust under different external operational conditions.

In this system, the accelerations are acquired directly from measurements through the sensors mounted on the bogie/body frame. The signals can be processed continuously and the results can be given instantly from every running time interval, so fast detection ability can also be achieved. It will be shown that the correlation change before and after the fault condition is quickly observed and that the fault(s) can be detected in a real-time manner, and also be isolated by comparing the different patterns between their correlation performances.

Based on a similar principle, a second processing method using relative variances is also studied which may be used as a supplementary approach to the cross correlation computations. The same measurements are required, so there is very little additional hardware/cost involved.

1.4 Structure of the Thesis

This thesis is divided into six chapters, outlined as follows:

Chapter 1 gives a brief introduction to condition monitoring technology in railway vehicle systems. The literature review gives the concept of the condition monitoring technology and a background study of the current approaches and applications in vehicle systems, where the features and limitations of these methods are

summarised. Finally, the new approaches and ideas which will be presented in this thesis are briefly described, followed by the structure of the thesis.

In Chapter 2, a conventional bogie vehicle is described and modelled both as a conceptual and numerical model. Linearisation is applied in order to simplify the modelling process. The vertical dynamic motions of the vehicle on random track irregularities are investigated.

Chapter 3 presents the development of the proposed fault detection and isolation technique in detail. Dynamic interactions introduced by suspension faults are explained using a simple side-view conventional bogie model, and initial results and effectiveness of the new FDI methods are illustrated. The detail of the data processing methods is also provided.

Chapter 4 details the simulation studies using the proposed approach for the suspension system under different operational conditions, and improvements to rectify the detection results are given. The feasibility of the approach when used with noisy measurements and for non-linear system is assessed.

In Chapter 5, a second fault data processing method using relative variance is developed and assessed.

Chapter 6 summarises the work undertaken and outcomes of the study. Conclusions for the effectiveness of the proposed FDI technique for railway vehicles are presented. Suggestions for future work are also given.

1.5 Publication List

A total of five academic publications have been produced from this study as listed below. A copy of the full papers are given in Appendix B.

- Mei, T. X. and Ding, X. J., Condition Monitoring of Rail Vehicle Suspensions Based on Changes in System Dynamic Interactions, *Vehicle System Dynamics*, Vol. 47, pp. 1167-1181, Taylor & Francis Ltd., 2009

- Mei, T. X. and Ding, X. J., A Model-less Technique for the Fault Detection of Rail Vehicle Suspensions, *Vehicle System Dynamics*, Volume 46, Supplement 1, pp. 277-287, Taylor and Francis Ltd., 2008

- Ding, X. J. and Mei, T. X., Condition Monitoring of Vehicle Suspensions using Relative Variances, *23rd IAR Workshop on Advanced Control and Diagnosis*, Coventry University, UK, 2008

- Ding, X. J. and Mei, T. X., Fault Detection for Vehicle Suspensions Based on System Dynamic Interactions, *Proceedings of UKACC International Conference on Control*, Manchester, UK, 2008

- Mei, T. X. and Ding, X. J., New Condition Monitoring Techniques for Vehicle Suspensions, *the 4th IET International Conference on Railway Condition Monitoring*, pp 1-6, Derby, UK, 2008

Chapter 2

Mathematical Models

2.1 Introduction

To develop an effective FDI scheme for a rail suspension system, it is important to have a good comprehension of the bogie and suspension system, and a clear understanding of the functions of each part and the relationship between individual components.

In this chapter, an introduction to the bogie and suspension systems of a conventional bogie vehicle system is presented, followed by the development of two mathematical models. The first model is for the side view dynamics of a conventional bogie. This simple model is used to simplify the theoretical analysis of the dynamic interaction changes in different suspension conditions, and to ease the development process of the proposed fault detection method as presented in chapter 3. The second and more comprehensive model includes all modes of a vehicle that are influenced by the primary vertical suspensions (the focus of this study), i.e. the bounce, pitch and roll motions of the bogies and the body frame. This model is used primarily for performance assessments in chapters 4 and 5.

The special feature of a railway vehicle compared with other types of wheeled transport is the constrained guidance provided by the track. The surface of the rails guides the wheelsets, and the wheelsets and suspension systems of the bogies support the carbody in its motion. With the development of high speed trains, the use of bogies plays a very important role in safe railway operation and, less obviously, high vehicle steering performance [44].

In a conventional bogie vehicle system, the bogie transmits all the longitudinal, lateral, and vertical forces between the carbody and the wheelsets. The bogie may also include tilting devices, lubrication devices for wheel-rail contact, and mechanisms to provide proper positioning of wheelsets on curves. Therefore, the design of bogies is crucial in achieving reliability and maintenance benefits [45] [46].

2.2 Structure of a Conventional Bogie and Basic Components

In order to understand railway vehicle dynamics, it is common to investigate the motion of a single vehicle carriage running on rails. The running equipment mounted on a separate frame that can turn relative motions to the carbody is known as a bogie (or truck as known in North America). This thesis will focus on a simple conventional bogie, which has the common two-axle structure, to help clarify the basic mechanism of railway vehicles. The key components of this type of bogie include the bogie frame, the suspension systems, the wheelsets, the traction devices and the brake equipments.

2.2.1 Bogie Frame

The bogie frame is a steel structure which is generally made of two side beams and two cross beams formed into an H-shape frame. Like the chassis of a lorry, it is a framework which carries wheelsets via the primary suspensions and attaches the carbody by the secondary suspensions. The force is transmitted from the wheelsets to the bogie frame by the primary suspension and to the carbody by the secondary suspension. The bogie frame can also carry the traction and braking drives. The bogie frame is a basic consideration for the bogie design scheme as it is located in the centre of the bogie and constitutes a large proportion of the total weight of the bogie. Irrespective of the design of the bogie system, the stability of vehicles in

motion is largely directed by the dynamics of the wheelset within the bogie frame [47]. The bogie frame with its linkages is normally considered as a sprung mass for the primary suspension systems and an unsprung mass for the secondary suspension systems. For a four axle vehicle, the mass and moment of inertia of the bogie frame are carefully selected so that the four axles can support the sprung loads under the normal operating conditions [48].

2.2.2 Suspension Systems

Suspension systems consist of a variety of energy storage dissipating components which may include simple mechanical springs, viscous and friction dampers, air springs, active or semi-active components, and other associated linkages which connect the wheelsets to the carbody. In general, a freight railway vehicle has only one layer of suspension, and is therefore less complex than the passenger railway vehicle which has more than one suspension system to improve passenger comfort. In this thesis, the most commonly used conventional passenger bogie vehicle with two suspension systems is used in the study. The two suspensions are located apart from different parts of the bogie, and are designed to have various functions in different frequency ranges. The primary suspension is mounted between the wheelsets and the bogie frame, while the secondary suspension is placed between the bogie frame and the bolster or the carbody. The whole suspension system is necessary, not only for reducing the forces between the wheels and rails and isolating the carriage from vibrations and bumps, but also for keeping the railway vehicle passengers comfortable and maintaining safe riding. Normally the primary suspension system comprises of elastic elements (springs) and dampers mounted on each axle, and works at a high frequency to reduce most of the frequency content to which the passengers are most sensitive. The secondary suspension system often consists of a pair of air springs in the vertical direction and a variety of springs, lateral and anti-yaw dampers working in the lateral and yaw directions. Operating

differently from the primary suspension, the secondary suspension can further reduce the vibration from the primary suspension to a lower level which is acceptable for the comfort of the human body. Both suspension systems also help to provide additional control and stability for the railway vehicle at high speed and allow the bogie and carbody to move relatively to each other on curves [49]. In this thesis, only the component faults in the primary suspension system are studied.

2.2.2.1 Primary Suspension

The springs in the primary suspension system play an important role for the railway vehicle dynamics [50]. These springs may consist of coil springs, leaf springs and torsion springs etc. They are commonly used as stiffness elements in the primary suspension system, and the coil springs are the most important. Usually coil springs are produced as a helix of steel wire, typically of circular cross-section. Compared with other springs such as torsion springs and rubber-metal springs in the bogie, the coil springs are cheap and commonplace. They are flexibly mounted not only in the vertical, but also in longitudinal and lateral directions. All these springs provide very little damping. The characteristic of spring stiffness may be linear or non-linear as illustrated in Figure 2.1, where the non-linearity is often represented as a symmetrical piecewise linear relationship, which passes through the origin of the force-displacement plane. In many research works, these elastic springs in the railway vehicle suspension systems are often treatewd with linear properties [50] [51].

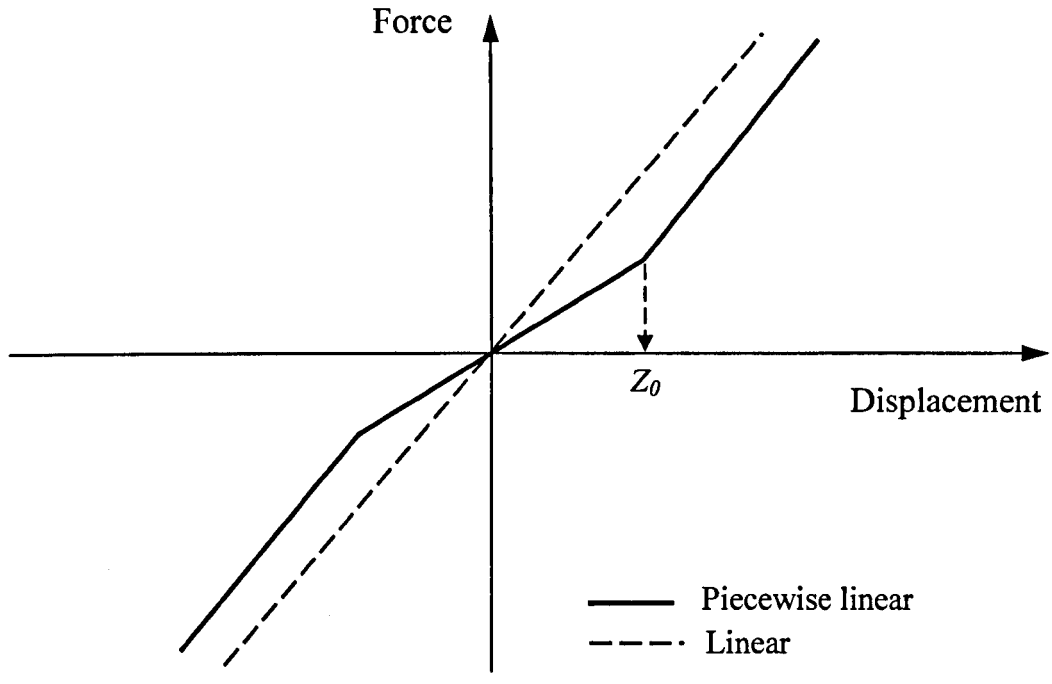

Figure 2.1 Spring stiffness characteristic [50]

In most common cases when the railway vehicle suspension model is investigated, the force generated by the suspension springs is proportional to the change in height regardless of their initial displacements. Conventional bogie vehicles often use stiffness components of which the spring rates are derived from the gravitational force. Spring rates that are too hard or too soft will both affect the suspension performance [51]. In practice the design or the selection of the stiffness is always a compromise between conflicting criteria, for instance the need for high stiffness for good high speed steering versus the requirement for soft stiffness to enhance passenger comfort. Much effort has been spent in exploiting optimal solutions for different applications. However, how to design the bogie or the selection of the suspension component is not the relevant issue in this thesis and thus it is mentioned but will not be studied further.

Dampers are as important as springs in railway vehicle suspension systems, and are commonly used. Damping or resistance force is often generated using viscous or friction damping devices, of which hydraulic dampers are the most common [52].

Hydraulic dampers have a major influence on the stability and passenger comfort of railway vehicles. Similar to the design considerations to the spring stiffness, the design of the damper is a compromise between these two aspects. Often, hard dampers are used for a railway vehicle running on very uneven rails at high speed, because it is easy to increase the adherence to the rail in steering. On the other hand, the hard damping may result in a reduction of passenger comfort. Unlike the springs which dissipate the energy by a force proportional to the compressing (or expanding) length, the dampers are characterised by a force in terms of the piston velocity. Figure 2.2 shows the force-velocity relation of a typical hydraulic damper.

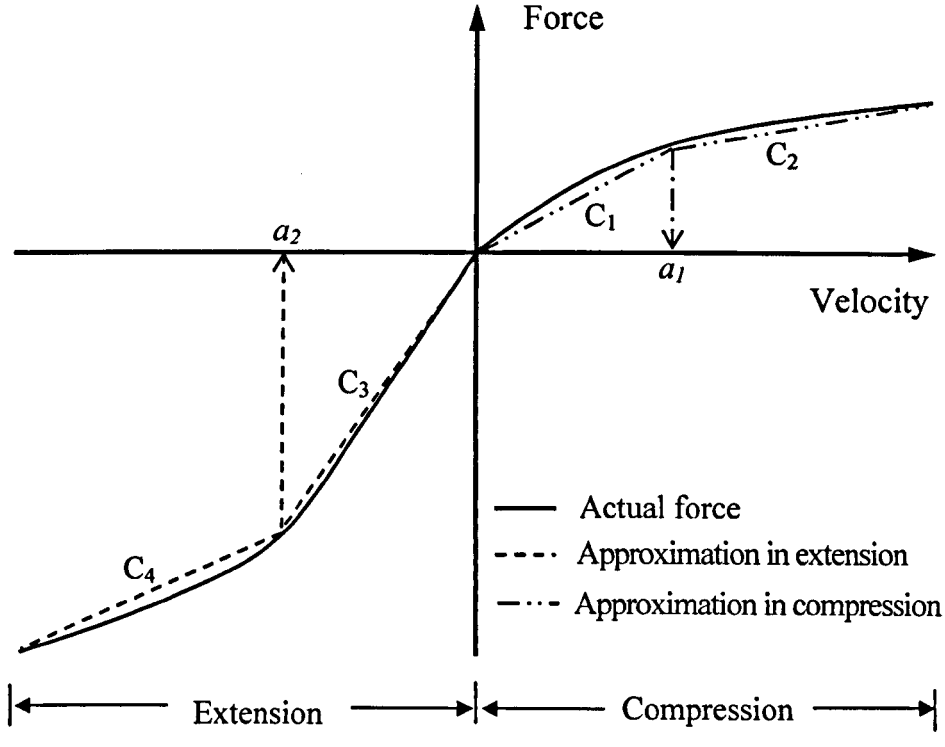

Figure 2.2 Typical force-velocity properties of a hydraulic damper

Studies of experimental test data show that asymmetrical dampers are considered for a more accurate treatment of the primary suspension systems in real designs [50]. The hydraulic damper has an asymmetrical characteristic of damping force which has a smaller value for compressing than for extending movement. The motion of the wheels running over convex irregularities causes larger forces than when travelling over concave ones. The hydraulic damper with an asymmetrical characteristic is typically suitable for providing a smaller force in compression and a greater one in extension [51].

In other designs, the hydraulic dampers also have a series of elastic elements (e.g., springs) from the mountings or oil chambers, which give the hydraulic damper the ability to provide both damping and stiffness. Nonetheless the separation is useful in the modelling procedure which focuses on the main property and application of each suspension component. For a real hydraulic damper, the condition of its seals can greatly affect its performance of absorbing the vibration or shock. The reliability of hydraulic dampers usually depends on the sealing between the shaft, piston and body. When applied in railway vehicle suspensions, occasional malfunction of this unit causes excessive pressure in the chamber which may result in leakage of the working fluid, and hence loss of damping [52].

Although in reality the characteristics of the damper force are nonlinear and also asymmetrical in the compression and extension motions, most vehicle dynamics and control strategies use linearised damping and represent it as symmetrical for simplicity [53] [54] [55]. Hence in this thesis, the modelling of the dampers in conventional bogie vehicle suspensions and theoretical analysis of the proposed FDI solutions will mainly be established using linear characteristics, which contributes the same resistance forces at the same speed of movements in compression and extension. It is noted that, the asymmetrical damping forces in compression and extension more accurately represent railway vehicle dynamics, thus affecting the availability of the proposed condition monitoring method in practical applications. In

this study, the bilinear (asymmetrical in compression and extension) damper mode is also included for performance assessments.

2.2.2.2 Secondary Suspension

Secondary suspension system is important in filtering out the frequencies of discomfort arising from the bogie frame and in maintaining the displacement of the carbody to acceptable limits. In the 1960s, secondary suspensions consisting of a pair of air springs were commercially used in Japanese conventional express railways. Afterwards such secondary suspensions became almost universal in modern passenger railway vehicle applications [45] [46]. Apart from other secondary spring stiffness and secondary hydraulic dampers in lateral and yaw directions, the air spring is particularly important in providing vertical support of the carbody [56]. Besides its practical advantages, the most significant are its provisions of constant suspension frequency and ride height regardless of the vehicle load. To enhance the possible safety standard in case of air loss that could result in a fall in suspension, most air springs are also fitted with a special rubber stack to ensure emergency carbody support [51].

The dynamic behaviour of an air spring is nonlinear and often complicated as it is mainly based on fluid dynamic and thermodynamic mechanisms [57]. Understanding the behaviour of the air spring is very important in modelling secondary suspension system. In this thesis, interest is solely focused on the vertical behaviour of the suspension systems and simplification of the air spring modelling is therefore necessary. The vertical behaviour of an air spring has both stiffness and damping characteristics. Unlike the hydraulic damper's asymmetrical characteristic in the primary suspension system, the equivalent symmetrical damping derived from the air spring is often used in the railway vehicle secondary suspension system. It is the only damping in that system and should be carefully considered in the modelling process. For the interest of the railway vehicle frequency range in the vertical direction, the

dynamic frequency of the primary suspension is high at 10-20Hz; however the secondary suspension only provides vertical vibration within the range of 0-1Hz. The differing frequency characteristic of various suspension systems is an important criterion for the validation of suspension designs. In different railway vehicle operational conditions, the deformation of the airspring will cause different force behaviour in lateral and vertical directions. However, these force changes will have little effect to the analysis of the force characteristic of the primary suspension systems, which is due to its filtering effect.

Figure 2.3 and Figure 2.4 show simple diagrams of a physical air spring with air reservoir and an equivalent mathematical representation used for modelling its behaviour [58]. Here K_a denotes the stiffness from the change-of-area of air springs, in which, as the height varies the effective area changes, resulting in a change of force even if the air pressure is constant. K_s is the stiffness representing the influence of air in the main volume. K_r is the stiffness representing the influence of air in the additional air reservoir. The damping C_r is parallel with the stiffness K_r, and it represents the damping of the surge pipe which connects the air chamber and the air reservoir. Although the air mass in the pipe is small, its equivalent inertia is significant when it passes through the narrow pipe at high velocity. This damping C_r arises from the air flow in the pipe or any orifices, which is often approximately as being linearly related to the velocity in many studies. The other factor which affects the air spring performance is the series stack stiffness, which rarely acts fast enough in the dynamic vehicle system and has less effect than the other stiffness as a contribution to air spring performance. For simplicity, the series stack stiffness does not appear in the following model [51].

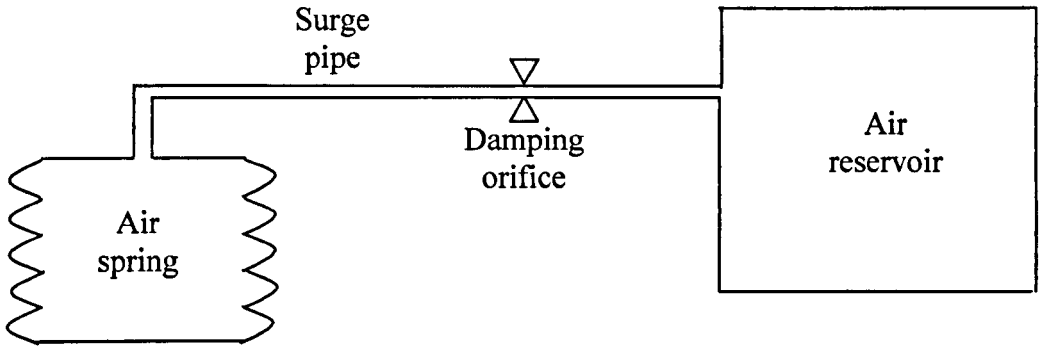

Figure 2.3 Physical air spring model with air reservoir

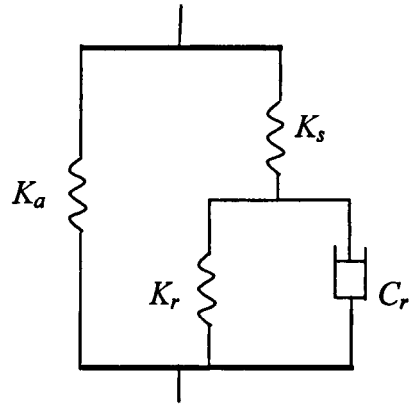

Figure 2.4 Air spring equivalent mathematical model [51]

Modern bogie design uses a smaller number of components in the secondary suspension system than in the primary. This arrangement has added benefits such as decreased component malfunctions and also reduced maintenance costs for the secondary suspension system.

2.2.3 Wheelset

The bottom part of the bogie is the wheelsets, each of which consists of two wheels connected by a common axle. The fixed solid axle is commonly used for conventional bogie, although Independently Rotating Wheels (IRW) for railway vehicles has recently engaged some consideration at a theoretical and experimental

level [59]. A wheelset is important in providing the safe gauge between the vehicle and rail tracks, and in guiding and determining the motion on straight and curved lines. Connected by the axle box, the wheels are critical factors in the railway rolling characteristic because they are in direct contact with the rails. The wheels are made from solid steel in specific shapes that can follow curves. In vehicle system dynamics, the track irregularities can be transmitted to the primary suspension systems via the rail-wheel interface.

2.3 Side View Model of a Bogie

This thesis does not cover the concept of wheel-rail contact, which has been the subject of many studies elsewhere [60]. For the basic analysis and development of the fault detection, a simple side view model extracted from a conventional bogie vehicle is first presented in this section, which only includes one bogie and two attached primary suspensions. The force exerted on the bogie from the secondary suspension is also considered.

The model has two motions in the vertical directions, bounce z_b and pitch ϕ_b, as shown in Figure 2.5. The standard dynamic equations for the two motions of the simple bogie under the normal condition are readily derived and can be found in references [43] [61] [62], as shown in equations (2.1) and (2.2).

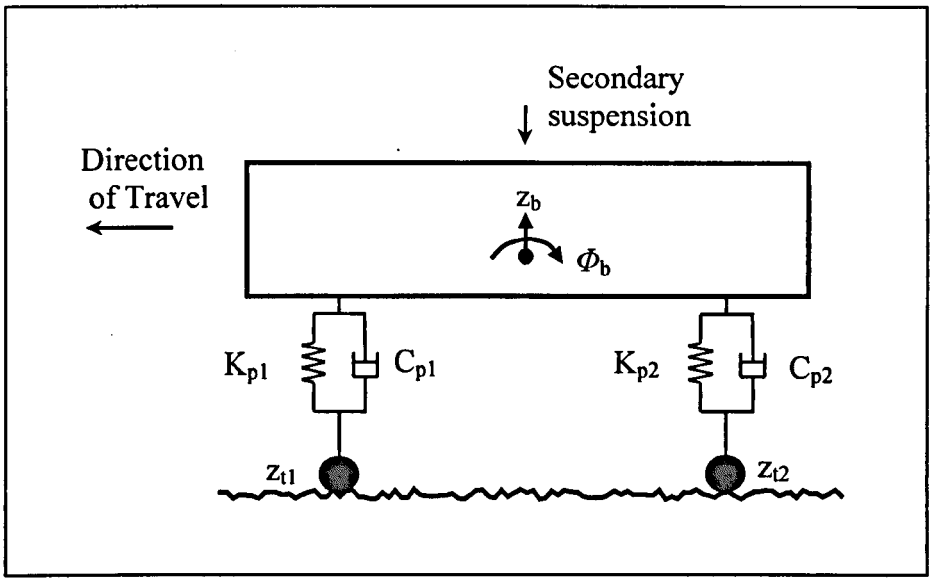

Figure 2.5 Side view diagram of a simple railway bogie

$$m_b\ddot{z}_b + 2C_p\dot{z}_b + 2K_p z_b = C_p(\dot{z}_{t1} + \dot{z}_{t2}) + K_p(z_{t1} + z_{t2}) + F_d \qquad (2.1)$$

$$I_b\ddot{\phi}_b + 2L_{bx}{}^2C_p\dot{\phi}_b + 2L_{bx}{}^2K_p\phi_b = L_{bx}C_p(\dot{z}_{t1} - \dot{z}_{t2}) + L_{bx}K_p(z_{t1} - z_{t2}) \qquad (2.2)$$

where

C_p - damping coefficient of primary suspensions (nominal)

F_d - Force exerted on the bogie from the secondary suspension

I_b - the bogie (pitch) moment of inertia

L_{bx} - semi wheel space

m_b - the bogie mass

K_p - stiffness constant of primary suspensions (nominal)

z_b - bogie bounce displacement

ϕ_b - bogie pitch (angular) displacement

z_{t1}, z_{t2} - track vertical displacement at the leading and trailing wheelsets

From equations (2.1) and (2.2), it is clear that there are no direct interactions between the bounce and pitch movements of the bogie. The main link between them is through the track inputs at the leading and trailing wheelsets, where the bounce mode is excited by their sum and the pitch mode by their difference.

However the above equations are only valid when the stiffness constants and the damping coefficients at both primary suspensions are the same, which is the case in most vehicles under normal circumstances. For a more general case where the two suspensions may not necessarily have the same values, equations (2.3) and (2.4) may be derived. They show potential interactions between the bounce and pitch motions when the suspension parameters are different, as the pitch movement may affect the bounce mode and vice versa.

$$\begin{aligned} m_b\ddot{z}_b + (C_{p1}+C_{p2})\cdot\dot{z}_b + (K_{p1}+K_{p2})\cdot z_b + L_{bx}\cdot(C_{p1}-C_{p2})\cdot\dot{\phi}_b + L_{bx}\cdot(K_{p1}-K_{p2})\cdot\phi_b \\ = C_{p1}\cdot\dot{z}_{t1} + K_{p1}\cdot z_{t1} + C_{p2}\cdot\dot{z}_{t2} + K_{p2}\cdot z_{t2} + F_d \end{aligned} \tag{2.3}$$

$$\begin{aligned} I_b\ddot{\phi}_b + L_{bx}^2(C_{p1}+C_{p2})\cdot\dot{\phi}_b + L_{bx}^2(K_{p1}+K_{p2})\cdot\phi_b + L_{bx}\cdot(C_{p1}-C_{p2})\cdot\dot{z}_b + L_{bx}\cdot(K_{p1}-K_{p2})\cdot z_b \\ = L_{bx}C_{p1}\cdot\dot{z}_{t1} + L_{bx}K_{p1}\cdot z_{t1} - L_{bx}C_{p2}\cdot\dot{z}_{t2} - L_{bx}K_{p2}\cdot z_{t2} \end{aligned} \tag{2.4}$$

where

C_{p1}, C_{p2} - damping coefficients of (front and rear) primary suspensions

K_{p1}, K_{p2} - stiffness constants of (front and rear) primary suspensions

A further analysis of the proposed fault detection scheme will be presented with respect to this side view model in Chapter 3.

2.4 Side/End View Model of a Vehicle

A more comprehensive model of a complete vehicle is used for the performance evaluation of the proposed fault detection technique.

A schematic diagram of a conventional railway bogie vehicle is shown in Figure 2.6, where the configuration and main components have been previously introduced in this chapter. The model consists of four wheelsets, two bogies (named leading and trailing bogies on front and rear sides) and a carbody frame interconnected by primary and secondary suspension systems. The main external excitations are track geometries (deterministic inputs) and irregularities (random track inputs) transmitted to the vehicle through the wheels, but attenuated through the use of the two layers of suspensions. In railway vehicle design, same suspension components are normally used at the four corners of each primary suspension and therefore the bogie configurations are mostly symmetrical. The primary suspensions are mainly used to control the running behaviour and stabilise the vehicle at high speeds and on curves, whereas the secondary suspensions are designed to maintain ride height and ensure reasonable ride comfort for passengers. Same air springs tend to be used for the secondary suspensions on both sides (referred to as left and right sides) of each of the two bogies.

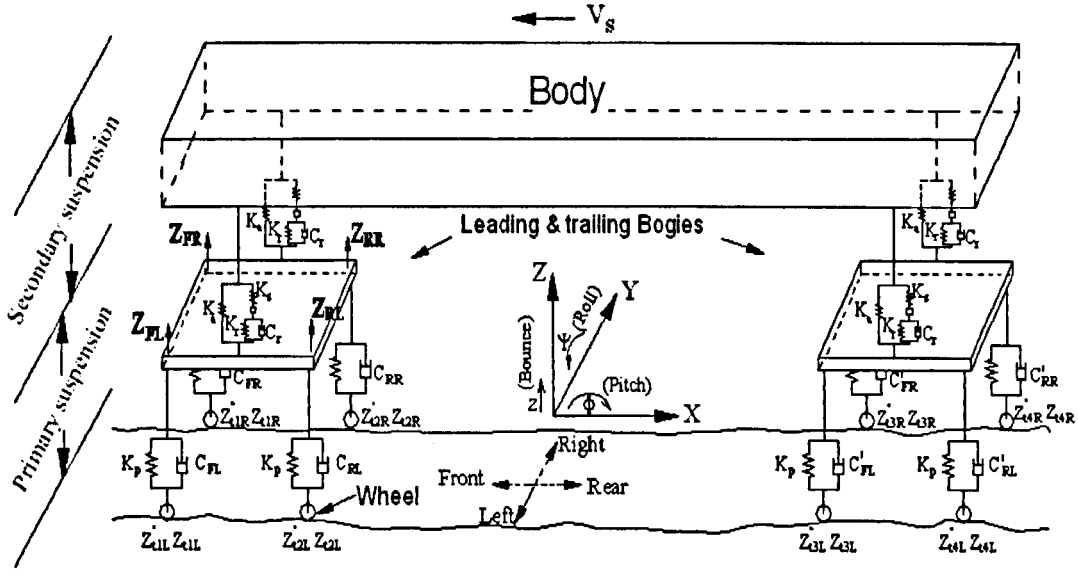

Figure 2.6 A comprehensive side and back view of a conventional bogie vehicle in vertical dynamics

The railway vehicle has several motions in different directions such as longitudinal, vertical, lateral and yaw. The corresponding suspension components in these directions may be different due to different vehicle ride requirements. Of all the directional motions, the vertical movement of the wheelsets is often directly constrained to the track surface. In this thesis, the FDI problem of the vertical primary suspensions is studied to demonstrate the principle and effectiveness of the proposed methods; however the techniques may be extended for the condition monitoring of suspensions in other directions or positions [43] [63]. According to the carbody and two bogies in Figure 2.6, only motions directly related to the vertical suspensions are modelled, including the bounce, pitch and roll movements of the carbody and those of the two bogie frames resulting in a 9 DoFs model.

On the side and back view of the conventional bogie vehicle shown in Figure 2.6, each bogie mass m_b is connected between the two layers of suspensions and it is supported by four springs and four dampers. The carbody mass m_v is mainly supported by two pairs of air springs in the secondary suspensions in the z direction. For a stationary vehicle system straddled over the rails, the weight of bogie mass m_b or carbody m_v is preloaded by the springs, and therefore its gravity is excluded from the following modelling process.

Using Newton's second law applied to the vertical motion, the equations of the bounce motion of the vertical vehicle system can be written as

$$m \cdot a_z = F_z \tag{2.5}$$

where, m is the mass of the car body or bogie, and a_z and F_z denote the acceleration and force respectively in the z direction.

Also, equations of motion in the pitch and roll directions can be expressed as

$$\begin{cases} I_x \cdot d\omega_x / dt = \Delta F_x \cdot L_x \\ I_y \cdot d\omega_y / dt = \Delta F_y \cdot L_y \end{cases} \tag{2.6}$$

where I_x, I_y are the moments of inertia in the pitch and roll directions of the bogie or carbody, ω_x, ω_y are their angular velocities, ΔF_x, ΔF_y are their force vectors acting on one point, and L_x, L_y are their vectors of position which point from points relative to the rotational axis, all along the pitch and roll direction respectively.

As the acceleration a_z can be described as the second derivative of the displacement z of the corresponding bogies or carbody in the bounce direction, the force equation (2.5) can be given as

$$m \cdot \ddot{z} = F_z \tag{2.7}$$

Also, the angular velocities ω_x, ω_y are the derivative of the corresponding pitch angle ϕ and roll angle ψ respectively. The derivatives of the angular velocities ω_x, ω_y representing the accelerations of the pitch and roll rotation angles, $d\omega_x/dt$ and $d\omega_y/dt$ can be substituted by $d^2\phi/dt$ and $d^2\psi/dt$ respectively. Thus the torque expression in equation (2.6) can be given as

$$\begin{cases} I_x \cdot \ddot{\phi} = \Delta F_x \cdot L_x \\ I_y \cdot \ddot{\psi} = \Delta F_y \cdot L_y \end{cases} \tag{2.8}$$

To consider that the vehicle operates along the rails, the track inputs z_t and $\dot{z}_t$ provide the external vertical stiffness force and damping force respectively through the excitations by springs and dampers in the primary suspension. These forces are attenuated through the primary suspensions and then regarded as the inputs to the secondary suspensions which maintain the motions of carbody. The supporting force applied by the secondary suspensions to the carbody simultaneously reacts back to the bogies; this retrieved force has the same magnitude as the supporting force but acts downwards. Therefore the overall forces related to every bogie include the interactive parts from both primary and secondary suspension systems. The magnitude of each of the forces is determined by the added multiplication of stiffness rate with their relative displacement, and the damping coefficient with their

relative velocity. These relative displacements and velocities are derived from the relative movement of each wheel, bogie and carbody. Those are not only defined by the inputs from the railway tracks, but also the performance of the mass-spring-damper systems.

The bounce movement of the leading bogie is therefore written as

$$m_b \ddot{z}_{b1} = F_{pfl} + F_{pfr} + F_{prl} + F_{prr} + F_{sl} + F_{sr} \tag{2.9}$$

where F_{pfl}, F_{pfr}, F_{prl} and F_{prr} are forces from the primary suspension system at the front left, front right, rear left and rear right corners respectively; F_{sl} and F_{sr} are forces from the secondary suspension system on the left and right sides (directions are denoted in Figure 2.6).

$$F_{pfl} = C_{FL} \cdot (\dot{z}_{t1l} - \dot{z}_{b1} - L_{bx}\dot{\phi}_{b1} - L_{by}\dot{\psi}_{b1}) + K_{FL} \cdot (z_{t1l} - z_{b1} - L_{bx}\phi_{b1} - L_{by}\psi_{b1}) \tag{2.10}$$

$$F_{pfr} = C_{FR} \cdot (\dot{z}_{t1r} - \dot{z}_{b1} - L_{bx}\dot{\phi}_{b1} + L_{by}\dot{\psi}_{b1}) + K_{FR} \cdot (z_{t1r} - z_{b1} - L_{bx}\phi_{b1} + L_{by}\psi_{b1}) \tag{2.11}$$

$$F_{prl} = C_{RL} \cdot (\dot{z}_{t2l} - \dot{z}_{b1} + L_{bx}\dot{\phi}_{b1} - L_{by}\dot{\psi}_{b1}) + K_{RL} \cdot (z_{t2l} - z_{b1} + L_{bx}\phi_{b1} - L_{by}\psi_{b1}) \tag{2.12}$$

$$F_{prr} = C_{RR} \cdot (\dot{z}_{t2r} - \dot{z}_{b1} + L_{bx}\dot{\phi}_{b1} + L_{by}\dot{\psi}_{b1}) + K_{RR} \cdot (z_{t2r} - z_{b1} + L_{bx}\phi_{b1} + L_{by}\psi_{b1}) \tag{2.13}$$

$$\begin{aligned} F_{sl} &= -K_a \cdot (z_{b1} + L_{by}\psi_{b1} - z_{bd} - L_{bdx}\phi_{bd} - L_{bdy}\psi_{bd}) \\ &\quad - C_r \cdot (\dot{z}_{b1} + L_{by}\dot{\psi}_{b1} - \dot{z}_{d1l}) - K_r \cdot (z_{b1} + L_{by}\psi_{b1} - z_{d1l}) \end{aligned} \tag{2.14}$$

$$\begin{aligned} F_{sr} &= -K_a \cdot (z_{b1} - L_{by}\psi_{b1} - z_{bd} - L_{bdx}\phi_{bd} + L_{bdy}\psi_{bd}) \\ &\quad - C_r \cdot (\dot{z}_{b1} - L_{by}\dot{\psi}_{b1} - \dot{z}_{d1r}) - K_r \cdot (z_{b1} - L_{by}\psi_{b1} - z_{d1r}) \end{aligned} \tag{2.15}$$

In equations (2.10) - (2.15), C_{FL}, C_{FR}, C_{RL} and C_{RR} are the dampings of the hydraulic dampers in the primary suspension system of the leading/trailing bogies, mounted at the front left, front right, rear left and rear right corners respectively. These dampers are the objects which will be studied later as the main subject of fault detection. In

the conventional bogie vehicle design, they are normally identical with the same damping coefficients. K_{FL}, K_{FR}, K_{RL} and K_{RR} are the springs with the same stiffness rates, parallel with corresponding C_{FL}, C_{FR}, C_{RL} and C_{RR} dampings at the four suspension corners. At the same four corners and in the same order, z_{t1l}, z_{t1r}, z_{t2l} and z_{t2r} represent the track inputs of the leading bogie in displacement, and $\dot{z}_{t1l}$, $\dot{z}_{t1r}$, $\dot{z}_{t2l}$ and $\dot{z}_{t2r}$ are their derivative track inputs in velocity.

Also, z_{bl}, ϕ_{bl} and ψ_{bl} represent the bounce, pitch and roll movements respectively for the leading bogie, z_{bd}, ϕ_{bd} and ψ_{bd} stand for the corresponding bounce, pitch and roll movements for the carbody. L_{bx} and L_{by} represent the half length of each bogie in the x and y directions, and L_{bdx} and L_{bdy} also denote the half lengths of the carbody in their corresponding directions.

In equations (2.14) and (2.15), z_{dll} and z_{dlr} represent the vertical displacements of the mid-point mass mm for the air springs assembled with the leading bogie. Figure 2.7 shows the arrangement of the alternative airspring model. Compared with the previous equivalent mathematical model of the airspring shown in Figure 2.4, the introduction of the mid-point mass m_m makes the force analysis in the secondary suspension systems easier, as it has very little effect on the dynamic performance. Therefore, this alternative airspring model shown in Figure 2.7 is applied in the following analysis and simulation.

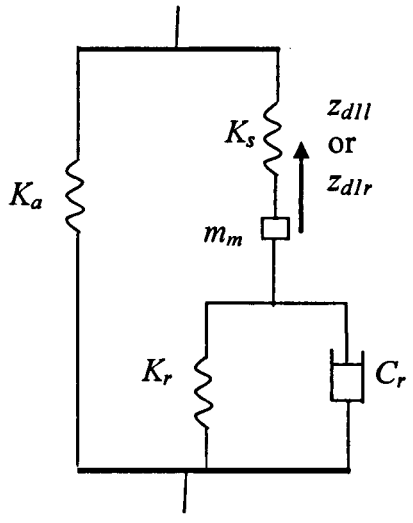

Figure 2.7 Air spring mathematical model with mid-point mass

In this thesis, attention is focused on the possible failure of the dampers, although the principle may be applied to the other components. Hence the springs in the primary suspension system can be assumed to have the same spring rate K_p for simplicity.

$$K_{FL} = K_{FR} = K_{RL} = K_{RR} = K_p \tag{2.16}$$

Substituting equations (2.10) - (2.16) into equation (2.9), forms the force equation for the leading bogie.

Bounce equation for leading bogie

$$\begin{aligned} &m_b\ddot{z}_{b1} + (C_{FL} + C_{FR} + C_{RL} + C_{RR})\dot{z}_{b1} + 4K_p z_{b1} \\ &= -L_{bx}(C_{FL} + C_{FR} - C_{RL} - C_{RR})\dot{\phi}_{b1} - L_{by}(C_{FL} - C_{FR} + C_{RL} - C_{RR})\dot{\psi}_{b1} \\ &+ (C_{FL}\dot{z}_{t1l} + K_p z_{t1l}) + (C_{FR}\dot{z}_{t1r} + K_p z_{t1r}) + (C_{RL}\dot{z}_{t2l} + K_p z_{t2l}) + (C_{RR}\dot{z}_{t2r} + K_p z_{t2r}) + \Sigma F_1 \end{aligned} \tag{2.17}$$

where ΣF_1 is the sum of the secondary force acted to the leading bogie

$$\begin{aligned}\Sigma F_1 &= F_{SL} + F_{SR} \\ &= -2C_r\dot{z}_{b1} - 2(K_a + K_r)z_{b1} + 2K_a z_{bd} + 2K_a L_{bdx}\phi_{bd} \\ &+ (C_r\dot{z}_{d1l} + K_r z_{d1l}) + (C_r\dot{z}_{d1r} + K_r z_{d1r})\end{aligned} \tag{2.18}$$

Similar to the bounce equation of the leading bogie, equation (2.6) represents the relationships between the moment of inertia and the torques in the pitch and roll directions. It can be expanded and simplified as follows:

Pitch equation for leading bogie (rotation in x direction),

$$\begin{aligned}&I_{bx}\ddot{\phi}_{b1} + L_{bx}^2(C_{FL} + C_{FR} + C_{RL} + C_{RR})\dot{\phi}_{b1} + 4L_{bx}^2 K_p\phi_{b1} \\ &= -L_{bx}(C_{FL} + C_{FR} - C_{RL} - C_{RR})\dot{z}_{b1} + L_{bx}(C_{FL}\dot{z}_{t1l} + K_p z_{t1l}) \\ &+ L_{bx}(C_{FR}\dot{z}_{t1r} + K_p z_{t1r}) - L_{bx}(C_{RL}\dot{z}_{t2l} + K_p z_{t2l}) - L_{bx}(C_{RR}\dot{z}_{t2r} + K_p z_{t2r})\end{aligned} \tag{2.19}$$

and roll equation for leading bogie (rotation in y direction),

$$\begin{aligned}&I_{by}\ddot{\psi}_{b1} + L_{by}^2(C_{FL} + C_{FR} + C_{RL} + C_{RR})\dot{\psi}_{b1} + 4L_{by}^2 K_p\psi_{b1} \\ &= -L_{by}(C_{FL} - C_{FR} + C_{RL} - C_{RR})\dot{z}_{b1} + L_{by}(C_{FL}\dot{z}_{t1l} + K_p z_{t1l}) \\ &- L_{by}(C_{FR}\dot{z}_{t1r} + K_p z_{t1r}) + L_{by}(C_{RL}\dot{z}_{t2l} + K_p z_{t2l}) - L_{by}(C_{RR}\dot{z}_{t2r} + K_p z_{t2r}) + L_{by}\Delta F_1\end{aligned} \tag{2.20}$$

where I_{bx} and I_{by} are the moments of the bogie inertia along the pitch and roll directions. ΔF_1 is the difference between the secondary forces acting on the leading bogie on the left and right sides

$$\begin{aligned}\Delta F_1 &= F_{SL} - F_{SR} \\ &= -2L_{by}C_r\dot{\psi}_{b1} - 2L_{by}(K_a + K_r)\psi_{b1} + 2L_{vy}K_a\psi_v \\ &+ (C_r\dot{z}_{d1L} + K_r z_{d1L}) - (C_r\dot{z}_{d1R} + K_r z_{d1R})\end{aligned} \tag{2.21}$$

Using a similar analysis approach, the force and torque equations for the trailing bogie are summarised as:

Bounce movement for trailing bogie,

$$
\begin{aligned}
&m_b\ddot{z}_{b2}+(C_{FL}+C_{FR}+C_{RL}+C_{RR})\dot{z}_{b2}+4K_pz_{b2}\\
&=-L_{bx}(C_{FL}+C_{FR}-C_{RL}-C_{RR})\dot{\phi}_{b2}-L_{by}(C_{FL}-C_{FR}+C_{RL}-C_{RR})\dot{\psi}_{b2}\\
&+(C_{FL}\dot{z}_{t3l}+K_pz_{t3l})+(C_{FR}\dot{z}_{t3r}+K_pz_{t3r})+(C_{RL}\dot{z}_{t4l}+K_pz_{t4l})+(C_{RR}\dot{z}_{t4r}+K_pz_{t4r})+\Sigma F_2
\end{aligned}
\tag{2.22}
$$

Pitch movement for trailing bogie,

$$
\begin{aligned}
&I_{bx}\ddot{\phi}_{b2}+L_{bx}^2(C_{FL}+C_{FR}+C_{RL}+C_{RR})\dot{\phi}_{b2}+4L_{bx}^2K_p\phi_{b2}\\
&=-L_{bx}(C_{FL}+C_{FR}-C_{RL}-C_{RR})\dot{z}_{b2}+L_{bx}(C_{FL}\dot{z}_{t3l}+K_pz_{t3l})\\
&+L_{bx}(C_{FR}\dot{z}_{t3r}+K_pz_{t3r})-L_{bx}(C_{RL}\dot{z}_{t4l}+K_pz_{t4l})-L_{bx}(C_{RR}\dot{z}_{t4r}+K_pz_{t4r})
\end{aligned}
\tag{2.23}
$$

and roll movement for trailing bogie,

$$
\begin{aligned}
&I_{by}\ddot{\psi}_{b2}+L_{by}^2(C_{FL}+C_{FR}+C_{RL}+C_{RR})\dot{\psi}_{b2}+4L_{by}^2K_p\psi_{b2}\\
&=-L_{by}(C_{FL}-C_{FR}+C_{RL}-C_{RR})\dot{z}_{b2}+L_{by}(C_{FL}\dot{z}_{t3l}+K_pz_{t3l})\\
&-L_{by}(C_{FR}\dot{z}_{t3r}+K_pz_{t3r})+L_{by}(C_{RL}\dot{z}_{t4l}+K_pz_{t4l})-L_{by}(C_{RR}\dot{z}_{t4r}+K_pz_{t4r})+L_{by}\Delta F_2
\end{aligned}
\tag{2.24}
$$

where z_{b2}, ϕ_{b2} and ψ_{b2} represent the bounce, pitch and roll movements respectively for the trailing bogie.

In equations (2.22) - (2.24), z_{t3l}, z_{t3r}, z_{t4l} and z_{t4r} represent the track inputs of the trailing bogie in displacement, and $\dot{z}_{t3l}$, $\dot{z}_{t3r}$, $\dot{z}_{t4l}$ and $\dot{z}_{t4r}$ are their derivative track inputs in velocity.

ΣF_2 is the sum of the secondary force acting on the trailing bogie

$$
\begin{aligned}
&\Sigma F_2=-2C_r\dot{z}_{b2}-2(K_a+K_r)z_{b2}+2K_az_{bd}-2K_aL_{bdx}\phi_{bd}\\
&+(C_r\dot{z}_{d2l}+K_rz_{d2l})+(C_r\dot{z}_{d2r}+K_rz_{d2r})
\end{aligned}
\tag{2.25}
$$

ΔF_2 is the difference between the secondary forces acting on the trailing bogie on the left and right sides

$$
\begin{aligned}
&\Delta F_2=-2L_{by}C_r\dot{\psi}_{b2}-2L_{by}(K_a+K_r)\psi_{b2}+2L_{vy}K_a\psi_v\\
&+(C_r\dot{z}_{d2L}+K_rz_{d2L})-(C_r\dot{z}_{d2R}+K_rz_{d2R})
\end{aligned}
\tag{2.26}
$$

The carbody also has 3 DoFs of bounce, pitch and roll movements in the vertical direction, which are expressed below:

Carbody bounce movement

$$\begin{aligned} & m_{bd}\ddot{z}_{bd} + 4(K_a + K_s)z_{bd} \\ & = 2K_a z_{b1} + 2K_a z_{b2} + K_s z_{d1l} + K_s z_{d1r} + K_s z_{d2l} + K_s z_{d2r} \end{aligned} \tag{2.27}$$

Carbody pitch movement

$$\begin{aligned} & I_{bdx}\ddot{\phi}_{bd} + 4L_{bdx}^2(K_a + K_s)\phi_{bd} \\ & = 2L_{bdx}K_a z_{b1} - 2L_{bdx}K_a z_{b2} + L_{bdx}K_s z_{d1l} + L_{bdx}K_s z_{d1r} - L_{bdx}K_s z_{d2l} - L_{bdx}K_s z_{d2r} \end{aligned} \tag{2.28}$$

Carbody roll movement

$$\begin{aligned} & I_{bdy}\ddot{\psi}_{bd} + 4L_{bdy}^2(K_a + K_s)\psi_{bd} \\ & = 2L_{bdy}L_{by}K_a\psi_{b1} + 2L_{bdy}L_{by}K_a\psi_{b2} + L_{bdy}K_s z_{d1l} - L_{vy}K_s z_{d1r} + L_{vy}K_s z_{d2l} - L_{vy}K_s z_{d2r} \end{aligned} \tag{2.29}$$

where z_{d2l} and z_{d2r} are the vertical displacements of the mid-point mass m_m for the air springs connected within the carbody and trailing bogie.

The equations for the mid-point masses of the air springs are given as:

$$\begin{aligned} & m_m\ddot{z}_{d1l} + C_r\dot{z}_{d1l} + (K_s + K_r)z_{d1l} \\ & = (C_r\dot{z}_{b1} + K_r z_{b1}) + (L_{by}C_r\dot{\psi}_{b1} + L_{by}K_r\psi_{b1}) + K_s z_{bd} + L_{bdx}K_s\phi_{bd} + L_{bdy}K_s\psi_{bd} \end{aligned} \tag{2.30}$$

$$\begin{aligned} & m_m\ddot{z}_{d1r} + C_r\dot{z}_{d1r} + (K_s + K_r)z_{d1r} \\ & = (C_r\dot{z}_{b1} + K_r z_{b1}) - (L_{by}C_r\dot{\psi}_{b1} + L_{by}K_r\psi_{b1}) + K_s z_{bd} + L_{bdx}K_s\phi_{bd} - L_{bdy}K_s\psi_{bd} \end{aligned} \tag{2.31}$$

$$\begin{aligned} & m_m\ddot{z}_{d2l} + C_r\dot{z}_{d2l} + (K_s + K_r)z_{d2l} \\ & = (C_r\dot{z}_{b2} + K_r z_{b2}) + (L_{by}C_r\dot{\psi}_{b2} + L_{by}K_r\psi_{b2}) + K_s z_{bd} - L_{bdx}K_s\phi_{bd} + L_{bdy}K_s\psi_{bd} \end{aligned} \tag{2.32}$$

$$\begin{aligned} & m_m\ddot{z}_{d2r} + C_r\dot{z}_{d2r} + (K_s + K_r)z_{d2r} \\ & = (C_r\dot{z}_{b2} + K_r z_{b2}) - (L_{by}C_r\dot{\psi}_{b2} + L_{by}K_r\psi_{b2}) + K_s z_{bd} - L_{bdx}K_s\phi_{bd} - L_{bdy}K_s\psi_{bd} \end{aligned} \tag{2.33}$$

Since the modelling of the conventional bogie vehicle in the vertical direction is of main interest, the longitudinal, lateral and yaw movements are not modelled above. The vertical vehicle model contains 13 DoFs in overall, i.e., bounce, pitch and roll modes for each bogie and the carbody, and a bounce mode for every air spring (defined in equations (2.17) - (2.33)). The mathematical model is therefore 26^{th} order.

2.5 Modal Analysis

Railway vehicle models are highly complex and of high order, even when a limited number of motions considered as in this study. It is therefore essential to ensure that correct and accurate models are used.

Modal analysis provides a powerful means to validate the models. The equations of the motions can be organised in a state-space form:

$$\dot{x} = A_{26}x + B_{16}u \tag{2.34}$$

where x and u are state variables and track input vectors respectively. A more detailed explanation of the variables in equation (2.34) is provided in Appendix A.

The state space equation (2.34) represents a linearised conventional bogie vehicle model with 13 DoFs in the vertical direction. The state variable x represents the bounce, pitch and roll motions of the carbody, bogies plus the additional mid-point mass of the air springs. All variables in the system matrix A_{26} and input matrix B_{16} are related to the characteristics of the vehicle system and the parameters of the two-layer suspension systems. The system response is also defined by the input vector u which is comprised of the random irregular vertical track inputs (as only the vertical motions of the vehicle system is emphasized in this thesis), although in the normal case railway track inputs may have two types of input, one being the deterministic

input (e.g. gradient) and the other the random input due to irregularities [38]. A more detailed property of the random track input in the vertical direction will be introduced in the next section.

The parameters of the conventional bogie vehicle model, which are taken from a typical passenger train, are given in Table 2.1.

Table 2.1 Relevant parameters of the conventional bogie vehicle model

Variables	Definitions and values
C_{FL}, C_{FR}, C_{RL}, C_{RR}	Damping of hydraulic dampers in bogies (17900Ns/m)
C_r	Damping for every airspring (30kNs/m)
I_{bdx}	Carbody pitch inertia (2310000kgm^2)
I_{bdy}	Carbody roll inertia (14400kgm^2)
I_{bx}	Leading or trailing bogie pitch inertia (2000kgm^2)
I_{by}	Leading or trailing bogie roll inertia (720kgm^2)
L_{bdx}	Half length of carbody in pitch motion (9.5m)
L_{bdy}	Half length of carbody in roll motion (0.75m)
L_{bx}	Half length of every bogie in pitch motion (1.25m)
L_{by}	Half length of every bogie in roll motion (0.75m)
K_a	Change of air stiffness for every airspring (1N/m)
K_p	Spring stiffness for leading or trailing bogie (2500kN/m)
K_r	Reservoir stiffness for every airspring (254kN/m)
K_s	Airspring stiffness (508kN/m)
m_b	Mass of leading or trailing bogie (2500kg)
m_{bd}	Mass of the carbody (38000kg)
m_m	Mid-point mass of every airspring (5kg)

Using MATLAB, the eigenvalues of the carbody and the two bogies can be calculated and are shown in Table 2.2.

Table 2.2 Eigenvalues for vertical vehicle model

		Frequency (Hz)	Damping
Carbody mode	Bounce	0.68	0.16
	Pitch	0.84	0.19
	Roll	0.84	0.19
Bogie mode (leading)	Bounce	10.57	0.23
	Pitch	14.07	0.32
	Roll	14.79	0.31
Bogie mode (trailing)	Bounce	10.57	0.23
	Pitch	14.07	0.32
	Roll	14.79	0.31

The eigenvalues given in the first three rows of Table 2.2 indicate that the carbody bounce, pitch and roll motions are of low frequencies (<1Hz), which is necessary to ensure comfort for the passengers. The last six rows, from fourth to ninth, represent the frequency mode for the leading and trailing bogies. The leading and trailing bogies have the same structures and identical components; they also have the same natural frequencies and damping ratios. It is clearly evident that after the filtering effect from the primary suspension systems, the dynamic frequency modes of bounce, pitch and roll for either bogie still have higher frequency vibrations (>10Hz) compared with the corresponding eigenvalues for the carbody. The damping ratio for the vertical motions of the carbody and two bogies are around 0.2.

For passenger railway vehicle with conventional bogie, the bogie bounce frequency between 10-20 Hz is generally accepted, for the carbody it is around 1Hz, and the effective damping ratio of the vertical vibration is usually located within the range of 0.1-0.3 [50]. Compared with these criteria, the side and end view of the model can be validated and thus accepted for further simulation assessments. The eigenvalues in the vertical direction are also independent of the vehicle operating speed, as expected.

2.6 The Properties of Vertical Track Inputs and Modelling

As only the vertical and related motions of the vehicle are considered in the study, only track irregularities in the vertical direction are included. Track geometries such as gradients are design features and tend to affect vehicle dynamics at low frequencies. Whilst it would not be a problem to include gradients in the simulations, they are not expected to affect the effectiveness of the proposed methods or to alter the conclusions of the study.

The rail track provides a displacement and its derivatives to each of the wheels of the railway vehicle. As a result of track misalignment, the track inputs are irregular. Some work has been done in modelling the track profile, using a stationary Gaussian stochastic process [50] [64].

Based on previous studies and experimental results in the track irregularities, some assumptions are made in the study:

(1) All track irregularities are considered as stationary random processes with zero mean;
(2) The probability density of the track irregularities is thought of as Gaussian;
(3) The cross-correlation between any two of the irregularities is zero [65] [66] [67].

To realise the stationary Gaussian random process of the track irregularity, the wave number Ω (rad/m) is introduced, which indicates the rate of cycle change with respect to the distance. For a train travelling along the track at a velocity V, it can be substituted by the angular frequency ω follows that

$$\omega = V\Omega \tag{2.35}$$

The relationship of the Power Spectral Density (PSD) between the wave number Ω and angular frequency ω can be expressed as

$$S(\Omega) = \frac{1}{V} S(\omega) \tag{2.36}$$

According to [67] the PSD of the vertical track irregularity can be modelled as follows

$$S_v(\Omega) = \frac{2\pi A_{rv} \Omega_c^2}{\Omega^2 (\Omega^2 + \Omega_c^2)} \tag{2.37}$$

where A_{rv} is the roughness factor in the vertical direction, Ω_c is the rail critical wave number above which the track input is negligible.

In many studies, a commonly employed form

$$S_v(\Omega) = \frac{A_{rv}}{\Omega^2} \tag{2.38}$$

is often applied to replace the PSD in equation (2.37) in order to get a simplified and appropriate vertical track inputs.

To reflect the rounding off effect at high frequencies in equation (2.37), an additional low pass filter is also used to give a more realistic generation of the power spectrum [61] [64] [67] [68].

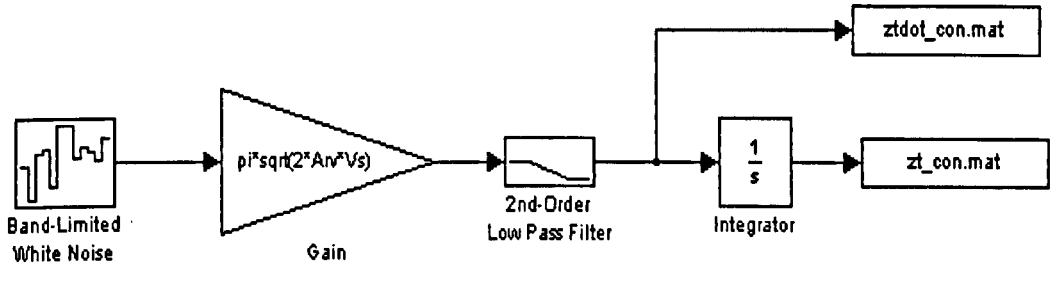

Figure 2.8 Vertical track irregularity generation scheme

As shown in Figure 2.8, the time series vertical track input is obtained from a Band-Limited White Noise block with a selected random seed. The magnitude of the track

input is dependent on the railway vehicle speed V, and a low pass filter with cut-off frequency of 80Hz is added in the loop in order to reduce the high frequency content above the critical wave number Ω_c and to reflect the general track irregularities which have high order in the denominator.

Figure 2.9 shows the vertical displacement of the track input obtained from the simulated data in Figure 2.8, and Figure 2.10 indicates its first-order derivative at the vehicle speed of 50m/s.

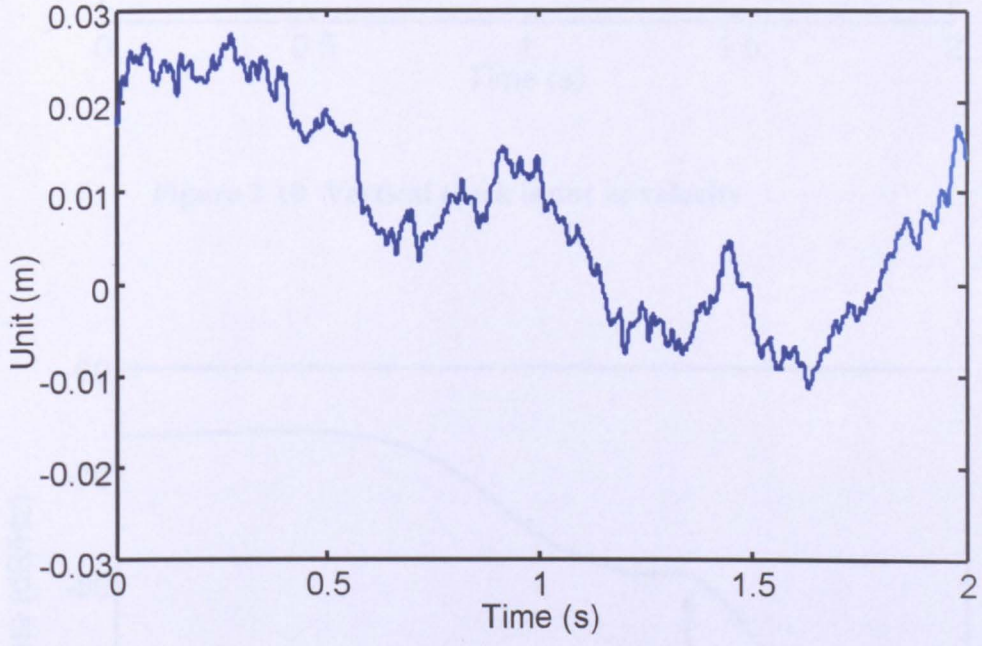

Figure 2.9 Vertical track input in displacement

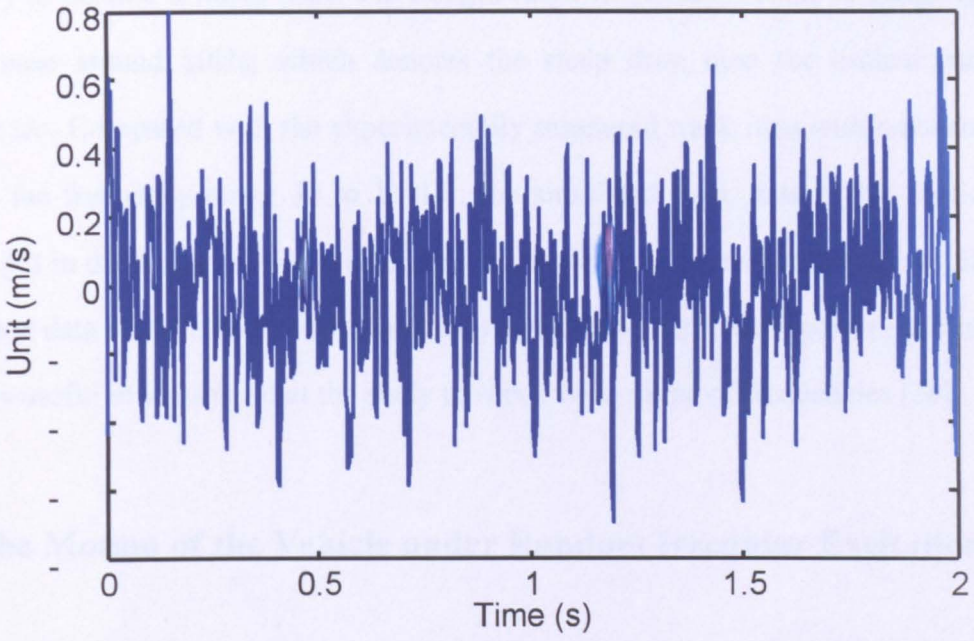

Figure 2.10 Vertical track input in velocity

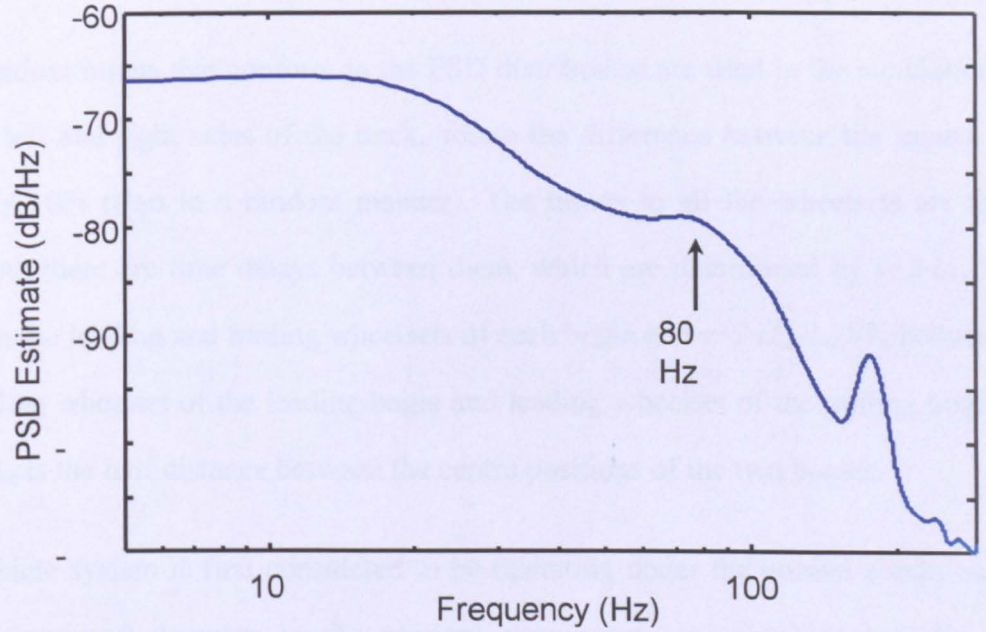

Figure 2.11 PSD of vertical track input in displacement (Vs=50m/s)

Figure 2.11 shows the PSD of the simulated vertical track input obtained from Figure 2.9. The PSD value is much richer at long wavelength (low frequency), with a

tendency to decline towards short wavelength (high frequency). There is a high rate of decrease around 80Hz, which denotes the steep drop near the critical wave number Ωc. Compared with the experimentally measured track data with resonance falls in the frequency range 30 to 100Hz, the simulated track data of the vertical track input in displacement and the derivatives shows they are reasonably close [68]. Simulated data tends to provide a richer and more evenly distributed power spectrum which is useful in ensuring that the study covers a wide range of frequencies [38].

2.7 The Motion of the Vehicle under Random Irregular Excitations

The time series vertical track inputs obtained from the Matlab/Simulink environment are used to simulate the railway vehicle response in the vertical direction. The operating speed of 50m/s (180km/h) for the vehicle is chosen. The typical parameters of the vehicle system used in the simulation are shown in Table 2.1.

Two random inputs that conform to the PSD distribution are used in the simulations for the left and right sides of the track, where the difference between the inputs is typically 10% (also in a random manner). The inputs to all the wheelsets are the same, but there are time delays between them, which are determined by $\tau=2\cdot L_{bx}/V_s$ between the leading and trailing wheelsets of each bogie and $\tau=2\cdot(L_b-L_{bx})/V_s$ between the trailing wheelset of the leading bogie and leading wheelset of the trailing bogie, where L_b is the half distance between the centre positions of the two bogies.

The vehicle system is first considered to be operating under the normal conditions. The springs and dampers in the primary suspensions are considered as linear components, together with a linearised air spring model used to simulate the secondary suspensions in the vertical direction. Because it is assumed that there are no faults in the springs and dampers in the suspensions, their corresponding parameters are identical and the vehicle structure is symmetrical.

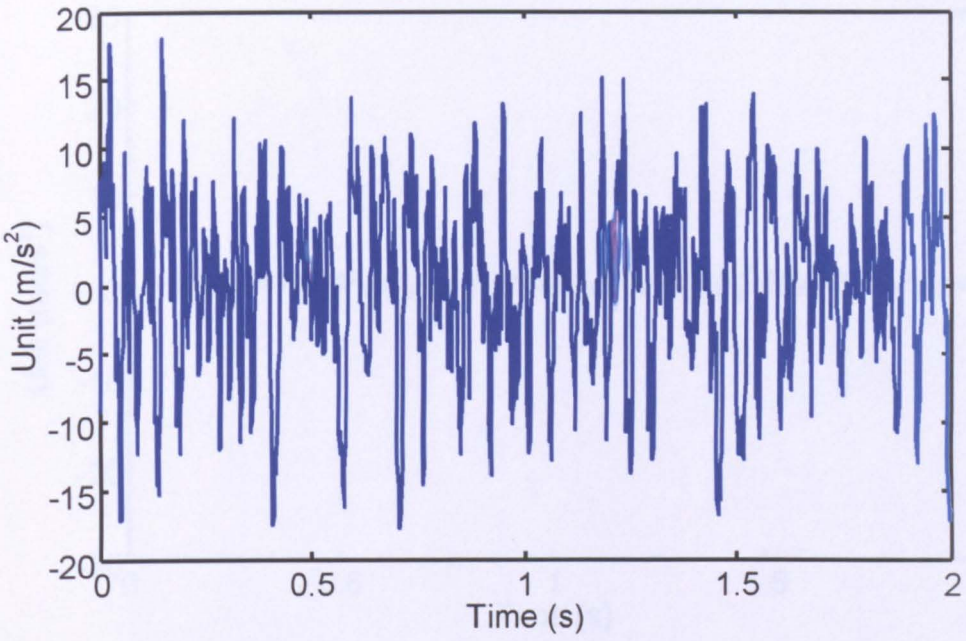

Figure 2.12 The bounce acceleration of leading bogie

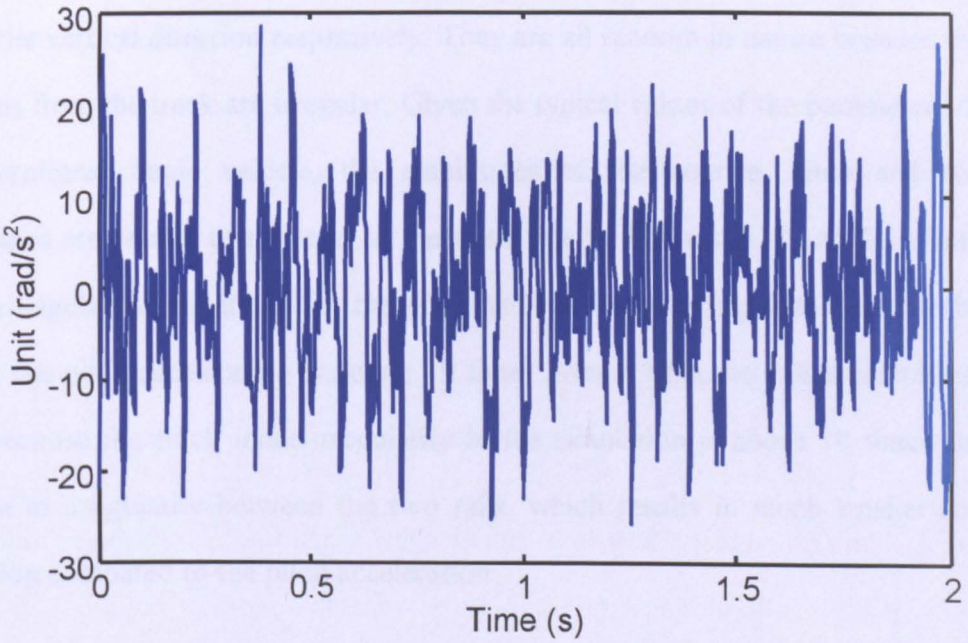

Figure 2.13 The pitch acceleration of leading bogie

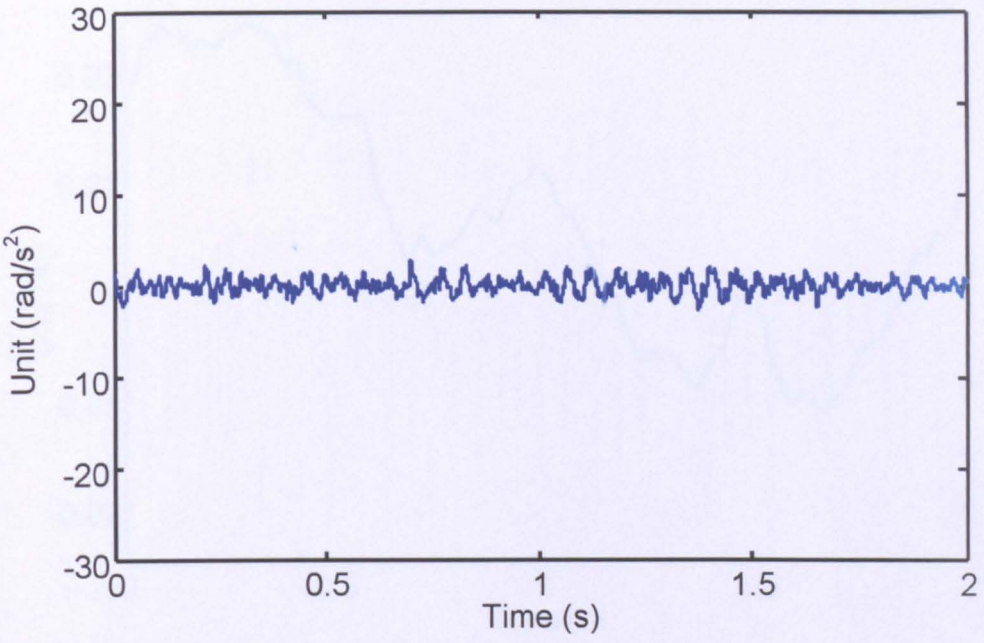

Figure 2.14 The roll acceleration of leading bogie

Figures 2.12 to Figure 2.14 show the bounce, pitch and roll motions of the leading bogie in the vertical direction respectively. They are all random in nature because the excitations from the track are irregular. Given the typical values of the parameters of the conventional bogie vehicle, the amplitudes of the bounce, pitch and roll accelerations are related to the level of the track inputs. Figures 2.13 and 2.14 both show the angular accelerations for the pitch and roll motions separately. It can be seen that the pitch acceleration is nearly 10 times greater then the roll acceleration. This is because the track input irregularity in the simulation is about 10 times the difference in irregularity between the two rails, which results in much smaller roll acceleration compared to the pitch acceleration.

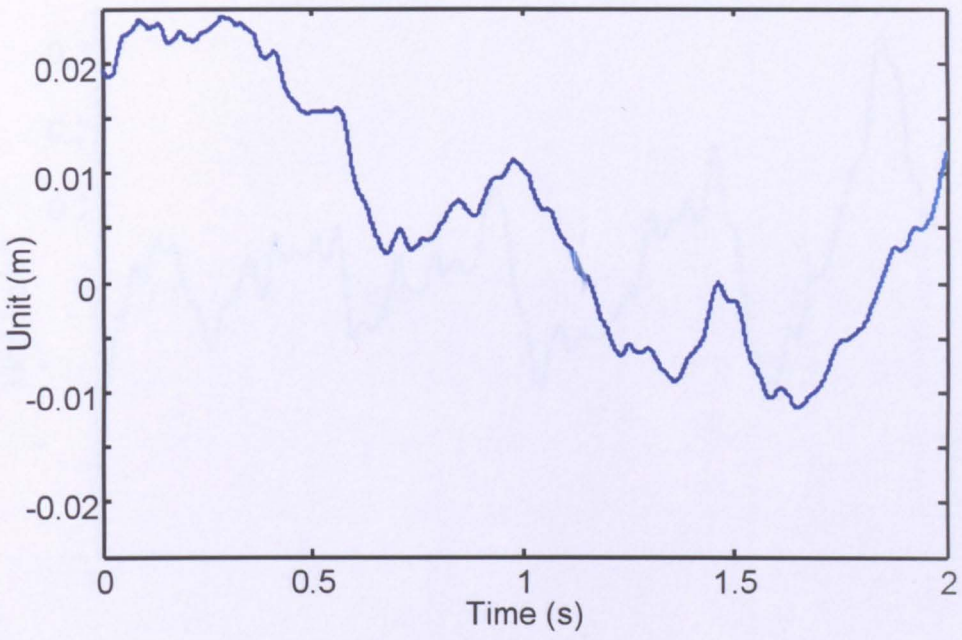

Figure 2.15 The bounce displacement of leading bogie

The simulation result for the bounce displacement of the leading bogie is shown in Figure 2.15. It is found that the bounce displacement is very similar to the vertical displacement track input shown in Figure 2.9 at low frequencies. The good match of the vertical movement of the bogie shows that the bogie follows the slow changes of the rail track. The difference between them is that the bounce displacement of the bogie is smoother than that of the vertical displacement track input. This difference is mostly due to the fact that the primary suspension system has a filtering effect which can filter out the higher frequency components of the track input.

For the trailing bogie, similar responses can be observed as those of the leading bogie.

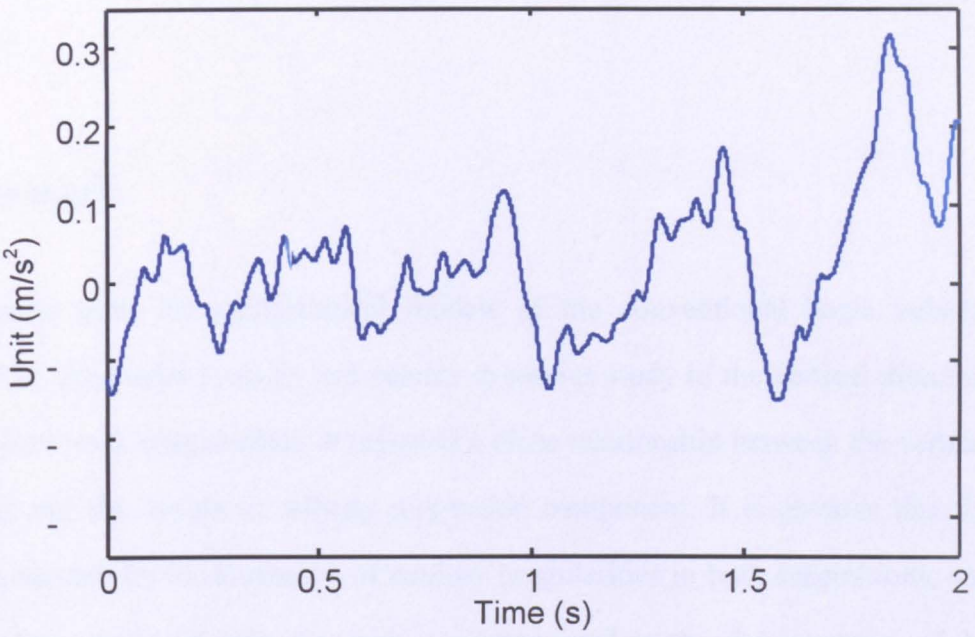

Figure 2.16 The bounce acceleration of the carbody

Figure 2.16 shows the bounce acceleration of the carbody at the mass centre. It is apparent that the random distribution of the carbody bounce acceleration is mainly due to the combination of the bounce motions of the leading and trailing bogies. Its magnitude ($0.2m/s^2$ in RMS) is much smaller than the bounce acceleration of the leading bogie shown in Figure 2.12 ($10m/s^2$ in RMS). Its waveform is also much smoother than the bogie bounce acceleration. Both effects are of course due to the filtering function of the secondary suspensions (i.e., the air springs).

It is also observed that the range of the bounce acceleration of the carbody is considerably smaller and smoother, which indicates that the height of the carbody changes very little in response to the excitation from the track input even if the train is running at high speeds. On the other hand, as the secondary suspension system works effectively in the very low frequency range; other vibrational effects in the high frequency range can be negligible. This property is very helpful in simplifying the following FDI problem, because the forces from the secondary suspensions are

filtered out at around 1Hz, and hence can be omitted in the following analysis for simplicity.

2.8 Summary

This chapter gave the mathematical models of the conventional bogie vehicle, followed by the modal analysis and vehicle dynamics study in the vertical direction with random track irregularities. It revealed a close relationship between the vertical dynamics and the design of railway suspension component. It is obvious that the vibration appears by the excitation of random irregularities in both suspensions, and the main frequencies of their vibrations are determined by the characteristics of the suspension systems.

By monitoring the vibrational information of the selected suspension, the faulty condition can be possibly indicated.

Chapter 3

Fault Detection Scheme Based on Changes in Dynamic Interactions

3.1 Introduction

In the development of a novel FDI scheme in railway vehicles, it is essential to understand the construction and configuration of the vehicle system. Their dynamic interactions also need to be understood clearly [69] [70]. In chapter 2, the fundamental structure and principal components of a conventional bogie vehicle are introduced and the side view model for a simple bogie has been developed for the FDI scheme analysis. With the aid of this model, this chapter presents the basic concepts of the proposed technique for the fault detection of vehicle suspensions, explained by examining the consequences of a component fault in terms of additional dynamic interactions.

This novel approach is simple but very effective for the FDI problem for railway vehicle suspensions, and it requires much less prior knowledge of the railway vehicle systems concerned in the study. There is no need for additional complex modelling and detailed knowledge of external conditions such as track irregularities. It also offers potential benefits of robustness against nonlinearities and uncertainties as well as that of easy tuning.

3.2 Fault Detection Concept from a Simple Railway Bogie

In this study, the FDI scheme focusing on damper failure in the primary suspension systems is developed. To clarify and simplify the basic concept, the side view bogie model in the vertical direction is used in the analysis, as shown in Figure 2.5. As

noted previously, the components used in the same railway vehicle suspension (i.e. springs and dampers) are largely identical. The proposed FDI technique is based on system dynamic interaction changes caused by component faults.

3.2.1 Analysis of Dynamic Interaction

The dynamic interactions caused by possible component faults have been illustrated using the equations of motions in the form of bounce and pitch movements of the simple bogie model as given in equations (2.3) and (2.4). By introducing the sum and difference of their corresponding damping coefficients and stiffnesses, they can be modified to give equations (3.1) and (3.2).

$$\begin{aligned} & m_b\ddot{z}_b + C_{ps}\dot{z}_b + K_{ps}z_b + L_{bx}C_{pd}\dot{\phi}_b + L_{bx}K_{pd}\phi_b \\ & = \frac{1}{2}\left[C_{ps}(\dot{z}_{t1} + \dot{z}_{t2}) + K_{ps}(z_{t1} + z_{t2}) + C_{pd}(\dot{z}_{t1} - \dot{z}_{t2}) + K_{pd}(z_{t1} - z_{t2})\right] + F_d \end{aligned} \tag{3.1}$$

$$\begin{aligned} & I_b\ddot{\phi}_b + L_{bx}{}^2C_{ps}\dot{\phi}_b + L_{bx}{}^2K_{ps}\phi_b + L_{bx}C_{pd}\dot{z}_b + L_{bx}K_{pd}z_b \\ & = \frac{L_{bx}}{2}\left[C_{ps}(\dot{z}_{t1} - \dot{z}_{t2}) + K_{ps}(z_{t1} - z_{t2}) + C_{pd}(\dot{z}_{t1} + \dot{z}_{t2}) + K_{pd}(z_{t1} + z_{t2})\right] \end{aligned} \tag{3.2}$$

where

$$C_{ps}=C_{p1}+C_{p2}$$

$$C_{pd}=C_{p1}-C_{p2}$$

$$K_{ps}=K_{p1}+K_{p2}$$

$$K_{pd}=K_{p1}-K_{p2}$$

When the bogie is operating under the normal condition ($K_{p1}=K_{p2}$, $C_{p1}=C_{p2}$), equations (3.1) and (3.2) may be simplified to equations (3.3) and (3.4), which indicate clearly that the bounce and pitch movements of the bogie are independent and that there is no direct dynamic coupling between these two motions. The force

F_d from the secondary suspension only affects the bounce motion but not the pitch motion.

$$m_b\ddot{z}_b + C_{ps}\dot{z}_b + K_{ps}z_b = \frac{1}{2}C_{ps}(\dot{z}_{t1} + \dot{z}_{t2}) + \frac{1}{2}K_{ps}(z_{t1} + z_{t2}) + (F_d) \tag{3.3}$$

$$I_b\ddot{\phi}_b + L_{bx}^2 C_{ps}\dot{\phi}_b + L_{bx}^2 K_{ps}\phi_b = \frac{1}{2}L_{bx}C_{ps}(\dot{z}_{t1} - \dot{z}_{t2}) + \frac{1}{2}L_{bx}K_{ps}(z_{t1} - z_{t2}) \tag{3.4}$$

However, when one of the faults occurs, the two suspensions become different and the structure of the suspension becomes asymmetrical. The imbalance between the suspensions cause interactions between the bounce and pitch motions in two ways. Dynamically, equations (3.1) and (3.2) are no longer independent as two pitch terms appear in the bounce equation and two bounce terms in the pitch equation. Externally, the bounce motion is now also affected by the difference between the track inputs at the front and rear suspensions which predominantly excites the pitch motion. The pitch movement is also affected by the sum of these two input signals which predominantly excites the bounce motion. The interaction between the two motions introduces an additional correlation between the different dynamic modes. The correlation will change with different types of suspension component faults (i.e. by not only the extent of the imbalance, but also the location of the failure), which will be used to detect how much unbalance (i.e. due to component fault) may exist in the system, and to isolate the fault.

In practice, the bounce and pitch accelerations may be readily obtained through the use of inertial sensors mounted on the bogie frame [18] [19]. The two accelerations may be expressed in the form of transfer functions in equations (3.5) and (3.6) replacing the general equations (3.1) and (3.2). It cab be seen that, in bounce equation (3.5), the 3rd and 4th terms are introduced due to the imbalance caused by a component failure, which represent a response change to the track inputs at the leading and trailing wheelsets respectively. The 5th term is represented as the

additional interaction stimulated by the pitch motion, and finally the 6th term is related to the secondary suspension force $F_d(s)$. In pitch equation (3.6), the imbalance also presents a response change to the leading and trailing wheelset track inputs shown in the 3rd and 4th terms, and the 5th term indicates the extra interaction which results from the bounce motion. The secondary suspension force $F_d(s)$ clearly has no effect on the pitch motion.

$$\begin{aligned}\ddot{z}_b(s) = &\frac{1}{2}\cdot\frac{C_{ps}s+K_{ps}}{m_b s^2+C_{ps}s+K_{ps}}\ddot{z}_{t1}(s)+\frac{1}{2}\cdot\frac{C_{ps}s+K_{ps}}{m_b s^2+C_{ps}s+K_{ps}}\ddot{z}_{t2}(s)\\ &+\frac{1}{2}\cdot\frac{C_{pd}s+K_{pd}}{m_b s^2+C_{ps}s+K_{ps}}\ddot{z}_{t1}(s)-\frac{1}{2}\cdot\frac{C_{pd}s+K_{pd}}{m_b s^2+C_{ps}s+K_{ps}}\ddot{z}_{t2}(s)\\ &-\frac{L_{bx}(C_{pd}s+K_{pd})}{m_b s^2+C_{ps}s+K_{ps}}\ddot{\phi}_b(s)+\frac{s^2}{m_b s^2+C_{ps}s+K_{ps}}F_d(s)\end{aligned} \tag{3.5}$$

$$\begin{aligned}\ddot{\phi}_b(s) = &\frac{L_{bx}}{2}\cdot\frac{C_{ps}s+K_{ps}}{I_b s^2+L_{bx}^2C_{ps}s+L_{bx}^2K_{ps}}\ddot{z}_{t1}(s)-\frac{L_{bx}}{2}\cdot\frac{C_{ps}s+K_{ps}}{I_b s^2+L_{bx}^2C_{ps}s+2L_{bx}^2K_{ps}}\ddot{z}_{t2}(s)\\ &+\frac{L_{bx}}{2}\cdot\frac{C_{pd}s+K_{pd}}{I_b s^2+L_{bx}^2C_{ps}s+L_{bx}^2K_{ps}}\ddot{z}_{t1}(s)+\frac{L_{bx}}{2}\cdot\frac{C_{pd}s+K_{pd}}{I_b s^2+L_{bx}^2C_{ps}s+2L_{bx}^2K_{ps}}\ddot{z}_{t2}(s)\\ &-\frac{L_{bx}(C_{pd}s+K_{pd})}{I_b s^2+L_{bx}^2C_{ps}s+2L_{bx}^2K_{ps}}\ddot{z}_b(s)\end{aligned} \tag{3.6}$$

The modal decomposition process can be applied by substituting equation (3.6) into equation (3.5) to remove the pitch acceleration from the bounce equation, and substituting equation (3.5) into equation (3.6) to remove the bounce acceleration from the pitch equation, which leads to equations (3.7) and (3.8) respectively:

$$\ddot{z}_b(s)=\frac{1}{2}\cdot G_0(s)\cdot\left[G_{11}(s)\ddot{z}_{t1}(s)+G_{12}(s)\ddot{z}_{t2}(s)\right]+\frac{s^2}{A_z(s)}F_d(s) \tag{3.7}$$

$$\ddot{\phi}_b(s)=\frac{L_{bx}}{2}\cdot G_0(s)\cdot\left[G_{21}(s)\ddot{z}_{t1}(s)-G_{22}(s)\ddot{z}_{t2}(s)\right]-\frac{L_{bx}B_d(s)s^2}{A_z(s)A_\phi(s)}F_d(s) \tag{3.8}$$

where

$$G_0(s) = \frac{A_z(s)A_\phi(s)}{A_z(s)A_\phi(s) - {L_{bx}}^2 B_d(s)^2}$$

$$G_{11}(s) = \frac{2\left(C_{p1}\cdot s + K_{p1}\right)}{A_z(s)} \cdot \left(1 - \frac{{L_{bx}}^2 B_d(s)}{A_\phi(s)}\right)$$

$$G_{12}(s) = \frac{2\left(C_{p2}\cdot s + K_{p2}\right)}{A_z(s)} \cdot \left(1 + \frac{{L_{bx}}^2 B_d(s)}{A_\phi(s)}\right)$$

$$G_{21}(s) = \frac{2\left(C_{p1}\cdot s + K_{p1}\right)}{A_\phi(s)} \cdot \left(1 - \frac{B_d(s)}{A_z(s)}\right)$$

$$G_{22}(s) = \frac{2\left(C_{p2}\cdot s + K_{p2}\right)}{A_\phi(s)} \cdot \left(1 + \frac{B_d(s)}{A_z(s)}\right)\Bigg]$$

$$A_z(s) = m_b s^2 + C_{ps}s + K_{ps}$$

$$A_\phi(s) = I_b s^2 + {L_{bx}}^2 C_{ps}s + {L_{bx}}^2 K_{ps}$$

$$B_s(s) = C_{ps}s + K_{ps}$$

$$B_d(s) = C_{pd}s + K_{pd}$$

Equations (3.7) and (3.8) can be further simplified to equations (3.9) and (3.10) by neglecting the term relating to the secondary suspension force $F_d(s)$, which has much smaller effects compared to that of the track inputs (due to the filtering effect).

$$\ddot{z}_b(s) = \frac{1}{2}\cdot G_0(s)\cdot\left[G_{11}(s)\ddot{z}_{t1}(s) + G_{12}(s)\ddot{z}_{t2}(s)\right] \tag{3.9}$$

$$\ddot{\phi}_b(s) = \frac{L_{bx}}{2}\cdot G_0(s)\cdot\left[G_{21}(s)\ddot{z}_{t1}(s) - G_{22}(s)\ddot{z}_{t2}(s)\right] \tag{3.10}$$

Equations (3.9) and (3.10) show clearly that the bounce and pitch motions of the railway bogie can be largely decoupled in the balanced condition, i.e. $B_d(s)=0$. Their simplest transfer function forms can therefore be expressed in equations (3.11) and (3.12).

$$\ddot{z}_b(s) = \frac{1}{2} \cdot \left[G_z(s)\ddot{z}_{t1}(s) + G_z(s)\ddot{z}_{t2}(s) \right] \tag{3.11}$$

$$\ddot{\phi}_b(s) = \frac{L_{bx}}{2} \cdot \left[G_\phi(s)\ddot{z}_{t1}(s) - G_\phi(s)\ddot{z}_{t2}(s) \right] \tag{3.12}$$

where

$$G_z(s) = \frac{B_s(s)}{A_z(s)}$$

$$G_\phi(s) = \frac{B_s(s)}{A_\phi(s)}$$

The difference between the normal (equations 3.11 and 3.12) and faulty (equations 3.9 and 3.10) conditions will be further analysed in frequency domain.

3.2.2 Frequency Response Comparisons of the Analytical Models

By comparing the two sets of transfer functions between the normal and fault conditions, it is obvious that the filtering effect of the primary suspensions on bogie motions would be different in different cases. The gain of the common term $G_0(s)$ is very close to unity in the no fault case, but in a fault condition the response is magnified in the frequency region around the two bogie modes (by up to 66% if the damping coefficient at the trailing damper becomes zero) as shown in Figure 3.1. However, there is no noticeable change at the high or low frequency ranges and therefore the overall effect of the term $G_0(s)$ will be limited.

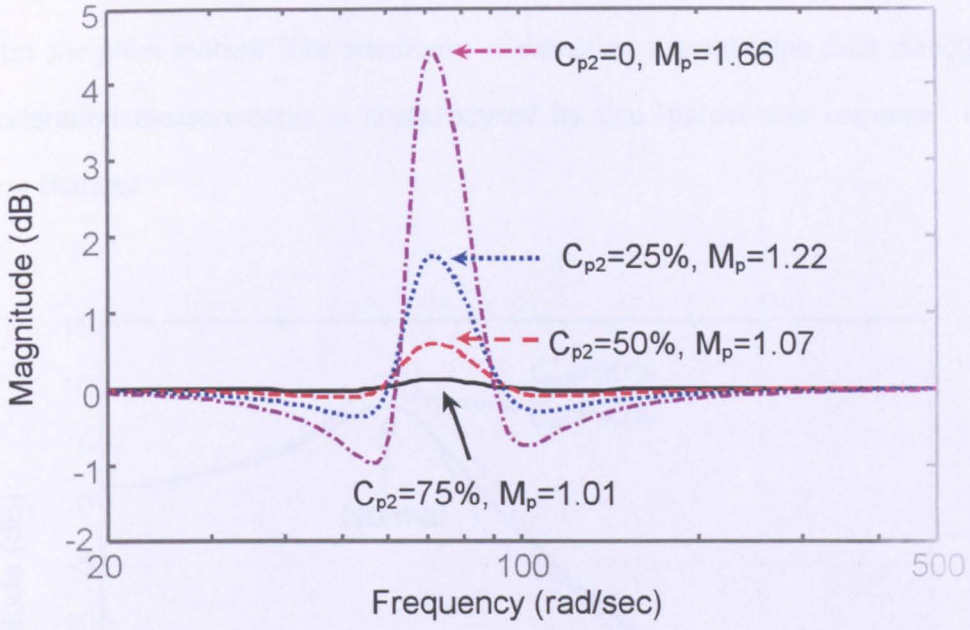

Figure 3.1 Bode plot of $G_0(s)$

Equations 3.9 - 3.12 also show how the bounce and pitch motions are excited by track inputs at the leading and trailing wheelsets. Each of the two inputs influences only one of the two terms in the dynamic equations through the corresponding suspension. Therefore the changes due to a component failure in one suspension will only be reflected in the corresponding part of the responses, while the effects to the other part will be insignificant. As demonstrated in Figure 3.2 and Figure 3.3, a reduction of the damping coefficient to half in the front suspension alters significantly how the bogie bounce mode responds to the track input at the leading wheelset (through G_{11}), but has little effect on its response to the delayed track input at the trailing wheelset (through G_{12}). On the other hand, a similar damper failure occurring at the rear suspension affects the bogie bounce motion mainly through the track input at the trailing wheelset (through G_{12}), but not at the leading wheelset (G_{11}). It is notable that for either G_{11} or G_{12}, the damping fault on the corresponding front or rear suspension side will cause an increase in gain around the resonant frequency but conversely a reduction across the wider range of the high frequency, which makes the

overall magnitude in performance decrease. A similar trend may be observed for G_{21} and G_{22} for the pitch motion. The sensitivity of detecting a suspension fault directly from acceleration measurements is compromised by this 'partial non response' to suspension changes.

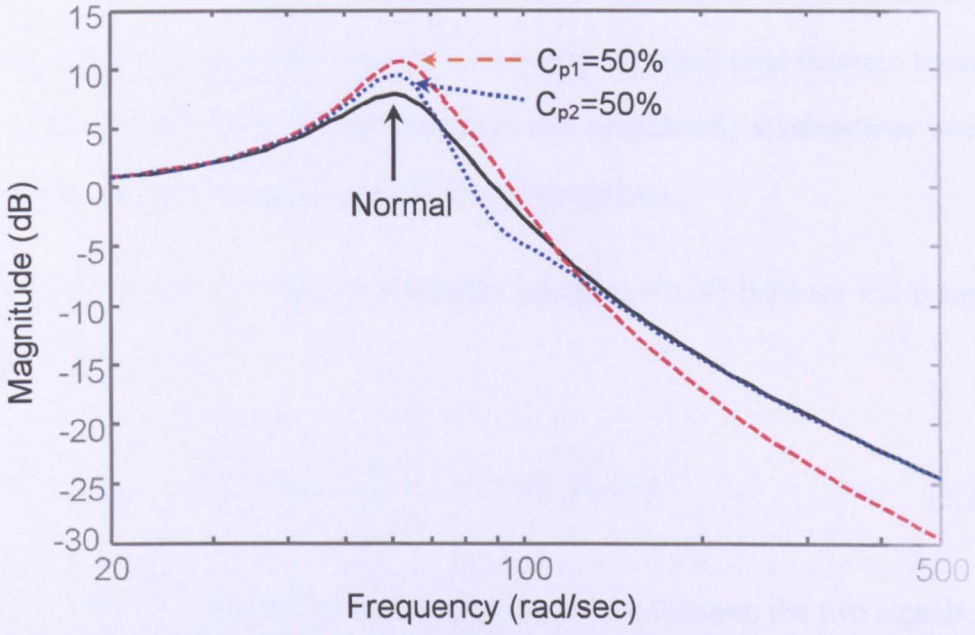

Figure 3.2 Bode plot of $G_{11}(s)$

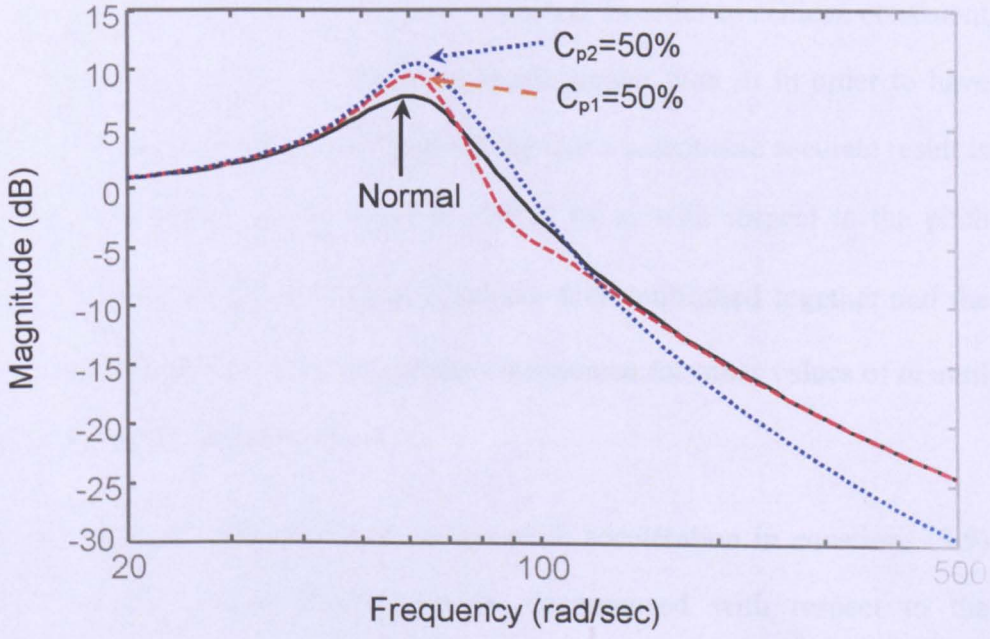

Figure 3.3 Bode plot of $G_{12}(s)$

3.3 Fault Detection Scheme by Correlation Evaluation

In contrast with other methods presented in Chapter 1, the proposed new method attempts to overcome the problem of insensitivity to component faults by detecting changes in dynamic correlations between the bounce and pitch (and between bounce and roll, pitch and roll when the roll motion is also considered) accelerations which can be readily achieved using cross correlation calculations.

Equation (3.13) shows the Cross Correlation Function (CCF) between the bounce and pitch accelerations.

$$R_{BP}(m) = \sum_{n=1}^{N} \ddot{z}_b(n+m) \cdot \ddot{\phi}_b(n) \tag{3.13}$$

where *m[-N, N]* is the number of the sampled time shift between the two signals. N is the number of sampled data for the CCF calculation. For a fixed sampling interval Δt ($\Delta t=0.001s$ in this thesis, with a fixed sampling rate of 1kHz), a time window T which contains a period of sampled signal is required. In order to achieve consistent results, the time window $T=N\cdot\Delta t$ should be much greater than Δt in order to have enough lagged products at the selected highest lag that a reasonable accurate result is still obtained. The bounce signal $\ddot{z}_b(n)$ is shifted by m with respect to the pitch signal $\ddot{\phi}_b(n)$. The signals $\ddot{z}_b(n+m)$ and $\ddot{\phi}_b(n)$ are then multiplied together and the sum of the product is determined. The process is repeated for other values of m until the whole set of $R_{BP}(m)$ is obtained.

Using the 'de-coupled ' forms of bounce and pitch acceleration in equations (3.9) and (3.10), the CCF value $R_{BP}(m)$ can be decomposed with respect to the relationships from different combinations of track input multiplications, as shown in equation (3.14).

$$R\left(\ddot{z}_b(n),\ddot{\phi}_b(n)\right)=-R\left(g_{11}(n),g_{22}(n)\right)+R\left(g_{12}(n),g_{21}(n)\right)+\left[R\left(g_{11}(n),g_{21}(n)\right)-R\left(g_{12}(n),g_{22}(n)\right)\right] \quad (3.14)$$

where *R(a, b)* denotes a cross correlation operation of *a* and *b*, and $g_{11}(n)$, $g_{12}(n)$, $g_{21}(n)$ and $g_{22}(n)$ represent the time domain representations of the relative terms in equations (3.9) and (3.10).

When a vehicle travels on a track, the track input profiles at the two wheelsets are exactly same and the only difference between them is the time delay which is determined by the vehicle speed and the length between the two wheelsets. g_{11} and g_{22} are the responses to the track inputs $\ddot{z}_{t1}$ and $\ddot{z}_{t2}$ respectively and hence the first term on the right hand side of equation (3.14) should give a peak negative cross correlation at the negative time shift (negative cross correlation is due to '– sign' of the CCF, negative time shift is because the track input $\ddot{z}_{t2}$ is left shifted to track input $\ddot{z}_{t1}$). Similarly, g_{12} and g_{21} are excited by the track inputs $\ddot{z}_{t2}$ and $\ddot{z}_{t1}$ respectively and their cross correlation in the second term on the right hand side of equation (3.14) has a positive peak at the positive time shift. However, the cross correlations at 0s time shift result from the combined effect of (g_{11}, g_{21}) and (g_{12}, g_{22}); g_{11} and g_{21} are caused by the same track input $\ddot{z}_{t1}$, g_{12} and g_{22} are also excited by the same track input but this time the track input $\ddot{z}_{t2}$. In the no fault condition, the two separate cross correlation functions contribute the same cross correlation in magnitude but act oppositely to cancel each other; therefore the third term in the square bracket should give an overall zero correlation at 0s time shift. The cancellation of cross correlation values at 0s time shift is helpful to understand the minimum interaction effect of the suspensions when no fault has occurred.

In the no fault condition, the cross correlations of the bounce and pitch accelerations are expected to be of largest magnitude at the positive and negative time shifts (±*Tshift*), but minimal (or near zero) at 0s time shift. Figure 3.4 illustrates expected

scenarios for the CCF values between the bounce and pitch motions at these specific time shifts.

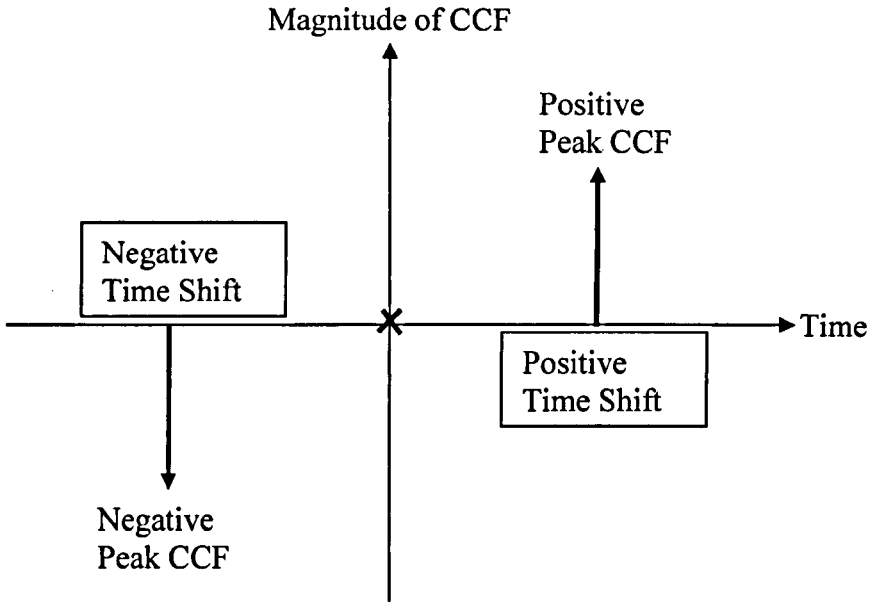

Figure 3.4 Demonstration of cross correlation for bounce and pitch motions

Under the abnormal conditions, where one of the suspension components has failed, the absolute value of cross correlations at the $\pm T_{shift}$ may be reduced due to the increased attenuation on the overall effect of the random track input in a wide range of frequencies as illustrated in Figure 3.2 and Figure 3.3. However, the cross correlations at 0s time shift can be significantly changed (in the positive or negative direction depending on the type and location of the fault) because the asymmetry between the two suspensions removes the balance in the 3rd term of equation (3.14) and hence cancellation is no longer possible.

The detection of suspension faults can therefore be achieved by monitoring cross correlation changes at the three specific time shifts. Figure 3.5 represents the overall scheme of the proposed fault detection and isolation approach using the basic bogie motions in the vertical direction. The scheme also considers the roll motion of a bogie, and therefore involves the cross correlations of any two motions of the bogie.

Similar to the cross correlation between the bounce and pitch motions given in equation (3.13), equations (3.15) and (3.16) give the other two cross correlations between the bounce and roll, and pitch and roll motions respectively.

$$R_{BR}(m) = \sum_{n=1}^{N} \ddot{z}_b(n+m) \cdot \ddot{\psi}_b(n) \tag{3.15}$$

$$R_{PR}(m) = \sum_{n=1}^{N} \ddot{\phi}_b(n+m) \cdot \ddot{\psi}_b(n) \tag{3.16}$$

where the definitions of m and N are as defined in equation (3.13).

To perform the fault detection/isolation, the acceleration signals are assumed to be measured using inertial sensors mounted on the bogie frame [19]. These acceleartions are then processed to derive the changes in the level of interaction by computing their cross correlations, and by taking into account the time shifts between the track inputs. If a suspension component fault occurs, a distinct peak or an obvious change of a peak may be found at the specific time shifts in the cross correlation of any two selected signals. Using the predefined tuned thresholds, it gives the faulty information that corresponds to different suspension changes. The changes in the cross correlations are monitored and the fault is therefore detected. On the other hand, the manner of the cross correlation changes differs with cross correlation computations of different combinations of two motions, depending on the locations of the faults. This property is very useful and makes the fault isolation possible. More details will be presented later in the following chapters.

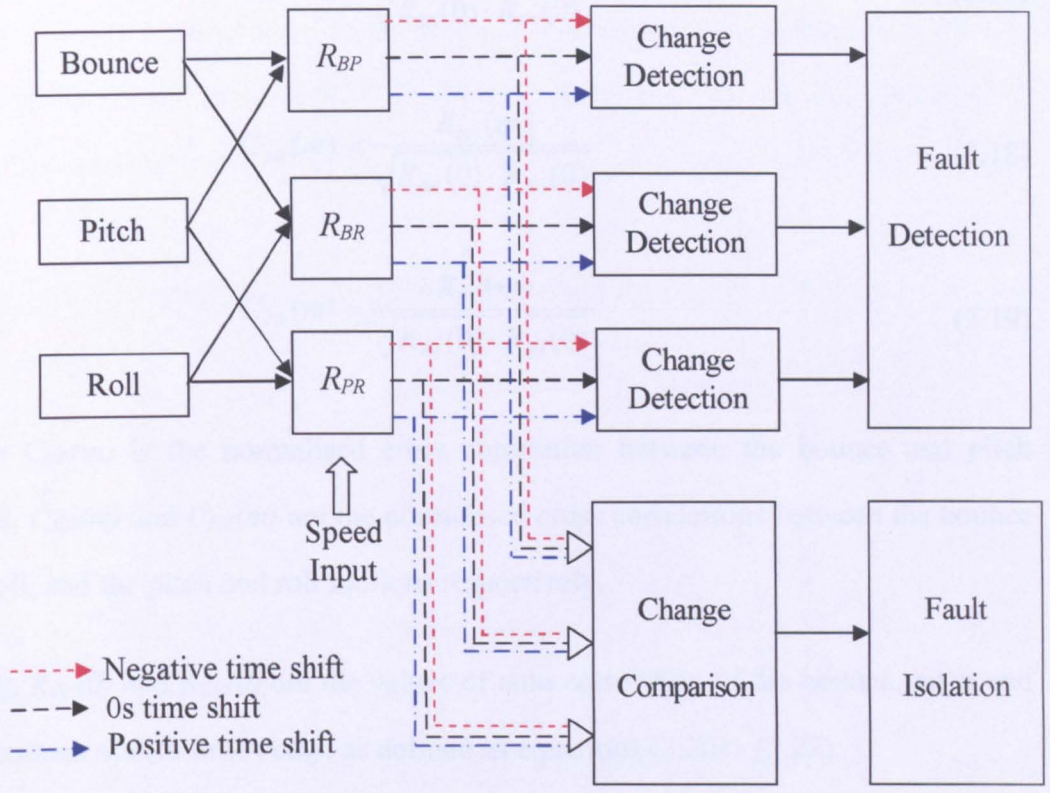

Figure 3.5 Overall fault detection and isolation scheme

The implementation of the proposed cross correlation techniques is straightforward. The measured acceleration signals from the sensors are directly sent to the selected correlator, the measurement of vehicle speed is also used as an additional data input to the computation process to determine the time delay between the two wheelsets. The cross correlation of two signals is computed and the results at the specific time shifts are selected according to the vehicle speed and wheel space. Their cross correlations present the relationships of the two related measured signals, and their changes in magnitude can be used as indicators of the suspension condition changes.

Rather than the use of the cross correlation magnitude, it is also useful to express the cross correlation function in a normalised form, which has a scale of [-1, +1]. Using the basic motions in the vertical direction, the corresponding normalised cross correlations of the studied bogie are defined in equations (3.17) - (3.19).

$$C_{BP}(m) = \frac{R_{BP}(m)}{\sqrt{R_{BB}(0) \cdot R_{PP}(0)}} \tag{3.17}$$

$$C_{BR}(m) = \frac{R_{BR}(m)}{\sqrt{R_{BB}(0) \cdot R_{RR}(0)}} \tag{3.18}$$

$$C_{PR}(m) = \frac{R_{PR}(m)}{\sqrt{R_{PP}(0) \cdot R_{RR}(0)}} \tag{3.19}$$

where $C_{BP}(m)$ is the normalised cross correlation between the bounce and pitch modes, $C_{BR}(m)$ and $C_{PR}(m)$ are the normalised cross correlations between the bounce and roll, and the pitch and roll motions respectively.

$R_{BB}(0)$, $R_{PP}(0)$ and $R_{RR}(0)$ are the values of auto correlation of the bounce, pitch and roll motions at zero time delay, as defined as equations (3.20) - (3.22).

$$R_{BB}(0) = \sum_{n=1}^{N} \ddot{z}_b(n) \cdot \ddot{z}_b(n) \tag{3.20}$$

$$R_{PP}(0) = \sum_{n=1}^{N} \ddot{\phi}_b(n) \cdot \ddot{\phi}_b(n) \tag{3.21}$$

$$R_{RR}(m) = \sum_{n=1}^{N} \ddot{\psi}_b(n) \cdot \ddot{\psi}_b(n) \tag{3.22}$$

The use of the normalised cross correlation offers a clear advantage in improving the detection reliability in changing conditions. As the track input is irregular and not a strictly stationary process in practice, the magnitude of the basic motions of the bogie may be different at different track sections. The cross correlation computations will therefore have certain unevenness even when the other operational conditions are unchanged. More significantly, the level of vibration on the bogie is highly dependent upon the travelling speed of the vehicle even when the track conditions remain the same. The fault detection would have to use fault thresholds that are tuned to speed as well as track conditions which can be very difficult in practice.

Those uncertainties are readily removed by using normalised cross correlation (CCF coefficient). As these CCF coefficients are generated from the CCF values by normalising the cross-spectrum with the auto-spectrums, they are therefore much less affected by changes in operational conditions. Due to the normalisation of the CCF coefficient technique, the detection accuracy can be well improved, in the aspects of either due to a vehicle travelling at different speeds and/or the difference of rail track geometries.

3.4 Pre-filtering

Last section has illustrated the possibility to use correlation evaluation in detecting suspension component faults. It is also studied from Figures 3.1 - 3.3 that the frequency responses of the studied bogie mode have the largest magnitudes near their natural frequencies. As the track irregularity used in this thesis has limited frequency distribution around up to 80Hz, the performance of the correlation evaluation will be easily affected by the resonance caused by the largest frequency responses near the natural frequencies. This effect will be occurred in both the normal and fault conditions, particularly in the fault condition where the resonance becomes increased due to the reduced damping by the damper failures, which could cause the associated oscillations in the cross correlation results and result in difficulties in detecting changes at the specific time shifts.

To remove the problem, the measurement signals should be filtered before the cross correlation computation is implemented. Band-stop filters are selected to remove the frequency contents near the resonance [7] [61].

As shown in Figure 3.6, the measured accelerations are fed to a band-stop filter, which is designed to suppress the content near the bogie natural frequencies. After filtering, the required magnitude of the signals consisting of other frequency contents can be obtained for the correlation evaluation.

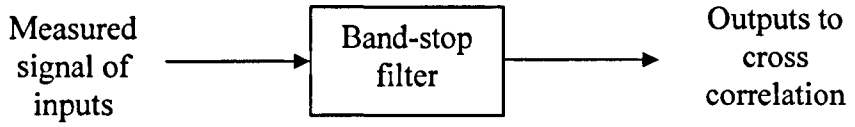

Figure 3.6 Band-stop filter mode for the acceleration measurements

The band-stop filter is designed as a second order filter which can effectively reduce the magnitude within its bandwidth at twice the rate of the basic first order filter, i.e. 40 dB per decade, as expressed in equation (3.23).

$$H(s) = \frac{s^2 + 2\eta\zeta\omega_n s + \omega_n^2}{s^2 + 2\zeta\omega_n s + \omega_n^2}, k < 1 \tag{3.23}$$

where ω_n is the notch frequency where the maximum attenuated frequency is located, and ζ is the damping of the band-stop filter. By tuning the parameter η, a suitable band-stop filter for the conventional bogie system is selected and equalised in (3.24).

$$H(s) = \frac{s^2 + 4.664s + 4352}{s^2 + 93.29s + 4352} \tag{3.24}$$

The bode diagram of the selected band-stop filter is shown in Figure 3.7, where the low cut-off frequency is set at 7Hz, and the high one is 20Hz.

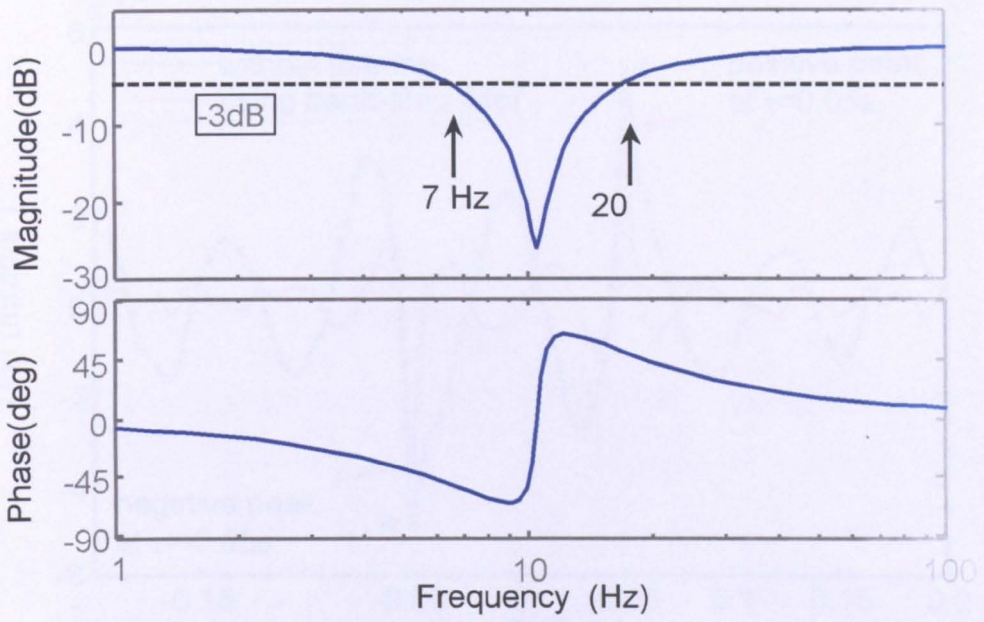

Figure 3.7 Bode diagram of the selected band-stop filter

To compare the difference of the cross correlation evaluation between the signals without filtering and those using band-stop filters before their calculations, the CCF values and coefficients between the bounce and pitch accelerations are computed. This example is illustrated in the no fault condition and at the vehicle speed of 50m/s, their simulation results are shown in Figure 3.8 and Figure 3.9, respectively. From both Figure 3.8 and Figure 3.9, it is noticed that a sinusoidal component exists in either the CCF value or coefficient computation when the band-stop filters are not applied, which is mainly caused by the resonances near the bogie natural frequencies as expected. However, the resonance of their corresponding CCF value or coefficient is largely removed in the band-stop filter mode, which makes the interested peak values more distinctively and easily identified.

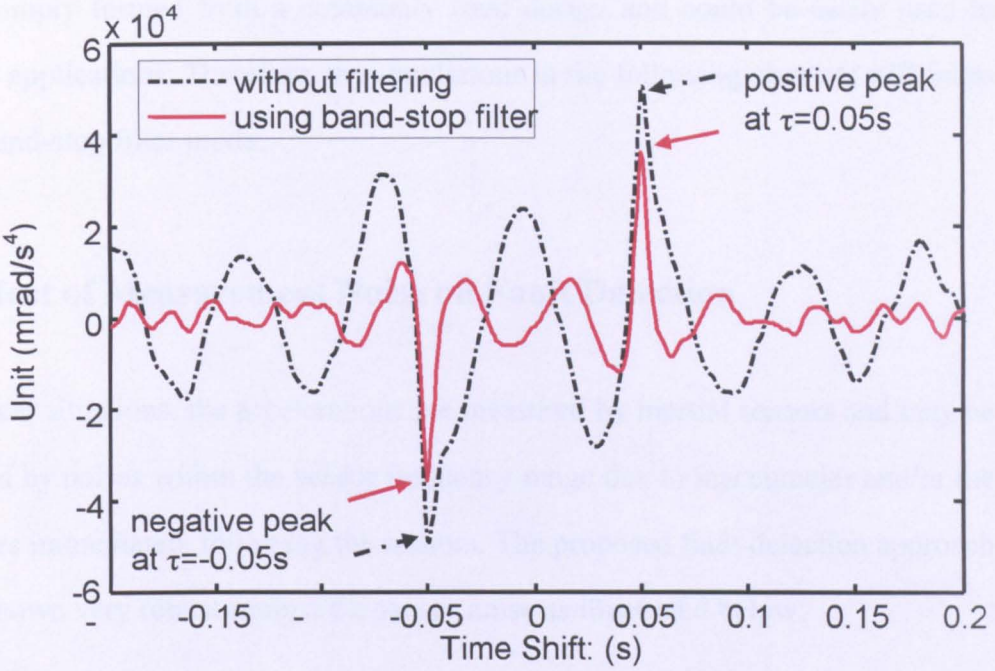

Figure 3.8 CCF value for bounce and pitch accelerations (without and with Band-stop filter, Vs=50m/s)

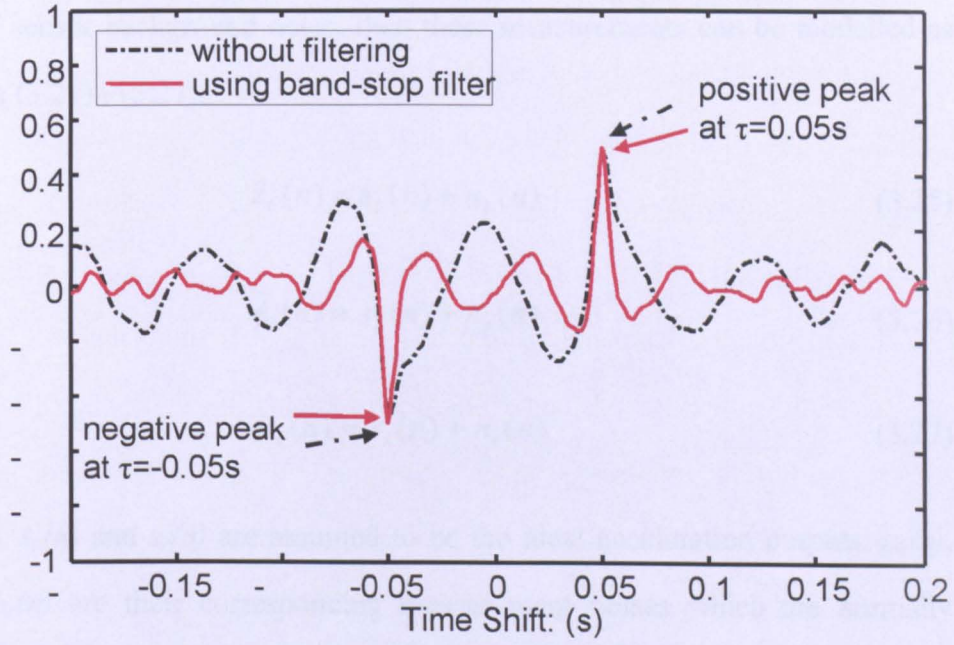

Figure 3.9 CCF coefficient for bounce and pitch accelerations (without and with Band-stop filter, Vs=50m/s)

The band-stop filtering mode is beneficial to deal with the resonant fluctuations during the correlation evaluations and give consistent clarified correlation results, hence the sensitivity of the fault detection can be improved. Furthermore, the filter

can be simply formed from a commonly used design and could be easily used in practical applications. Therefore, the simulations in the following chapters will focus on the band-stop filter mode.

3.5 Effect of Measurement Noise on Fault Detection

In practical situations, the accelerations are measured by inertial sensors and may be corrupted by noises within the sensor frequency range due to inaccuracies and/or the amplifiers immediately following the sensors. The proposed fault detection approach can be shown very robust against the sensor noise as illustrated below.

3.5.1 Noise Effect on Cross Correlation Magnitude

If it is assumed that the bounce, pitch and roll accelerations are measured in the presence of sensor background noise, then these measurements can be modelled as in equations (3.25) - (3.27).

$$\ddot{z}_b(n) = s_b(n) + n_b(n) \tag{3.25}$$

$$\ddot{\phi}_b(n) = s_p(n) + n_p(n) \tag{3.26}$$

$$\ddot{\psi}_b(n) = s_r(n) + n_r(n) \tag{3.27}$$

where $s_b(n)$, $s_p(n)$ and $s_r(n)$ are assumed to be the ideal acceleration outputs. $n_b(n)$, $n_p(n)$ and $n_r(n)$ are their corresponding measurement noises which are normally uncorrelated with each other and with the ideal acceleration signals, as expressed in equations (3.28) and (3.29).

$$R_{n_b n_p}(m) = R_{n_b n_r}(m) = R_{n_p n_r}(m) \approx 0 \tag{3.28}$$

$$R_{s_b n_b}(m) = R_{s_b n_p}(m) = R_{s_b n_r}(m) = R_{s_p n_b}(m) = R_{s_p n_p}(m) = R_{s_p n_r}(m)$$
$$= R_{s_r n_b}(m) = R_{s_r n_p}(m) = R_{s_r n_r}(m) \approx 0 \tag{3.29}$$

Hence the effects of the uncorrelated sensor noise can be neglected from the correlations between the measured accelerations. Equations (3.30) - (3.32) present the approximation of the cross correlations of the measurements with and without noise.

$$R_{BP}(m) \approx R_{s_b s_p}(m) \tag{3.30}$$

$$R_{BR}(m) \approx R_{s_b s_r}(m) \tag{3.31}$$

$$R_{PR}(m) \approx R_{s_p s_r}(m) \tag{3.32}$$

3.5.2 Noise Effect on Normalised Cross Correlation

The effect of the measurement noise cannot be directly removed for the CCF coefficient computation, because the normalisation involves auto correlation processing between the noise signals which will result in non-zero auto-correlated values at 0s time shift. To illustrate this, equations (3.33) shows the relationship of the normalised cross correlations between the bounce and pitch motions with measurement noise.

$$C_{BP}(m) = \frac{R_{BP}(m)}{\sqrt{R_{BB}(0) \cdot R_{PP}(0)}}$$
$$= \frac{R_{s_b s_p}(m) + R_{s_b n_p}(m) + R_{n_b s_p}(m) + R_{n_b n_p}(m)}{\sqrt{[R_{s_b s_b}(0) + R_{s_b n_b}(0) + R_{n_b s_b}(0) + R_{n_b n_b}(0)] \cdot [R_{s_p s_p}(0) + R_{s_p n_p}(0) + R_{n_p s_p}(0) + R_{n_p n_p}(0)]}} \tag{3.33}$$

As given in equations (3.28) and (3.29), the correlation of the noise signal with each other and with the ideal acceleration signals tend to zero, $C_{BP}(m)$ can be written as

$$C_{BP}(m)=\frac{R_{s_b s_p}(m)}{\sqrt{[R_{s_b s_b}(0)+R_{n_b n_b}(0)]\cdot[R_{s_p s_p}(0)+R_{n_p n_p}(0)]}} \tag{3.34}$$

To compare with its normalised cross correlation without measurement noise, the theoretical normalised cross correlation prediction between the bounce and pitch motions $C_{sbsp}(m)$ is defined in equation (3.35).

$$C_{s_b s_p}(m)=\frac{R_{s_b s_p}(m)}{\sqrt{R_{s_b s_b}(0)\cdot R_{s_p s_p}(0)}} \tag{3.35}$$

Dividing $\sqrt{R_{s_b s_b}(0)\cdot R_{s_p s_p}(0)}$ in the numerator and denominator of the right term of equation (3.34), and substituting equation (3.35) into equation (3.34), $C_{BP}(m)$ is given in equation (3.36) in the form of

$$C_{BP}(m)=\frac{C_{s_b s_p}(m)}{\sqrt{[1+\frac{R_{n_b n_b}(0)}{R_{s_b s_b}(0)}]\cdot[1+\frac{R_{n_p n_p}(0)}{R_{s_p s_p}(0)}]}} \tag{3.36}$$

Let

$$\begin{cases}\sigma_{s_b}^2 = R_{s_b s_b}(0)\\ \sigma_{s_p}^2 = R_{s_p s_p}(0)\\ \sigma_{n_b}^2 = R_{n_b n_b}(0)\\ \sigma_{n_p}^2 = R_{n_p n_p}(0)\end{cases} \tag{3.37}$$

where $\sigma_{s_b}^2$, $\sigma_{s_p}^2$, $\sigma_{n_b}^2$ and $\sigma_{n_p}^2$ are the variances for the ideal bounce and pitch accelerations, and their corresponding sensor noise signals respectively.

Substituting equation (3.37) into equation (3.36), it gives equation (3.38)

$$C_{BP}(m) = \frac{C_{s_b s_p}(m)}{\sqrt{(1+\frac{\sigma_{n_b}^2}{\sigma_{s_b}^2}) \cdot (1+\frac{\sigma_{n_p}^2}{\sigma_{s_p}^2})}} \tag{3.38}$$

It is noticed although the CCF coefficient may be affected by the noise to signal ratio (NSR), for the railway acceleration measurements which have relatively small (typically 1~2%) sensor noises, the noise effect on the normalised cross correlation is very trivial. For instance, the CCF coefficient only reduces 0.01% for NSR at 1%, and decreases less than 0.07% for a NSR at 2.5%. Thus a similar relationship for the normalised cross correlation (CCF coefficient) can also be expressed in equations (3.39) - (3.41).

$$C_{BP}(m) \approx C_{s_b s_p}(m) \tag{3.39}$$

$$C_{BR}(m) \approx C_{s_b s_r}(m) \tag{3.40}$$

$$C_{PR}(m) \approx C_{s_p s_r}(m) \tag{3.41}$$

It is therefore clear that the sensor noises from the measurements have little effect on the overall correlation results, this will be further verified in chapter 4 using both the normal and fault conditions.

3.6 Running Detection Scheme

For an on-line detection, a running cross correlation calculation is more useful. The running detection can be achieved by selecting an appropriate fixed moving time window T, where a constant amount of acceleration measurements within the period of the latest time window are stored and used for cross correlation calculations. Given a chosen sampling rate Δt, the acceleration signals for the cross correlation evaluation are measured and updated at each sampling.

Equation (3.42) - (3.44) give the expressions of the running CCF coefficients between the bounce and pitch, the bounce and roll, and the pitch and roll motions respectively.

$$f_{BP}(k\cdot\Delta t,m)=\frac{\sum_{n=1}^{N}\ddot{z}_b(n+m+k\cdot\Delta t)\cdot\ddot{\phi}_b(n+k\cdot\Delta t)}{\sqrt{\sum_{n=1}^{N}\ddot{z}_b^2(n+k\cdot\Delta t)\cdot\sum_{n=1}^{N}\ddot{\phi}_b^2(n+k\cdot\Delta t)}} \tag{3.42}$$

$$f_{BR}(k\cdot\Delta t,m)=\frac{\sum_{n=1}^{N}\ddot{z}_b(n+m+k\cdot\Delta t)\cdot\ddot{\psi}_b(n+k\cdot\Delta t)}{\sqrt{\sum_{n=1}^{N}\ddot{z}_b^2(n+k\cdot\Delta t)\cdot\sum_{n=1}^{N}\ddot{\psi}_b^2(n+k\cdot\Delta t)}} \tag{3.43}$$

$$f_{PR}(k\cdot\Delta t,m)=\frac{\sum_{n=1}^{N}\ddot{\phi}_b(n+m+k\cdot\Delta t)\cdot\ddot{\psi}_b(n+k\cdot\Delta t)}{\sqrt{\sum_{n=1}^{N}\ddot{\phi}_b^2(n+k\cdot\Delta t)\cdot\sum_{n=1}^{N}\ddot{\psi}_b^2(n+k\cdot\Delta t)}} \tag{3.44}$$

with

$$k = 0, 1, 2, \cdots, \frac{T_{total}}{\Delta t} - 1$$

where $f_{BP}(k\cdot\Delta t,m)$, $f_{BR}(k\cdot\Delta t,m)$ and $f_{PR}(k\cdot\Delta t,m)$ denote the running CCF coefficients of the $k\cdot\Delta t$ time instance at time shift m, between the bounce and pitch, the bounce and roll, and the pitch and roll motions respectively. k represents the samples, and T_{total} is the total processing time for the fault detection.

For each new computation step, equations (3.42) - (3.44) are repeated and only one newest sampled data is added and therefore the buffer for data storage will be updated at every step. Assuming the bogie accelerations begin to change due to a component failure, their relevant CCF coefficient computation will also start to vary. As time passes, more and more acceleration measurements under the fault conditions

are acquired and buffered in their time windows, and consequently their CCF coefficient levels gradually deviate from fault-free positions to the new steady values till the buffers are fully filled with acceleration signals under the fault conditions. The duration of their cross correlation changes lasts approximately the same time as the selected time window. Figure 3.10 shows the diagram of the running detection scheme.

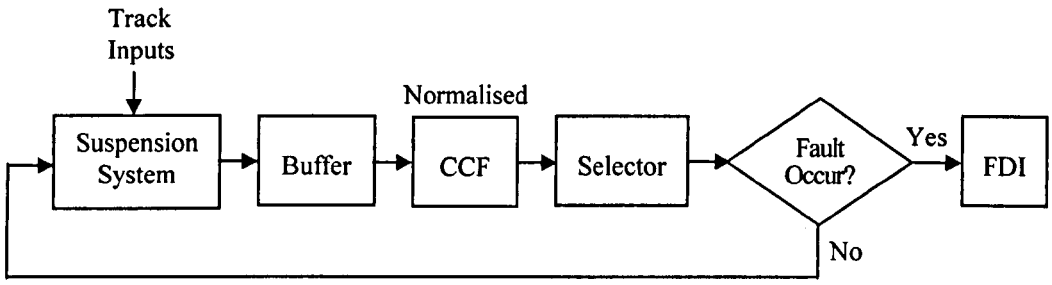

Figure 3.10 Running detection scheme

In the running detection scheme, the selection of the size of the time window is a trade-off between the speed and reliability of the fault detection. If the length of the time window is short, the detection is quick but cross correlation is more likely to be affected by other changes or uncertainties in the system, which may cause a false alarm. On the other hand, a long time window increases the reliability of the fault detection, at the cost of slow detection speed. A moving time window of 2 seconds has been found in this study to give a satisfactory compromise between false alarm probability and detection speed, although this may change in practice for different vehicles and/or operating conditions.

3.7 Summary

From the analysis of a simple railway bogie model with symmetrical components used in the suspensions, it was obvious that there is a close link between the

interaction change and the suspension component imbalance. This link was exploited in order to develop a new and effective fault detection scheme using cross correlation evaluation, which is expected to be sensitive in detecting suspension faults directly from its acceleration measurements, as it will be shown in the performance assessments. The tuning of the scheme and noise effect on the cross correlation computation were analysed. The feasibility for fault isolation by comparing cross correlations between different bogie motions was also described and more detail will be provided in the following chapter. Additionally, the on-line detection scheme processed with a running time window has been briefly introduced.

Chapter 4

Simulation Results and Assessments

4.1 Introduction

The previous chapter presents the development of a novel fault detection and isolation scheme which exploits the relationship between component fault(s) and changes in dynamic interactions in the primary suspension. This chapter will study the performance of this novel approach in detail. Assessments are carried out using simulation results using the model involving the bounce, pitch and roll motions of a conventional vehicle as illustrated in Figure 2.6 in the MATLAB/Simulink software environment.

4.2 Results from Direct Simulated Data

As shown in Figure 2.6, there are four primary suspensions on each bogie, identified as front left and front right at either side of the leading wheelset and rear left and rear right at either side of the trailing wheelset. Simulation results from the leading bogie of the vehicle model are used in the assessment. Similar performance of the fault detection and isolation for the trailing bogie is expected. The focus is on the primary suspension and the coupling effect of the secondary suspensions is relatively small.

It is possible to use direct measurement of the bogie acceleration and typically use of the RMS value to monitor the suspension performance, but as stated before the sensitivity and robustness to the fault conditions are not expected to be as good as the proposed method. In this section, the RMS values of the bounce acceleration of the leading bogie in normal and with its front left damper at 50% failure are given

performance comparison, as case 4.1 shown in Figure 4.1 and Figure 4.2. Unless otherwise specified, this chapter will use the same front left damper fault.

Case 4.1: front left damper has 50% damping loss, vehicle speed at 50m/s.

Computations: bounce acceleration measurement and running RMS (2s of data)

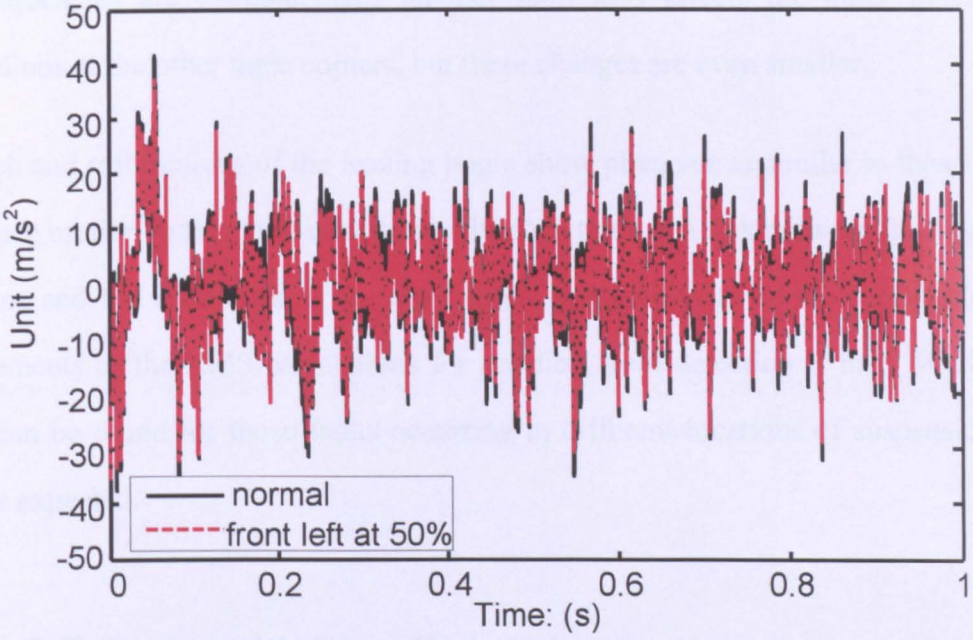

Figure 4.1 Bounce acceleration for case 4.1

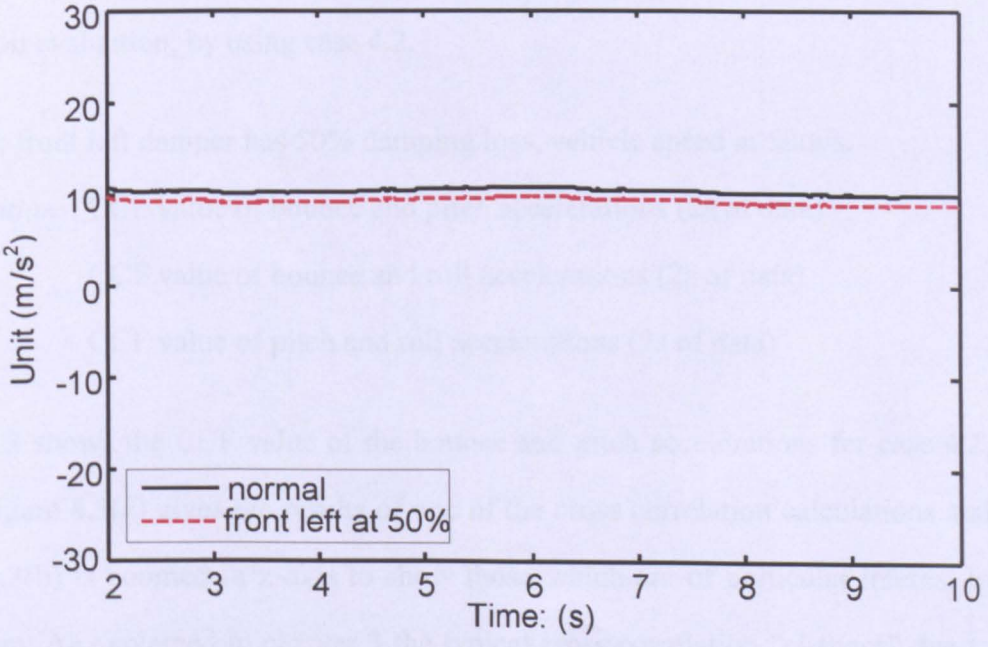

Figure 4.2 Running RMS of bounce acceleration for case 4.1

It is observed the difference between the normal and fault conditions is small. In both Figure 4.1 and Figure 4.2, the overall acceleration of the leading bogie is only slightly reduced, as although the damper fault reduces the damping of the bogie mode and increases the resonance near the natural frequency, the responses at wider high frequencies are lowered. This damper fault also affects the other bounce accelerations at the other three corners, but these changes are even smaller.

The pitch and roll motions of the leading bogie show phenomena similar to those of the bounce motion in this fault condition. Although there is a link between the bogie vibrations and the conditions of the suspension, the sensitivity of the acceleration measurements or the RMS calculations for practical fault detection is low. Similar results can be found for those faults occurring in different locations of suspension, which is expected.

4.3 Fault Detection with Cross Correlation

Clear improvements may be achieved via the proposed approach using cross correlation evaluation, by using case 4.2.

Case 4.2: front left damper has 50% damping loss, vehicle speed at 50m/s.

Computations: CCF value of bounce and pitch accelerations (2s of data)

CCF value of bounce and roll accelerations (2s of data)

CCF value of pitch and roll accelerations (2s of data)

Figure 4.3 shows the CCF value of the bounce and pitch accelerations for case 4.2, where Figure 4.3(a) gives the results of one of the cross correlation calculations and Figure 4.3(b) is zoomed in x-axis to show those which are of particular interest to the system. As explained in chapter 3 the typical cross correlation "changes" due to component fault occur at the points of the specific time shifts 0 and $\pm T$ seconds and

this case $T = 2L_{bx}/V_s = 0.05s$ for the semi-wheel space of 1.25m and the railway vehicle travelling at a speed of 50m/s. Under the normal conditions, the two peaks at ±0.05s time shifts in Figure 4.2 indicate that the correlation between the bounce and pitch motions is mainly caused by the inputs to the two wheelsets (same input with a time shift of 0.05s and on both left and right track sides). The negative peak at -0.05s time shift is due to there is a negative sign for the correlation between the front and the rear track inputs to the bounce and pitch motions respectively, and the positive peak at +0.05s time shift is due to the rear track inputs to bounce motion being positively correlated with the front track inputs to pitch motion. However the two peaks at ±0.05s time shifts are similar in magnitude, because under the no fault condition the corresponding suspension components have the same parameters and their track inputs are also the same except for the time delay. At 0s time shift, their correlation is minimal (near to zero) because of the cross correlation cancellation between the front and rear parts of the suspensions, as explained in the development of the FDI technique in the previous chapter.

Those are changed as a result of a damper fault, which leads to reduced levels of correlation at ±0.05s time shifts and a negative spike at 0s time shift. The reduction in correlation at ±0.05s time shifts is mostly due to the reduced damping which results in an overall decrease in bounce and pitch responses. The spike at 0s time shift is due to the imbalance between suspensions at the leading and trailing wheelsets, as the effect of inputs at the leading side can no longer cancel out those at the trailing side. As it can be seen from equation (3.14), this cross correlation under the fault condition of case 4.2 will give a negative sign, because the front left damper failure gives rise to a decreased correlation in the positive direction. The sign of the spike at 0s time shift is therefore dependent on the different damper fault conditions, and its correlation change appears to be far more sensitive than those at ±0.05s time shifts, consequently it can potentially provide a more useful indicator of the faults [63].

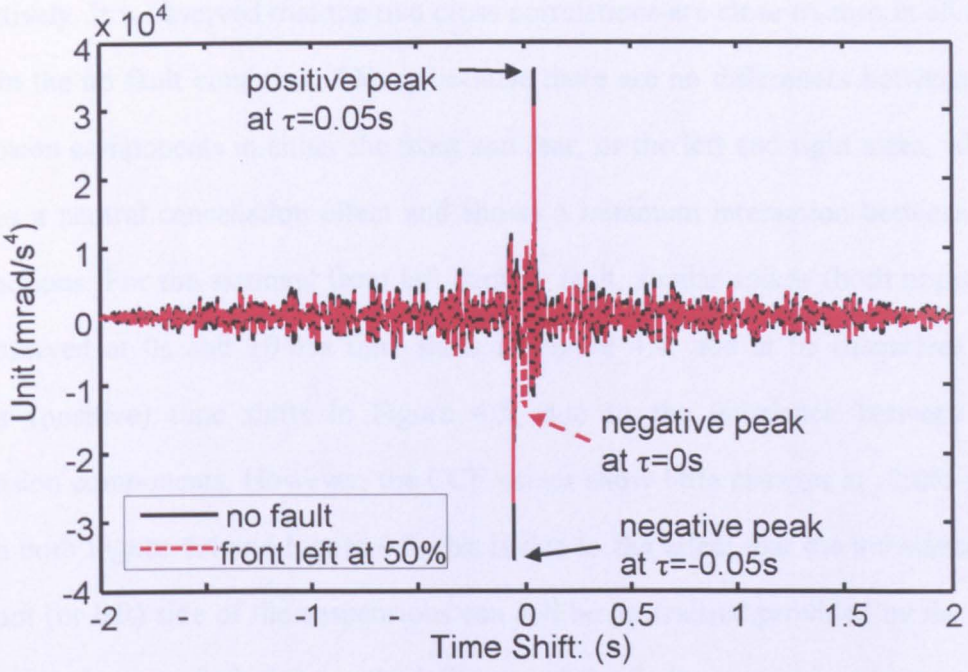

(a) Detailed CCF value for all time delay in [-2s, 2s]

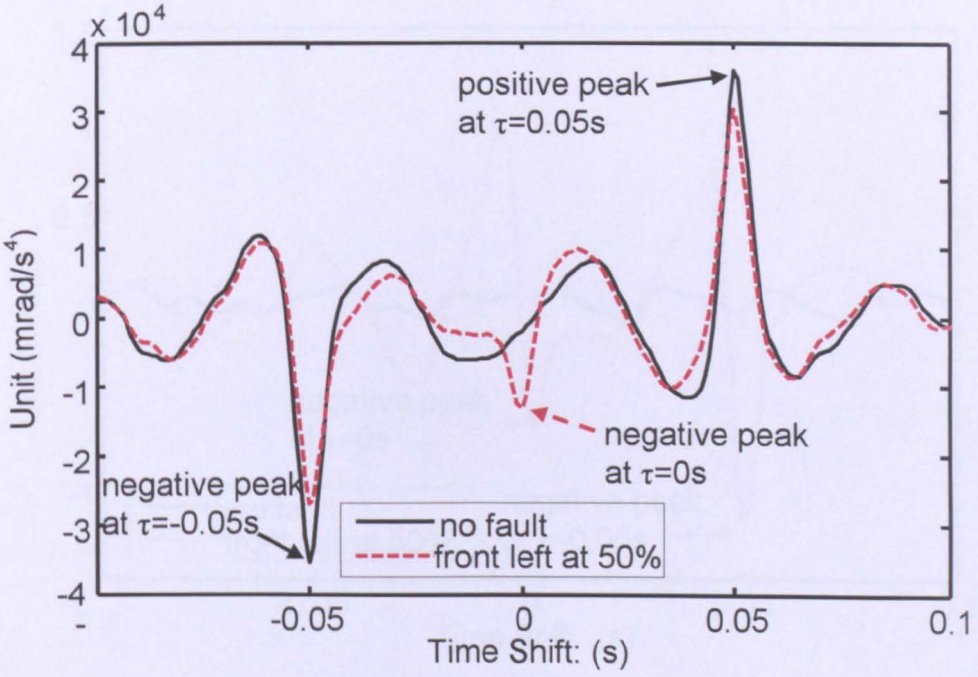

(b) Close-up CCF value from Figure 4.3(a)

Figure 4.3 CCF value of bounce and pitch accelerations for case 4.2

The CCF values in the same fault condition are also processed from the bounce and roll motions, and the pitch and roll motions as shown in Figures 4.4 and Figure 4.5

respectively. It is observed that the two cross correlations are close to zero in all time shifts in the no fault condition. This is because there are no differences between the suspension components in either the front and rear, or the left and right sides, which denotes a neutral cancellation effect and shows a minimum interaction between the two motions. For the assumed front left damper fault, similar spikes (both negative) are observed at 0s and +0.05s time shifts in Figure 4.4, and at 0s (negative) and +0.05s (positive) time shifts in Figure 4.5, due to the imbalance between the suspension components. However, the CCF values show little changes at -0.05s time shift in both Figure 4.4 and Figure 4.5, this is due to the effect that the imbalance on the front (or left) side of the suspensions can still be neutralised provided by the rear side suspensions are fault-free, as the influence of the faulty suspensions is cancelled processed mutually with symmetric suspension parameters on the rear side.

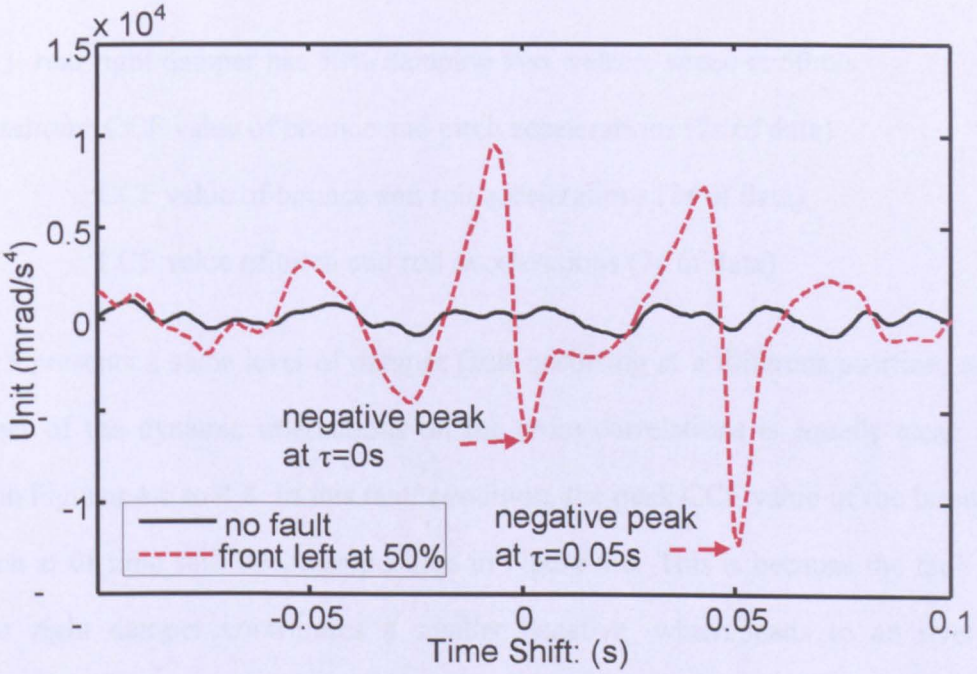

Figure 4.4 CCF value of bounce and roll accelerations for case 4.2

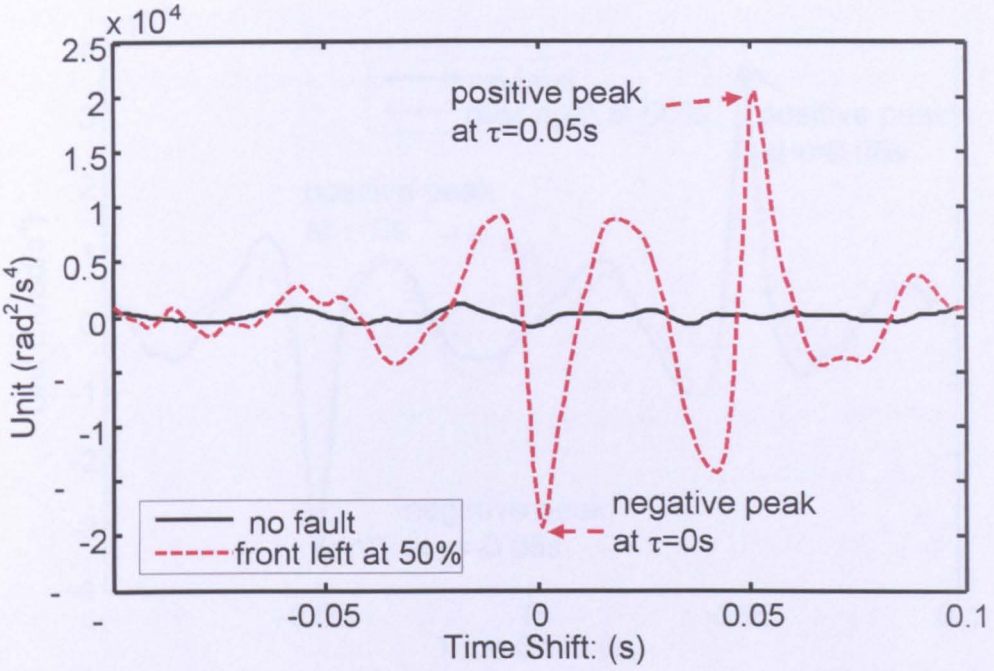

Figure 4.5 CCF value of pitch and roll accelerations for case 4.2

Case 4.3: rear right damper has 50% damping loss, vehicle speed at 50m/s.

Computations: CCF value of bounce and pitch accelerations (2s of data)

CCF value of bounce and roll accelerations (2s of data)

CCF value of pitch and roll accelerations (2s of data)

Case 4.3 presents a same level of damper fault occurring at a different position, and the effect of the dynamic interactions on the cross-correlations is equally clear, as shown in Figures 4.6 to 4.8. In this fault condition, the peak CCF value of the bounce and pitch at 0s time shift becomes positive in Figure 4.6. This is because the fault in the rear right damper contributes a smaller negative, which leads to an overall positive correlated peak. In Figure 4.7, the bounce and roll CCF also results in positive peaks at 0s and -0.05s (rather than negative peaks at 0s and +0.05s time shifts as in case 2) time shifts. For the CCF value between pitch and roll motion in Figure 4.8, their correlation changes occur at 0s and -0.05s time shifts, but it gives a negative peak at 0s time shift compared with a positive value (also at 0s time shift) previously shown in Figure 4.7.

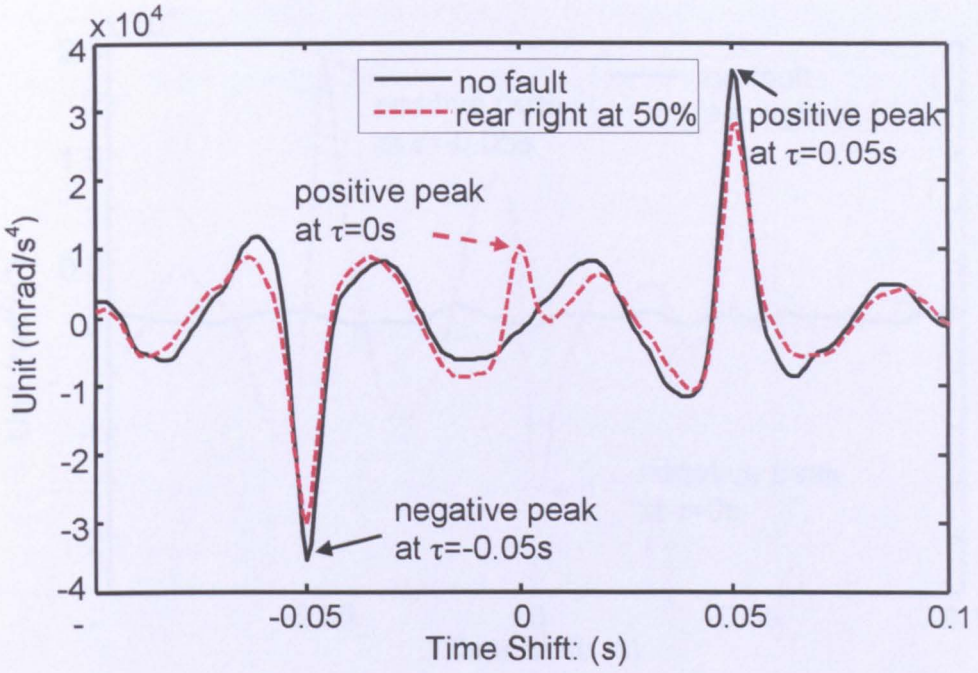

Figure 4.6 CCF value of bounce and pitch accelerations for case 4.3

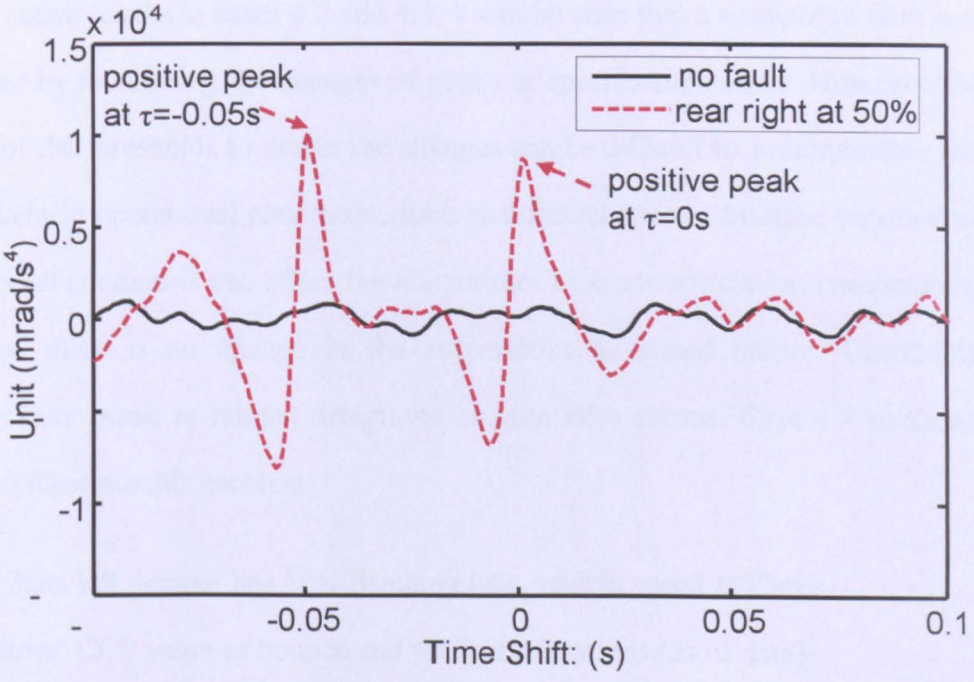

Figure 4.7 CCF value of bounce and roll accelerations for case 4.3

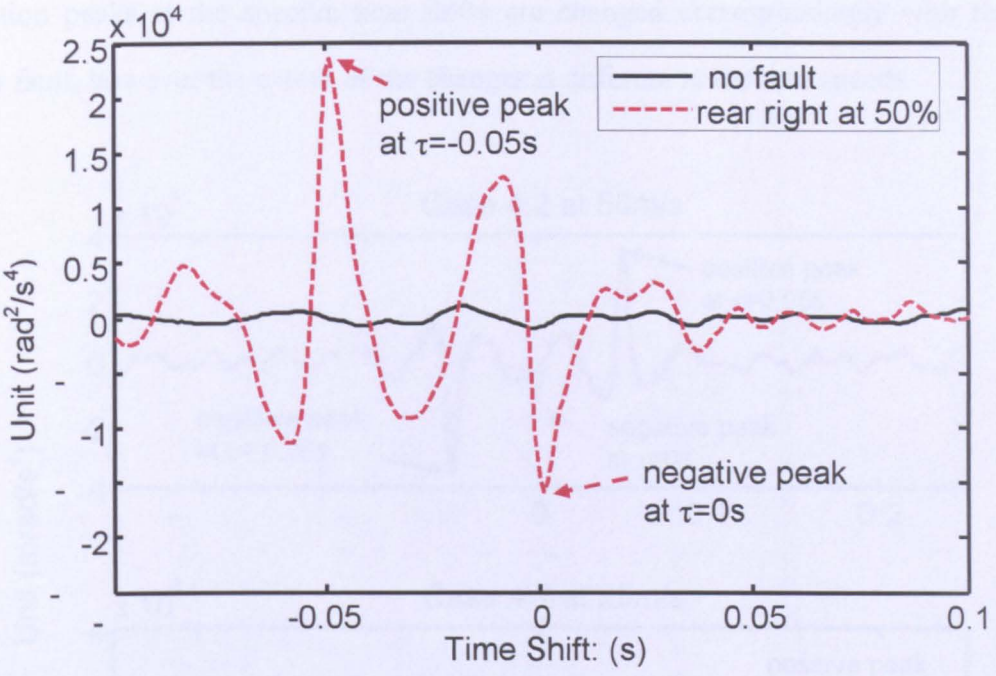

Figure 4.8 CCF value of pitch and roll accelerations for case 4.3

From the above results in cases 4.2 and 4.3, it can be seen that a suspension fault can be detected by monitoring the changes of peaks at specific time shifts. However the selection of the thresholds to detect the changes can be difficult to accommodate for different vehicle operational conditions, such as different speeds, because variance of these external conditions can affect the magnitudes of cross correlation computation even when there is no change in the suspensions as stated before. Unsuitable thresholds may result in missed detections or give false alarms. Case 4.4 gives an example to illustrate this problem.

Case 4.4: front left damper has 50% damping loss, vehicle speed at 25m/s.

Computations: CCF value of bounce and pitch accelerations (2s of data)

Figure 4.9 compares cross correlations of the bounce and pitch motions of the same condition as in case 4.2, but at two different speeds of (a) 50m/s and (b) 25m/s. It is clear that the peaks of the cross correlations under the normal condition at ±0.05s time shifts at high sped (50m/s) are much higher than those at ±0.10s at low speed (double time shifts due to the vehicle speed being halved to 25m/s). All the cross

correlation peaks at the specific time shifts are changed correspondingly with the damper fault, however the extent of the changes is different at the two speeds.

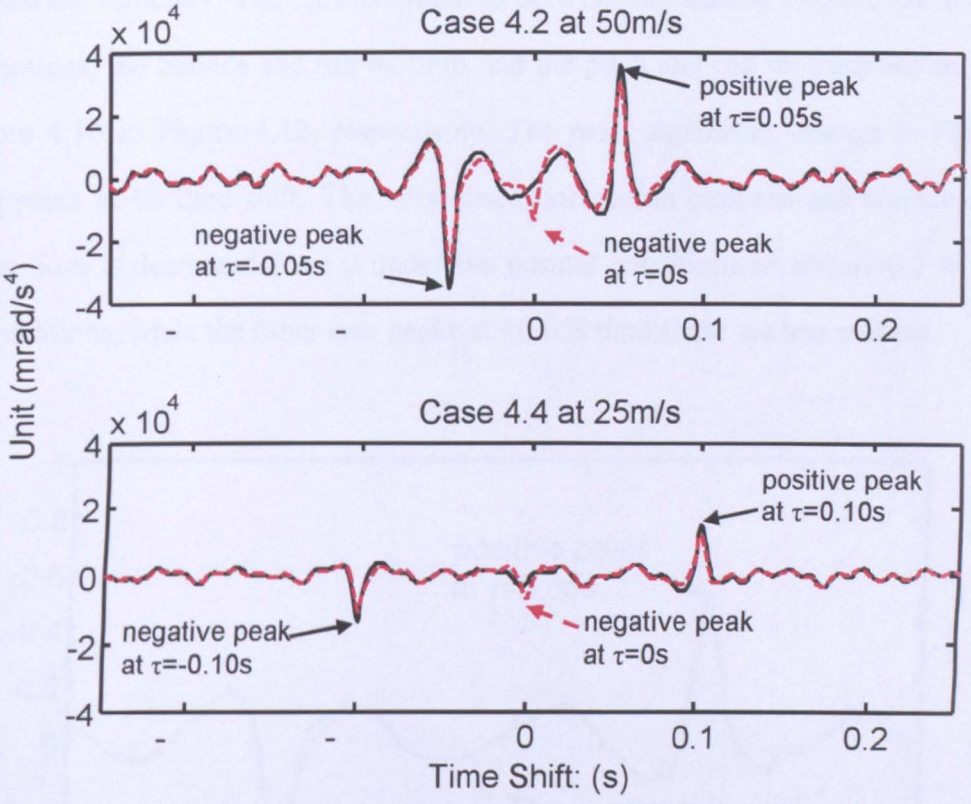

Figure 4.9 CCF value of bounce and pitch accelerations for cases 4.2 & 4.4

It is clear that the cross correlation changes at the special time shifts can provide an essential monitoring of the suspension health conditions, and different damper faults may have different change patterns, which are useful in determining the fault location. However the use of CCF value has the limitation that the detection would have to be tuned to different train operational conditions and/or different track inputs [43].

4.4 FDI with Normalised Cross Correlation

Case 4.5: front left damper has 50% damping loss, vehicle speed at 50m/s.

Computations: CCF coefficient of bounce and pitch accelerations (2s of data)

CCF coefficient of bounce and roll accelerations (2s of data)

CCF coefficient of pitch and roll accelerations (2s of data)

The use of the normalised cross correlation technique is therefore proposed to overcome the difficulty. The CCF coefficients between the leading bogie bounce and pitch motions, the bounce and roll motions and the pitch and roll motions are shown in Figure 4.10 to Figure 4.12, respectively. The most significant change in Figure 4.10 appears at 0s time shift. The normalised correlation between the bounce and pitch motions is decreased from 0 under the normal conditions to about -0.2 in the fault conditions, while the other two peaks at ±0.05s time shifts are less evident.

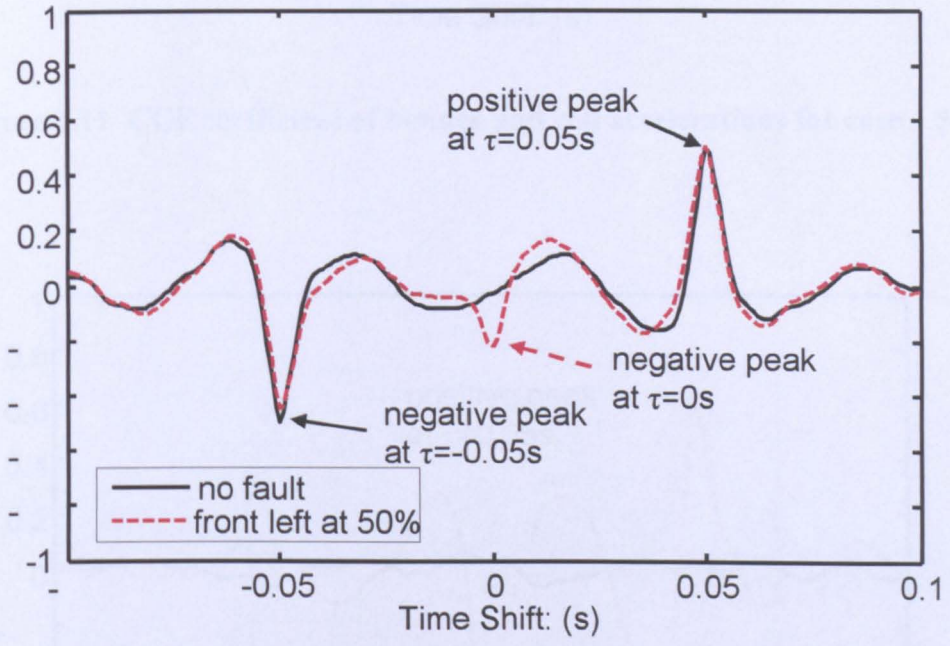

Figure 4.10 CCF coefficient of bounce and pitch accelerations for case 4.5

For the CCF coefficients between the bounce and roll motions in Figure 4.11, the most sensitive correlation change to the fault is at +0.05s time shift where a decrease from around 0 to -0.4 is observed. The changes to the CCF coefficients of the pitch and roll motions also occur at +0.05s time shift, but it increases from around 0 to +0.5 in the positive direction as shown in Figure 4.12.

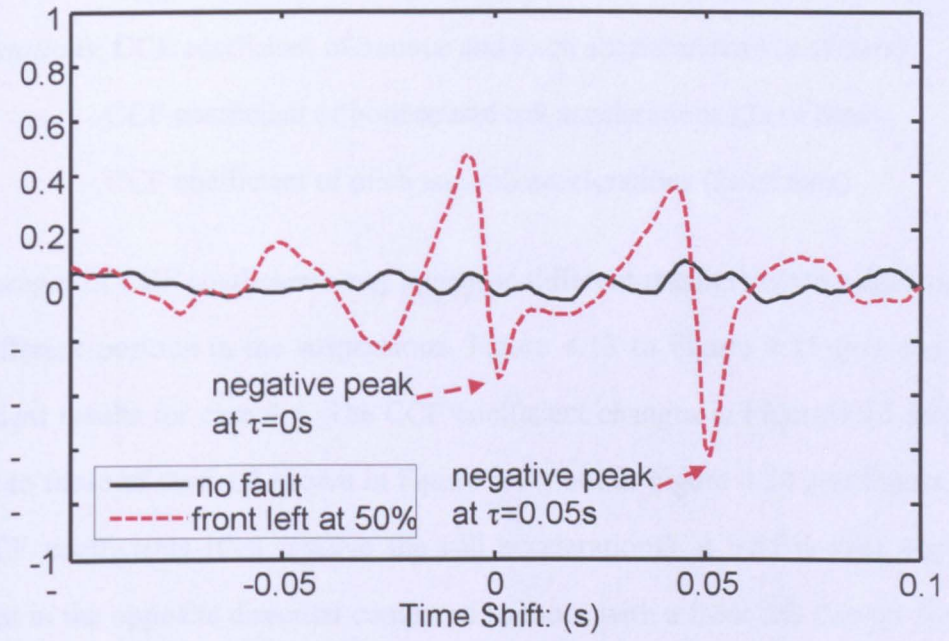

Figure 4.11 CCF coefficient of bounce and roll accelerations for case 4.5

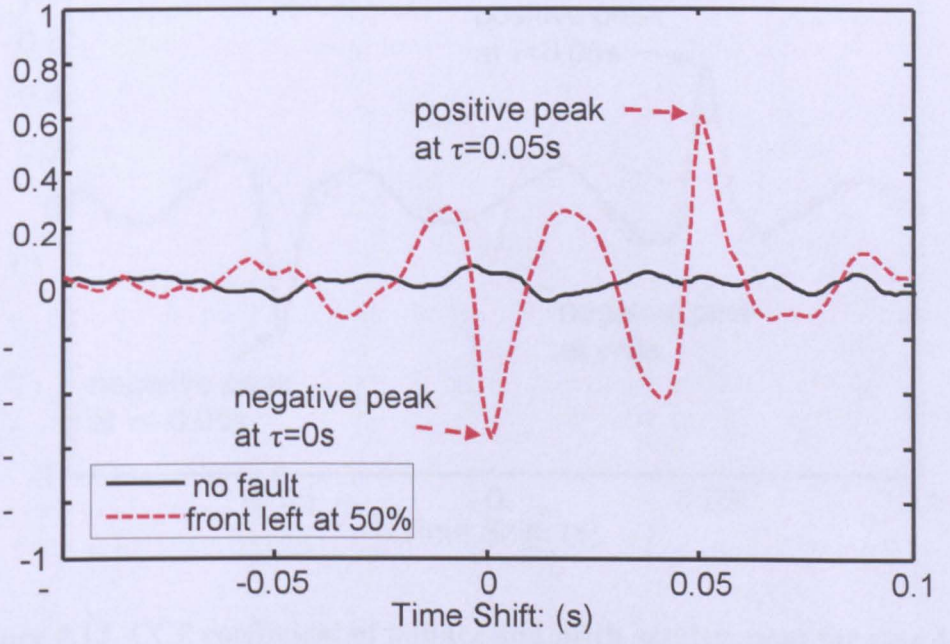

Figure 4.12 CCF coefficient of pitch and roll accelerations for case 4.5

In both Figure 4.11 and Figure 4.12, there are additional CCF coefficient reductions at 0s time shift but relatively small compared with those at +0.05s time shift.

Case 4.6: front right damper has 50% damping loss, vehicle speed at 50m/s.

Computations: CCF coefficient of bounce and pitch accelerations (2s of data)

CCF coefficient of bounce and roll accelerations (2s of data)

CCF coefficient of pitch and roll accelerations (2s of data)

The changes of CCF coefficients may appear in different manners when a fault occurs at a different position in the suspensions. Figure 4.13 to Figure 4.15 give the CCF coefficient results for case 4.6. The CCF coefficient changes in Figure 4.13 are very similar to those of case 4.5 shown in Figure 4.10, but in Figure 4.14 and Figure 4.15 the CCF coefficients (that involve the roll accelerations) at +0.05s time shift are changed in the opposite direction compared to those with a front left damper fault as in Figure 4.11 and Figure 4.12.

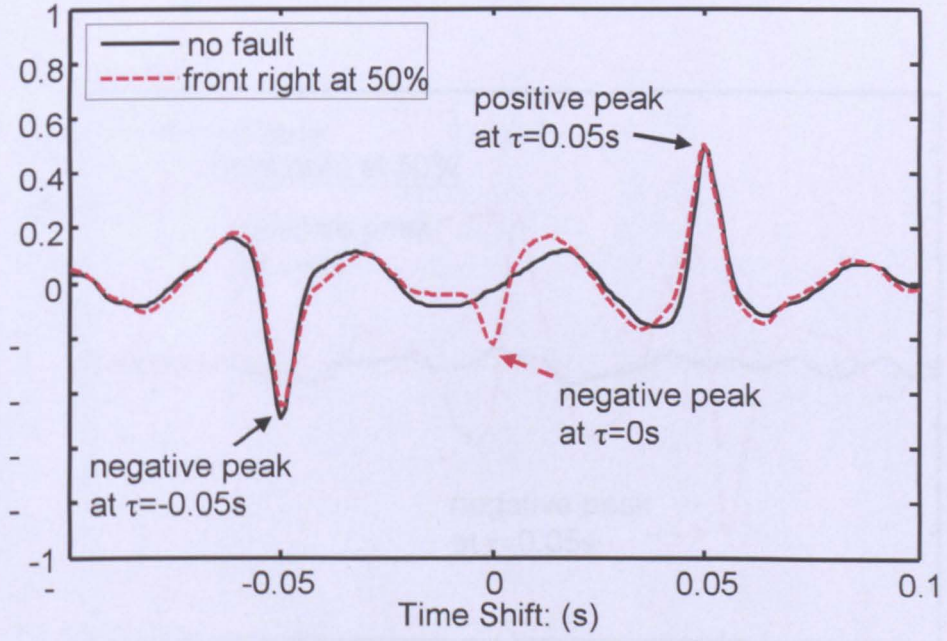

Figure 4.13 CCF coefficient of bounce and pitch accelerations for case 4.6

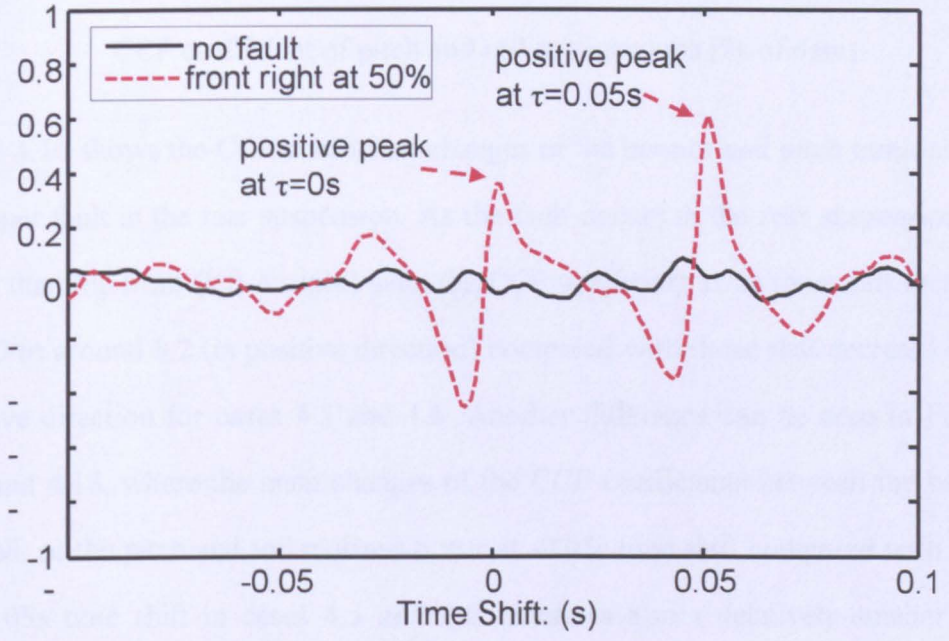

Figure 4.14 CCF coefficient of bounce and roll accelerations for case 4.6

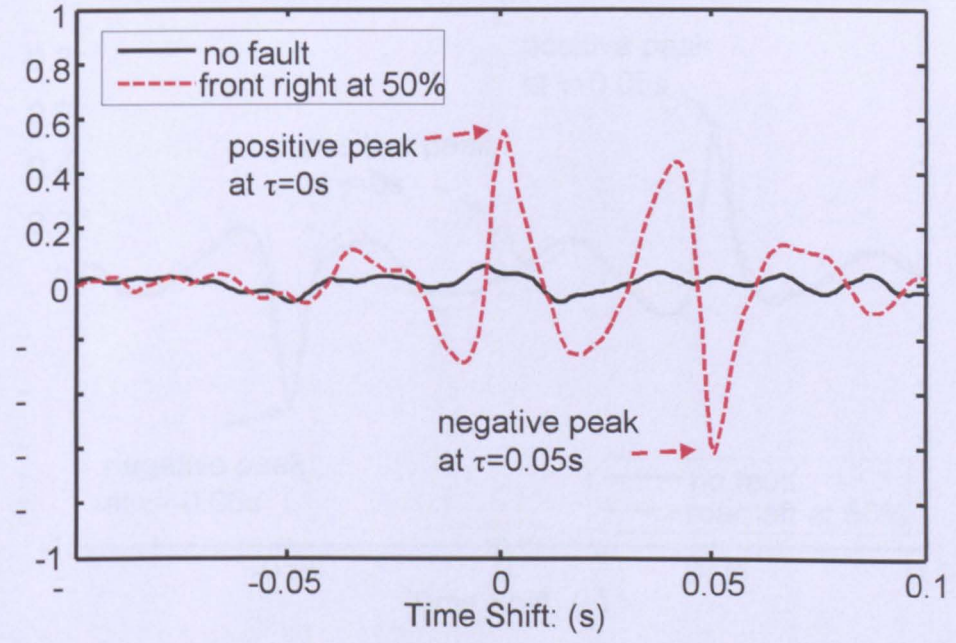

Figure 4.15 CCF coefficient of pitch and roll accelerations for case 4.6

Case 4.7: rear left damper has 50% damping loss, vehicle speed at 50m/s.

Computations: CCF coefficient of bounce and pitch accelerations (2s of data)

CCF coefficient of bounce and roll accelerations (2s of data)

CCF coefficient of pitch and roll accelerations (2s of data)

Figure 4.16 shows the CCF coefficient changes of the bounce and pitch motions with a damper fault in the rear suspension. As the fault occurs in the rear suspension side rather than the front (left & right) side, the CCF coefficient at 0s time shift increases from 0 to around 0.2 (in positive direction) compared with those that decrease in the negative direction for cases 4.5 and 4.6. Another difference can be seen in Figures 4.17 and 4.18, where the main changes of the CCF coefficients between the bounce and roll, or the pitch and roll motions occur at -0.05s time shift compared with those at +0.05s time shift in cases 4.5 and 4.6. There is also a relatively smaller CCF coefficient change at 0s time shift in Figures 4.14 to 4.15 and Figures 4.17 to 4.18, for similar reasons as those in Figures 4.11 to 4.12.

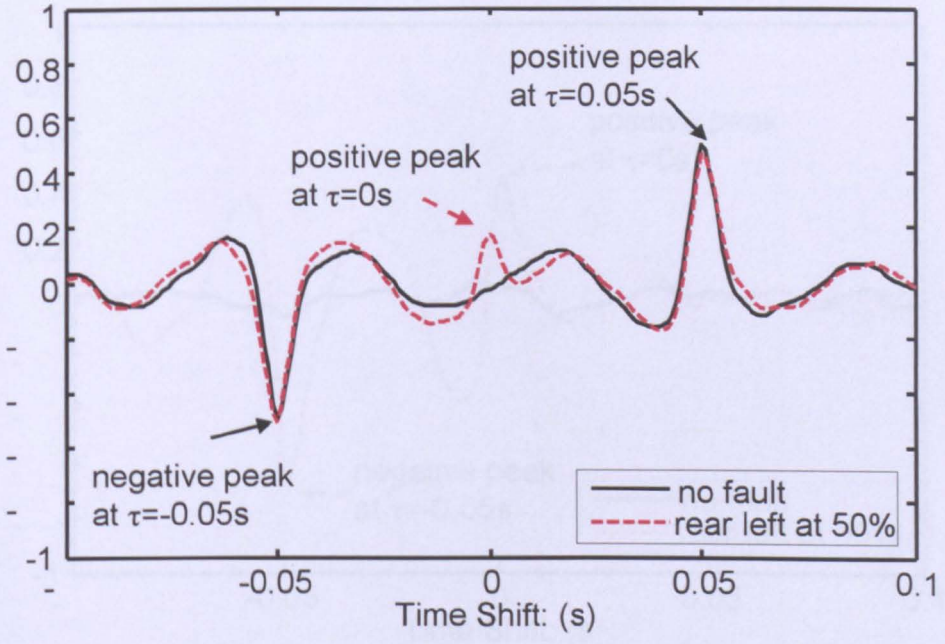

Figure 4.16 CCF coefficient of bounce and pitch accelerations for case 4.7

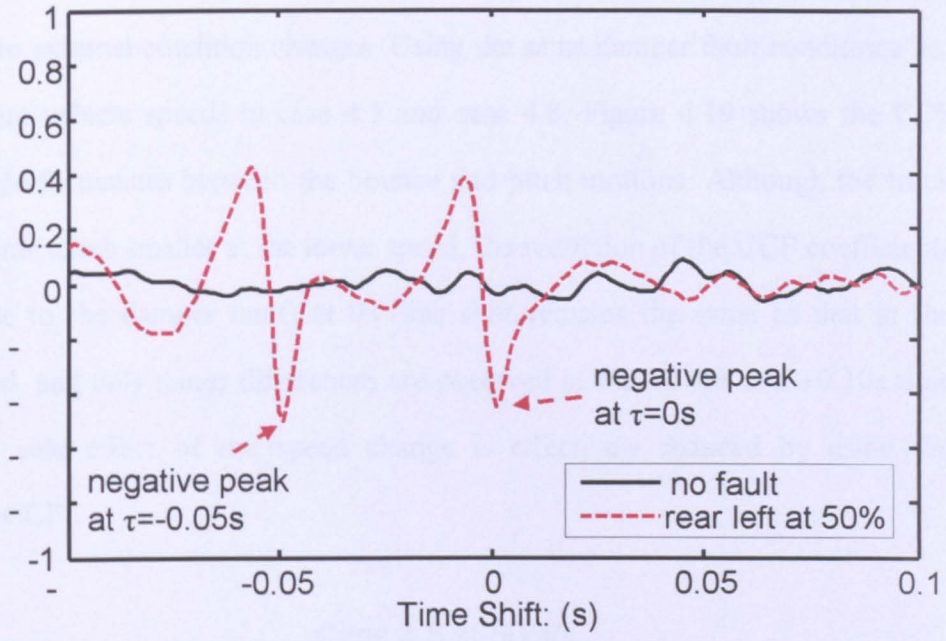

Figure 4.17 CCF coefficient of bounce and roll accelerations for case 4.7

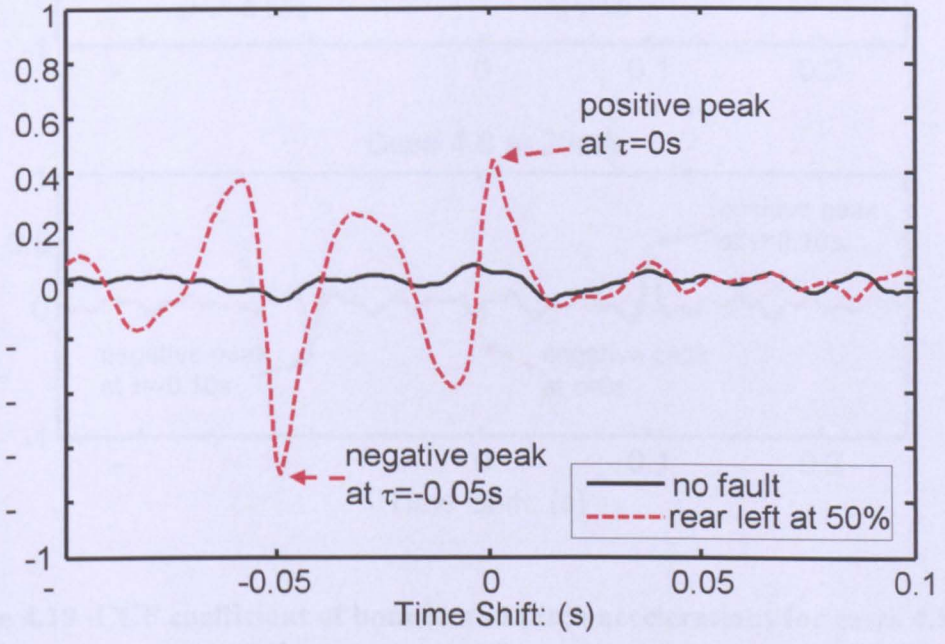

Figure 4.18 CCF coefficient of pitch and roll accelerations for case 4.7

Case 4.8: front left damper has 50% damping loss, vehicle speed at 25m/s.

Computations: CCF coefficient of bounce and pitch accelerations (2s of data)

Because of the normalisation, the CCF coefficient evaluation is expected to be insensitive to external condition changes. Using the same damper fault conditions but with different vehicle speeds in case 4.5 and case 4.8, Figure 4.19 shows the CCF coefficient performances between the bounce and pitch motions. Although the track inputs become much smaller at the lower speed, the reduction of the CCF coefficients (in response to the damper fault) at 0s time shift remains the same as that at the higher speed, and only minor differences are observed at the ±0.05s and ±0.10s time shifts. The side effect of the speed change is effectively reduced by using the normalised CCF.

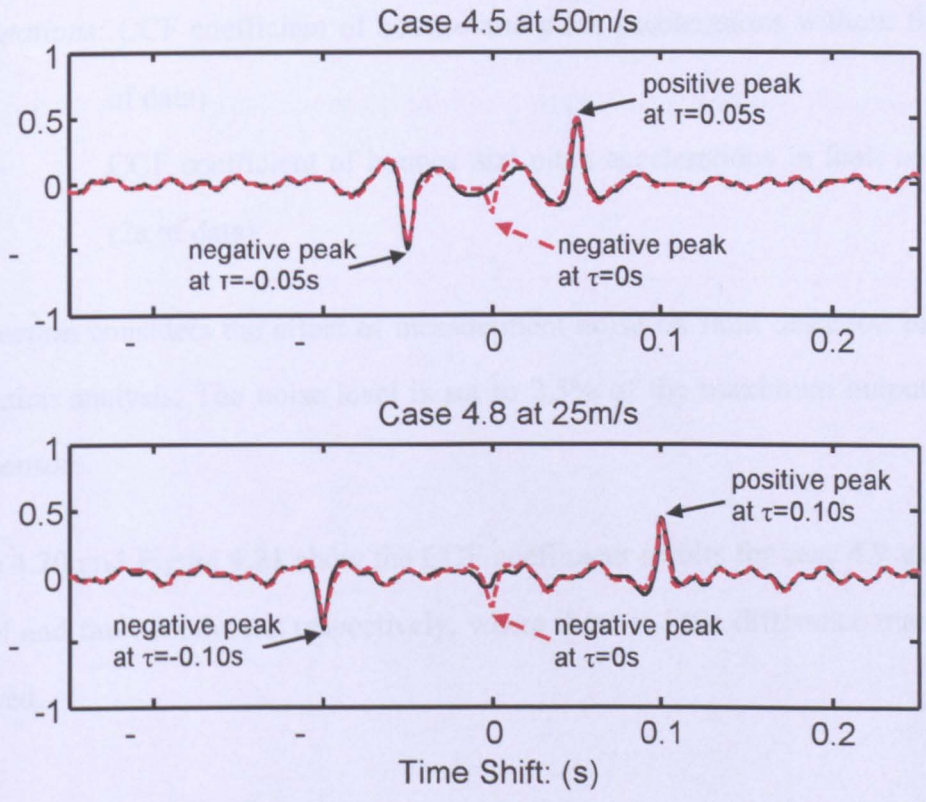

Figure 4.19 CCF coefficient of bounce and pitch accelerations for cases 4.5 & 4.8

From above simulation results, it is realised that either the CCF value or coefficient evaluation can be used as an indicator of suspension component faults by monitoring the correlation changes at the selected time shifts [43]. Same level of component fault

fault tends to give similar level of cross correlation changes for a selected CCF computation, although faults in different suspension location may lead to different change patterns. This CCF coefficient technique is particularly useful in the fault detection, as it can be made largely independent of the different external situations such as vehicle speed, and the use and tuning of thresholds can be made easier.

4.5 Results with Random Noise

Case 4.9: front left damper has 50% damping loss, vehicle speed at 50m/s, bounce and pitch accelerations with 2.5% measurement noises.

Computations: CCF coefficient of bounce and pitch accelerations without fault (2s of data)

CCF coefficient of bounce and pitch accelerations in fault condition (2s of data)

This section considers the effect of measurement noise on fault detection based on correlation analysis. The noise level is set to 2.5% of the maximum output of the ideal sensors.

Figure 4.20 and Figure 4.21 show the CCF coefficient results for case 4.9 under the normal and fault conditions respectively, where there is little difference that can be observed.

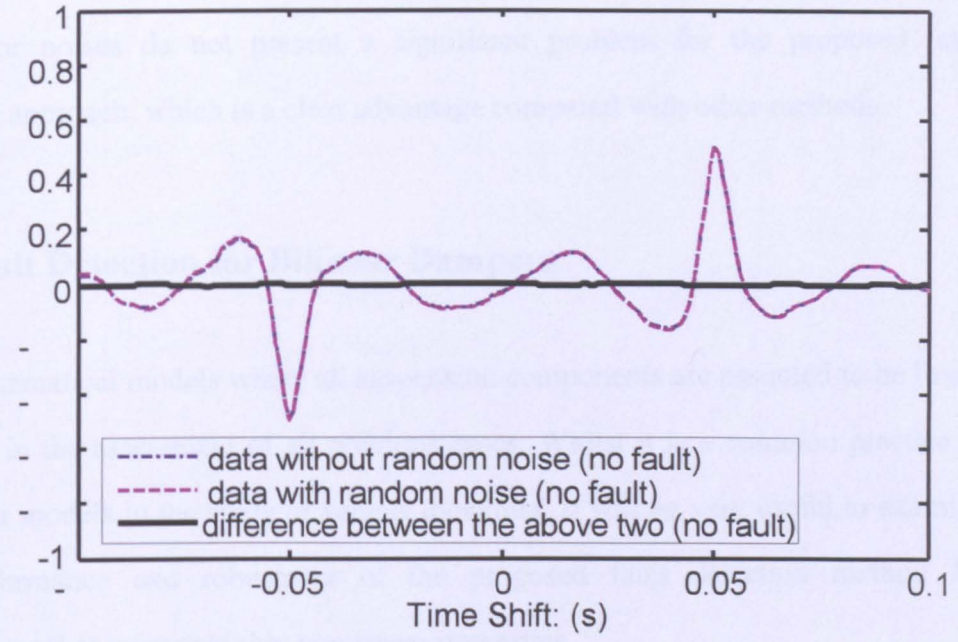

Figure 4.20 CCF coefficient of bounce and pitch accelerations for case 4.9 (no fault)

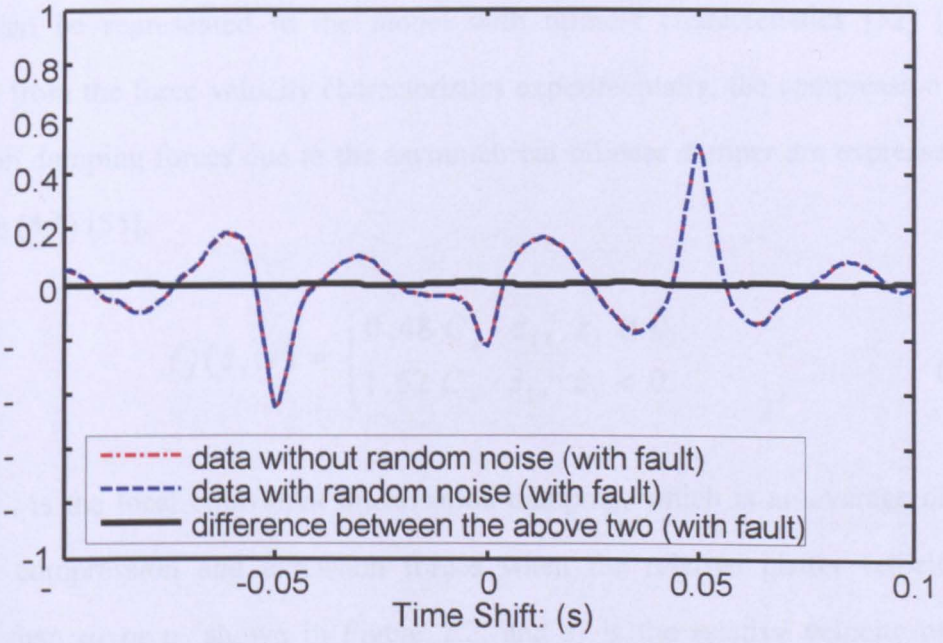

Figure 4.21 CCF coefficient of bounce and pitch accelerations for case 4.9 (fault condition)

These results support the theoretical analysis presented in the previous chapter that the sensor noises do not present a significant problem for the proposed fault detection approach, which is a clear advantage compared with other methods.

4.6 Fault Detection for Bilinear Dampers

The mathematical models where all suspension components are assumed to be linear are used in the assessment of all previous cases. Whilst it is a common practice to use linear models in the study of vehicle dynamics, it will be very useful to examine the performance and robustness of the proposed fault detection method for suspensions that present highly non-linear properties.

For the typical hydraulic damper used in railway vehicle primary suspensions, their damping forces of compression and extension movements are not necessarily equal, and the extension damping force is considerably larger than that in compression, which can be represented in the model with bilinear characteristics [52] [55]. Derived from the force-velocity characteristics experimentally, the compression and extension damping forces due to the asymmetrical bilinear damper are expressed in equation (4.1) [55].

$$f_d(\dot{z}_1, t) = \begin{cases} 0.48\, C_s \cdot \dot{z}_1, & \dot{z}_1 \geq 0 \\ 1.52\, C_s \cdot \dot{z}_1, & \dot{z}_1 < 0 \end{cases} \tag{4.1}$$

where C_s is the local equivalent linearisation damping, which is an average of the bilinear compression and extension forces when the relative piston velocity is smaller than a_1 or a_2 shown in Figure 2.2, and $\dot{z}_1$ is the relative velocity of the damper piston.

Case 4.10: bilinear damper models, front left damper has 50% damping loss, vehicle speed at 50m/s.

CCF coefficient of pitch and roll accelerations (2s of data)

Using the bilinear dampers, the following simulation is focused on the CCF coefficient evaluation as it is unaffected by the change in external conditions. Figure 4.22 shows the simulation results of bounce and pitch motions for case 4.10, indicating a similar level of sensitivity to the fault compared with the result using the linear damper for case 4.5 shown in Figure 4.10.

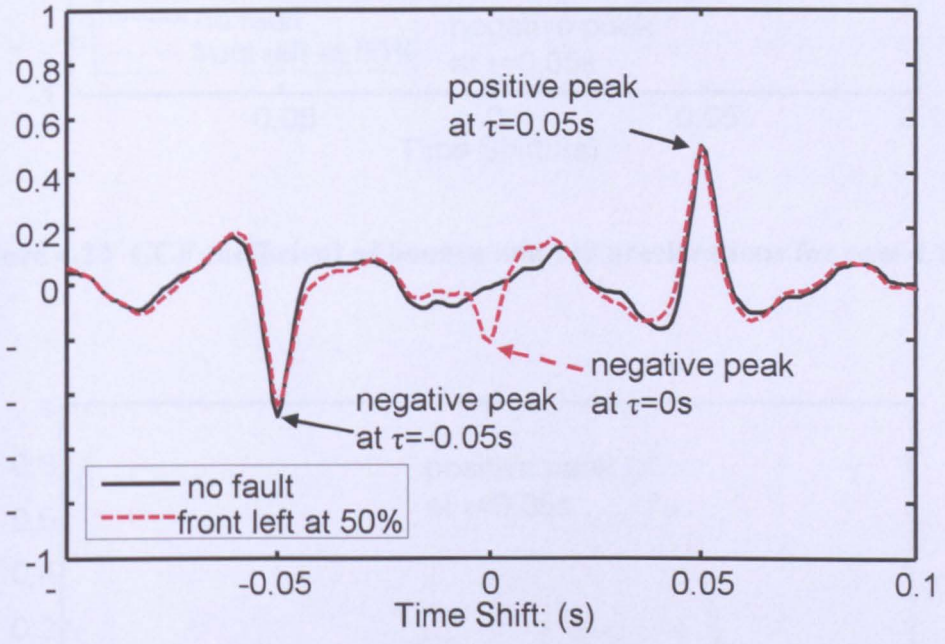

Figure 4.22 CCF coefficient of bounce and pitch accelerations for case 4.10

Similar CCF coefficient results using the bilinear dampers can also be observed by comparing the performances between the bounce and roll, and the pitch and roll motions shown in Figure 4.23 and Figure 4.24, respectively. Compared with the corresponding CCF coefficient results involved roll acceleration in case 4.5, their correlation results show the consistent results are also achievable for the proposed method for both linear and bilinear damper models. A fuller assessment of different types and levels of faults using linear or bi-linear dampers is given in Table 4.1 and Table 4.2 respectively. From the data in these two tables it is equally found that the similarities can be observed for any possible damper fault and in any location.

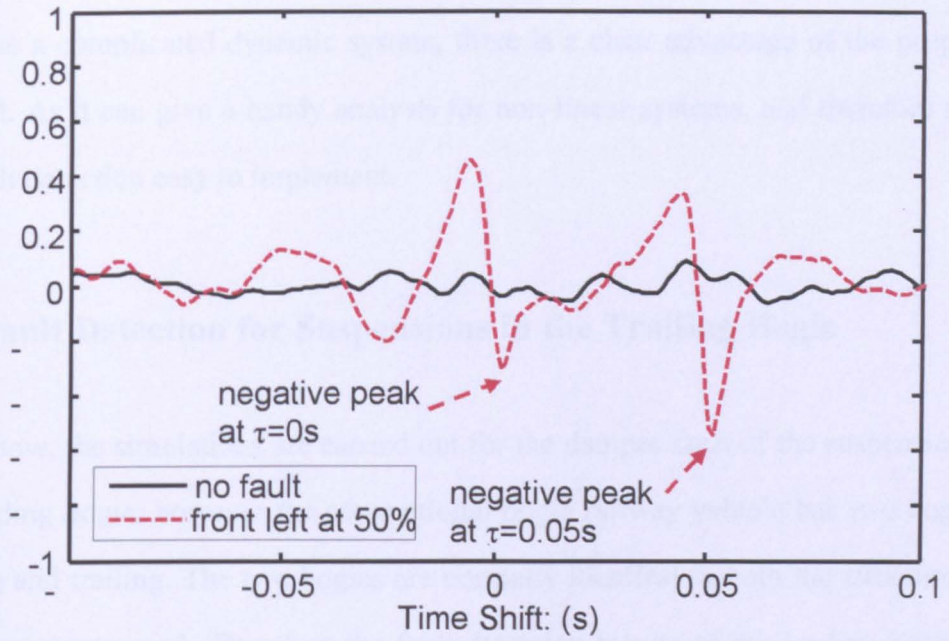

Figure 4.23 CCF coefficient of bounce and roll accelerations for case 4.10

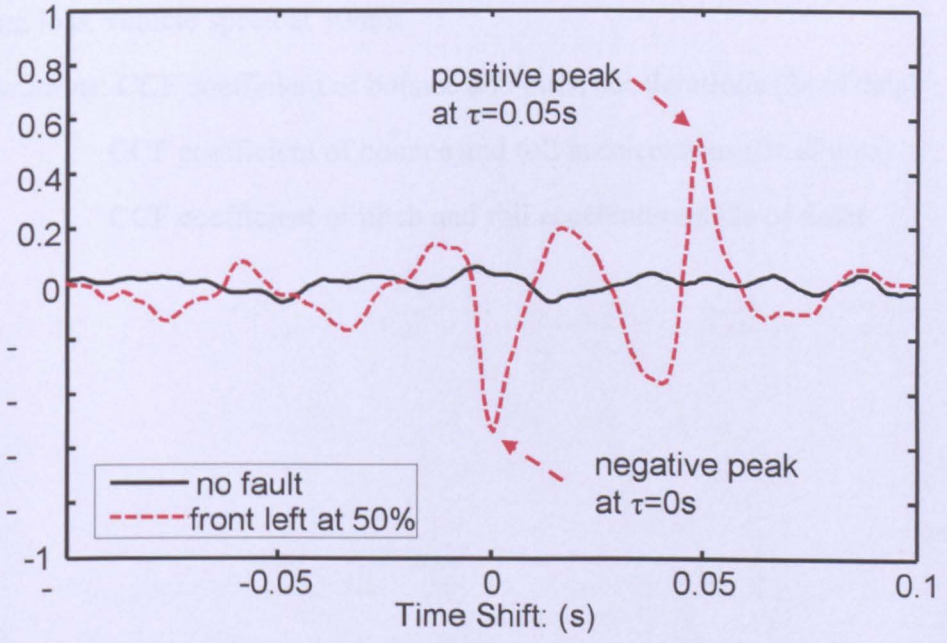

Figure 4.24 CCF coefficient of pitch and roll accelerations for case 4.10

Compared to other model-based fault detection schemes which normally need to linearise a complicated dynamic system, there is a clear advantage of the proposed

Compared to other model-based fault detection schemes which normally need to linearise a complicated dynamic system, there is a clear advantage of the proposed method. As it can give a handy analysis for non-linear systems, and therefore make the fault detection easy to implement.

4.7 Fault Detection for Suspensions in the Trailing Bogie

Up to now, the simulations are carried out for the damper fault of the suspensions in the leading bogie, however the conventional bogie railway vehicle has two bogies - leading and trailing. The two bogies are normally identical in both the structure and the components used. Therefore the fault detection results of the leading bogie are expected to be equally applicable to the trailing one.

Case 4.11: linear damper models, front left damper in the trailing bogie has 50% damping loss, vehicle speed at 50m/s.

Computations: CCF coefficient of bounce and pitch accelerations (2s of data)

CCF coefficient of bounce and roll accelerations (2s of data)

CCF coefficient of pitch and roll accelerations (2s of data)

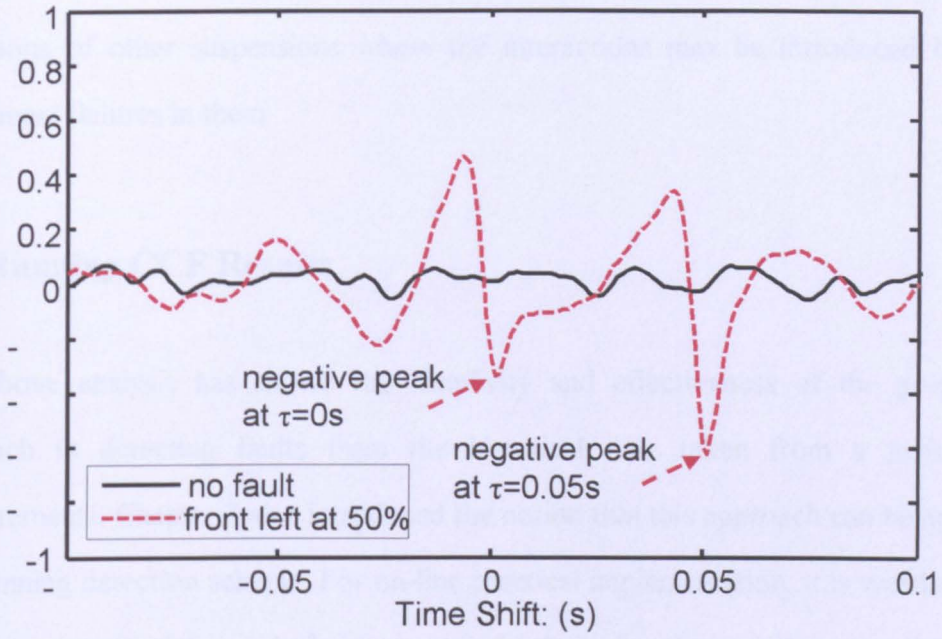

Figure 4.26 CCF coefficient of bounce and roll accelerations for case 4.11

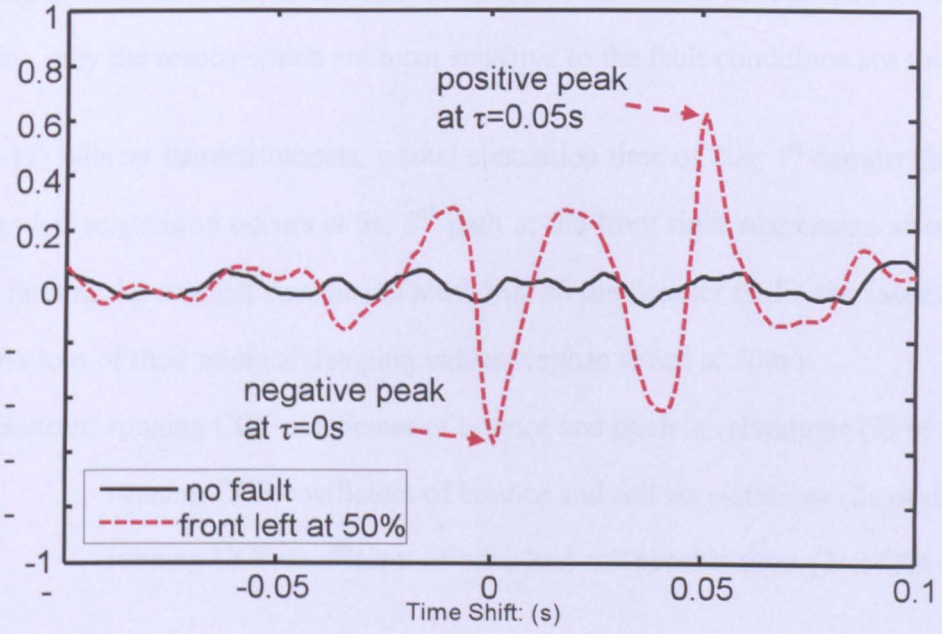

Figure 4.27 CCF coefficient of pitch and roll accelerations for case 4.11

It is clearly seen from Figure 4.25 to Figure 4.27 that the CCF coefficient results from either bounce, pitch and roll motions of the trailing bogie are very close to those

of case 4.5, which shows the proposed technique may be expandable to monitor conditions of other suspensions where the interactions may be introduced by the component failures in them.

4.8 Running CCF Results

The above analysis has shown the simplicity and effectiveness of the proposed approach in detecting faults from the historical data taken from a period of measurements. Chapter 3 also introduced the notion that this approach can be applied as a running detection scheme. For on-line practical implementation, it is worth using running cross correlation calculations with a fixed moving time window to reduce the latency of the fault detection process.

In this section, the running detection scheme is examined with the damper fault(s) occurring in different time periods and, as usual, in different locations. In the interest of clarity, only the results which are most sensitive to the fault conditions are shown.

Case 4.12: bilinear damper models, a total simulation time of 20s; 1st damper fault at the front left suspension occurs at 5s, 2nd fault at the front right suspension after 10s, and 3rd fault at the rear left suspension after 15s; all the damper faults are assumed to be a 50% loss of their nominal damping values; vehicle speed at 50m/s.

Computations: running CCF coefficient of bounce and pitch accelerations (2s of data)
running CCF coefficient of bounce and roll accelerations (2s of data)
running CCF coefficient of pitch and roll accelerations (2s of data)

Figure 4.28 shows the CCF coefficient between the bounce and pitch motions for case 4.12 at 0s time shift, where the CCF coefficient is increased in the negative direction after 5s when the first damper fault occurs in one of the front suspensions (on the left side). The coefficient is further increased negatively at the time of 10s due to a second damper fault occurring in another front suspension (on the right side), as

In this section, the running detection scheme is examined with the damper fault(s) occurring in different time periods and, as usual, in different locations. In the interest of clarity, only the results which are most sensitive to the fault conditions are shown.

Case 4.12: bilinear damper models, a total simulation time of 20s; 1st damper fault at the front left suspension occurs at 5s, 2nd fault at the front right suspension after 10s, and 3rd fault at the rear left suspension after 15s; all the damper faults are assumed to be a 50% loss of their nominal damping values; vehicle speed at 50m/s.

Computations: running CCF coefficient of bounce and pitch accelerations (2s of data)
running CCF coefficient of bounce and roll accelerations (2s of data)
running CCF coefficient of pitch and roll accelerations (2s of data)

Figure 4.28 shows the CCF coefficient between the bounce and pitch motions for case 4.12 at 0s time shift, where the CCF coefficient is increased in the negative direction after 5s when the first damper fault occurs in one of the front suspensions (on the left side). The coefficient is further increased negatively at the time of 10s due to a second damper fault occurring in another front suspension (on the right side), as the two front side faults worsens the asymmetry in the suspension system. When a third damper fault occurs in the rear suspension after the time of 15s, the CCF coefficient is actually improved because the imbalance between the front and rear suspension sides becomes less severe.

Figure 4.29 gives their CCF coefficient between the bounce and roll motions. The changes of their CCF coefficient indicate that an asymmetry between the left and right suspensions exists when there is a fault at the front left damper only (between 5 - 10s), or when the fault on the one side of the bogie is more severe than the other side (after 15s), which deviates the CCF coefficients apart from zero. When the roll motion is in balance before the time of 5s or retrieved to balance again between 10 - 15s, their cross correlations are very close to zero as expected.

A similar scenario is observed from the CCF coefficient between the pitch and roll motions as shown in Figure 4.30. Their CCF coefficients reflect not only the imbalance level of the roll motion but also the pitch in the suspension system. Their correlations are very close to zero under the normal condition (0 - 5s), as the same as those in Figure 4.28 and Figure 4.29. The CCF coefficient appears to be insensitive to fault when there is only an asymmetry in the pitch motion until the roll motion also becomes asymmetric, as it is shown that the front left & right damper faults (between 10 - 15s) cause an imbalance in the pitch direction, which contributes no change to the CCF coefficient. Only in the time periods 5 - 10s and 15 - 20s when both pitch and roll motions are imbalanced, obvious change of the CCF coefficients can be observed.

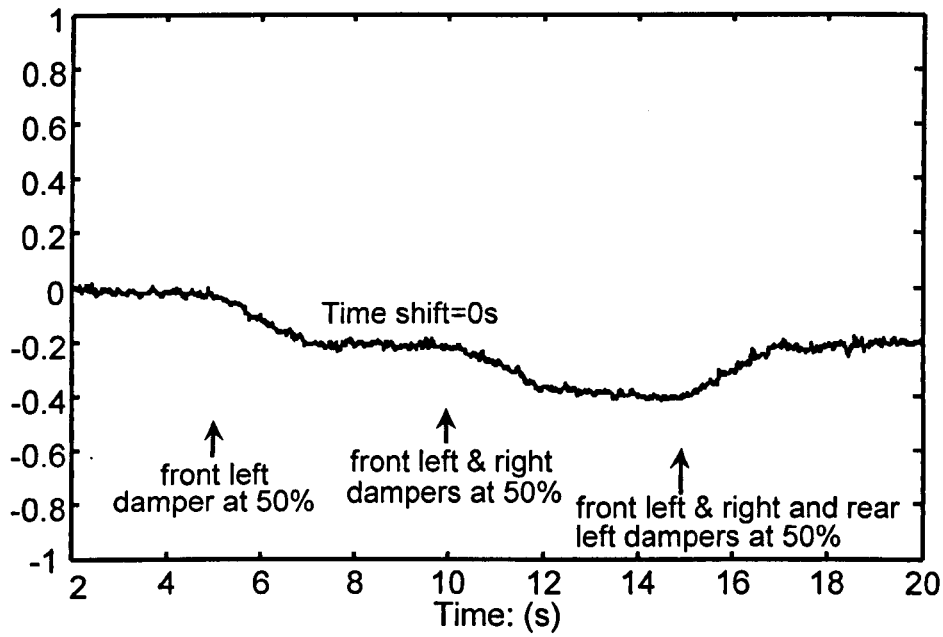

Figure 4.28 Running CCF coefficient of bounce and pitch accelerations for case 4.12

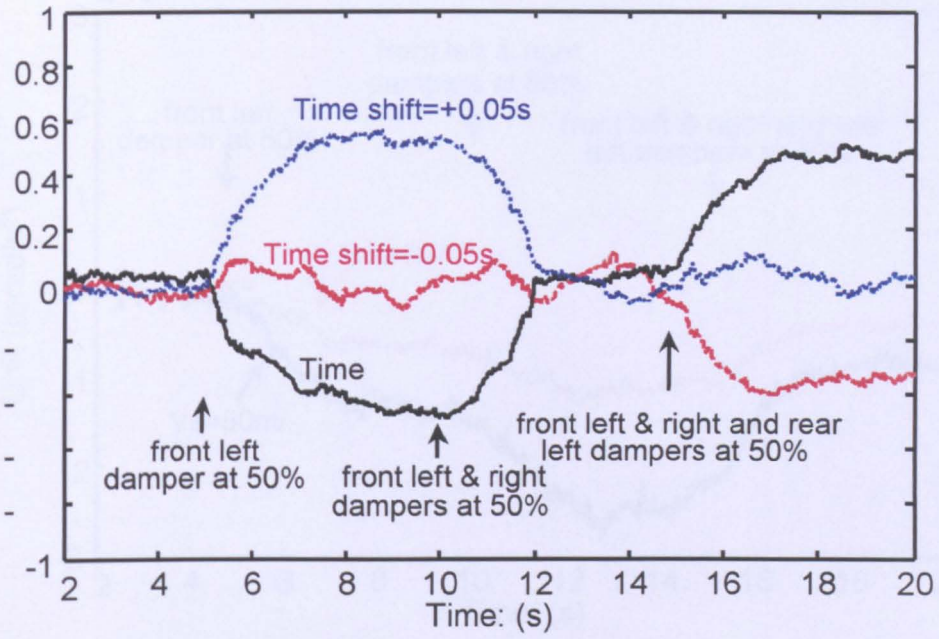

Figure 4.30 Running CCF coefficient of pitch and roll accelerations for case 4.12

Case 4.13: bilinear damper models, a total simulation time of 20s; 1st damper fault at the front left suspension occurs at 5s, 2nd fault at the front right suspension after 10s, and 3rd fault at the rear left suspension after 15s; all the damper faults are assumed to be a 50% loss of their nominal damping values; vehicle speed at 50m/s and 25m/s respectively.

Computations: running CCF value of bounce and pitch accelerations at two speeds (2s of data)

running CCF coefficient of bounce and pitch accelerations at two speeds (2s of data)

The running simulation results are also carried out to compare the performance of the cross correlations at different vehicle speeds. Figure 4.31 shows the running CCF values results, it is observed that the changes of the two correlations correspond to the same faults, but the level of change at low speed is obviously smaller as the CCF values are largely dependent on the magnitude of the track irregularities.

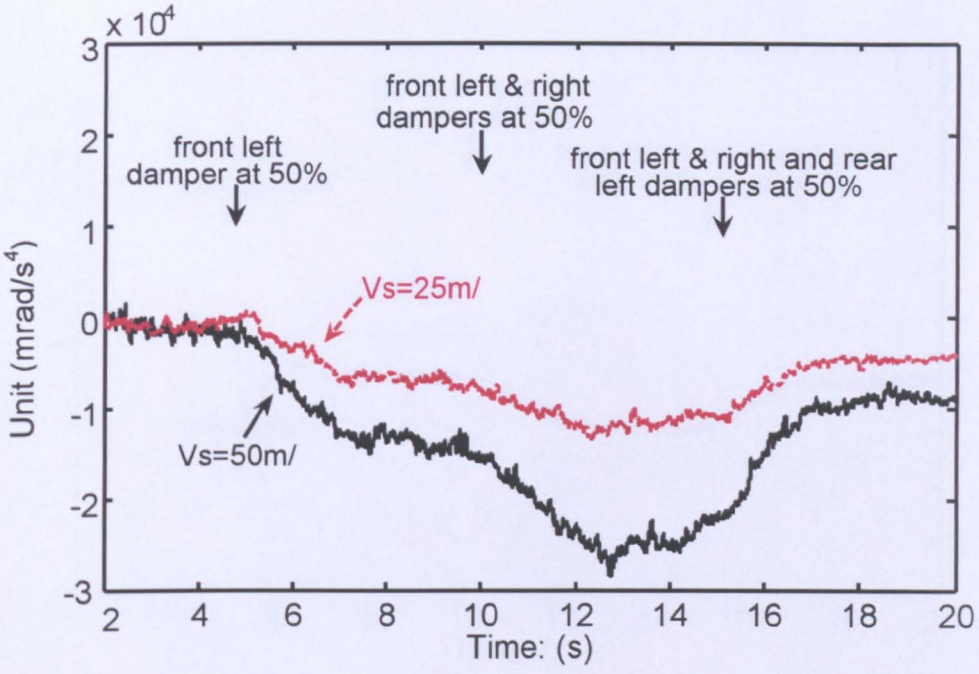

Figure 4.31 Comparison of running CCF values of bounce and pitch accelerations for case 4.13 at different speeds

However, the running CCF coefficients in Figure 4.32 only show minor differences between them at the different speeds. This makes the use of running CCF coefficient more convenient than the running CCF value in the fault detection, and therefore the use and tuning of the thresholds can be easily achieved

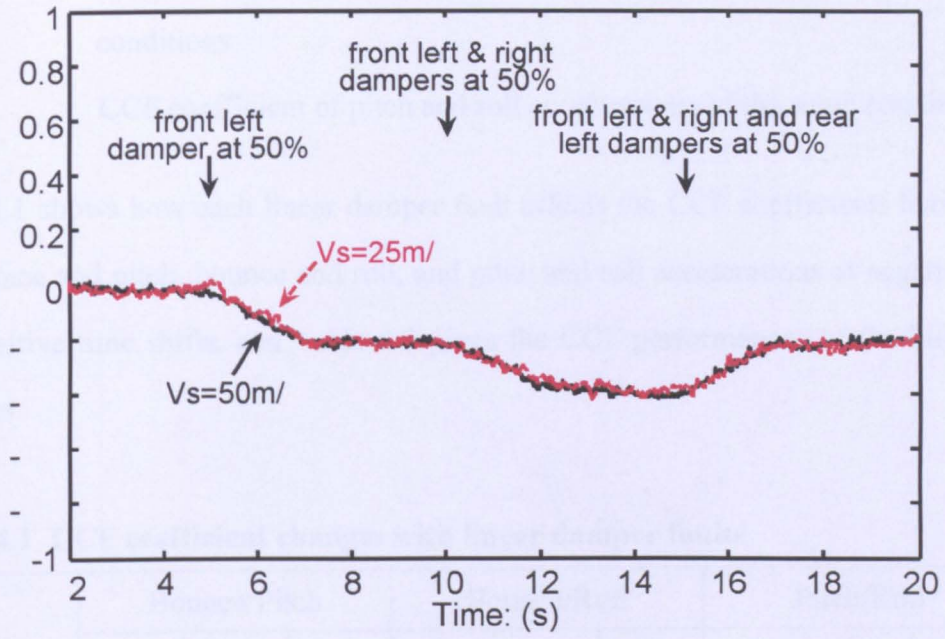

Figure 4.32 Comparison of running CCF coefficients of bounce and pitch accelerations for case 4.13 at different speeds

4.9 Fault Isolation

Previous assessments have shown that proposed detection method reacts to different fault(s) in different manners, in terms of the sensitivity at different time shifts (negative, 0 and positive) of the cross correlations and/or the sign (negative, positive) of the CCF results. This feature can be therefore used to determine the exact location of a fault.

Case 4.14: using linear and bilinear dampers, vehicle speed at 50m/s.

Computations: CCF coefficient of bounce and pitch accelerations, with 75%, 50%, 25% and 0% of the normal damping coefficient, and for different locations of dampers

CCF coefficient of bounce and roll accelerations of the same conditions

CCF coefficient of pitch and roll accelerations of the same conditions

CCF coefficient of bounce and roll accelerations of the same conditions

CCF coefficient of pitch and roll accelerations of the same conditions

Table 4.1 shows how each linear damper fault affects the CCF coefficients between the bounce and pitch, bounce and roll, and pitch and roll accelerations at negative, 0 and positive time shifts, and Table 4.2 gives the CCF performances of the bilinear dampers.

Table 4.1 CCF coefficient changes with linear damper faults

	Bounce/Pitch			Bounce/Roll			Pitch/Roll		
	$-T_{shift}$	*0s*	$+T_{shift}$	$-T_{shift}$	*0s*	$+T_{shift}$	$-T_{shift}$	*0s*	$+T_{shift}$
No Fault	-0.50	-0.03	+0.49	-0.03	-0.05	-0.02	-0.03	+0.02	+0.02
C_{FL} 75%	-0.48	-0.12			-0.32	-0.49		-0.50	+0.48
C_{FL} 50%	-0.46	-0.22			-0.28	-0.57		-0.49	+0.56
C_{FL} 25%	-0.43	-0.31			-0.22	-0.61		-0.44	+0.60
C_{FL} 0%	-0.38	-0.41			-0.14	-0.65		-0.36	+0.64
C_{FR} 75%	-0.48	-0.12			+0.27	+0.47		+0.52	-0.46
C_{FR} 50%	-0.46	-0.22			+0.25	+0.56		+0.50	-0.55
C_{FR} 25%	-0.43	-0.32			+0.19	+0.61		+0.45	-0.59
C_{FR} 0%	-0.38	-0.41			+0.12	+0.64		+0.37	-0.63
C_{RL} 75%		+0.06	+0.48	-0.38	-0.42		-0.57	+0.40	
C_{RL} 50%		+0.16	+0.46	-0.46	-0.40		-0.66	+0.37	
C_{RL} 25%		+0.26	+0.43	-0.51	-0.34		-0.70	+0.30	
C_{RL} 0%		+0.35	+0.38	-0.56	-0.26		-0.73	+0.22	
C_{RR} 75%		+0.06	+0.48	+0.37	+0.38		+0.55	-0.39	
C_{RR} 50%		+0.16	+0.46	+0.45	+0.38		+0.65	-0.37	
C_{RR} 25%		+0.26	+0.43	+0.50	+0.32		+0.69	-0.30	
C_{RR} 0%		+0.35	+0.38	+0.55	+0.25		+0.73	-0.22	

Table 4.2 CCF coefficient changes with bilinear damper faults

	Bounce/Pitch			Bounce/Roll			Pitch/Roll		
	$-T_{shift}$	*0s*	$+T_{shift}$	$-T_{shift}$	*0s*	$+T_{shift}$	$-T_{shift}$	*0s*	$+T_{shift}$
No Fault	-0.49	-0.02	+0.48	-0.03	-0.04	-0.02	-0.01	+0.02	+0.01
C_{FL} 75%	-0.47	-0.11			-0.28	-0.42		-0.42	+0.41
C_{FL} 50%	-0.45	-0.21			-0.27	-0.53		-0.45	+0.52
C_{FL} 25%	-0.42	-0.31			-0.22	-0.59		-0.41	+0.58
C_{FL} 0%	-0.37	-0.41			-0.15	-0.62		-0.34	+0.61
C_{FR} 75%	-0.47	-0.12			+0.24	+0.40		+0.44	-0.41
C_{FR} 50%	-0.45	-0.21			+0.24	+0.52		+0.47	-0.52
C_{FR} 25%	-0.42	-0.31			+0.20	+0.58		+0.42	-0.57
C_{FR} 0%	-0.37	-0.41			+0.13	+0.61		+0.34	-0.61
C_{RL} 75%		+0.07	+0.47	-0.33	-0.35		-0.47	+0.35	
C_{RL} 50%		+0.17	+0.45	-0.43	-0.36		-0.60	+0.36	
C_{RL} 25%		+0.27	+0.41	-0.48	-0.31		-0.65	+0.31	
C_{RL} 0%		+0.37	+0.37	-0.53	-0.23		-0.69	+0.23	
C_{RR} 75%		+0.07	+0.47	+0.30	+0.31		+0.47	-0.34	
C_{RR} 50%		+0.17	+0.45	+0.41	+0.34		+0.59	-0.35	
C_{RR} 25%		+0.27	+0.41	+0.47	+0.29		+0.65	-0.30	
C_{RR} 0%		+0.37	+0.37	+0.52	+0.22		+0.69	-0.23	

The CCF coefficients at a time shift that not sensitive to a particular faults are not included in the two tables. There is a clear correlation between the degree of a fault(s) and the level of change in CCF coefficients, which can be very useful to determine if a replacement is needed, and the urgency of the replacement. For the purpose of fault isolation, only two of the three cross correlation results (i.e. bounce/pitch, bounce/roll & pitch/roll) are sufficient to identify a fault. For instance, a fault on the front side (either left or right direction) of the bogie decreases the CCF coefficient between the bounce and pitch motions, and the CCF coefficient between the bounce and roll motions will also be reduced if this damper fault occurs in the

left direction of the bogie. Using this unique information provided by the two combined CCF coefficient results, the fault can be thereby isolated.

Tables 4.1 and 4.2 can be simplified to Table 4.3 which illustrates the relationship between different suspension faults and the CCF results. The arrows in bold indicate one being more sensitive to fault(s).

Table 4.3 Cross correlation changes with different damper faults

Type of damper fault	Bounce/Pitch			Bounce/Roll			Pitch/Roll		
	$-T_{shift}$	$0s$	$+T_{shift}$	$-T_{shift}$	$0s$	$+T_{shift}$	$-T_{shift}$	$0s$	$+T_{shift}$
Front left	↗	↘			↘	↘		↘	↗
Front right	↗	↘			↗	↗		↗	↘
Rear left		↗	↘	↘	↘		↘	↗	
Rear right		↗	↘	↗	↗		↗	↘	

Table 4.4 illustrates how a damper fault can be isolated using the results at zero time shift of bounce and pitch, and bounce and roll cross correlations.

Table 4.4 Logic sequences for fault detection and isolation

Change tendency		Faulty damper isolation			
Bounce/Pitch	Bounce/Roll	Front left	Front right	Rear left	Rear right
↘	↘	√	--	--	--
	↗	--	√	--	--
↗	↘	--	--	√	--
	↗	--	--	--	√

Similar results can be obtained from the different correlation combinations such as between the bounce and roll, the pitch and roll motions, or between bounce and roll, pitch and roll motions. The cross correlation changes at ±0.05s time shifts (at the

vehicle speed of 50m/s) also enable isolation of faults, so there is no shortage of information.

4.10 Summary

In this chapter the concept and scheme for fault detection using the described correlation technique was examined under different conditions. The simulation results were assessed by studying the sensitivity of this technology. Special attention has been given to the CCF coefficient computation as it is robust to the changes of external operational conditions. The reliability of the technique was also verified by examining the proposed method for the vehicle model with bilinear dampers. The effect of measurement noise was studied. The results and analysis show the feasibility and consistency of the proposed technique for detecting faults in railway vehicle suspensions.

Based on this fault detection study, fault isolation performance was also verified by exploring the link between different patterns of correlation changes and individual faults. The results show that the proposed approach is helpful not only in detecting a fault in the suspension systems, but also in isolating the location of the fault and identifying the severity of the failure.

Chapter 5

Condition Monitoring Using Relative Variance

5.1 Introduction

A novel data processing scheme using cross correlation has been developed for the FDI problem in railway suspension systems. In Chapter 4, simulation results and assessments of the scheme have demonstrated that suspension component faults can be effectively detected and isolated via monitoring the correlation changes.

The present chapter introduces a supplementary technique based on the same fault detection principle as described in Chapter 3. This approach will focus on the changes in variance of the bogie accelerations.

5.2 Fault Detection Scheme

So far, this thesis has described the development and validation of cross correlation as a data processing tool which could provide acceptable fault detection and isolation results, with the advantage of avoiding a complicated system model and providing easy threshold tuning. The same principle of detecting the dynamic changes and asymmetry caused by a component fault can be exploited using a different data processing technique. This chapter investigates the suspension health conditions by using short-term variances and further the relative variances method. An important issue is to determine how the variance or relative variance changes are related to component failures under different operational conditions. Firstly, characteristics of this fault detection scheme are briefly introduced. Secondly their performances are studied and compared with the previous technique. The issue of

the measurement noise and the use in non-linear systems are also investigated. Finally, the use of relative variance in the context of fault isolation has also been assessed and compared.

To examine the practical use of the method, the overall computational requirements are now studied in terms of the relationship between the bogie accelerations at the positions above the suspensions and the suspension components. In practice, the measurements of the bounce, pitch and roll motions can be readily measured using inertial sensors mounted on the bogie frame [19]. By using the same conventional bogie vehicle system shown in Figure 2.6, the dynamic equations of the accelerations above the four primary suspensions may be easily derived from the three basic measurements and bogie geometrical parameters as given in equations (5.1) - (5.4).

$$\ddot{z}_{FL} = \ddot{z}_b + L_{bx} \cdot \ddot{\phi}_b + L_{by} \cdot \ddot{\psi}_b \tag{5.1}$$

$$\ddot{z}_{FR} = \ddot{z}_b + L_{bx} \cdot \ddot{\phi}_b - L_{by} \cdot \ddot{\psi}_b \tag{5.2}$$

$$\ddot{z}_{RL} = \ddot{z}_b - L_{bx} \cdot \ddot{\phi}_b + L_{by} \cdot \ddot{\psi}_b \tag{5.3}$$

$$\ddot{z}_{RR} = \ddot{z}_b - L_{bx} \cdot \ddot{\phi}_b - L_{by} \cdot \ddot{\psi}_b \tag{5.4}$$

where $\ddot{z}_{FL}$, $\ddot{z}_{FR}$, $\ddot{z}_{RL}$ and $\ddot{z}_{RR}$ are the corner accelerations corresponding to the front left, front right, rear left and rear right primary suspensions of the studied bogie.

It is noticed from equations (5.1) - (5.4) that the responses of the four corner accelerations will be very similar until a fault occurs, because a fault can break the system symmetry and change the responses by affecting the corresponding parts of bounce, pitch and roll motions.

The basic bounce, pitch and roll motions can also be inversely described in the form of the four corner accelerations outlined in equations (5.1) - (5.4), which gives equations (5.5) - (5.7).

$$\ddot{z}_b = \frac{\ddot{z}_{FL} + \ddot{z}_{FR} + \ddot{z}_{RL} + \ddot{z}_{RR}}{4} \tag{5.5}$$

$$\ddot{\phi}_b = \frac{\ddot{z}_{FL} + \ddot{z}_{FR} - \ddot{z}_{RL} - \ddot{z}_{RR}}{4L_{bx}} \tag{5.6}$$

$$\ddot{\psi}_b = \frac{\ddot{z}_{FL} - \ddot{z}_{FR} + \ddot{z}_{RL} - \ddot{z}_{RR}}{4L_{by}} \tag{5.7}$$

To study the relationship among the four corner accelerations, equations (5.1) - (5.4) can be firstly transformed by replacing equation (2.17) and equations (2.19) - (2.20) into them, which leads to equations (5.8) - (5.11).

$$\begin{aligned}
&I_{by}/L_{by}^2 \cdot \ddot{z}_{FL} + (C_{FL} + C_{FR} + C_{RL} + C_{RR}) \cdot \dot{z}_{FL} + 4K_P \cdot z_{FL} \\
&-(I_{by}/L_{by}^2 - m_b) \cdot \ddot{z}_b - (I_{by}/L_{by}^2 - I_{bx}/L_{bx}^2) L_{bx} \cdot \ddot{\phi}_b \\
&+(C_{FL} + C_{FR} - C_{RL} - C_{RR}) \cdot (\dot{z}_b + L_{bx} \cdot \dot{\phi}_b) \\
&+(C_{FL} - C_{FR} + C_{RL} - C_{RR}) \cdot (\dot{z}_b + L_{by} \cdot \dot{\psi}_b) \\
&= 3(C_{FL} \cdot \dot{z}_{t1L} + K_P \cdot z_{t1L}) + (C_{FR} \cdot \dot{z}_{t1R} + K_P \cdot z_{t1R}) \\
&+(C_{RL} \cdot \dot{z}_{t2L} + K_P \cdot z_{t2L}) - (C_{RR} \cdot \dot{z}_{t2R} + K_P \cdot z_{t2R}) + \Sigma F_1 + \Delta F_1
\end{aligned} \tag{5.8}$$

$$\begin{aligned}
&I_{by}/L_{by}^2 \cdot \ddot{z}_{FR} + (C_{FL} + C_{FR} + C_{RL} + C_{RR}) \cdot \dot{z}_{FR} + 4K_P \cdot z_{FR} \\
&-(I_{by}/L_{by}^2 - m_b) \cdot \ddot{z}_b - (I_{by}/L_{by}^2 - I_{bx}/L_{bx}^2) L_{bx} \cdot \ddot{\phi}_b \\
&+(C_{FL} + C_{FR} - C_{RL} - C_{RR}) \cdot (\dot{z}_b + L_{bx} \cdot \dot{\phi}_b) \\
&-(C_{FL} - C_{FR} + C_{RL} - C_{RR}) \cdot (\dot{z}_b - L_{by} \cdot \dot{\psi}_b) \\
&= (C_{FL} \cdot \dot{z}_{t1L} + K_P \cdot z_{t1L}) + 3(C_{FR} \cdot \dot{z}_{t1R} + K_P \cdot z_{t1R}) \\
&-(C_{RL} \cdot \dot{z}_{t2L} + K_P \cdot z_{t2L}) + (C_{RR} \cdot \dot{z}_{t2R} + K_P \cdot z_{t2R}) + \Sigma F_1 - \Delta F_1
\end{aligned} \tag{5.9}$$

$$
\begin{aligned}
&I_{by}/L_{by}^2\cdot\ddot{z}_{RL}+(C_{FL}+C_{FR}+C_{RL}+C_{RR})\cdot\dot{z}_{RL}+4K_P\cdot z_{RL}\\
&-(I_{by}/L_{by}^2-m_b)\cdot\ddot{z}_b+(I_{by}/L_{by}^2-I_{bx}/L_{bx}^2)L_{bx}\cdot\ddot{\phi}_b\\
&-(C_{FL}+C_{FR}-C_{RL}-C_{RR})\cdot(\dot{z}_b-L_{bx}\cdot\dot{\phi}_b)\\
&+(C_{FL}-C_{FR}+C_{RL}-C_{RR})\cdot(\dot{z}_b+L_{by}\cdot\dot{\psi}_b)\\
&=(C_{FL}\cdot\dot{z}_{t1L}+K_P\cdot z_{t1L})-(C_{FR}\cdot\dot{z}_{t1R}+K_P\cdot z_{t1R})\\
&+3(C_{RL}\cdot\dot{z}_{t2L}+K_P\cdot z_{t2L})+(C_{RR}\cdot\dot{z}_{t2R}+K_P\cdot z_{t2R})+\Sigma F_1+\Delta F_1
\end{aligned}
\tag{5.10}
$$

$$
\begin{aligned}
&I_{by}/L_{by}^2\cdot\ddot{z}_{RR}+(C_{FL}+C_{FR}+C_{RL}+C_{RR})\cdot\dot{z}_{RR}+4K_P\cdot z_{RR}\\
&-(I_{by}/L_{by}^2-m_b)\cdot\ddot{z}_b+(I_{by}/L_{by}^2-I_{bx}/L_{bx}^2)L_{bx}\cdot\ddot{\phi}_b\\
&-(C_{FL}+C_{FR}-C_{RL}-C_{RR})\cdot(\dot{z}_b-L_{bx}\cdot\dot{\phi}_b)\\
&-(C_{FL}-C_{FR}+C_{RL}-C_{RR})\cdot(\dot{z}_b-L_{by}\cdot\dot{\psi}_b)\\
&=-(C_{FL}\cdot\dot{z}_{t1L}+K_P\cdot z_{t1L})+(C_{FR}\cdot\dot{z}_{t1R}+K_P\cdot z_{t1R})\\
&+(C_{RL}\cdot\dot{z}_{t2L}+K_P\cdot z_{t2L})+3(C_{RR}\cdot\dot{z}_{t2R}+K_P\cdot z_{t2R})+\Sigma F_1-\Delta F_1
\end{aligned}
\tag{5.11}
$$

Then, by substituting equations (5.5) - (5.7) into to equations (5.8) - (5.11) removes the bounce, pitch and roll motions, the relationship of the four corner accelerations can be formed and their simplified expressions are given in equations (5.12) - (5.15).

$$
\begin{aligned}
&(3I_{by}/L_{by}^2+m_b)/4\cdot\ddot{z}_{FL}+(2C_{FL}+C_{FR}+C_{RL})\cdot\dot{z}_{FL}+4K_P\cdot z_{FL}\\
&-(I_{by}/L_{by}^2-m_b)/4\cdot\ddot{z}_{FR}+(C_{FL}+C_{FR}-C_{RL}-C_{RR})/2\cdot\dot{z}_{FR}\\
&-(I_{by}/L_{by}^2-m_b)/4\cdot\ddot{z}_{RL}+(C_{FL}-C_{FR}+C_{RL}-C_{RR})/2\cdot\dot{z}_{RL}\\
&-(I_{by}/L_{by}^2-m_b)/4\cdot\ddot{z}_{RR}\\
&=(3C_{FL}\cdot\dot{z}_{t1L}+C_{FR}\cdot\dot{z}_{t1R}+C_{RL}\cdot\dot{z}_{t2L}-C_{RR}\cdot\dot{z}_{t2R})\\
&+K_P(3z_{t1L}+z_{t1R}+z_{t2L}-z_{t2R})+\Sigma F_1+\Delta F_1
\end{aligned}
\tag{5.12}
$$

$$
\begin{aligned}
&(3I_{by}/L_{by}^2+m_b)/4\cdot\ddot{z}_{FR}+(C_{FL}+2C_{FR}+C_{RR})\cdot\dot{z}_{FR}+4K_P\cdot z_{FR}\\
&-(I_{by}/L_{by}^2-m_b)/4\cdot\ddot{z}_{FL}+(C_{FL}+C_{FR}-C_{RL}-C_{RR})/2\cdot\dot{z}_{FL}\\
&-(I_{by}/L_{by}^2-m_b)/4\cdot\ddot{z}_{RL}\\
&-(I_{by}/L_{by}^2-m_b)/4\cdot\ddot{z}_{RR}-(C_{FL}-C_{FR}+C_{RL}-C_{RR})/2\cdot\dot{z}_{RR}\\
&=(C_{FL}\cdot\dot{z}_{t1L}+3C_{FR}\cdot\dot{z}_{t1R}-C_{RL}\cdot\dot{z}_{t2L}+C_{RR}\cdot\dot{z}_{t2R})\\
&+K_P(z_{t1L}+3z_{t1R}-z_{t2L}+z_{t2R})+\Sigma F_1-\Delta F_1
\end{aligned}
\tag{5.13}
$$

$$
\begin{aligned}
&(3I_{by}/L_{by}^2 + m_b)/4 \cdot \ddot{z}_{RL} + (C_{FL} + 2C_{RL} + C_{RR}) \cdot \dot{z}_{RL} + 4K_P \cdot z_{RL} \\
&-(I_{by}/L_{by}^2 - m_b)/4 \cdot \ddot{z}_{FL} + (C_{FL} - C_{FR} + C_{RL} - C_{RR})/2 \cdot \dot{z}_{FL} \\
&-(I_{by}/L_{by}^2 - m_b)/4 \cdot \ddot{z}_{FR} \\
&-(I_{by}/L_{by}^2 - m_b)/4 \cdot \ddot{z}_{RR} - (C_{FL} + C_{FR} - C_{RL} - C_{RR})/2 \cdot \dot{z}_{RR} \\
&= (C_{FL} \cdot \dot{z}_{t1L} - C_{FR} \cdot \dot{z}_{t1R} + 3C_{RL} \cdot \dot{z}_{t2L} + C_{RR} \cdot \dot{z}_{t2R}) \\
&+ K_P(z_{t1L} - z_{t1R} + 3z_{t2L} + z_{t2R}) + \Sigma F_1 + \Delta F_1
\end{aligned}
\tag{5.14}
$$

$$
\begin{aligned}
&(3I_{by}/L_{by}^2 + m_b)/4 \cdot \ddot{z}_{RR} + (C_{FL} + C_{RL} + 2C_{RR}) \cdot \dot{z}_{RR} + 4K_P \cdot z_{RR} \\
&-(I_{by}/L_{by}^2 - m_b)/4 \cdot \ddot{z}_{FL} \\
&-(I_{by}/L_{by}^2 - m_b)/4 \cdot \ddot{z}_{FR} - (C_{FL} - C_{FR} + C_{RL} - C_{RR})/2 \cdot \dot{z}_{FR} \\
&-(I_{by}/L_{by}^2 - m_b)/4 \cdot \ddot{z}_{RL} - (C_{FL} + C_{FR} - C_{RL} - C_{RR})/2 \cdot \dot{z}_{RL} \\
&= (-C_{FL} \cdot \dot{z}_{t1L} + C_{FR} \cdot \dot{z}_{t1R} + C_{RL} \cdot \dot{z}_{t2L} + 3C_{RR} \cdot \dot{z}_{t2R}) \\
&+ K_P(-z_{t1L} + z_{t1R} + z_{t2L} + 3z_{t2R}) + \Sigma F_1 - \Delta F_1
\end{aligned}
\tag{5.15}
$$

For the four corner accelerations under the normal condition, there are little interactions among them due to the balance in the design which is symmetric in structure and in which identical components are commonly used, as shown in equations (5.12) - (5.15). Apart from that, the corner accelerations are also caused by the non-uniform distribution of the bogie mass ($I_{by}/L_{by}^2 \neq m_b$) and the effect of the forces from the secondary suspensions.

From equations (5.12) - (5.15), it is clear that the four track inputs for each corner accelerations are not equally distributed. The track input at the suspension concerned is three times the magnitude compared to the others that are not directly connected. The random track inputs at both sides of a track are normally expected to have similar magnitude and frequency distributions, so the overall response of the four corner suspensions should present a very similar variance with only a time shift between leading and trailing suspensions. Unless a suspension fault occurs, the variance change of the bogie acceleration will be expected to be very small. This characteristic will be used in the following detection scheme and the changes of the variances at the corner accelerations will be used to determine the health condition for the studied suspensions.

The concept of variance change detection is investigated using the same leading primary suspension system which is specified in Figure 2.5. A schematic diagram of the technique is shown in Figure 5.1, with three stages included in the implementation.

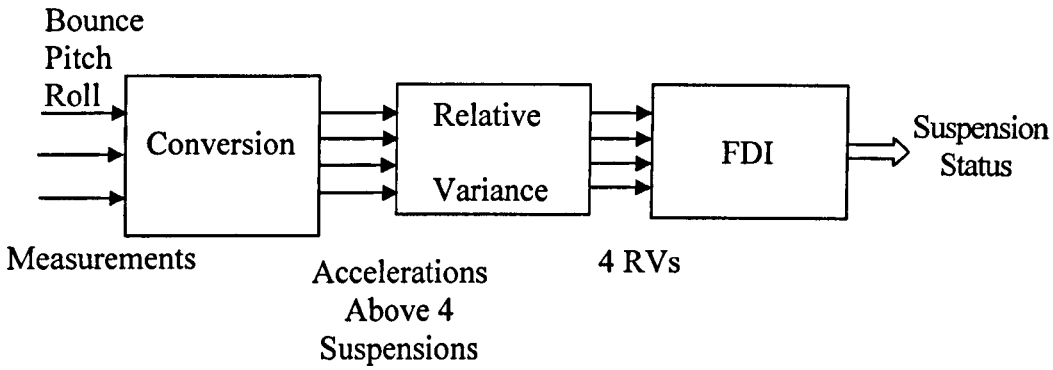

Figure 5.1 Schematic Diagram of FDI Using Relative Variance

The first stage is to derive the four corner accelerations from the basic bounce, pitch and roll motions, which can be measured with a single sensor box, using equations (5.1) - (5.4). Secondly the variances of the four accelerations can be estimated over a fixed number n by buffering the samples of the derived accelerations in a fixed time window, as shown in equations (5.16) - (5.19).

$$V_{FL}(k) = \sum_{i=k}^{k+n-1} (\ddot{z}_{FL}(i) - \overline{\ddot{z}_{FL}})^2 \Big/ n \tag{5.16}$$

$$V_{FR}(k) = \sum_{i=k}^{k+n-1} (\ddot{z}_{FR}(i) - \overline{\ddot{z}_{FR}})^2 \Big/ n \tag{5.17}$$

$$V_{RL}(k) = \sum_{i=k}^{k+n-1} (\ddot{z}_{RL}(i) - \overline{\ddot{z}_{RL}})^2 \Big/ n \tag{5.18}$$

$$V_{RR}(k) = \sum_{i=k}^{k+n-1} (\ddot{z}_{RR}(i) - \overline{\ddot{z}_{RR}})^2 \Big/ n \tag{5.19}$$

where k is the step for each set of the sampling acceleration, n is the number of samples in the time window.

Then the FDI problem may be investigated by using variance estimation over a running time window, as for the cross correlation evaluation. It is possible to use the variance values in fault detection, as any changes in the suspensions will influence the bogie accelerations especially at the location where a faulty component is directly connected. However the direct use of the variance values will be affected by changes in external conditions in the same way as in the previous scheme with the direct use of cross correlation calculations, because the variance values can be affected by the track inputs which are non-deterministic and may vary in different time periods. Also, the change of railway vehicle speeds causes different input excitations to the suspensions and consequently affects directly variance changes. It is impractical to measure the track inputs directly or to predict their changes in magnitude under different locations and at different speeds. However, because all suspensions are assumed to have the same configuration and components under the normal conditions, the variance for each corner acceleration will be similar when the studied suspensions are excited by the same set of track inputs. On the other hand, the variance of one corner acceleration located above a faulty suspension will have a distinct change compared to the others. Therefore, the variance disturbance problem due to external conditions may be overcome by comparing the four outputs of the variance calculations using the concept of majority 'voting', as the variance values should be similar under nominal conditions but differ if there is a fault at one or more of the suspensions - as far as the probability of all the four suspensions failing at the same time in the same manner would be extremely low. The process of 'voting' is achieved/simplified through the use of normalisation similar to that for the cross correlations, as shown in equations (5.20) - (5.23). The normalisation essentially provides a means of relation comparison of the variances of the bogie

accelerations above the four accelerations, without the need to examine directly the difference between them.

$$RV_{FL}(k) = \frac{4 \times V_{FL}(k)}{V_{FL}(k) + V_{FR}(k) + V_{RL}(k+m) + V_{RR}(k+m)} \tag{5.20}$$

$$RV_{FR}(k) = \frac{4 \times V_{FR}(k)}{V_{FL}(k) + V_{FR}(k) + V_{RL}(k+m) + V_{RR}(k+m)} \tag{5.21}$$

$$RV_{RL}(k) = \frac{4 \times V_{RL}(k)}{V_{FL}(k-m) + V_{FR}(k-m) + V_{RL}(k) + V_{RR}(k)} \tag{5.22}$$

$$RV_{RR}(k) = \frac{4 \times V_{RR}(k)}{V_{FL}(k-m) + V_{FR}(k-m) + V_{RL}(k) + V_{RR}(k)} \tag{5.23}$$

where m is the number of delayed sampling time steps which is decided by the wheel space and the vehicle speed.

It is noted that the relative variance calculations at the two rear suspensions in equations (5.22) and (5.23) are almost identical to those for the two front suspensions in equations (5.20) and (5.21) except for a delayed time interval m. As m is the exact time delay of the track inputs between the front and rear suspensions, these four equations (5.20) - (5.23) should always give the normalised variances for the same track input conditions. The relative variance for each corner acceleration will remain largely similar under the normal condition even when the railway vehicle speed changes. Only a fault in a component (e.g., a damper fault pre-assumed in this thesis) is expected to cause relevant changes to their relative variances. The most significant variance change is expected to coincide with the fault at the particular suspension and therefore fault isolation will also be possible.

5.3 Performance Assessments

In this section, simulations are carried out to assess the performance of the proposed supplementary fault detection technique. The running RMS and variance values of the corner accelerations are given for comparison, and the performances of their relative variances are assessed under different operational conditions. The inclusion of RMS results in the study is to demonstrate the improved fault detection sensitivity of the new scheme.

5.3.1 Fault Detection Using RMS Values

Case 5.1: front left damper has 50% damping loss.

Computations: running RMS of front left acceleration at 50m/s (2s of data)

running RMS of front left acceleration at 25m/s (2s of data)

In Figure 5.2, the RMS value of the front left acceleration shows a clear difference between the normal and fault conditions. At a higher speed of 50m/s, the RMS value of the front left acceleration decreases from around $11 m/s^2$ to $8.5 m/s^2$ ($2.5 m/s^2$ reduction) when the fault occurs. It is known that a reduced damping increases resonances for the basic bogie motions, but suppresses higher frequency content more severely, which results in an overall reduced acceleration for the random track inputs [61]. The accelerations above the other three suspensions remain largely unchanged, which is expected because of the location of the only fault assumed in this case.

At the lower speed of 25m/s, a similar pattern of RMS changes can be observed in Figure 5.3. However, the magnitude of the change is less, its RMS value only decreases from $7.8 m/s^2$ to $6 m/s^2$ ($1.8 m/s^2$ reduction). The difference of the RMS value and also its reduction at the lower speed is expected because of the smaller track irregularities. This could make fault detection difficult to determine as the RMS reductions are more dependent on the operational conditions.

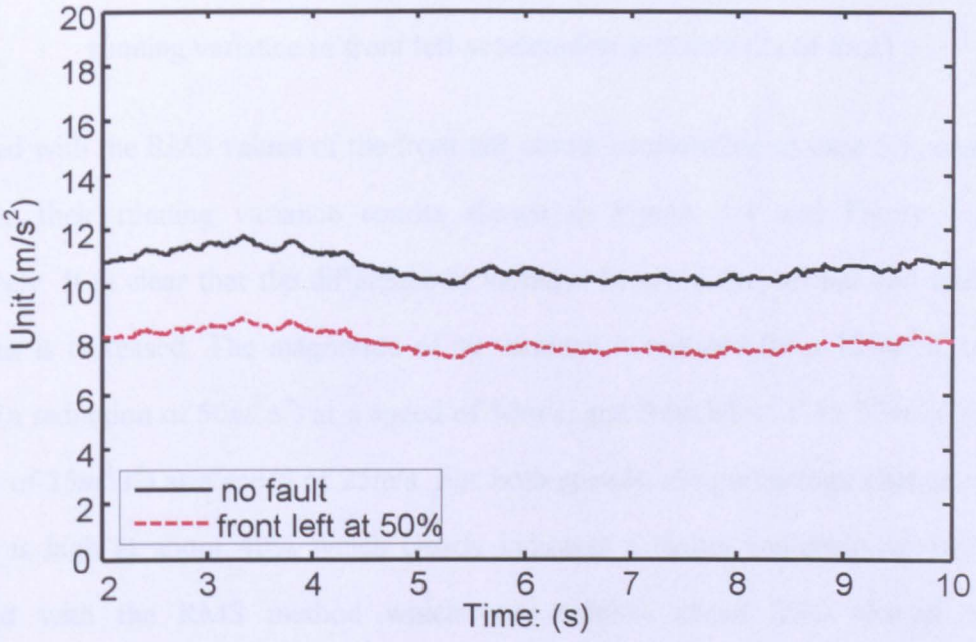

Figure 5.2 Running RMS of front left acceleration for case 5.1 at 50m/s

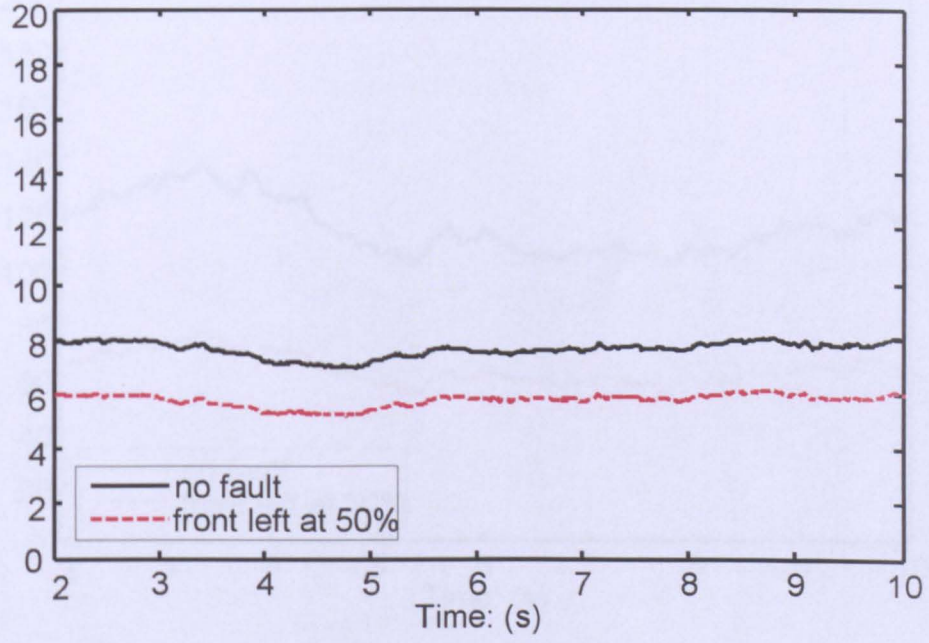

Figure 5.3 Running RMS of front left acceleration fro case 5.1 at 25m/s

5.3.2 Fault Detection Using Variance Values

Case 5.2: front left damper has 50% damping loss.

Computations: running variance of front left acceleration at 50m/s (2s of data)

running variance of front left acceleration at 25m/s (2s of data)

Compared with the RMS values of the front left corner acceleration in case 5.1, case 5.2 gives their running variance results shown in Figure 5.4 and Figure 5.5 respectively. It is clear that the difference in variance between the normal and fault conditions is increased. The magnitude of its variance is reduced from $120m^2/s^4$ to $70m^2/s^4$ (a reduction of $50m^2/s^4$) at a speed of 50m/s, and from $62m^2/s^4$ to $37m^2/s^4$ (a decrease of $25m^2/s^4$) at a speed of 25m/s. For both speeds, the percentage change in variance is high at about 40% which clearly indicates a higher sensitivity to fault compared with the RMS method which only exhibits about 20% change in magnitude. There are also changes to the other corner accelerations, but they are smaller for similar reasons as for the RMS calculation.

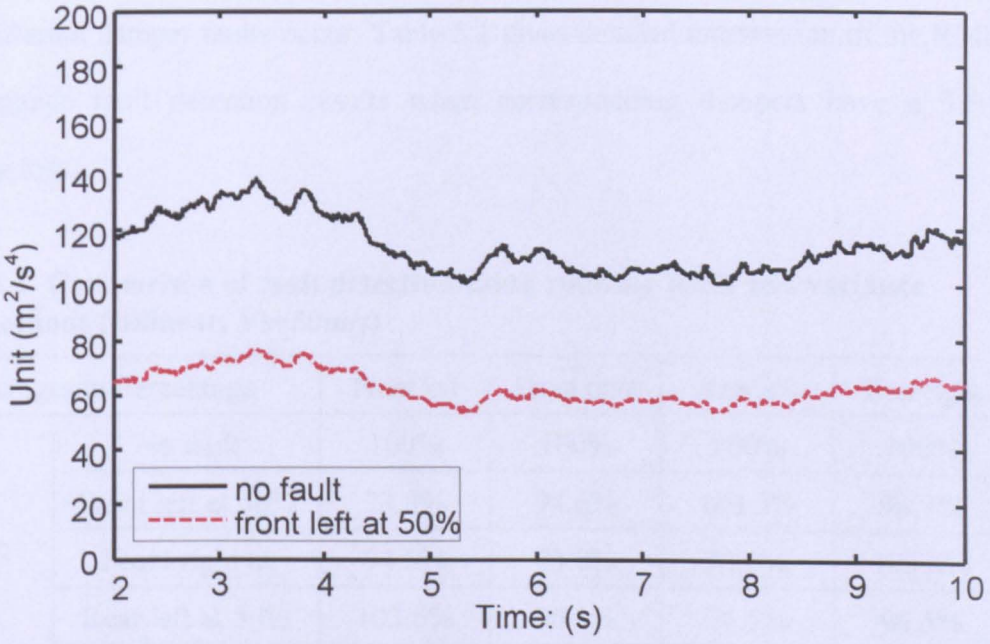

Figure 5.4 Running variance of front left acceleration for case 5.2 at 50m/s

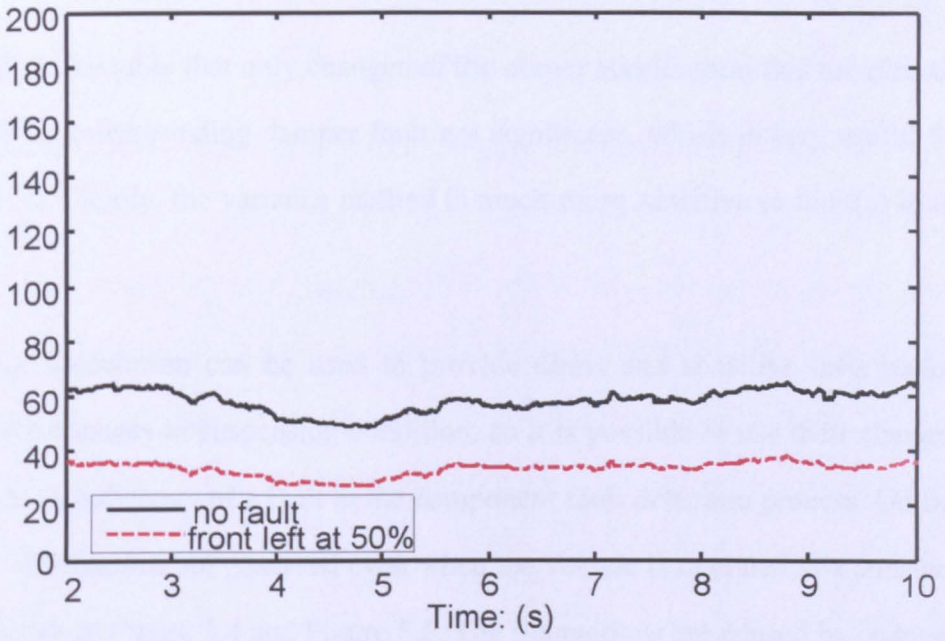

Figure 5.5 Running variance of front left acceleration for case 5.2 at 25m/s

A similar pattern of changes for the other corner accelerations can also be observed when different damper faults occur. Table 5.1 gives detailed information of the RMS and variance fault detection results when corresponding dampers have a 50% damping loss.

Table 5.1 Comparison of fault detection using running RMS and variance methods (Bilinear, Vs=50m/s)

Changes in Percentage		Front left	Front right	Rear left	Rear right
RMS	No fault	100%	100%	100%	100%
	Front left at 50%	73.8%	94.6%	103.5%	93.7%
	Front right at	94.5%	73.8%	93.6%	103.4%
	Rear left at 50%	103.6%	96.3%	76.5%	94.5%
	Rear right at 50%	95.9%	103.8%	94.7%	76.2%
Variance	No fault	100%	100%	100%	100%
	Front left at 50%	54.5%	89.6%	107.1%	87.8%
	Front left at 50%	89.3%	54.5%	87.7%	107.0%
	Front left at 50%	107.3%	92.7%	58.6%	89.3%
	Front left at 50%	92.0%	107.8%	89.7%	58.1%

It is clear from the table that only changes of the corner acceleration that are directly related to their corresponding damper fault are significant, which is very useful for fault isolation. Clearly, the variance method is much more sensitive to fault(s) in all cases.

The variance calculation can be used to provide direct and sensitive information relating to the changes in suspension condition, so it is possible to use their changes in magnitude as indicators of a fault in the component fault detection process. On the other hand, fluctuations are observed even when the vehicle is operated at a constant speed, as shown in Figure 5.4 and Figure 5.5. The fluctuations are caused by changes in track input irregularities, especially where low frequency components become more dominant. Due to the uncertainty, it may not always be clear that a fault has occurred for a higher RMS or variance value under the normal conditions or a lower value under the fault conditions. Similar to the fault detection using the CCF value for the bounce, pitch and roll motions, the selection of the fault detection thresholds will have to be highly adaptive to both vehicle speed and track conditions which would not be straight forward to achieve in practical applications [71] [72].

5.3.3 Fault Detection Using Relative Variance

The proposed use of relative variance (i.e., normalised) in equations (5.20) - (5.23) is intended to overcome the problem. It minimizes the influences associated with the variation in track irregularities and the difference in travel speeds, as all variance calculations are normalised over four accelerations which effectively removes the effects of external conditions.

Case 5.3: front left damper has 50% damping loss.

Computations: running relative variance of front left acceleration at 50m/s (2s of data)

running relative variance of front left acceleration at 25m/s (2s of data)

Figure 5.6 and Figure 5.7 show the running relative variance for case 5.3 at the two different speeds. At either speed, the relative variance results show two advantages compared with variance value evaluation. Firstly, their relative variances are much smoother under both the normal and fault conditions, the fluctuation seen in the variance values is much less significant. Secondly the relative variances have a similar reduction from 1 to around 0.6 ~ 0.7 (a reduction of 30% ~ 40%) regardless of the speed changes. This improved robustness against external condition changes is very beneficial in fault detection processing, as the selection and tuning of the thresholds will be comparatively easier when applied with the relative variance approach.

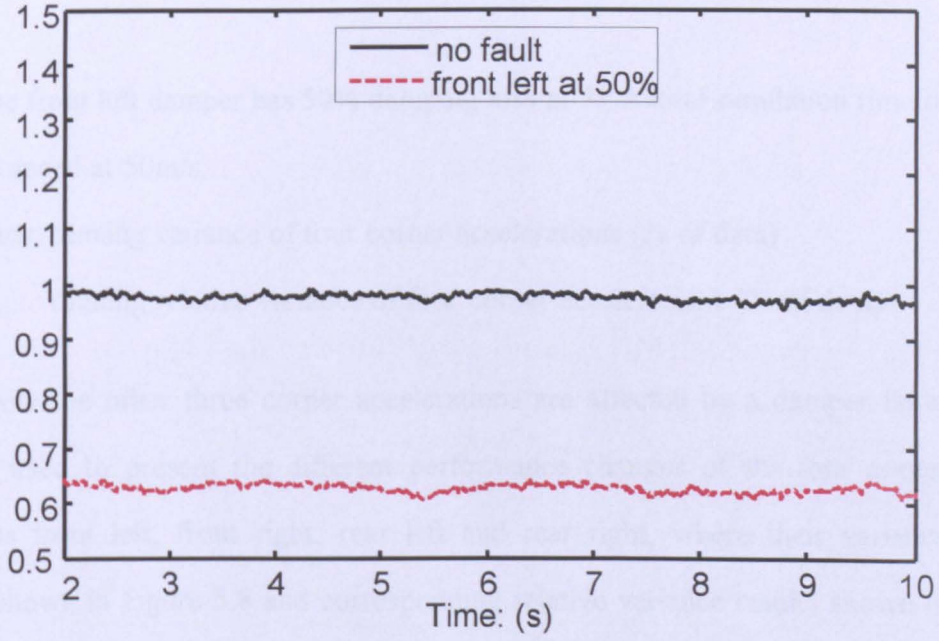

Figure 5.6 Running relative variance of front left acceleration for case 5.3 at 50m/s

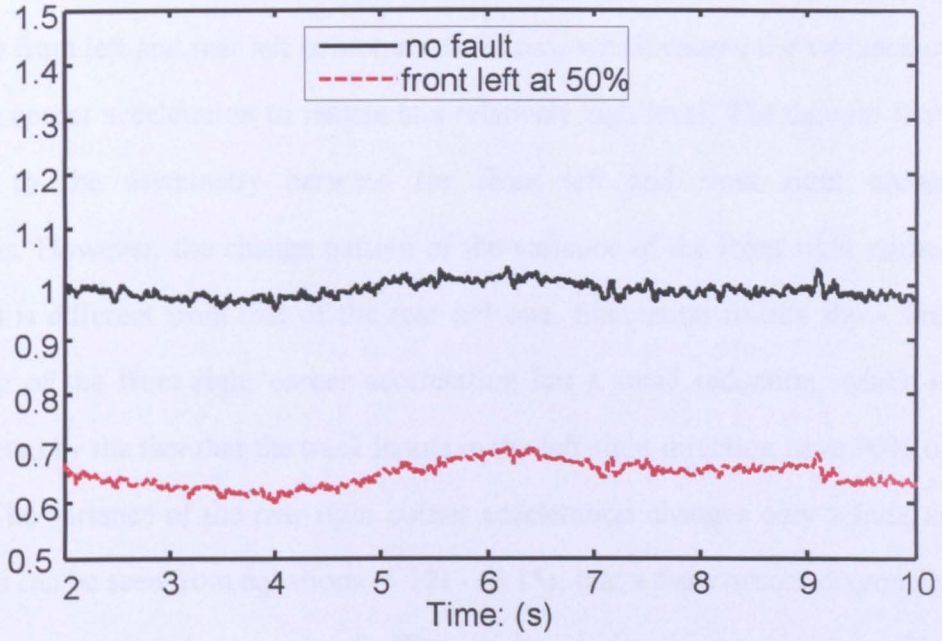

Figure 5.7 Running relative variance of front left acceleration for case 5.3 at 25m/s

Case 5.4: the front left damper has 50% damping loss at 5s, a total simulation time of 10s, vehicle speed at 50m/s.

Computations: running variance of four corner accelerations (2s of data)

running relative variance of four corner accelerations (2s of data)

To study how the other three corner accelerations are affected by a damper fault, case 5.4 is used to present the different performance changes of the four corner accelerations front left, front right, rear left and rear right, where their variance results are shown in Figure 5.8 and corresponding relative variance results shown in Figure 5.9.

In Figure 5.8, it can be seen that the variance for the four corner accelerations are very similar under the normal condition (0-5s). However, it is observed that an overall reduction of the system damping after 5s due to the damper fault at the front left suspension is observed, leading to the magnitude of variances of the four corner accelerations being reduced. The variance of the front left corner acceleration has the

largest reduction as expected. The front left damper fault causes an unbalance between the front left and rear left corner accelerations, which causes the variance of the rear left corner acceleration to remain at a relatively high level. The damper fault also leads to the asymmetry between the front left and front right corner accelerations. However, the change pattern of the variance of the front right corner acceleration is different from that of the rear left one. Simulation results show that the variance of the front right corner acceleration has a small reduction, which is mainly affected by the fact that the track inputs in the left-right direction have 90% of similarity. The variance of the rear right corner acceleration changes only a little as expected, as can be seen from equations (5.12) - (5.15), that a fault occurs diagonally across in the suspensions has very small effect on the acceleration at this point. The understanding of their corner acceleration changes in variance is helpful in recognising the different performances of the relative variances normalised from their variance combinations, even when the fault conditions are changed.

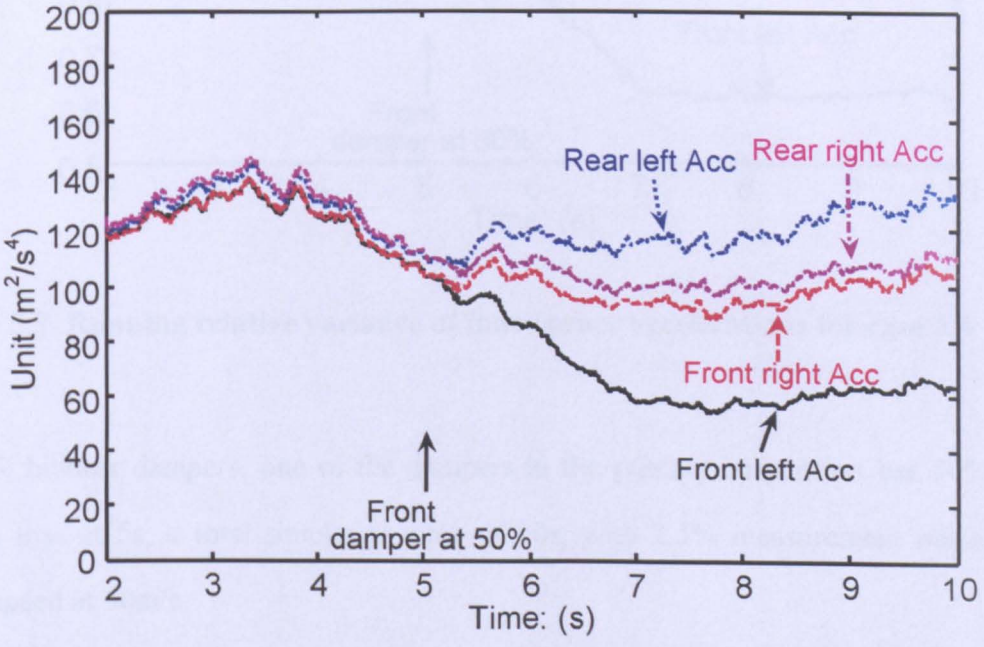

Figure 5.8 Running variance of four corner accelerations for case 5.4

In Figure 5.9, it is observed that the relative variance of the front left corner acceleration is the most sensitive to the fault for obvious reasons. Its magnitude has a significant reduction of 40%. There are also smaller changes in the other three relative variances. The relative variances of the front right and rear right corner accelerations are only slightly varied whereas that of the rear left corner acceleration is increased by 20% - 30%. The increase of the relative variance of rear left corner acceleration is because its variance is the largest in the fault condition shown in Figure 5.8.

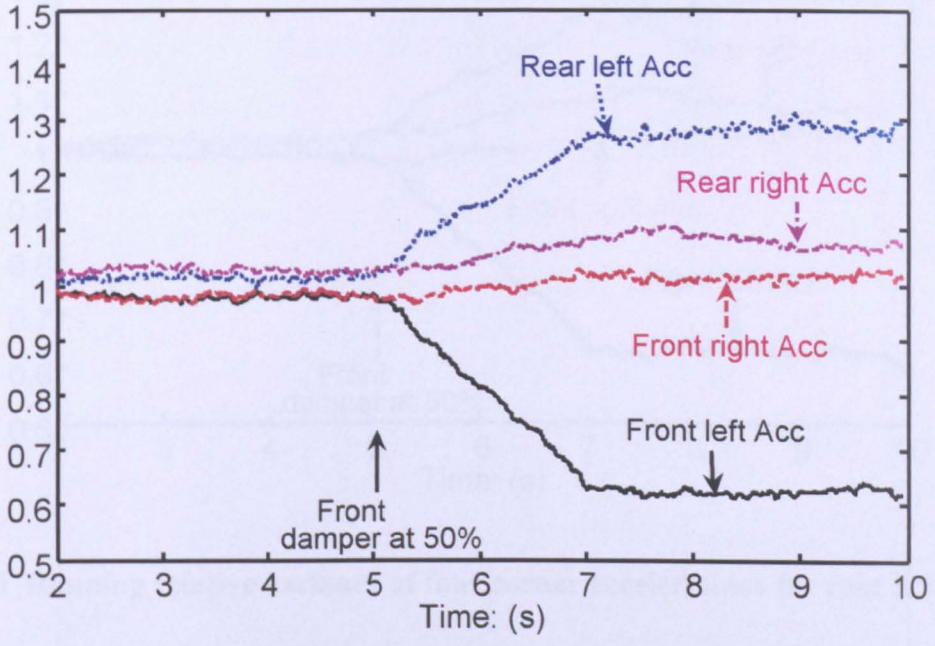

Figure 5.9 Running relative variance of four corner accelerations for case 5.4

Case 5.5: bilinear dampers, one of the dampers in the primary suspension has 50% damping loss at 5s, a total simulation time of 10s, with 2.5% measurement noise, vehicle speed at 50m/s.

Computations: running relative variance of four corner accelerations with fault occurred in the front left damper (2s of data)

The issue of measurement noise and its performance with bilinear dampers are also considered. Figure 5.10 shows the relative variance results in detecting the bilinear

damper fault occurred in the front left damper, with an additional 2.5% measurement noise on all the corner accelerations. It is clear from Figure 5.10 of case 5.5 that the outcomes have a consistent match with those relative variance changes in Figure 5.9, hence the effects of measurement noise on the relative variance detection method is very low. It is also shown that it can work effectively in both linearised and non-linear systems.

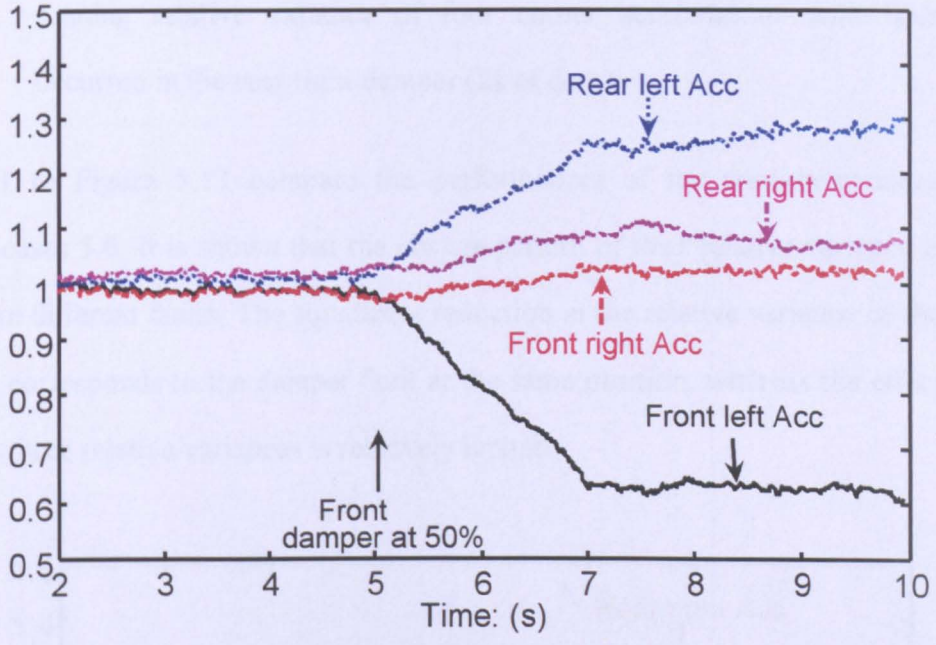

Figure 5.10 Running relative variance of four corner accelerations for case 5.5

5.4 Fault Isolation

The proposed relative variance approach is not only valid for detecting suspension faults, but also useful in their isolation. This is due to the strong link between the relative variance of any particular acceleration and the corresponding suspension. To outline this, the cases of one single damper fault occurring separately in the other three suspensions are also studied by evaluating their relative variance changes.

Case 5.6: bilinear dampers, one of the dampers in the primary suspension has 50% damping loss at 5s, a total simulation time of 10s, with 2.5% measurement noise, vehicle speed at 50m/s.

Computations: running relative variance of four corner accelerations with fault occurred in the front right damper (2s of data)

running relative variance of four corner accelerations with fault occurred in the rear left damper (2s of data)

running relative variance of four corner accelerations with fault occurred in the rear right damper (2s of data)

Figures 5.11 to Figure 5.13 compare the performances of the relative variance changes for cases 5.6. It is shown that the change pattern of their relative variance is different from different faults. The significant reduction in the relative variance of the acceleration corresponds to the damper fault at the same position, whereas the effect on the other three relative variances is relatively limited.

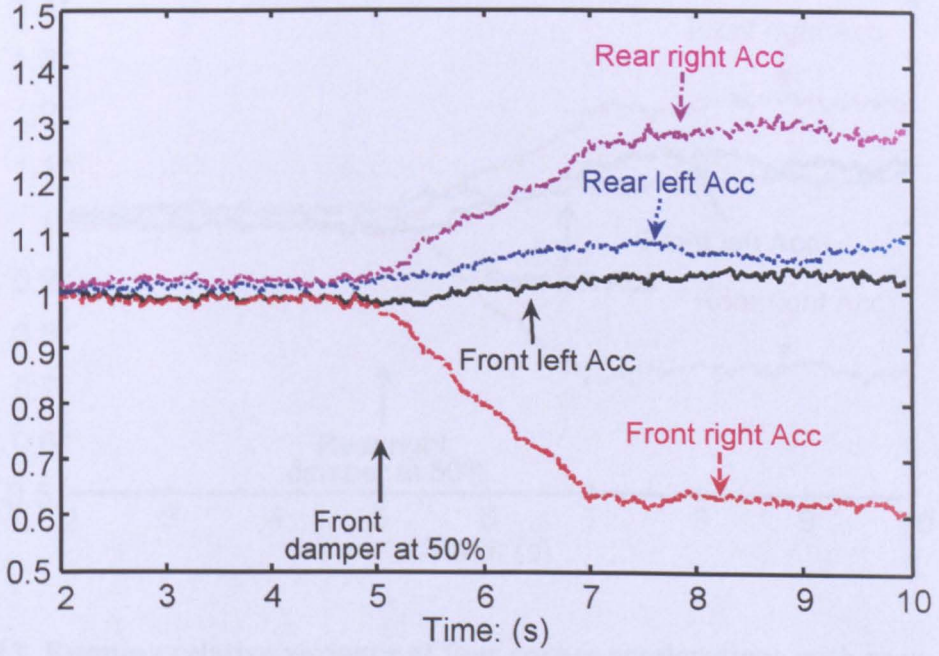

Figure 5.11 Running relative variance of four corner accelerations with front right damper fault in case 5.6

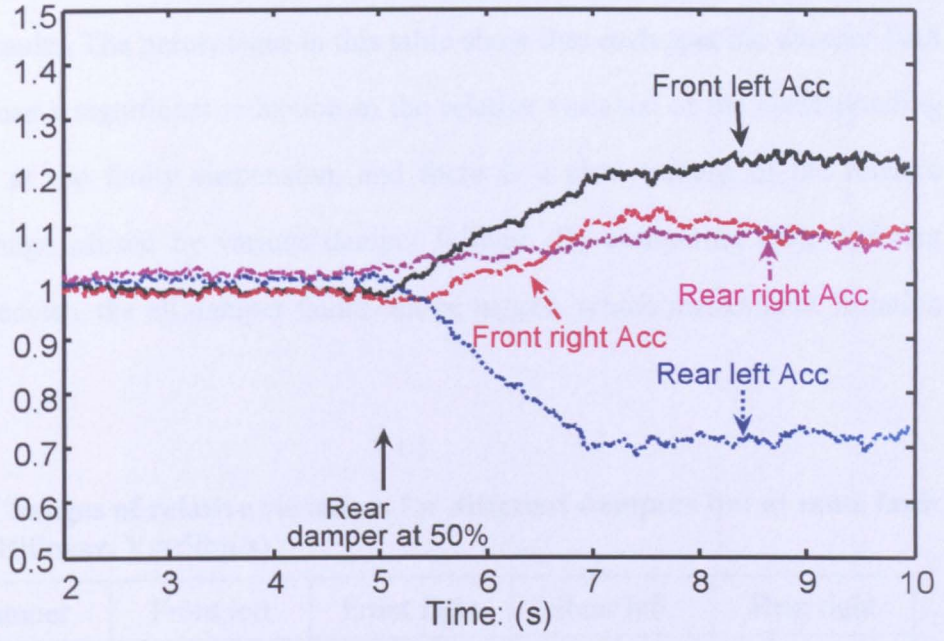

Figure 5.12 Running relative variance of four corner accelerations with rear left damper fault in case 5.6

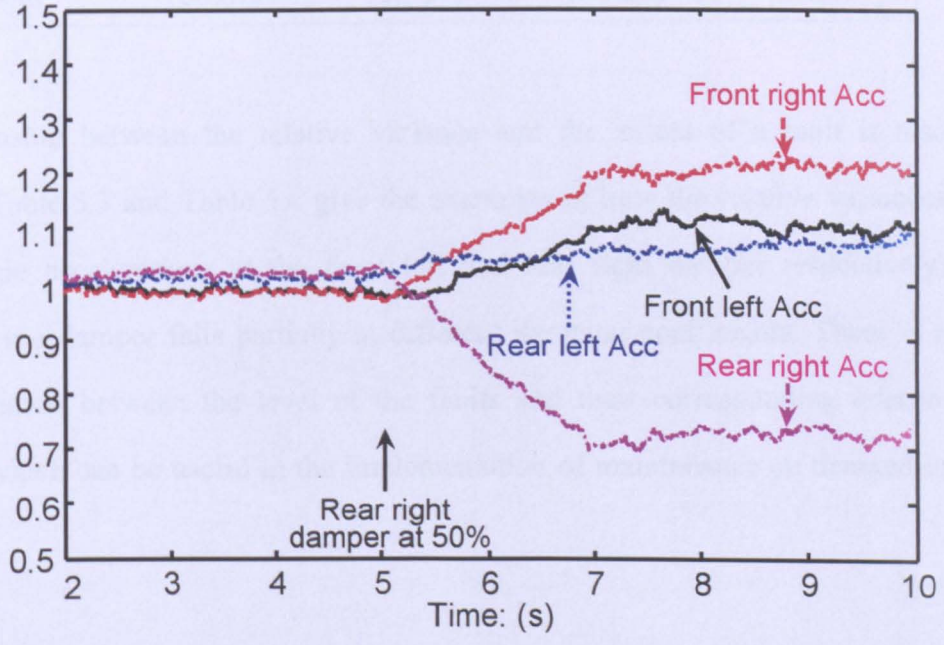

Figure 5.13 Running relative variance of four corner accelerations with rear right damper fault in case 5.6

Table 5.2 confirms how the relative variance performances are affected by each of the

Table 5.2 confirms how the relative variance performances are affected by each of the damper faults. The percentages in this table show that each specific damper fault will only cause a significant reduction in the relative variance of the corresponding acceleration at the faulty suspension, and there is a clear pattern of the relative variance change caused by various damper failures. By comparing their different change tendencies, the all damper faults can be tagged, which makes fault isolation possible.

Table 5.2 Changes of relative variances for different dampers but at same fault level (Bilinear, Vs=50m/s)

Faulty damper	Front left	Front right	Rear left	Rear right
No fault	99.2%	99.8%	100.2%	100.9%
Front left	64.4%	104.3%	125.6%	105.7%
Front right	103.7%	64.7%	105.9%	125.6%
Rear left	121.2%	107.9%	67.7%	103.2%
Rear right	106.6%	122.6%	103.2%	67.6%

The relationship between the relative variance and the extent of a fault is also evaluated. Table 5.3 and Table 5.4 give the examples of how the relative variances (of the bogie accelerations at the front left and rear right damper respectively) change when a damper fails partially at different damping coefficients. There is a clear correlation between the level of the faults and their corresponding relative variances, which can be useful in the implementation of maintenance on demand in the future.

Table 5.3 Changes of relative variances for front left damper faults at different levels (Bilinear, Vs=50m/s)

Front left	Front left	Front right	Rear left	Rear right
75%	80.5%	103.3%	113.3%	102.8%
50%	64.4%	104.3%	125.6%	105.7%
25%	52.4%	102.6%	135.8%	109.3%
0%	47.5%	97.0%	141.3%	115.1%

Table 5.4 Changes of relative variances for rear right damper faults at different levels (Bilinear, Vs=50m/s)

Rear right	Front left	Front right	Rear left	Rear right
75%	102.3%	111.7%	103.0%	83.0%
50%	106.6%	122.6%	103.2%	67.6%
25%	111.2%	131.6%	100.0%	57.0%
0%	115.8%	137.6%	94.4%	50.1%

5.5 Summary

This chapter has presented a supplementary and similarly convenient fault detection scheme focused on the comparison of the different behaviours of the bogie corner accelerations. Different with the cross correlation method which investigates the dynamic interaction change between the basic bogie motions, the relative variance approach studies the relationship of corner acceleration changes in variance under different fault conditions. Calculation and comparison of their relative variances at all the four suspensions reveal a close link between their changes and different fault conditions, which can be used as an easy way for both fault detection and isolation in suspension systems.

The feasibility of this technology is evaluated in different conditions and with measurement noise for non-linearity in the system. Similar with the FDI performance

using normalised CCF, their results also show the effectiveness and robustness of the technique as the FDI problem can be simply solved by comparing the relative variances in most cases, without detailed knowledge of the bogie and external conditions.

Chapter 6

Conclusions and Future Work

This dissertation is summarised in section 6.1, and future work is proposed in section 6.2.

6.1 Conclusions

Focused mainly on the primary suspensions of a conventional bogie railway vehicle, this research has investigated a novel fault detection and isolation technique, which is expected to provide improved sensitivity to component faults in the railway suspension systems. The research methodology is detailed in the chapters and brief summaries are given here.

Firstly, a side view of a simple bogie and a side and end view of a conventional railway bogie vehicle were modelled. The suspension systems were reviewed, with emphasis on the primary suspensions, and the response of the bogie and carbody in the vertical direction was investigated using a series of irregular track inputs. As the railway vehicle with conventional bogie design is very popular for passenger vehicles, its study is essential for improving condition monitoring techniques.

Secondly, based on the simple bogie model, the basic concept of the proposed fault detection scheme was investigated. The study of the mathematical model revealed an important property of the vehicle, where symmetric components are commonly used. The analysis of its dynamic equations shows their basic motions have minimum interactions unless there is a fault which may deteriorate the balance and magnify their interactions. The introduction of cross correlation technology can effectively

improve the detection ability and sensitivity, by detecting the changes caused by the faulty suspension component at specific time shifts.

Thirdly the cross correlation was studied in order to detect a primary suspension component fault. Attention was mainly paid to the damper failure in the primary suspension as this is the most common component fault in railway suspensions. The basic bounce, pitch and roll motions in the vertical direction were measured directly, and fault detection was carried out by the correlation computation between the selected motions with filtering. The performance of fault detection using this approach was studied between different bogie motions and under different conditions, the simulation results showed that faults could be detected quickly on the basis of their corresponding correlation changes. Fault detection performance was further improved by introducing normalised cross correlation (CCF coefficient), which can overcome the influence of track irregularities on geometry and speed change. The CCF coefficient is more robust and effective than the CCF value. The cross correlation approach also exhibits good performance in dealing with noisy measurements, performs well in non-linear vehicle systems and also gives equal detection ability for faults occurred in both bogie, which shows the feasibility and potential for practical usage.

In addition, a supplementary approach using relative variance was studied. It focused on the corner suspension accelerations derived from the basic bogie motions. It was also simply in implementation and sensitive to suspension faults. Affected by a damper fault, the dynamics and asymmetry of the corner accelerations may change compared with the nominal fault-free condition. The relationship of their relative variance changes with the suspension health status was analysed. The detections were processed under different fault conditions, and their simulation results showed that the relative variance approach was as robust as that of the normalised cross correlation approach. It was also proved a reliable method of faults in noisy measurement environments and for non-linear systems.

Finally, the fault isolation scheme was developed, in which the results of either cross correlation or relative variance changes were not only sensitive in fault detection but also beneficial in fault isolation as each of them is specifically partial to different suspension changes. The performance of fault isolation was evaluated in different fault conditions; the pattern of their changes for a designated fault was found to be unique which indicates that an individual fault can be isolated from the different change patterns. Using a running scheme, both fault detection and isolation could be achieved after 2 seconds of the selected time window.

The key points noted from this work can be briefly concluded and highlighted as follows:

(1) A suspension component fault can unbalance the suspension symmetry, leading to increased interactions between the selected features. The interaction can be analysed as a level of indication of the fault.

(2) A fault condition can be detected effectively by monitoring the cross correlation or relative variance changes directly calculated from the motion measurements under different vehicle operation conditions. The cross correlation or relative variance results of different suspension faults show that any individual fault may also be readily isolated by exploring and comparing their different change patterns.

(3) The proposed methods are very sensitive and reliable in distinguishing different fault conditions; the use of normalisation and relative quantities enhance the robustness of the detection schemes against non-fault changes such as the operating speed and statistical non-stationary of the track irregularities.

(4) The scheme is simple as there is no need to model difficult characteristics for complex dynamics. The proposed methods take advantages of the vehicle suspension configurations are often symmetrical, therefore it is largely independent of detailed vehicle profile and parameters, making it easy to implement and tune in practice.

(5) The fault detection and isolation scheme based on cross correlation or relative variance can yield accurate results despite measurement noise from sensors and is also viable for non-linear systems.

(6) The technique may be equally applied to monitor conditions of other suspension systems including lateral primary suspensions, secondary suspensions and possibly extended to report health conditions in other dynamic systems with symmetrical configurations.

6.2 Future Work

Although the methodology has been well studied, and has verified the cross correlation or the relative variance approaches as practical tools for the FDI analysis of suspension systems in railway vehicles, there is still potential for improvement. Future work is therefore needed to develop the generality, improve the accuracy and broaden the applicability. This future work includes:

(1) To assess the detection method for other railway vehicles in order to achieve better and generalised results, this may be applicable to other common passenger railway vehicles, freight wagons and light trams.

(2) To include the present proposal to track irregularity with gradients, from which the dynamics of railway suspension systems may be affected; therefore it is useful to carry out some comparison studies between them.

(3) To verify the accuracy of the proposed approach via experiments, possibly via a scaled-down test rig firstly, and then followed by the experimentation to a real railway vehicle.

References

[1] Goda, K. and Goodall, R.M., Fault Detection and Isolation System for A Railway Vehicle Bogie, *Vehicle System Dynamics*, Vol. 41, Supplement, pp. 468-476, 2004

[2] Bruni, S., Goodall, R., Mei, T.X., Tsunashima, H., Control and Monitoring for Railway Vehicle Dynamics, *Vehicle System Dynamics*, Vol. 45, pp. 743-779, 2007

[3] Patton, R.J., P.M. Frank and R.N. Clark, Fault Diagnosis in Dynamic Systems - Theory and Applications, *Prentice Hall (Control Engineering Series)*, 1989

[4] Deckert, J.C., Desal, M.N., Deyst, J.J. and Willsky, A.S., Dual Redundant Sensor FDI Techniques Applied to the NASA F8C DFBW Aircraft, *AIAA Guidance and Control Conf.* San Diego, CA, 1976

[5] Patton, R.J. and Chen, J., Robust Fault Detection of Jet Engine Sensor System by Eigenstructure Assignment, J. *Guidance, Control & Dynamics*, Vol. 15(6), pp. 1491-1496, 1992

[6] Isermann, R., Diagnosis Methods for Electronic Controlled Vehicles, *Vehicle System Dynamics*, Vol. 36, pp. 77-117, 2001

[7] Isermann, R., Model-based Fault-detection and Diagnosis - Status and Applications, *Annual Reviews in Control*, Vol. 29, pp. 71-85, 2005

[8] Goodall, R.M. and Mei, T.X., Advanced Control and Monitoring for Railway Vehicle Suspensions, *Proceedings of International Symposium on Speed-up ands Service Technology for Railway and Maglev Systems*, STECH'06, pp. 10-16, 2006

[9] Li, P., Goodall, R.M., Weston, P., Ling, C.S., Goodman, C. and Roberts, C., Estimation of Railway Vehicle Suspension Parameters for Condition Monitoring, *Control Engineering Practice*, Vol. 15, pp. 43-55, 2007

[10] Hayashi, Y., Tsunashima, H. and Marumo, Y., Fault Detection of Railway Vehicle Suspensions Using Multiple Model Approach, *SICE Auunal Conference*, Japan, pp. 1540-1543, 2007

[11] Isermann, R., Process Fault Detection Based on Modelling and Estimation Methods - A Survey, *Automatica*, Vol. 20, pp. 387-404, 1984

[12] Patton, R.J., Frank, P.M. and Clark, R.N., Issues of Fault Diagnosis for Dynamic System, *Springer*, 2000

[13] Willsky, A.S., A Survey of Design Methods for Failure Detection in Dynamic System, *Automatica*, Vol. 12, pp. 601-611, 1976

[14] Isermann, R. and Balle, P., Trends in the Application of Model-based Fault Detection and Diagnosis of Technical Process, *Control Engineering Practice*, Vol. 5, No. 5, pp. 709-719, 1997

[15] Tran, T.J. and Zaborszky, J., A Practical Nondiverging Filter, *AIAA Jl*, Vol. 8, pp. 1127-1133, 1970

[16] Jazwinski, A.H., Limited Memory Optimal Filtering, *IEEE Trans. Aut. Control*, Vol. 13, pp. 558-563, 1968

[17] Frssois, S.D. and Sakellariou, J.S., Time-series Methods for Fault Detection and Identification in Vibrating Structures, *Philosophical Transactions of the Royal Society A*, pp. 411-448, 2007

[18] Metallidis, P., Verros, G. and Natsiavas, S., Fault Detection and Optimal Sensor Location in Vehicle Suspensions, *Journal of Vibration and Control*, Vol. 9, pp. 337-359, 2003

[19] Charles, G., Goodall, R.M. and Dixon, R., Model-based Condition Monitoring at the Wheel-rail Interface, *Vehicle System Dynamics*, Vol. 46, Supplement, pp. 415-430, 2008

[20] Tandon, N. and Nakra, B.C., Detection of Defects in Rolling Element Bearings by Vibration Monitoring, *Mechanical Engineering Division*, Vol. 73, pp. 271-282, 1993

[21] Morando L.E., Measuring Shock Pulses Is Ideal for Bearing Condition Monitoring, *Pulp & Paper*, Vol. 62(12), pp. 96-98, 1988

[22] Fong, K.F. and Loh, A.P., A Frequency Domain Approach for Fault Detection, *Proceedings of the 40th IEEE Conference on Decision and Control*, Oriando, USA, pp. 1023-1028, 2001

[23] Weispfenning T., Fault Detection and Diagnosis of Components of the Vehicle Vertical Dynamics, *Meccanica*, Vol. 32, pp. 459-472, 1997

[24] Tandon, N. and Choudhury, A., A review of Vibration and Acoustic Measurement Methods for the Detection of Defects in Rolling Element Bearings, *Tribology International*, Vol. 32, pp. 469-480, 1999

[25] Azadi, S. and Soltani, A., Fault Detection of Vehicle Suspension System Using Wavelet Analysis, *Vehicle System Dynamics*, Vol. 47, No. 4, pp. 403-418, 2009

[26] Bayissa, W.L., Haritos, N. and Thelandersson, S., Vibration-based Structual Damage Identification Using Wavelet Transform, *Mechanical System and Signal Processing*, Vol. 22, pp. 1194-1215, 2008

[27] Scanlan, J. and O'Leary, K., Knowledge-based Process Control for Fault Detection and Classification, *Advanced Process Control and Automation*, Vol. 5044, pp. 139-149, 2003

[28] Zhao, Q. and Xu, Z., Design of a Novel Knowledge-Based Fault Detection and Isolation Scheme, *IEEE Transactions on Systems, Man and Cybernetics- Part B: Cybernetics*, Vol. 34, No. 2, pp. 1089-1095, 2004

[29] Fisher, D., Borner, M., Schmitt, J. and Isermann, R., Fault Detection for Lateral and Vertical Vehicle Dynamics, *Control Engineering Practice*, Vol. 15, pp. 315-324, 2007

[30] Li, P. and Goodall, R.M., Model-based Condition Monitoring for Railway Vehicle Systems, *UKACC 2004*, University of Bath, 2004

[31] Hayash, Y., Tsnashima, H. and Marumo, Y., Fault Detection of Railway Vehicle Using Multiple Model Approach, *SICE-ICASE International Joint Conference*, Korea, pp. 2812-2817, 2006

[32] Gertler, J.J., Fault Detection and Diagnosis in Engineering Systems, *Marcel Dekker Inc.*, New York, 1998

[33] Holfling, T. and Isermann, R., Fault Detection Based on Adaptive Parity Equations and Single-Parameter Tracking, *Control Engineering Practice*, Vol. 4, No. 10, pp.1361-1369, 1996

[34] Hofling, T. and Isermann, R., Parameter Estimation Triggered by Continuous-Time Parity Equations, *Proceedings of the American Control Conference*, Vol. 2, pp. 1145-1146, 1995

[35] Frank, P.M., Fault Diagnosis in Dynamic Systems Using Analytical and Knowledge-based Redundancy- A Survey and Some New Results, *Automation*, Vol. 26, No. 3, pp. 459-474, 1990

[36] Kalman, R.E., A New Approach to Linear Filtering and Prediction Problems, *Transaction of the ASME--Journal of Basic Engineering*, pp. 35-45, 1960

[37] Grewal, M.S. and Andrews, A.P., Kalman Filtering, Theory and Practice, *Prentice-Hall, Inc.*, New Jersey, 1993

[38] Mei, T.X., Li, H. and Goodall, R.M., Kalman Filters Applied to Actively Controlled Railway Vehicle Suspensions, *Transactions of the Institute of Measurement and Control*, Vol. 23, pp. 163-181, 2001

[39] Ljung, L., Asymptotic Behavior of the Extended Kalman Filter as A Parameter Estimator for Linear System, *IEEE Transactions on Automatic Control*, AC-24(1), pp.36-50, 1979

[40] Alessandri, A., Caccia, M. and Veruggio, G., Fault Detection of Actuator Faults in Unmanned Underwater Vehicles, *Control Engineering Practice*, Vol. 7, pp. 357-368, 1999

[41] Patton, R.J., Robustness in Model-based Fault Diagnosis, *International Federation of Automatic Control*, Vol. 21, pp. 103-123, 1997

[42] Himmelblau, D.M., Fault Detection and Diagnosis in Chemical and Petrochemical Processes, *Elsevier Science Publishing Company*, New York, 1978

[43] Ding, X.J. and Mei, T.X., Fault Detection for Vehicle Suspensions Based on System Dynamic Interactions, *UKACC 2008*, University of Manchester, 2008

[44] Feilden, G.B.R., Wickens, A.H. and Yates, I.R., Passenger Transport after 2000 AD, *E&FN Spon Publishing Company*, London, 1995

[45] Okamoto, I. and Wako, K., How Bogies Work, *Japan Railway & Transport Review 18*, pp. 52-61, 1998

[46] Okamoto, I. and Wako, K., Shinkansen Bogies, *Japan Railway & Transport Review 19*, pp. 46-53, 1999

[47] Wickens, A.H., Fundamentals of Rail Vehicle Dynamics: Guidance and Stability. Lisse: *Swets & Zeitlinger BV.*, 2003

[48] Park, B.H. and Lee, K.Y., Bogie Frame Design in Consideration of Fatigue Strength and Weight Reduction, *Proc. IMechE*, Vol. 220, Part F: Rail and Rapid Transit, 2006

[49] Perez, J., Busturia, J.M., Goodall, R.M., Control Strategies for Active Steering of Bogie-based Railway Vehicles, *Control Engineering Practice*, Vol. 10, pp. 1005-1012, 2002

[50] Iwnicki, S., Handbook of Railway Vehicle Dynamics, *Taylor & Francis Groups*, 2006

[51] Eickhoff, B.M., Evans, J.R. and Minnis, A.J., A Review of Modelling Methods for Railway Vehicle Suspension Components, *Vehicle System Dynamics*, Vol. 24, pp. 469-496, 1995

[52] Calarasu, D. and Serbanb, E., Mathematical Model of the Double Effect Telescopic Hydraulic Damper, *The 6th International Conference on Hydraulic Machinery Hydradynamics Timisoara*, pp. 331-334, 2004

[53] Gillespie, T.D., Fundamentals of Vehicle Dynamics, *Society of Automotive Engineers, Inc.*, Warrendale, PA, 1992

[54] Rajamani, R., Vehicle Dynamics and Control, *Springer*, New York, USA, 2006

[55] Ahmed, A.K.W. and Rakhja, S., An Equivalent Linearization technique for the Frequency Response Analysis of Asymmetric Dampers, *Journal of Sound and Vibration*, Vol. 153, pp. 537-542, 1992

[56] Pellegrini, C., Gherardi, F., Spinelli, D., Saporito, G. and Romani, M., Wheel-rail Dynamic of DMU IC4 Car for DSB: Modelling of the Secondary Air Springs and Effects on Calculation Results, *Vehicle System Dynamics*, Vol. 44, Supplement, pp. 433-442, 2006

[57] Quaglia, G. and Soli, M., Air Suspension Dimensionless Analysis and Design Procedure, *Vehicle System Dynamics*, Vol. 35, pp. 443-475, 2001

[58] Docquier, N., Fisette, P. and Jeanmart, H., Multiphysic Modelling of Railway Vehicles Equipped with Pneumatic Suspensions, *Vehicle System Dynamics*, Vol. 45, pp. 505-524, 2007

[59] Perez, J., Busturia, J.B., Mei, T.X. and Vinolas, J., Combined active steering and traction for mechatronic bogie vehicles with independently rotating wheels, *Annual Reviews in Control*, Vol. 28, pp. 207-217, 2004

[60] Kalker, J.J., Survey of Wheel-rail Rolling Contact Theory, *Vehicle System Dynamics*, Vol. 8, pp. 317-358, 1979

[61] Mei, T. X. and Ding, X. J., Condition Monitoring of Rail Vehicle Suspensions Based on Changes in System Dynamic Interactions, *Vehicle System Dynamics*, Vol. 47, pp. 1167-1181, 2009

[62] Bonaventura, C.S., Palese, J.W. and Zarembski, A.M., Intelligent System for Real-Time Prediction of Railway Vehicle Response to the Interaction with Track Geometry, *Railroad Conference 2000, Proceedings of the 2000 ASME/IEEE joint*, Newark, USA, pp. 31-45, 2000

[63] Mei, T. X. and Ding, X. J., A Model-less Technique for the Fault Detection of Rail Vehicle Suspensions, *Vehicle System Dynamics*, Volume 46, Supplement 1, pp. 277-287, 2008

[64] Sun, J.L. and Li, L.Q., Lateral Vibration of Railway Bridge-Vehicle System Caused by Track Irregularities, *Vehicle System Dynamics*, Vol. 17, pp. 281-293, 1988

[65] Robson, J.D. and Kamash, K.M. A., Road Surface Description in Relation to Vehicle Response, *Vehicle System Dynamics*, Vol. 6, pp. 153-157, 1977

[66] Rill, G., The Influence of Correlated Random Road-Excitation Processeson Vehicle Vibrations, *Vehicle System Dynamics*, Vol. 12, pp. 50-54, 1983

[67] Garivaltis, D.S., Garg. V.K. and Dsouza, A.F., Dynamic Response of a Six-axle Locomotive to Random Track Inputs, *Vehicle System Dynamics*, Vol. 9, pp. 117-147, 1980

[68] Cheng, G., The Analysis on Random Vibration of Vehicle/Track Coupling System, *Ph.D. Dissertation (in Chinese)*, Southwest Jiaotong University

[69] McDonald, M. and Richard, A., Vehicle Health Monitoring on the Docklands Light Railway, *IEE Power Division Colloquium on Advanced Condition Monitoring System for Railways*, London, 1995

[70] Nicks, S., Condition Monitoring of the Track/Train Interface, *IEE Seminar Condition Monitoring for Railway Transport Systems*, London, 1998

[71] Mei, T.X. and Ding, X.J., New Condition Monitoring Techniques for Vehicle Suspensions, *The 4th IET International Conference on Railway Condition Monitoring*, pp 1-6, Derby, UK, 2008

[72] Ding, X.J. and Mei, T.X., Condition Monitoring of Vehicle Suspensions Using Relative Variances, *23rd IAR Workshop on Advanced Control and Diagnosis*, Coventry University, UK, 2008

Appendix A

The matrix and variables of equation (2.34)

In this appendix each element of the matrices A_{26} and B_{16} used in equation (2.34) are given, where A_{26} is a 26×26 system matrix and B_{16} is a 16×16 input matrix of the conventional bogie vehicle, x and u present the state variables and track input vectors respectively.

where

$$A_{26}=\begin{bmatrix}
0 & a_{1\text{-}2} & 0 & 0 & 0 & 0 & 0 & a_{1\text{-}8} & 0 & a_{1\text{-}10} & 0 & a_{1\text{-}12} & 0 & a_{1\text{-}14} & 0 & a_{1\text{-}16} & 0 & 0 & 0 & 0 & 0 & a_{1\text{-}22} & 0 & 0 & 0 & 0 \\
1 & 0 & 0 & 0 & 0 & 0 & 0 & 0 & 0 & 0 & 0 & 0 & 0 & 0 & 0 & 0 & 0 & 0 & 0 & 0 & 0 & 0 & 0 & 0 & 0 & 0 \\
0 & 0 & 0 & a_{3\text{-}4} & 0 & 0 & 0 & a_{3\text{-}8} & 0 & a_{3\text{-}10} & 0 & a_{3\text{-}12} & 0 & a_{3\text{-}14} & 0 & a_{3\text{-}14} & 0 & 0 & 0 & 0 & 0 & a_{3\text{-}22} & 0 & 0 & 0 & 0 \\
0 & 0 & 1 & 0 & 0 & 0 & 0 & 0 & 0 & 0 & 0 & 0 & 0 & 0 & 0 & 0 & 0 & 0 & 0 & 0 & 0 & 0 & 0 & 0 & 0 & 0 \\
0 & 0 & 0 & 0 & 0 & a_{5\text{-}6} & 0 & a_{5\text{-}8} & 0 & a_{5\text{-}10} & 0 & a_{5\text{-}12} & 0 & a_{5\text{-}14} & 0 & 0 & 0 & 0 & 0 & a_{5\text{-}20} & 0 & 0 & 0 & 0 & 0 & a_{5\text{-}26} \\
0 & 0 & 0 & 0 & 1 & 0 & 0 & 0 & 0 & 0 & 0 & 0 & 0 & 0 & 0 & 0 & 0 & 0 & 0 & 0 & 0 & 0 & 0 & 0 & 0 & 0 \\
0 & a_{7\text{-}2} & 0 & a_{7\text{-}4} & 0 & a_{7\text{-}6} & a_{7\text{-}7} & a_{7\text{-}8} & 0 & 0 & 0 & 0 & 0 & 0 & a_{7\text{-}15} & a_{7\text{-}16} & 0 & 0 & a_{7\text{-}19} & a_{7\text{-}20} & 0 & 0 & 0 & 0 & 0 & 0 \\
0 & 0 & 0 & 0 & 0 & 0 & 1 & 0 & 0 & 0 & 0 & 0 & 0 & 0 & 0 & 0 & 0 & 0 & 0 & 0 & 0 & 0 & 0 & 0 & 0 & 0 \\
0 & a_{9\text{-}2} & 0 & a_{9\text{-}4} & 0 & a_{9\text{-}6} & 0 & 0 & a_{9\text{-}9} & a_{9\text{-}10} & 0 & 0 & 0 & 0 & a_{9\text{-}15} & a_{9\text{-}16} & 0 & 0 & a_{9\text{-}19} & a_{9\text{-}20} & 0 & 0 & 0 & 0 & 0 & 0 \\
0 & 0 & 0 & 0 & 0 & 0 & 0 & 0 & 1 & 0 & 0 & 0 & 0 & 0 & 0 & 0 & 0 & 0 & 0 & 0 & 0 & 0 & 0 & 0 & 0 & 0 \\
0 & a_{1\text{-}2} & 0 & a_{1\text{-}4} & 0 & a_{1\text{-}6} & 0 & 0 & 0 & 0 & a_{1\text{-}11} & a_{1\text{-}12} & 0 & 0 & 0 & 0 & 0 & 0 & 0 & 0 & a_{1\text{-}21} & a_{1\text{-}22} & 0 & 0 & a_{1\text{-}25} & a_{1\text{-}26} \\
0 & 0 & 0 & 0 & 0 & 0 & 0 & 0 & 0 & 0 & 1 & 0 & 0 & 0 & 0 & 0 & 0 & 0 & 0 & 0 & 0 & 0 & 0 & 0 & 0 & 0 \\
0 & a_{3\text{-}2} & 0 & a_{3\text{-}4} & 0 & a_{3\text{-}6} & 0 & 0 & 0 & 0 & 0 & 0 & a_{3\text{-}13} & a_{3\text{-}14} & 0 & 0 & 0 & 0 & 0 & 0 & a_{3\text{-}21} & a_{3\text{-}22} & 0 & 0 & a_{3\text{-}25} & a_{3\text{-}26} \\
0 & 0 & 0 & 0 & 0 & 0 & 0 & 0 & 0 & 0 & 0 & 0 & 1 & 0 & 0 & 0 & 0 & 0 & 0 & 0 & 0 & 0 & 0 & 0 & 0 & 0 \\
0 & a_{5\text{-}2} & 0 & a_{5\text{-}4} & 0 & 0 & a_{5\text{-}7} & a_{5\text{-}8} & a_{5\text{-}9} & a_{5\text{-}10} & 0 & 0 & 0 & 0 & a_{5\text{-}15} & a_{5\text{-}16} & a_{5\text{-}17} & 0 & a_{5\text{-}19} & 0 & 0 & 0 & 0 & 0 & 0 & 0 \\
0 & 0 & 0 & 0 & 0 & 0 & 0 & 0 & 0 & 0 & 0 & 0 & 0 & 0 & 1 & 0 & 0 & 0 & 0 & 0 & 0 & 0 & 0 & 0 & 0 & 0 \\
0 & 0 & 0 & 0 & 0 & 0 & 0 & 0 & 0 & 0 & 0 & 0 & 0 & 0 & a_{7\text{-}15} & 0 & a_{7\text{-}17} & a_{7\text{-}18} & 0 & 0 & 0 & 0 & 0 & 0 & 0 & 0 \\
0 & 0 & 0 & 0 & 0 & 0 & 0 & 0 & 0 & 0 & 0 & 0 & 0 & 0 & 0 & 0 & 1 & 0 & 0 & 0 & 0 & 0 & 0 & 0 & 0 & 0 \\
0 & 0 & 0 & 0 & 0 & a_{9\text{-}6} & a_{9\text{-}7} & a_{9\text{-}8} & a_{9\text{-}9} & a_{9\text{-}10} & 0 & 0 & 0 & 0 & a_{9\text{-}15} & 0 & 0 & 0 & a_{9\text{-}19} & a_{9\text{-}20} & 0 & 0 & 0 & 0 & 0 & 0 \\
0 & 0 & 0 & 0 & 0 & 0 & 0 & 0 & 0 & 0 & 0 & 0 & 0 & 0 & 0 & 0 & 0 & 0 & 1 & 0 & 0 & 0 & 0 & 0 & 0 & 0 \\
0 & a_{2\text{-}2} & 0 & a_{2\text{-}4} & 0 & 0 & 0 & 0 & 0 & 0 & a_{2\text{-}11} & a_{2\text{-}12} & a_{2\text{-}13} & a_{2\text{-}14} & 0 & 0 & 0 & 0 & 0 & 0 & a_{2\text{-}21} & a_{2\text{-}22} & a_{2\text{-}23} & 0 & a_{2\text{-}25} & 0 \\
0 & 0 & 0 & 0 & 0 & 0 & 0 & 0 & 0 & 0 & 0 & 0 & 0 & 0 & 0 & 0 & 0 & 0 & 0 & 0 & 1 & 0 & 0 & 0 & 0 & 0 \\
0 & 0 & 0 & 0 & 0 & 0 & 0 & 0 & 0 & 0 & 0 & 0 & 0 & 0 & 0 & 0 & 0 & 0 & 0 & 0 & a_{23\text{-}21} & 0 & a_{23\text{-}23} & a_{23\text{-}24} & 0 & 0 \\
0 & 0 & 0 & 0 & 0 & 0 & 0 & 0 & 0 & 0 & 0 & 0 & 0 & 0 & 0 & 0 & 0 & 0 & 0 & 0 & 0 & 0 & 1 & 0 & 0 & 0 \\
0 & 0 & 0 & 0 & 0 & a_{25\text{-}6} & 0 & 0 & 0 & 0 & a_{25\text{-}11} & a_{25\text{-}12} & a_{25\text{-}13} & a_{25\text{-}14} & 0 & 0 & 0 & 0 & 0 & 0 & a_{25\text{-}21} & 0 & 0 & 0 & a_{25\text{-}25} & a_{25\text{-}26} \\
0 & 0 & 0 & 0 & 0 & 0 & 0 & 0 & 0 & 0 & 0 & 0 & 0 & 0 & 0 & 0 & 0 & 0 & 0 & 0 & 0 & 0 & 0 & 0 & 1 & 0
\end{bmatrix} \quad \text{(A.1)}$$

$$
B_{16} = \begin{bmatrix}
0 & 0 & 0 & 0 & 0 & 0 & 0 & 0 & 0 & 0 & 0 & 0 & 0 & 0 & 0 & 0 \\
0 & 0 & 0 & 0 & 0 & 0 & 0 & 0 & 0 & 0 & 0 & 0 & 0 & 0 & 0 & 0 \\
0 & 0 & 0 & 0 & 0 & 0 & 0 & 0 & 0 & 0 & 0 & 0 & 0 & 0 & 0 & 0 \\
0 & 0 & 0 & 0 & 0 & 0 & 0 & 0 & 0 & 0 & 0 & 0 & 0 & 0 & 0 & 0 \\
0 & 0 & 0 & 0 & 0 & 0 & 0 & 0 & 0 & 0 & 0 & 0 & 0 & 0 & 0 & 0 \\
0 & 0 & 0 & 0 & 0 & 0 & 0 & 0 & 0 & 0 & 0 & 0 & 0 & 0 & 0 & 0 \\
0 & 0 & 0 & 0 & 0 & 0 & 0 & 0 & 0 & 0 & 0 & 0 & 0 & 0 & 0 & 0 \\
0 & 0 & 0 & 0 & 0 & 0 & 0 & 0 & 0 & 0 & 0 & 0 & 0 & 0 & 0 & 0 \\
0 & 0 & 0 & 0 & 0 & 0 & 0 & 0 & 0 & 0 & 0 & 0 & 0 & 0 & 0 & 0 \\
0 & 0 & 0 & 0 & 0 & 0 & 0 & 0 & 0 & 0 & 0 & 0 & 0 & 0 & 0 & 0 \\
0 & 0 & 0 & 0 & 0 & 0 & 0 & 0 & 0 & 0 & 0 & 0 & 0 & 0 & 0 & 0 \\
0 & 0 & 0 & 0 & 0 & 0 & 0 & 0 & 0 & 0 & 0 & 0 & 0 & 0 & 0 & 0 \\
0 & 0 & 0 & 0 & 0 & 0 & 0 & 0 & 0 & 0 & 0 & 0 & 0 & 0 & 0 & 0 \\
0 & 0 & 0 & 0 & 0 & 0 & 0 & 0 & 0 & 0 & 0 & 0 & 0 & 0 & 0 & 0 \\
b_{15-1} & b_{15-2} & b_{15-3} & b_{15-4} & b_{15-5} & b_{15-6} & b_{15-7} & b_{15-8} & 0 & 0 & 0 & 0 & 0 & 0 & 0 & 0 \\
0 & 0 & 0 & 0 & 0 & 0 & 0 & 0 & 0 & 0 & 0 & 0 & 0 & 0 & 0 & 0 \\
b_{17-1} & b_{17-2} & b_{17-3} & b_{17-4} & b_{17-5} & b_{17-6} & b_{17-7} & b_{17-8} & 0 & 0 & 0 & 0 & 0 & 0 & 0 & 0 \\
0 & 0 & 0 & 0 & 0 & 0 & 0 & 0 & 0 & 0 & 0 & 0 & 0 & 0 & 0 & 0 \\
b_{19-1} & b_{19-2} & b_{19-3} & b_{19-4} & b_{19-5} & b_{19-6} & b_{19-7} & b_{19-8} & 0 & 0 & 0 & 0 & 0 & 0 & 0 & 0 \\
0 & 0 & 0 & 0 & 0 & 0 & 0 & 0 & 0 & 0 & 0 & 0 & 0 & 0 & 0 & 0 \\
0 & 0 & 0 & 0 & 0 & 0 & 0 & 0 & b_{21-9} & b_{21-10} & b_{21-11} & b_{21-12} & b_{21-13} & b_{21-14} & b_{21-15} & b_{21-16} \\
0 & 0 & 0 & 0 & 0 & 0 & 0 & 0 & 0 & 0 & 0 & 0 & 0 & 0 & 0 & 0 \\
0 & 0 & 0 & 0 & 0 & 0 & 0 & 0 & b_{23-9} & b_{23-10} & b_{23-11} & b_{23-12} & b_{23-13} & b_{23-14} & b_{23-15} & b_{23-16} \\
0 & 0 & 0 & 0 & 0 & 0 & 0 & 0 & 0 & 0 & 0 & 0 & 0 & 0 & 0 & 0 \\
0 & 0 & 0 & 0 & 0 & 0 & 0 & 0 & b_{25-9} & b_{25-10} & b_{25-11} & b_{25-12} & b_{25-13} & b_{25-14} & b_{25-15} & b_{25-16} \\
0 & 0 & 0 & 0 & 0 & 0 & 0 & 0 & 0 & 0 & 0 & 0 & 0 & 0 & 0 & 0
\end{bmatrix} \quad \text{(A.2)}
$$

$$
x = \left[\dot{z}_{bd} \; z_{bd} \; \dot{\phi}_{bd} \; \phi_{bd} \; \dot{\psi}_{bd} \; \psi_{bd} \; \dot{z}_{d1l} \; z_{d1l} \; \dot{z}_{d1r} \; z_{d1r} \; \dot{z}_{d2l} \; z_{d2l} \; \dot{z}_{d2r} \; z_{d2r} \; \dot{z}_{b1} \; z_{b1} \; \dot{\phi}_{b1} \; \phi_{b1} \; \dot{\psi}_{b1} \; \psi_{b1} \; \dot{z}_{b2} \; z_{b2} \; \dot{\phi}_{b2} \; \phi_{b2} \; \dot{\psi}_{b2} \; \psi_{b2}\right] \quad \text{(A.3)}
$$

$$
u = \left[\dot{z}_{t1l} \; z_{t1l} \; \dot{z}_{t1r} \; z_{t1r} \; \dot{z}_{t2l} \; z_{t2l} \; \dot{z}_{t2r} \; z_{t2r} \; \dot{z}_{t3l} \; z_{t3l} \; \dot{z}_{t3r} \; z_{t3r} \; \dot{z}_{t4l} \; z_{t4l} \; \dot{z}_{t4r} \; z_{t4r}\right] \quad \text{(A.4)}
$$

The coefficients in matrices A_{26} and B_{16} are defined as:

$$a_{1-2} = -4(K_a + K_s)/m_{bd}$$

$$a_{1-8} = a_{1-10} = a_{1-12} = a_{1-14} = K_s / m_{bd}$$

$$a_{1-16} = a_{1-22} = 2K_a / m_{bd}$$

$$a_{3-4} = -4(K_a + K_s)L_{bdx}^2 / I_{bdx}$$

$$a_{3-8} = a_{3-10} = -a_{3-12} = -a_{3-14} = K_s L_{bdx} / I_{bdx}$$

$$a_{3-16} = -a_{3-22} = 2K_a L_{bdx} / I_{bdx}$$

$$a_{5-6} = -4(K_a + K_s) L_{bdy}^2 / I_{bdy}$$

$$a_{5-8} = -a_{5-10} = a_{5-12} = -a_{5-14} = K_s L_{bdy} / I_{bdy}$$

$$a_{5-20} = a_{5-26} = 2K_a L_{bdy} L_{by} / I_{bdy}$$

$$a_{7-2} = a_{9-2} = a_{11-2} = a_{13-2} = 2K_s / m_m$$

$$a_{7-4} = a_{9-4} = -a_{11-4} = -a_{13-4} = 2K_s L_{bdx} / m_m$$

$$a_{7-6} = -a_{9-6} = a_{11-6} = -a_{13-6} = 2K_s L_{bdy} / m_m$$

$$a_{7-7} = -a_{7-15} = a_{9-9} = -a_{9-15} = a_{11-11} = -a_{11-21} = a_{13-13} = -a_{13-21} = -2C_r / m_m$$

$$a_{7-8} = a_{9-10} = a_{11-12} = a_{13-14} = -2(K_s + K_r) / m_m$$

$$a_{7-16} = a_{9-16} = a_{11-22} = a_{13-22} = 2K_r / m_m$$

$$a_{7-19} = -a_{9-19} = a_{11-25} = -a_{13-25} = -2C_r L_{by} / m_m$$

$$a_{7-20} = -a_{9-20} = a_{11-26} = -a_{13-26} = 2K_r L_{by} / m_m$$

$$a_{15-2} = a_{21-2} = 2K_a / m_b$$

$$a_{15-4} = a_{21-4} = 2K_a L_{bdx} / m_b$$

$$a_{15-7} = a_{15-9} = a_{21-11} = a_{21-13} = C_r / m_b$$

$$a_{15-8} = a_{15-10} = a_{21-12} = a_{21-14} = K_r / m_b$$

$$a_{15-15} = -(C_{FL} + C_{FR} + C_{RL} + C_{RR} + 2C_r) / m_b$$

$$a_{15-16} = a_{21-22} = -(4K_p + 2K_a + 2K_r)/m_b$$

$$a_{15-17} = -(C_{FL} + C_{FR} - C_{RL} - C_{RR})L_{bx}/m_b$$

$$a_{15-19} = -(C_{FL} - C_{FR} + C_{RL} - C_{RR})L_{by}/m_b$$

$$a_{17-15} = -(C_{FL} + C_{FR} - C_{RL} - C_{RR})L_{bx}/I_{bx}$$

$$a_{17-17} = -(C_{FL} + C_{FR} + C_{RL} + C_{RR})L_{bx}^2/I_{bx}$$

$$a_{17-18} = a_{23-24} = -4K_pL_{bx}^2/I_{bx}$$

$$a_{19-6} = a_{25-6} = -2L_{bdy}L_{by}/I_{by}$$

$$a_{19-7} = -a_{19-9} = a_{25-11} = -a_{25-13} = C_rL_{by}/I_{by}$$

$$a_{19-8} = -a_{19-10} = a_{25-12} = -a_{25-14} = K_rL_{by}/I_{by}$$

$$a_{19-15} = -(C_{FL} + C_{FR} - C_{RL} - C_{RR})L_{by}/I_{by}$$

$$a_{19-19} = -(C_{FL} + C_{FR} + C_{RL} + C_{RR})L_{by}^2/I_{by}$$

$$a_{19-20} = a_{25-26} = -(4K_p + 2K_r + 2K_a)L_{by}^2/I_{by}$$

$$a_{21-21} = -(C'_{FL} + C'_{FR} + C'_{RL} + C'_{RR} + 2C_r)/m_b$$

$$a_{21-23} = -(C'_{FL} + C'_{FR} - C'_{RL} - C'_{RR})L_{bx}/m_b$$

$$a_{21-25} = -(C'_{FL} - C'_{FR} + C'_{RL} - C'_{RR})L_{by}/m_b$$

$$a_{23-21} = -(C'_{FL} + C'_{FR} - C'_{RL} - C'_{RR})L_{bx}/I_{bx}$$

$$a_{23-23} = -(C'_{FL} + C'_{FR} + C'_{RL} + C'_{RR})L_{bx}^2/I_{bx}$$

$$a_{25-21} = -(C'_{FL} + C'_{FR} - C'_{RL} - C'_{RR})L_{by} / I_{by}$$

$$a_{25-25} = -(C'_{FL} + C'_{FR} + C'_{RL} + C'_{RR})L^2_{by} / I_{by}$$

and

$$b_{15-1} = C_{FL} / m_b$$

$$b_{15-2} = b_{15-4} = b_{15-6} = b_{15-8} = b_{21-10} = b_{21-12} = b_{21-14} = b_{21-16} = K_p / m_b$$

$$b_{15-3} = C_{FR} / m_b$$

$$b_{15-5} = C_{RL} / m_b$$

$$b_{15-7} = C_{RR} / m_b$$

$$b_{17-1} = C_{FL} L_{bx} / I_{bx}$$

$$b_{17-2} = b_{17-4} = -b_{17-6} = -b_{17-8} = b_{23-10} = b_{23-12} = -b_{23-14} = -b_{23-16} = K_{FL} L_{bx} / I_{bx}$$

$$b_{17-3} = C_{FR} L_{bx} / I_{bx}$$

$$b_{17-5} = -C_{RL} L_{bx} / I_{bx}$$

$$b_{17-7} = -C_{RR} L_{bx} / I_{bx}$$

$$b_{19-1} = C_{FL} L_{bY} / I_{bY}$$

$$b_{19-2} = -b_{19-4} = b_{19-6} = -b_{19-8} = b_{25-10} = -b_{25-12} = b_{25-14} = -b_{25-16} = K_p L_{bY} / I_{bY}$$

$$b_{19-3} = -C_{FR} L_{by} / I_{by}$$

$$b_{19-5} = C_{RL} L_{by} / I_{by}$$

$$b_{19-7} = -C_{RR} L_{by} / I_{by}$$

$$b_{21-9} = C'_{FL} / m_b$$

$$b_{21-11} = C'_{FR} / m_b$$

$$b_{21-13} = C'_{RL} / m_b$$

$$b_{21-15} = C'_{RR} / m_b$$

$$b_{23-9} = C'_{FL} L_{bx} / I_{bx}$$

$$b_{23-11} = C'_{FR} L_{bx} / I_{bx}$$

$$b_{23-13} = -C'_{RL} L_{bx} / I_{bx}$$

$$b_{23-15} = -C'_{RR} L_{bx} / I_{bx}$$

$$b_{25-9} = C'_{FL} L_{by} / I_{by}$$

$$b_{25-11} = -C'_{FR} L_{by} / I_{by}$$

$$b_{25-13} = C'_{RL} L_{by} / I_{by}$$

$$b_{25-15} = -C'_{RR} L_{by} / I_{by}$$

Appendix B
Publications

Vehicle System Dynamics
Vol. 47, No. 9, September 2009, 1167–1181

Taylor & Francis
Taylor & Francis Group

Condition monitoring of rail vehicle suspensions based on changes in system dynamic interactions

T.X. Mei[a]* and X.J. Ding[b]

[a]*School of Computing, Science and Engineering, Salford University, Salford, UK;* [b]*School of Electronic and Electrical Engineering, University of Leeds, Leeds, UK*

(Received 17 July 2008; final version received 13 October 2008)

A novel scheme for the fault detection and condition monitoring of vehicle suspensions is presented in this study. The new technique exploits the dynamic interactions between different vehicle modes caused by component failures in the system, leading to a simple but effective solution. Compared with many model-based fault detection techniques, the proposed technique does not require complex mathematical models of the system and it overcomes potential difficulties associated with nonlinearities and parameter variations in the system. The use of inexpensive inertial sensors and ease of tuning make the practical implementation of the proposed scheme straightforward. A conventional railway vehicle is used in the study to illustrate the basic ideas as well as the effectiveness of the novel fault detection method, although the general principle is applicable to other systems.

Keywords: fault detection; suspensions; vehicle dynamics

1. Introduction

On-line fault detection and condition monitoring for dynamic systems are becoming increasingly important because of the potential benefits of detecting component failures at their early stages, to prevent further deterioration in performance as well as to ensure timely repair/replacement of faulty components. In the long term, the availability of reliable condition monitoring systems can replace scheduled regular services with maintenance on demand, leading to substantial savings in the total life cycle costs.

The most commonly used fault detection schemes directly measure signals using sensors mounted as close to the point of interest as possible and analyse the data using time and/or frequency domain signal processing, e.g. to find signatures or footprints related to particular faults [1,2]. The approach of direct measurement requires in-depth understanding of the system concerned and its effectiveness in fault detection may also be affected by variations or uncertainties of external conditions such as the level and properties of input signals and disturbances.

*Corresponding author. Email: t.x.mei@theiet.org

ISSN 0042-3114 print/ISSN 1744-5159 online

DOI: 10.1080/00423110802553087
http://www.informaworld.com

Model-based approaches compare a real 'physical' system with mathematical representations of the system (the model). Fault detection may typically be achieved by either finding the coefficients in the models that are associated with particular components using parameter identification techniques or analysing the difference in measured and estimated outputs (the residual). There have been a number of studies of the approach for both automotive [3,4,5] and railway [6,7] applications. Clearly, the development of an appropriate model for model-based methods is essential, in addition to a detailed knowledge of the system concerned. For systems that are dynamically complex and/or nonlinear, model-based approaches may lead to the use of high-order and/or linearised multiple models which can be difficult for practical implementation.

This paper presents a novel approach that is simple but very effective for fault detection for vehicle suspensions, which would not require the knowledge of many of the system parameters as needed for model-based approaches. The proposed technique is focused on the comparison of dynamic behaviours between the two suspensions where identical components are normally used. When there are no faults in the system, it can be readily shown that the bounce and pitch motions of the bogie (and to a large extent the vertical movements at the leading and trailing suspensions) are decoupled because of the symmetrical suspension configurations. Therefore, there is little interaction between the two motions. However, a component failure (e.g. a damper) in either of the suspensions will introduce an imbalance into the system, resulting in dynamic interferences between the motions. The level of interactions therefore provides a key indication of suspension conditions.

This paper is structured as follows. The general principles of the proposed detection method are explained in Section 2. Section 3 introduces a conventional railway vehicle, the mathematical model of which includes the bounce, pitch and roll motions of the vehicle body and two bogies. The algorithms for the proposed fault detection technique are also given in Section 3. The performance assessments are given in Section 4 and main conclusions are described in Section 5.

2. Basic principle of the fault detection technique

With the help of the side-view model of a simple railway bogie (or truck as known in North America) as illustrated in Figure 1, the basic principle of the proposed technique for the fault detection and condition monitoring of vehicle suspensions may be explained by examining the consequences of a component fault in terms of additional dynamic interactions [8].

The dynamic interactions introduced due to faults in the system are best illustrated using the equations of motions in the form of pitch and bounce movements of the bogie as given in

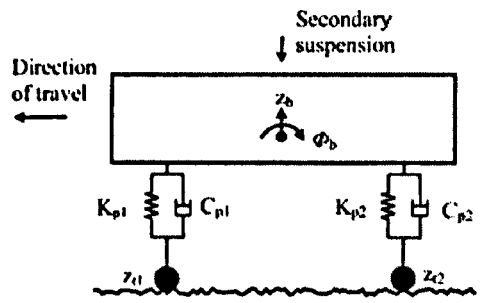

Figure 1. Side-view diagram of a conventional railway bogie.

Equations (1) and (2).

$$m_b\ddot{z}_b + C_{ps}\dot{z}_b + K_{ps}z_b + L_{bx}C_{pd}\dot{\phi}_b + L_{bx}K_{pd}\phi_b$$
$$= \frac{1}{2}\left[C_{ps}(\dot{z}_{t1} + \dot{z}_{t2}) + K_{ps}(z_{t1} + z_{t2}) + C_{pd}(\dot{z}_{t1} - \dot{z}_{t2}) + K_{pd}(z_{t1} - z_{t2})\right] + F_d \quad (1)$$

$$I_b\ddot{\phi}_b + L_{bx}^2C_{ps}\dot{\phi}_b + L_{bx}^2K_{ps}\phi_b + L_{bx}C_{pd}\dot{z}_b + L_{bx}K_{pd}z_b$$
$$= \frac{L_{bx}}{2}\left[C_{ps}(\dot{z}_{t1} - \dot{z}_{t2}) + K_{ps}(z_{t1} - z_{t2}) + C_{pd}(\dot{z}_{t1} + \dot{z}_{t2}) + K_{pd}(z_{t1} + z_{t2})\right] \quad (2)$$

where

$$C_{ps} = C_{p1} + C_{p2}, \quad K_{pd} = K_{p1} - K_{p2}$$
$$K_{ps} = K_{p1} + K_{p2}, \quad C_{pd} = C_{p1} - C_{p2}.$$

In most rail vehicles, the same components are commonly used for the two suspensions and hence the same (or at least closely matched) coefficients are expected. Therefore, in the no-fault condition ($K_{p1} = K_{p2}, C_{s1} = C_{s2}$), Equations (1) and (2) may be simplified to Equations (3) and (4), which indicate clearly that the bounce and pitch movements of the bogie are largely independent and there is no direct dynamic coupling between the two motions. The main link between the two is through the track inputs at the leading and trailing wheelsets – the bounce mode is excited by the sum of the two and the pitch mode by the difference between the two.

$$m_b\ddot{z}_b + C_{ps}\dot{z}_b + K_{ps}z_b = \frac{1}{2}C_{ps}(\dot{z}_{t1} + \dot{z}_{t2}) + \frac{1}{2}K_{ps}(z_{t1} + z_{t2}) + (F_d). \quad (3)$$

$$I_b\ddot{\phi}_b + L_{bx}^2C_{ps}\dot{\phi}_b + L_{bx}^2K_{ps}\phi_b = \frac{1}{2}L_{bx}C_{ps}(\dot{z}_{t1} - \dot{z}_{t2}) + \frac{1}{2}L_{bx}K_{ps}(z_{t1} - z_{t2}). \quad (4)$$

However, in abnormal conditions where the two suspensions become different, the imbalance between the suspensions causes interactions between the bounce and pitch motions in two ways. Dynamically, Equations (1) and (2) are no longer independent as two pitch terms appear in the bounce equation and two bounce terms in the pitch equation. Externally, the bounce motion is now also affected by the difference between the track inputs at the front and rear suspensions, which predominantly excites the pitch motion, and the pitch movement is also affected by the sum of the two input signals, which predominantly excites the bounce motion. Therefore, the degree of correlations may be used to detect how much imbalance (i.e. due to component fault) may exist in the system.

In practice, the bounce and pitch accelerations may be readily obtained through the use of inertial sensors. The two signals may be expressed in the form of transfer functions in Equations (5) and (6) for the general case from Equations (1) and (2), where the term related to the secondary suspension force (F_d) is neglected because its effect is much smaller when compared with that of the track input (due to the filtering effect). Note that the last three terms (in the second line) in both equations are introduced due to the imbalance caused by a component failure, the first two of which represent a changed response to the track input mainly at the wheelset where the suspension failure occurs and the third represents the

additional interaction between the two motions.

$$\ddot{Z}_b(s) = \frac{1}{2}\cdot\frac{C_{ps}s + K_{ps}}{m_b s^2 + C_{ps}s + K_{ps}}\ddot{Z}_{t1}(s) + \frac{1}{2}\cdot\frac{C_{ps}s + K_{ps}}{m_b s^2 + C_{ps}s + K_{ps}}\ddot{Z}_{t2}(s)$$
$$+ \frac{1}{2}\cdot\frac{C_{pd}s + K_{pd}}{m_b s^2 + C_{ps}s + K_{ps}}\ddot{Z}_{t1}(s) - \frac{1}{2}\cdot\frac{C_{pd}s + K_{pd}}{m_b s^2 + C_{ps}s + K_{ps}}\ddot{Z}_{t2}(s)$$
$$- \frac{L_{bx}(C_{pd}s + K_{pd})}{m_b s^2 + C_{ps}s + K_{ps}}\ddot{\Phi}_b(s), \tag{5}$$

$$\ddot{\Phi}_b(s) = \frac{L_{bx}}{2}\cdot\frac{C_{ps}s + K_{ps}}{I_b s^2 + L_{bx}^2 C_{ps}s + L_{bx}^2 K_{ps}}\ddot{Z}_{t1}(s) - \frac{L_{bx}}{2}\cdot\frac{C_{ps}s + K_{ps}}{I_b s^2 + L_{bx}^2 C_{ps}s + 2L_{bx}^2 K_{ps}}\ddot{Z}_{t2}(s)$$
$$+ \frac{L_{bx}}{2}\cdot\frac{C_{pd}s + K_{pd}}{I_b s^2 + L_{bx}^2 C_{ps}s + L_{bx}^2 K_{ps}}\ddot{Z}_{t1}(s) + \frac{L_{bx}}{2}\cdot\frac{C_{pd}s + K_{pd}}{I_b s^2 + L_{bx}^2 C_{ps}s + 2L_{bx}^2 K_{ps}}\ddot{Z}_{t2}(s)$$
$$- \frac{L_{bx}(C_{pd}s + K_{pd})}{I_b s^2 + L_{bx}^2 C_{ps}s + 2L_{bx}^2 K_{ps}}\ddot{Z}_b(s), \tag{6}$$

where

$$A_z(s) = m_b s^2 + C_{ps}s + K_{ps},$$
$$A_\phi(s) = I_b s^2 + L_{bx}^2 C_{ps}s + L_{bx}^2 K_{ps},$$
$$B_s(s) = C_{ps}s + K_{ps},$$
$$B_d(s) = C_{pd}s + K_{pd}.$$

Substituting Equation (6) into (5) removes the pitch acceleration from the bounce equation and substituting Equation (5) into (6) removes the bounce acceleration from the pitch equation, which leads to

$$\ddot{Z}_b(s) = \frac{1}{2}\cdot G_0(s)\cdot[G_{11}(s)\ddot{Z}_{t1}(s) + G_{12}(s)\ddot{Z}_{t2}(s)], \tag{7}$$

$$\ddot{\Phi}_b(s) = \frac{L_{bx}}{2}\cdot G_0(s)\cdot[G_{21}(s)\ddot{Z}_{t1}(s) - G_{22}(s)\ddot{Z}_{t2}(s)] \tag{8}$$

where

$$G_0(s) = \frac{A_z(s)A_\phi(s)}{A_z(s)A_\phi(s) - L_{bx}^2 B_d(s)^2},$$
$$G_{11}(s) = \frac{2(C_{p1}\cdot s + K_{p1})}{A_z(s)}\cdot\left(1 - \frac{L_{bx}^2 B_d(s)}{A_\phi(s)}\right),$$
$$G_{12}(s) = \frac{2(C_{p2}\cdot s + K_{p2})}{A_z(s)}\cdot\left(1 + \frac{L_{bx}^2 B_d(s)}{A_\phi(s)}\right)$$
$$G_{21}(s) = \frac{2(C_{p1}\cdot s + K_{p1})}{A_\phi(s)}\cdot\left(1 - \frac{B_d(s)}{A_z(s)}\right),$$
$$G_{22}(s) = \frac{2(C_{p2}\cdot s + K_{p2})}{A_\phi(s)}\cdot\left(1 + \frac{B_d(s)}{A_z(s)}\right)\Bigg].$$

In the balanced condition, i.e. $B_d(s)=0$, Equations (7) and (8) may be simplified into Equations (9) and (10).

$$\ddot{Z}_b(s) = \frac{1}{2} \cdot \left[G_z(s)\ddot{Z}_{t1}(s) + G_z(s)\ddot{Z}_{t2}(s)\right], \tag{9}$$

$$\ddot{\Phi}_b(s) = \frac{L_{bx}}{2} \cdot \left[G_\phi(s)\ddot{Z}_{t1}(s) - G_\phi(s)\ddot{Z}_{t2}(s)\right], \tag{10}$$

where

$$G_z(s) = \cdot\frac{B_s(s)}{A_z(s)}, \quad G_\phi(s) = \frac{B_s(s)}{A_\phi(s)}.$$

By comparing the two sets of transfer functions between the normal and fault conditions, it is obvious that the filtering effect of primary suspensions on bogie motions would be different in different cases. The common term $G_0(s)$ is of the unity gain in the no-fault case, but in a fault condition magnifies the responses in the frequency region around the two bogie modes (e.g. by up to 66% if the damping constant at one of the dampers becomes 0 and the other remains as normal). However, the overall effect of this term will be limited as the magnitude response in the high- or low-frequency regions is almost unity in all conditions.

Equations (7)–(10) also show how the bounce and pitch motions are excited by the track inputs at the two wheelsets. Each of the two inputs influences only one of the two terms in the dynamic equations through the corresponding suspension. Therefore, changes in one suspension (e.g. due to component failure) will only be reflected in the corresponding part of the responses. A reduction of the damping coefficient in the front suspension alters largely how the bogie bounce mode responds to the track input at the leading wheelset (through G_{11}), but has little effect on its response to the delayed input at the trailing wheelset (through G_{12}). On the other hand, a damper failure at the rear suspension affects the bounce motion mainly through the track input at the trailing wheelset (i.e. through G_{12}), but not that at the leading wheelset (G_{11}). A similar observation may be made on G_{21} and G_{22} for the pitch motion. The sensitivity for detecting a suspension fault directly from acceleration measurements is compromised by this 'partial nonresponse' to suspension changes.

The proposed new method overcomes the problem of insensitivity (to faults) by detecting changes in dynamic correlations between the bounce and pitch accelerations, which can be readily achieved using simple cross-correlation calculations. If $\mathbf{X}(a, b)$ is used to denote a cross-correlation operation of a and b, the following relation may be derived from Equations (7) and (8) (or Equations (9) and (10)), where $g_{11}(t)$, $g_{12}(t)$, $g_{21}(t)$ and $g_{22}(t)$ correspond to the time domain representations of the relative terms in the two equations:

$$\begin{aligned}\mathbf{X}(\ddot{z}(t), \quad \ddot{\phi}(t)) = \mathbf{X}(g_{11}(t), \quad -g_{22}(t)) + \mathbf{X}(g_{12}(t), \quad g_{21}(t)) \\ + \mathbf{X}(g_{11}(t), \quad g_{21}(t)) - \mathbf{X}(g_{12}(t), \quad g_{22}(t))\end{aligned} \tag{11}$$

Because profiles of track inputs at the two wheelsets are exactly same and the only difference between the signals is the time delay (T_{shift}) determined by the vehicle speed and wheel-base, g_{11} and g_{22} are the responses to the track inputs 1 and 2, respectively, and hence the first term on the right-hand side of Equation (11) should give a peak cross-correlation at the negative time shift T_{shift}. Similarly, g_{12} and g_{21} are excited by the track inputs 2 and 1, respectively, and their cross-correlation (the second term on the right-hand side) should peak at the positive time shift T_{shift}. On the other hand, the third term should give the maximum correlation at zero time shifts as g_{11} and g_{21} are both caused by the track input 1. The fourth term also peaks at zero time shift because g_{12} and g_{22} are related to the track input 2.

In the nominal condition (with no faults in the system), the cross-correlations of the bounce and pitch accelerations are expected to be at the largest values at positive and negative time shifts ($\pm T_{shift}$), but at the minimum (or zero) at the zero time shift. The latter is because the last two terms in Equation (11) tend to cancel each other out as the two suspensions are the same and the track inputs are also the same albeit with a time delay.

When one of the suspensions fails, the cross-correlations at the $\pm T_{shift}$ may be modified due to the increased attenuation on the effect of the random track input over a wide range of frequencies. More critically, the cross-correlations at the zero time shift can be significantly increased because the asymmetry between the two suspensions removes the balance between the last two terms of Equation (11) and hence cancellation is no longer possible.

Detection and isolation of suspension faults can therefore be achieved by changes at the three specific time-shift points in cross-correlation calculations. A more comprehensive assessment of the effectiveness of the proposed fault detection technique is carried out using a full bogie railway vehicle as presented in the following sections.

3. System description and fault detection algorithms

The conventional railway vehicle consists of a body frame and two bogies, a schematic diagram of which is given in Figure 2. The fault detection of the vertical primary suspensions is studied to demonstrate the principle and effectiveness of the proposed method, although the techniques may be extended for the condition monitoring of suspensions in other directions or positions. Therefore, only motions directly related to the vertical suspensions are modelled, including the bounce, pitch and roll movements of the body and those of the two bogies, resulting in a nine-DoF model. The dynamics of the air springs in the secondary suspensions are approximated using a linearised model. The mathematical models used in the simulation study are developed in Matlab/Simulink with two different types of dampers in the primary suspension. One is the linear damper model and the other is a bilinear damper model (with the damping coefficients in the rebound and compression modes of $1.52C_s$ and $0.48C_s$, respectively) – the latter is used to evaluate the performance and robustness of the new techniques for nonlinear systems.

A random track, representing the roughness of a typical main line, is derived to give an appropriate spatial power spectrum (A_{rv}/f_t^2) for the track vertical position, which is then filtered using an additional low-pass filter to take into account the generalised power spectrum that has higher order terms in the denominator.

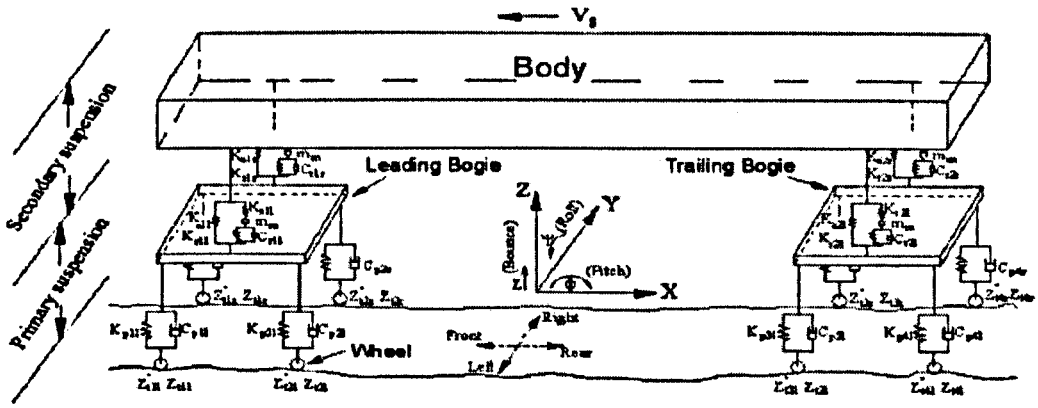

Figure 2. Conventional bogie vehicle for the study.

The detection scheme involves the use of a single sensor box mounted on the bogie frame in a centre position to measure the bounce, pitch and roll accelerations of the bogie. The issue of sensor noises has been considered in the study, but it has been found to have little effect on the outcome of cross-correlation computations, as sensor noises are relatively small (typically 1%) and more significantly uncorrelated – hence the effect at any specific time shift of the correlation calculations is very low.

The principle introduced in Section 2 may be extended to explore the cross-correlations between any two of the bounce, pitch and roll accelerations. The results are compared at three specific time shifts – 0 time delay for correlations due to the same input excitations and +/− time delays due to the time difference between the track inputs at the leading and trailing wheelsets. Equations (12)–(14) give the cross-correlation coefficients between the bounce and pitch accelerations, between the bounce and roll accelerations and between the pitch and roll accelerations. The cross-correlation coefficients reflect the normalised correlations between the two signals and, therefore, are much less affected by the changes in operation conditions due to a vehicle travelling at different speeds and/or on different tracks where the vibrations experienced on the bogie frame would vary even when the vehicle condition remains the same.

$$SC_{BP}(k) = \frac{S_{BP}(k)}{\sqrt{S_{BB}(0)S_{PP}(0)}}, \tag{12}$$

$$SC_{BR}(k) = \frac{S_{BR}(k)}{\sqrt{S_{BB}(0)S_{RR}(0)}}, \tag{13}$$

$$SC_{PR}(k) = \frac{S_{PR}(k)}{\sqrt{S_{PP}(0)S_{RR}(0)}}. \tag{14}$$

The auto-correlation S_{xx} of a signal (x) and the cross-correlation S_{xy} of any two signals (x, y) may be calculated using Equations (15) and (16), respectively. For any chosen sampling interval of T_s, the time window for each cross-correlation calculation is $T_w = N^*T_s$ from a total of N number of sampling intervals. The number of shifted intervals k may be varied from $-N$ to N for a complete set of cross-correlation calculations, although in practice only values at and near $k = 0$ and $\pm$ time delay between the two wheelsets (T_{shift}) are of particular interest for the proposed fault detection scheme.

$$S_{xx}(0) = \sum_{i=1}^{N} x(i) \cdot x(i), \tag{15}$$

$$S_{xy}(k) = \sum_{i=1}^{N} x(i+k) \cdot y(i). \tag{16}$$

4. Performance assessments

There are four primary suspensions on each bogie, identified as front left and front right at either side of the leading wheelset and rear left and rear right at either side of the trailing wheelset. The desired output of any effective scheme is not only to detect fault(s) in the system, but also to identify the location of the fault(s) as well as the degree of failure if possible.

Figures 3–5 show the normalised cross-correlations (i.e. the coefficients) between the bogie bounce and pitch accelerations, that of bounce and roll motions and that of pitch and roll motions, respectively, where three different conditions of the front left damper are compared: (1) no fault, (2) damping coefficient set to 50% of its normal value and (3) complete failure

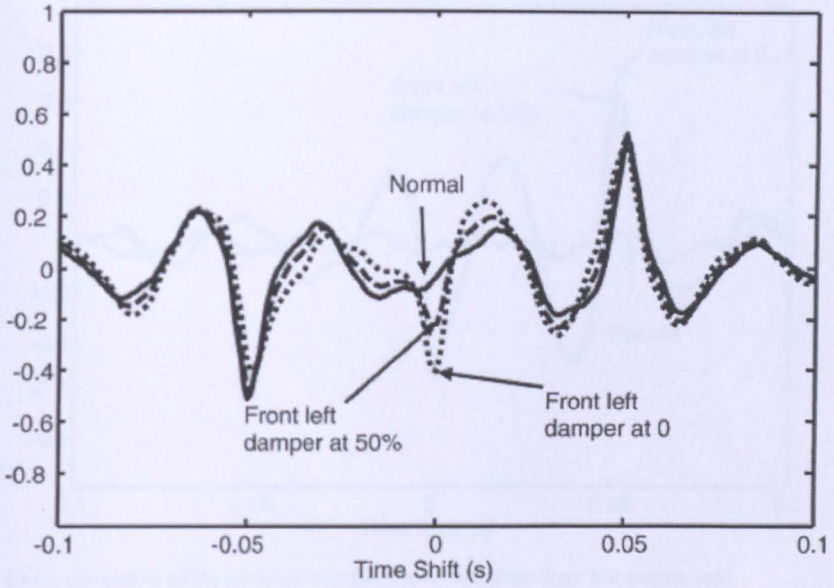

Figure 3. Cross-correlation of the bounce/pitch accelerations (fault at the front left suspension).

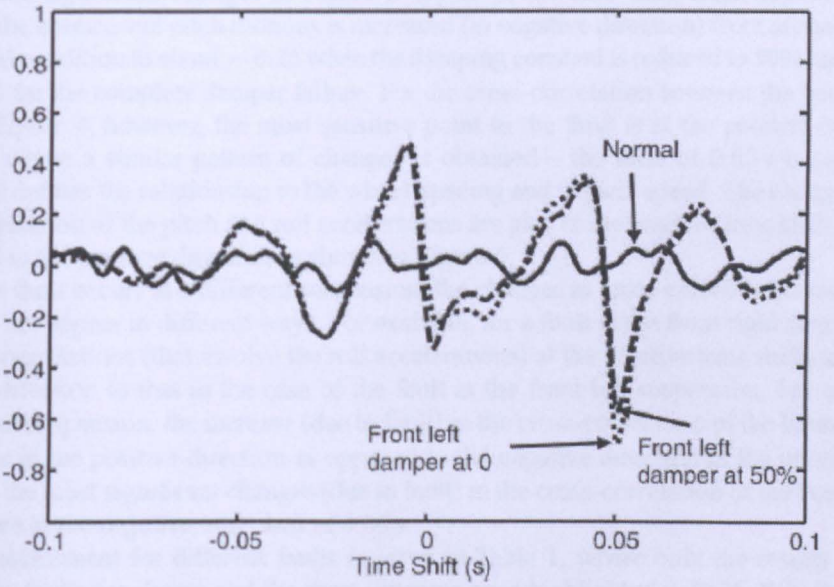

Figure 4. Cross-correlation of the bounce/roll accelerations (fault at the front left suspension).

of the front left damper. The vehicle speed is set at 50 m/s, as in most other cases unless indicated otherwise. The time delay from the leading wheelset to the trailing one is calculated as 0.05 s for the wheelbase of 2.5 m. A second-order band stop (notch) filter is also used in data processing before cross-correlation calculations and is tuned to have the low and high cut-off frequencies at 7 and 20 Hz, respectively, between which natural frequencies of the bogies modes are normally found. The use of the filter is to reduce the effect of increased resonance of the bogie modes due to the reduced damping by the damper failures, as the associated oscillations in the cross-correlation results can cause difficulties in detecting changes at the specific time shifts.

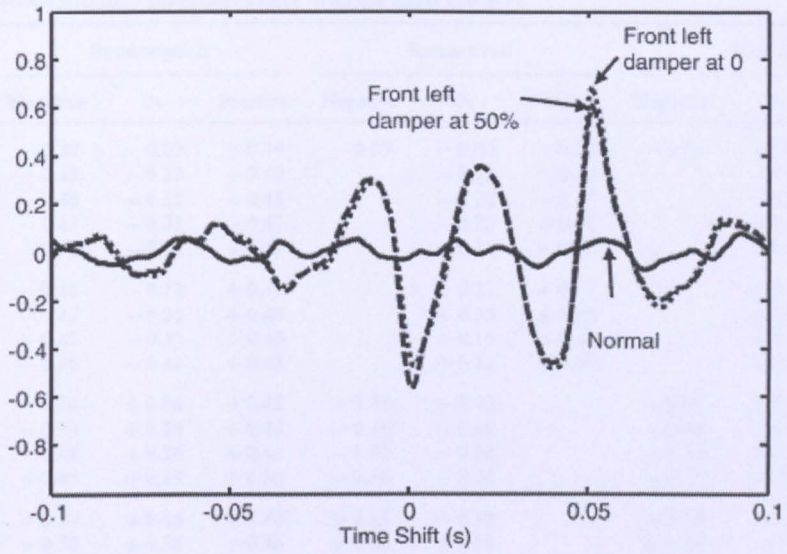

Figure 5. Cross-correlation of the pitch/roll accelerations (fault at the front left suspension).

The most significant changes in Figure 3 appear at the zero time shift. The correlation between the bounce and pitch motions is increased (in negative direction) from around zero in the normal condition to about -0.25 when the damping constant is reduced to 50% and further to -0.45 for the complete damper failure. For the cross-correlation between the bounce and pitch in Figure 4, however, the most sensitive point to the fault is at the positive time shift of 0.05 s where a similar pattern of changes is obtained – the time of 0.05 s is significant because it defines the relationship to the wheel-spacing and vehicle speed. The changes in the cross-correlation of the pitch and roll accelerations are also at the positive time shift, but it is increased in the positive direction as shown in Figure 5.

When a fault occurs at a different suspension, the changes in cross-correlations are equally sensitive, but appear in different ways. For example, for a fault at the front right suspensions, the cross-correlations (that involve the roll accelerations) at the positive time shifts are in the opposite direction to that in the case of the fault at the front left suspension. For a fault at the rear left suspension, the increase (due to fault) in the cross-correlation of the bounce/pitch motions is in the positive direction as opposed to the negative direction in the previous two cases and the most significant changes (due to fault) in the cross-correlation of the bounce/roll motions are at the negative time shift of 0.05 s.

A full assessment for different faults is given in Table 1, where only the results that are affected by faults are shown and the most sensitive ones highlighted in bold. It is clear from the table that not only different faults may be isolated using a combination of two or three cross-correlation calculations (and their results at different time shifts), but also a strong correlation exists between the degree of damper failure and the cross-correlation values, although the relationships appear to be nonlinear.

The proposed fault detection method remains effective when there are nonlinearities in the system. For a bilinear damper with the damping coefficients in the rebound and compression modes of $1.52C_s$ and $0.48C_s$, respectively, Figures 6 and 7 show the normalised cross-correlation of the bounce/pitch accelerations and that of the bounce/roll motions respectively, which indicates a similar level of sensitivity to the fault compared with results from the linear dampers as in Figures 3 and 4. A full assessment of different faults with the bilinear damper is given in Table 2, and again the same pattern of changes to any possible fault

Table 1. Cross-correlation coefficient values (with the linear damper).

	Bounce/pitch			Bounce/roll			Pitch/roll		
	Negative	0s	Positive	Negative	0s	Positive	Negative	0s	Positive
Normal	−0.50	−0.03	+0.49	−0.03	−0.05	−0.02	−0.03	+0.02	+0.02
C_{FL} 75%	−0.48	−0.12	+0.49		−0.32	−0.49		−0.50	+0.48
C_{FL} 50%	−0.46	−0.22	+0.48		−0.28	−0.57		−0.49	+0.56
C_{FL} 25%	−0.43	−0.31	+0.47		−0.22	−0.61		−0.44	+0.60
C_{FL} 0%	−0.38	−0.41	+0.43		−0.14	−0.65		−0.36	+0.64
C_{FR} 75%	−0.48	−0.12	+0.49		+0.27	+0.47		+0.52	−0.46
C_{FR} 50%	−0.46	−0.22	+0.48		+0.25	+0.56		+0.50	−0.55
C_{FR} 25%	−0.43	−0.32	+0.46		+0.19	+0.61		+0.45	−0.59
C_{FR} 0%	−0.38	−0.41	+0.43		+0.12	+0.64		+0.37	−0.63
C_{RL} 75%	−0.50	+0.06	+0.48	−0.38	−0.42		−0.57	+0.40	
C_{RL} 50%	−0.50	+0.16	+0.46	−0.46	−0.40		−0.66	+0.37	
C_{RL} 25%	−0.48	+0.26	+0.43	−0.51	−0.34		−0.70	+0.30	
C_{RL} 0%	−0.45	+0.35	+0.38	−0.56	−0.26		−0.73	+0.22	
C_{RR} 75%	−0.50	+0.06	+0.48	+0.37	+0.38		+0.55	−0.39	
C_{RR} 50%	−0.50	+0.16	+0.46	+0.45	+0.38		+0.65	−0.37	
C_{RR} 25%	−0.48	+0.26	+0.43	+0.50	+0.32		+0.69	−0.30	
C_{RR} 0%	−0.45	+0.35	+0.38	+0.55	+0.25		+0.73	−0.22	

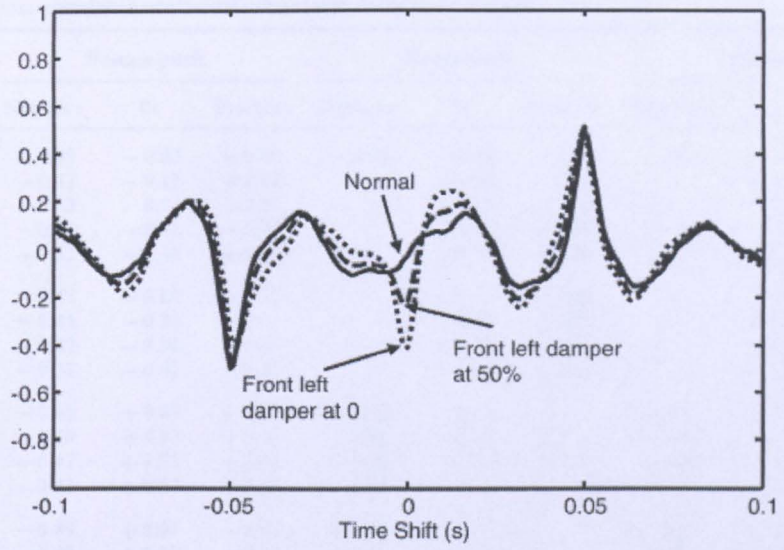

Figure 6. Cross-correlation of the bogie bounce/pitch accelerations (with a bilinear damper).

conditions is observed. Compared with modern model-based fault detection schemes, there is therefore a clear advantage of the proposed technique that it works well without the need for modelling often complex and sometimes difficult nonlinear characteristics which exist in many dynamic systems.

The proposed method reveals a general link between the level of dynamic imbalance in the system and the cross-correlation calculations, although the relationship appears to be nonlinear as indicated in the tables. In practice, some level of asymmetries may exist even in normal conditions as the suspensions cannot be assumed to be perfectly identical. This problem of normal asymmetries may be overcome in practice by detecting derivations of the cross-correlations from the original/normal conditions.

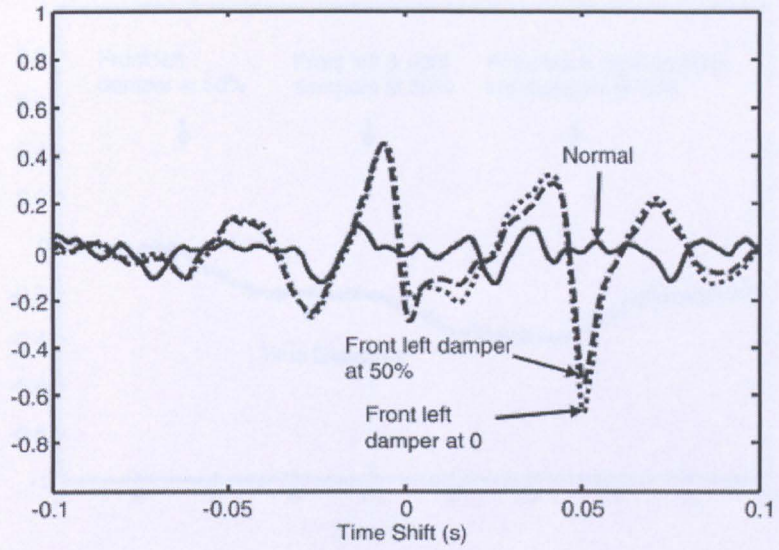

Figure 7. Cross-correlation of the bogie bounce/roll accelerations (with a bilinear damper).

Table 2. Cross-correlation coefficient values (with the bilinear damper).

	Bounce/pitch			Bounce/roll			Pitch/roll		
	Negative	0s	Positive	Negative	0s	Positive	Negative	0s	Positive
Normal	−0.49	−0.02	+0.48	−0.03	−0.04	−0.02	−0.01	+0.02	+0.01
C_{FL} 75%	−0.47	−0.11	+0.48		−0.28	−0.42		−0.42	+0.41
C_{FL} 50%	−0.45	−0.21	+0.47		−0.27	−0.53		−0.45	+0.52
C_{FL} 25%	−0.42	−0.31	+0.45		−0.22	−0.59		−0.41	+0.58
C_{FL} 0%	−0.37	−0.41	+0.42		−0.15	−0.62		−0.34	+0.61
C_{FR} 75%	−0.47	−0.12	+0.48		+0.24	+0.40		+0.44	−0.41
C_{FR} 50%	−0.45	−0.21	+0.47		+0.24	+0.52		+0.47	−0.52
C_{FR} 25%	−0.42	−0.31	+0.45		+0.20	+0.58		+0.42	−0.57
C_{FR} 0%	−0.37	−0.41	+0.42		+0.13	+0.61		+0.34	−0.61
C_{RL} 75%	−0.49	+0.07	+0.47	−0.33	−0.35		−0.47	+0.35	
C_{RL} 50%	−0.49	+0.17	+0.45	−0.43	−0.36		−0.60	+0.36	
C_{RL} 25%	−0.47	+0.27	+0.41	−0.48	−0.31		−0.65	+0.31	
C_{RL} 0%	−0.44	+0.37	+0.37	−0.53	−0.23		−0.69	+0.23	
C_{RR} 75%	−0.49	+0.07	+0.47	+0.30	+0.31		+0.47	−0.34	
C_{RR} 50%	−0.49	+0.17	+0.45	+0.41	+0.34		+0.59	−0.35	
C_{RR} 25%	−0.47	+0.27	+0.41	+0.47	+0.29		+0.65	−0.30	
C_{RR} 0%	−0.43	+0.37	+0.37	+0.52	+0.22		+0.69	−0.23	

For on-line real-time detection, running cross-correlation coefficients with a moving time window of fixed duration may be used to monitor the changes at the three specific time shifts. Figures 8–10 show the normalised cross-correlations of the bounce/pitch, bounce/roll and pitch/roll accelerations, respectively, where a partial fault at the front left suspension is set at 5 s; a second fault at the front right suspension is set at 10 s and a third fault at the rear left suspension is set at 15 s. For clarity of the figures, only the results that are most sensitive to the set fault conditions are shown.

In Figure 8, the cross-correlation between the bounce/pitch motions is increased in the negative direction at 5 s for the first fault (in one of the front suspensions) and further increased

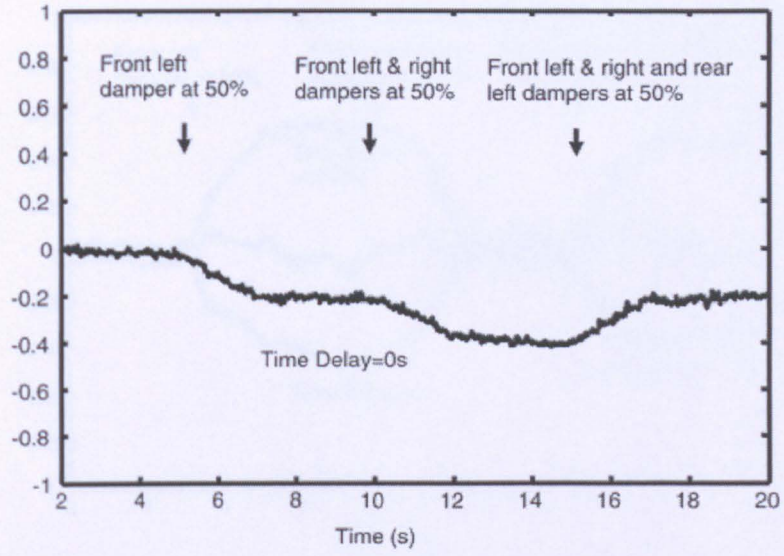

Figure 8. Running cross-correlation coefficient of the bogie bounce/pitch accelerations (with a bilinear damper).

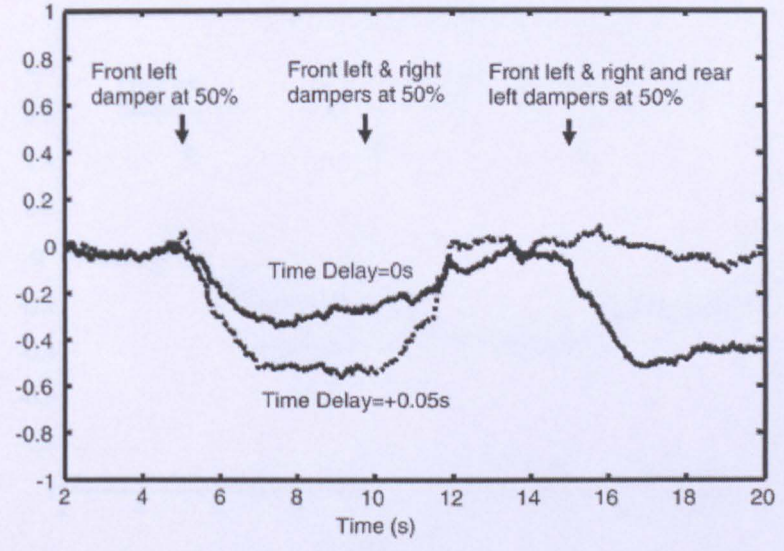

Figure 9. Running cross-correlation coefficient of the bogie bounce/roll accelerations (with a bilinear damper).

at 10 s due to the second fault (also in the front suspensions), as the fault worsens the asymmetry in the pitch direction. When the third fault occurs at 15 s, the cross-correlation is actually improved because the imbalance between the front and rear suspensions is made less severe for the pitch mode.

In Figure 9, the changes in the cross-correlations indicate that an asymmetry between the left and right suspensions exists when there is a fault at the front left damper only (between 5 and 10 s) or when the fault on the one side of the bogie is more severe than the other side (after 15 s). Before 5 s and between 10 and 15 s, the bogie is balanced in the roll direction and the cross-correlations are close to zero. A similar scenario is observed in Figure 10, where the cross-correlations also reflect the level of the roll motion imbalance in the system. The asymmetry in the pitch motion appears to be only sensitive to the bounce/pitch correlation.

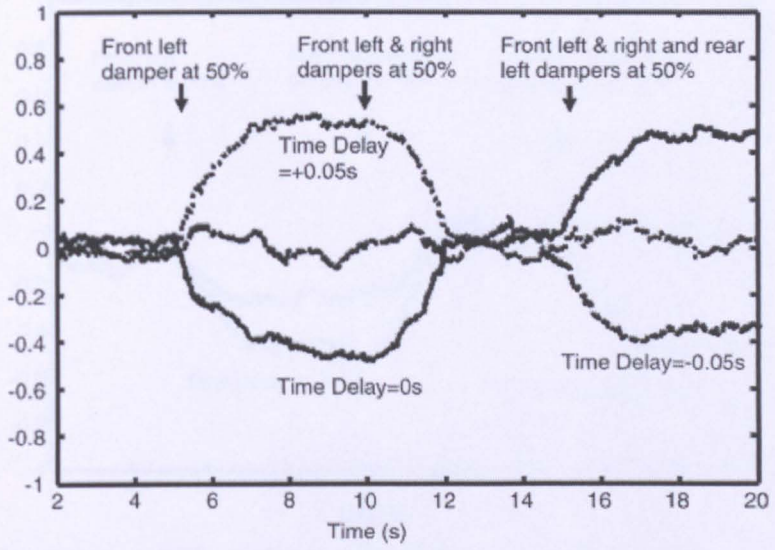

Figure 10. Running cross-correlation coefficient of the bogie pitch/roll accelerations (with a bilinear damper).

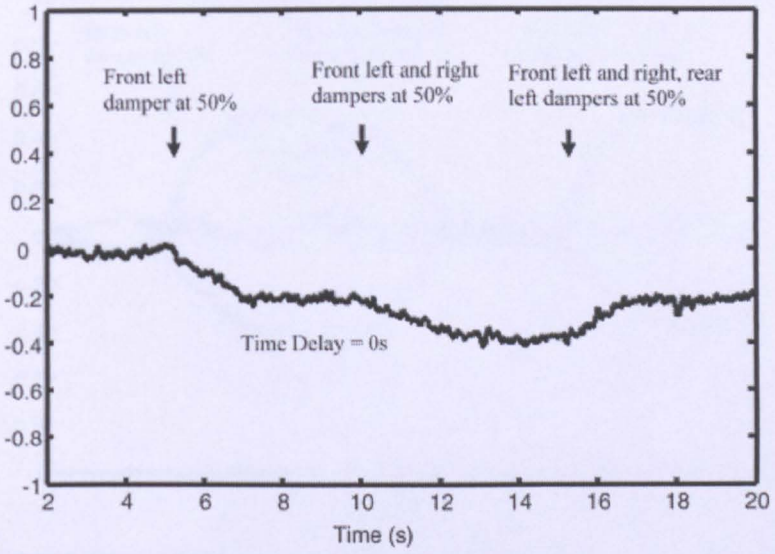

Figure 11. Running cross-correlation coefficient of the bogie bounce/pitch accelerations (with a bilinear damper, at 25 m/s).

Because of the normalisation, the cross-correlation coefficients are insensitive to changes in the vehicle speed. Figures 11–13 show the same cross-correlation results as in Figures 8–10, but at half of the speed (25 m/s). Although the track input excitation becomes much smaller at the lower speed, only minor differences may be observed between the two sets of results. This is significant because it implies that fault detection is largely independent of the input excitations and therefore the use and tuning of thresholds for fault detection can be made easier regardless of the vehicle operation conditions such as speed.

Comparisons with other (more conventional) fault detection schemes have suggested that the new method can be significantly more sensitive to suspension faults, e.g. the relative sensitivity of a detection based on rms accelerations is about 10% for a half-failed damper

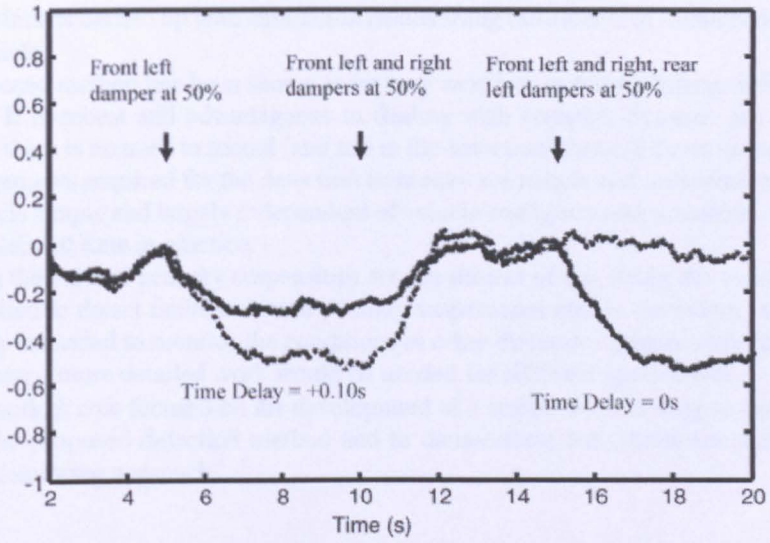

Figure 12. Running cross-correlation coefficient of the bogie bounce/roll accelerations (with a bilinear damper, at 25 m/s).

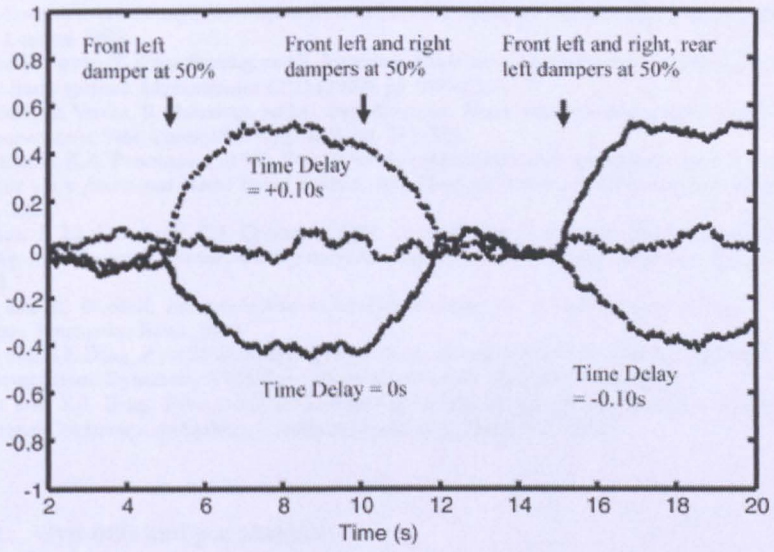

Figure 13. Running cross-correlation coefficient between the bogie pitch and roll accelerations (with a bilinear damper, at 25 m/s).

when compared with 20% or better for the proposed technique – more detailed information may be found in [9].

5. Conclusions

Effective fault detection and condition monitoring of vehicle suspensions do not necessarily require sophisticated and/or difficult to implement techniques. This paper has presented a radically new method based on cross-correlations between the measurements from bogie-mounted inertial sensors. A detailed analysis of the proposed detection method has been

provided, which is backed up with simulation results using the models of a conventional bogie railway vehicle.

The proposed method has been shown to be very sensitive in distinguishing different fault conditions. It is robust and advantageous in dealing with complex dynamic and nonlinear systems, as there is no need to model (and use in the detection) those difficult characteristics. The measurements required for the detection technique are simple and inexpensive to obtain. The scheme is simple and largely independent of vehicle configuration/parameters, and hence easy to implement/tune in practice.

Although the vertical primary suspensions are the subject of this study, the technique may be also applied to detect faults in lateral primary suspensions and in secondary suspensions and possibly extended to monitor the conditions in other dynamic systems with symmetrical configurations – more detailed work would be needed for different applications.

Further work is now focused on the development of a scaled-down test rig to verify experimentally the proposed detection method and to demonstrate the effectiveness of the new condition monitoring approach.

References

[1] M. McDonald and A. Richards, *Vehicle health monitoring on the Docklands Light Railway*, IEE Power Division Colloquium on Advanced Condition Monitoring Systems for Railways, London, 1995.

[2] S. Nicks, *Condition monitoring of the track/train interface*, IEE Seminar Condition Monitoring for Rail Transport Systems, London, 1998.

[3] M. Borner, H. Straky, T. Weispfenning, and R. Isermann, *Model based fault detection of vehicle suspension and hydraulic brake systems*, Mechatronics 12(8) (2002), pp. 999–1010.

[4] P. Metallidis, G. Verros, S. Natsiavas, and C. Papadimitriou, *Fault detection and optimal sensor location in vehicle suspensions*, Vibr. Control 9(3–4) (2003), pp. 337–359.

[5] J.S. Sakellariou, K.A. Petsounis, and S.D. Fassois, *On board fault detection and identification in railway vehicle suspensions via a functional model based method*, Intl. Conf. on Noise and Vibration Engineering, Leuven, Belgium, 2002.

[6] P.F. Weston, P. Li, C.S. Ling, C.J. Goodman, R.M. Goodall, and C. Roberts, *Track and vehicle condition monitoring during normal operation using reduced sensor sets*, Trans. Hong Kong Inst. Eng. 13(1) (2006), pp. 47–53.

[7] K. Goda and R. Goodall, *Fault-detection-and-isolation system for a railway vehicle bogie*, 18th IAVSD Symposium, Kanagawa, Japan, 2003.

[8] T.X. Mei and X.J. Ding, *A model-less technique for the fault detection of rail vehicle suspensions*, Proc. 20th IAVSD Symposium: Dynamics of Vehicles on Roads and Tracks, Berkeley, USA, 2007.

[9] T.X. Mei and X.J. Ding, *New condition monitoring techniques for vehicle suspensions*, Proc. 3rd IET International Conference on Railway Condition Monitoring, Derby, UK, 2008.

Appendix 1. Symbols and parameters

C_{p1}, C_{p2}	damping coefficients at the front and rear primary suspensions
I_b	pitch inertia of bogie
K_{p1}, K_{p2}	spring stiffnesses of the front and rear primary suspensions
L_{bx}	half-axle space of the bogie
L_{vx}, L_{vy}	half space of the vehicle body (pitch and roll directions)
m_b	bogie mass
z_{f1}, z_{f2}	vertical track inputs at the front and rear wheelsets

Vehicle System Dynamics
Vol. 46, Supplement, 2008, 277–287

Taylor & Francis
Taylor & Francis Group

A model-less technique for the fault detection of rail vehicle suspensions

T.X. Mei* and X.J. Ding

School of Electronic and Electrical Engineering, The University of Leeds, Leeds, UK

(*Received 25 July 2007; final version received 23 January 2008*)

This paper presents a novel method for the fault detection and condition monitoring of rail vehicle suspensions. The proposed technique takes advantage of the vehicle (suspension) configurations that are often symmetrical, and explores the additional dynamic interactions between different motions of a bogie or body caused by the failure of suspension components. The basic principle of the proposed detection method is presented and the interactions due to suspension fault conditions are analysed using a conventional two-axle bogie. Side-view models of a bogie vehicle are used in the study to demonstrate the effectiveness of the novel method in detecting damper faults in the suspensions. Both linear and bi-linear dampers are studied.

Keywords: fault detection; vehicle suspension; dampers

1. Introduction

On line fault detection and condition monitoring for rail vehicles offer a number of benefits to railway systems/operations. Detection of component failures at their early stages will prevent further deterioration in vehicle performance and enhance vehicle safety. Timely repair/replacement of the faulty components will lead to increased operational reliability and availability. The need for scheduled maintenance and associated costs can be significantly reduced, because maintenance in the future may be carried out on demand.

The condition monitoring systems developed so far in rail vehicle applications are mainly based on the direct measurement of relevant signals which are analysed using time and/or frequency domain signal processing, e.g. to find features or signatures related to particular faults [1,2]. There are some recent studies that look into parameter identification and estimation techniques based on physical models of the vehicles [3–7]. Those model-based techniques compare a real system with a mathematical model of the system, and the performances are therefore affected by the appropriateness and complexity of the models.

This paper presents a novel approach that is simple but very effective for the detection of suspension faults. The new detection method requires very little knowledge of the system

*Corresponding author. Email: t.x.mei@leeds.ac.uk

ISSN 0042-3114 print/ISSN 1744-5159 online

DOI: 10.1080/00423110801939154
http://www.informaworld.com

(i.e. the bogie), apart from some basic parameters such as vehicle travelling speed and distance between suspensions. The proposed technique is focussed on the comparison of dynamic behaviours between the two suspensions where identical components are normally used. When there are no faults in the system, it can be readily shown that the bounce and pitch motions of the bogie (and to a large extent the vertical movements at the leading and trailing suspensions) are decoupled because of the symmetrical suspension configurations. Therefore, there is little interaction between the two motions. However, a component failure (e.g. a damper) in either of the suspensions will introduce an imbalance into the system, resulting in dynamic interferences between the motions. The level of the interactions therefore provides a key indication of suspension conditions.

The basic idea of the proposed technique is explained in Section 2, with the help of a conventional bogie. In Section 3, the side-view models of a full bogie vehicle are used to demonstrate the effectiveness of the proposed technique in monitoring hydraulic dampers used in primary suspensions. Non-linearity of the dampers and associated fault detection are considered. Practical issues such as sensing and data processing are also discussed. Main conclusions are described in Section 4.

2. Concept of the detection method

The principle of the proposed technique can be illustrated by using the side view model of a single conventional bogie as shown in Figure 1. Standard dynamic equations for the bounce and pitch motions of the bogie may be readily derived and can be found in many references, as given in Equations 1 and 2. From the two equations, it is clear that there are no direct interactions between the bounce and pitch movements of the bogie. The main link between the two is through the track inputs at the leading and trailing wheelsets–the bounce mode is excited by the sum of the two and the pitch mode by the difference of the two. Also the force from the secondary suspension only affects the bounce motion and not the pitch.

$$m_b\ddot{z}_b + 2C_p\dot{z}_b + 2K_p z_b = C_p(\dot{z}_{t1} + \dot{z}_{t2}) + K_p(z_{t1} + z_{t2}) + (F_d) \tag{1}$$

$$I_b\ddot{\phi}_b + 2L_{bx}^2 C_p\dot{\phi}_b + 2L_{bx}^2 K_p\phi_b = L_{bx}C_p(\dot{z}_{t1} - \dot{z}_{t2}) + L_{bx}K_p(z_{t1} - z_{t2}) \tag{2}$$

where C_p, damping coefficient of primary suspensions (nominal); F_d, Force exerted on the bogie from the secondary suspension; I_b, the bogie (pitch) moment of inertia; L_{bx}, semi wheel space; m_b, the bogie mass; K_p, stiffness constant of primary suspensions (nominal); z_b, bogie

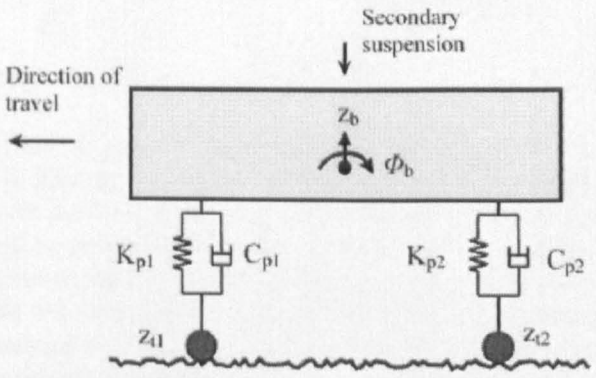

Figure 1. Side view diagram of a conventional railway bogie.

bounce displacement; Φ_b, bogie pitch (angular) displacement; z_{t1}, z_{t1}, track vertical displacement at the leading and trailing wheelsets.

However, Equations 1 and 2 are only valid when the stiffness constants and the damping coefficients at the two primary suspensions are the same, which is the case in most vehicles under the normal circumstances. For the case where the two suspensions may not necessarily have the same values, two more generic equations (Equations 3 and 4) can be derived. The new equations show clear interactions between the two motions, as the pitch movement affects the bounce mode and vice versa. Therefore, the degree of correlations may be used to determine how much unbalance (i.e., due to component fault) may exist in the system.

$$m_b\ddot{z}_b + (C_{p1} + C_{p2}) \cdot \dot{z}_b + (K_{p1} + K_{p2}) \cdot z_b + L_{bx} \cdot (C_{p1} - C_{p2}) \cdot \dot{\phi}_b + L_{bx} \cdot (K_{p1} - K_{p2}) \cdot \phi_b = C_{p1} \cdot \dot{z}_{t1} + K_{p1} \cdot z_{t1} + C_{p2} \cdot \dot{z}_{t2} + K_{p2} \cdot z_{t2} + (F_d) \quad (3)$$

$$I_b\ddot{\phi}_b + L_{bx}^2(C_{p1} + C_{p2}) \cdot \dot{\phi}_b + L_{bx}^2(K_{p1} + K_{p2}) \cdot \phi_b + L_{bx} \cdot (C_{p1} - C_{p2}) \cdot \dot{z}_b + L_{bx} \cdot (K_{p1} - K_{p2}) \cdot z_b = L_{bx}C_{p1} \cdot \dot{z}_{t1} + L_{bx}K_{p1} \cdot z_{t1} - L_{bx}C_{p2} \cdot \dot{z}_{t2} - L_{bx}K_{p2} \cdot z_{t2} \quad (4)$$

where C_{p1}, C_{p2}, damping coefficients of (front and rear) primary suspensions; K_{p1}, K_{p2}, stiffness constants of (front and rear) primary suspensions.

The dynamic equations can be manipulated and expressed in terms of the bogie motions at the front and rear suspensions, i.e. $z_b + L_b\Phi_b$ and $z_b - L_b\Phi_b$, which are shown in Equations 5 and 6. The two equations are almost identical in structure and also in parameters if the two suspensions are the same. The main difference is that the input of Equation 6 is that of Equation 5 delayed by the lagging time of the trailing wheelset to the leading one (i.e. $T = 2L_b/V_x$). Therefore, the responses of the bogie at the front and rear suspensions will be very similar and will have a fixed time delay determined by the wheel-space and vehicle speed, unless a fault occurs and the suspensions become asymmetrical. The level of difference between the two responses may be used to determine the health conditions of the system.

$$\left[m_b\ddot{z}_b + \frac{I_b}{L_{bx}^2}L_{bx}\ddot{\phi}_b\right] + 2C_{p1}\left[\dot{z}_b + L_{bx}\dot{\phi}_b\right] + 2K_{p1}\left[z_b + L_{bx}\phi_b\right] = 2C_{p1} \cdot \dot{z}_{t1} + 2K_{p1} \cdot z_{t1} + (F_d) \quad (5)$$

$$\left[m_b\ddot{z}_b - \frac{I_b}{L_{bx}^2}L_{bx}\ddot{\phi}_b\right] + 2C_{p2}\left[\dot{z}_b - L_{bx}\dot{\phi}_b\right] + 2K_{p2}\left[z_b - L_{bx}\phi_b\right] = 2C_{p2} \cdot \dot{z}_{t2} + 2K_{p2} \cdot z_{t2} + (F_d) \quad (6)$$

The above analyses provide a useful insight for the development of the proposed fault detection method which is illustrated in Figure 2. Only the two accelerations at the leading and trailing suspensions (or the bounce and pitch accelerations) are required in this example. The measured signals will be processed to derive the level of the interactions by computing the cross-correlations between the two measurements, taking into account the time shift between the track inputs at the two suspensions. As it will be shown in the next section, the detection scheme is highly sensitive to component faults (partial or complete), with a large change in the cross-correlation calculations within 1–2 s of a fault occurring.

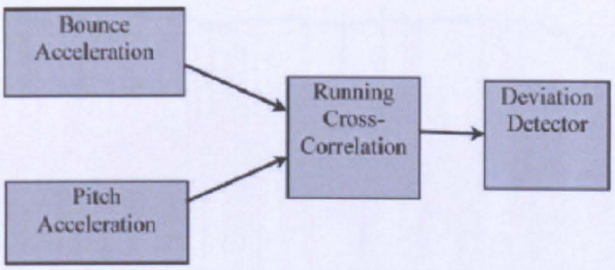

Figure 2. Block diagram of the proposed fault detection scheme.

3. Assessment of the fault detection technique

The side view models of a conventional bogie vehicle are used to study the effectiveness of the proposed fault detection method, which include the bounce and pitch motions of the body frame and the two bogies. Linear dampers in the primary suspension are first studied, followed by an investigation for bilinear dampers. The track irregularities of a typical main line are generated in the simulation to give an appropriate spatial power spectrum (A_{rv}/f_t^2) for the track vertical displacement. The vehicle speed of 50 m/s is used in the simulations. The leading bogie is used in the study for the simulation of damper faults and assessment of different fault detection possibilities, but the outcome will equally applied to the trailing bogie.

Figure 3 shows the acceleration and its running rms (×2) just above the front suspension of the leading bogie, and Figure 4 gives those for the rear suspension. To simulate fault conditions, the damping coefficient of the front suspension is reduced to 50% at the time of 6 s and that of the rear suspension at 12 s. The reduction in damping has an effect of better filtering of high frequency excitations from the track, at the expense of a worse resonance of the bogie modes. The overall responses to the random track data used in the study are reduced at 6 s for the front acceleration and 12 s for the rear acceleration as indicated in the figures. It may be possible to use the acceleration measurements as indicator of suspension conditions, either by computing the running rms or using its frequency responses. Rows 2 and 3 in Table 1

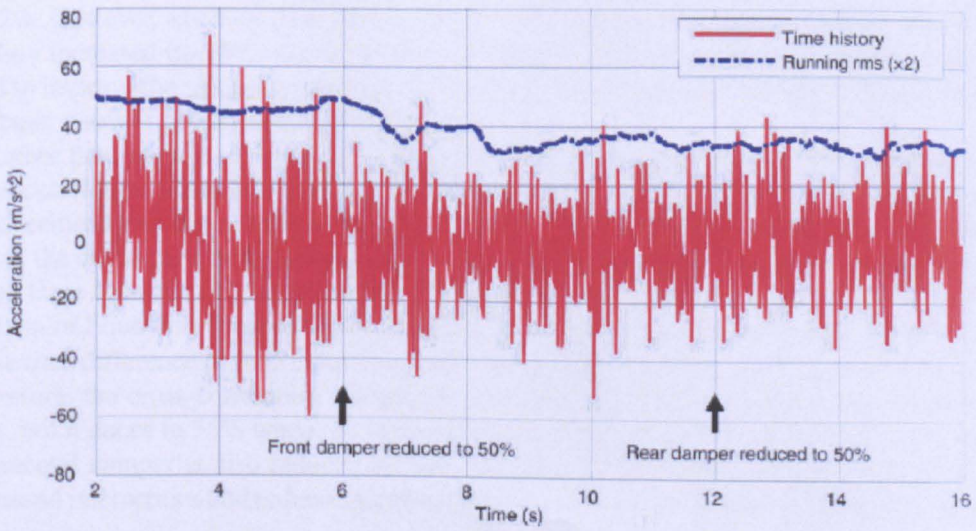

Figure 3. Acceleration above the front primary suspension.

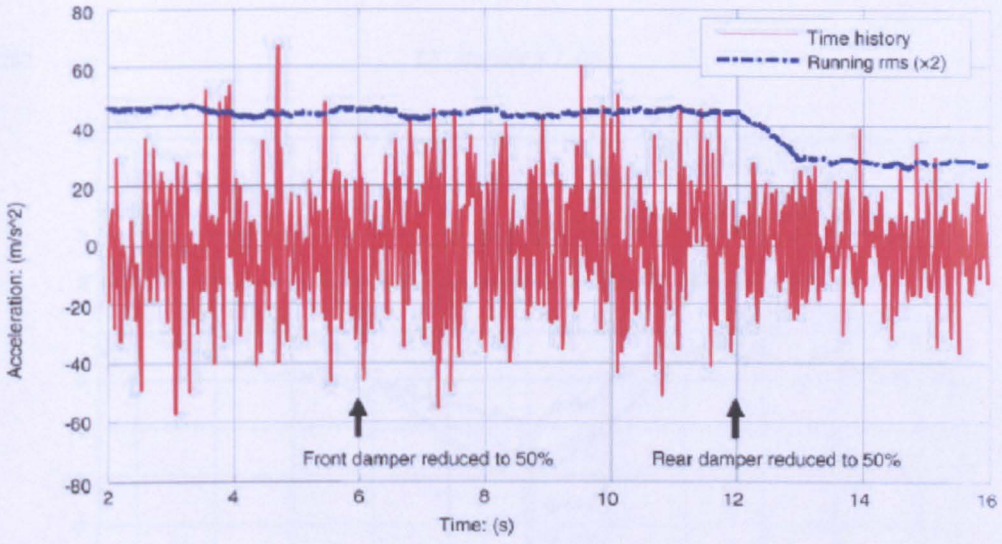

Figure 4. Acceleration above the rear primary suspension.

Table 1. Comparison of different detection options, in % (linear dampers).

	No fault (%)	1 fault (50%)	1 fault (25%)	2 fault (50%)
Front acceleration	100	76.10	78.25	73.24
Rear acceleration	100	98.05	99.71	63.88
Bounce acceleration	100	82.50	82.36	60.20
Pitch acceleration	100	88.47	90.80	70.93
CCF, front and rear accelerations (at −0.05 s time shift)	100	55.51	30.43	40.95
CCF, front and rear accelerations (at zero time shift)	100	81.79	87.80	55.12
CCF, bounce and pitch accelerations (at −0.05 s time shift)	100	58.42	36.47	44.76
CCF, bounce and pitch accelerations (at zero time shift)	100	−497.86	−492.39	214.50
CCF, bounce and pitch accelerations (at +0.05 s time shift)	100	42.71	2.46	30.00

show how the rms values of the two accelerations are affected by the fault dampers. When the damping coefficient in the front suspension is reduced to 50%, the acceleration at the suspension is reduced to about 76% – a change of 24%. For the rear suspension, when its damping coefficient is reduced by 50%, the acceleration is reduced to about 68% – a change of 32%. However, when the damping coefficient is reduced to 25%, the acceleration is actually slightly increased (to 78%) caused by the increased resonance. Additional measures may be used to improve the reliability, but the sensitivity to damper faults is clearly less than desirable to obtain a robust detection for the faults.

Rather than the use of absolute signals directly from the acceleration measurements, the cross-correlation method explored in this study makes relative comparisons between two measurements and hence reduces the effect of the factors that influence both outputs. Figure 5 shows the cross-correlation between the two accelerations at the front and rear suspensions. When there is no fault, the two accelerations are largely independent as explained earlier with the help of Equations 5 and 6. The track input to the two dynamic equations is the same, but at the time difference of 0.05 s (for the semi-wheel space of 1.25 m and the speed of 50 m/s). Therefore, the cross-correlation is the highest at the time shift of −0.05 s when there is no fault, but reduces to 56% when the front damper is reduced to 50% and to about 41% when the second damper is also reduced to 50% (see also Table 1) due to a combination of the increased interactions and reduced accelerations. There is a similar pattern of change (but less

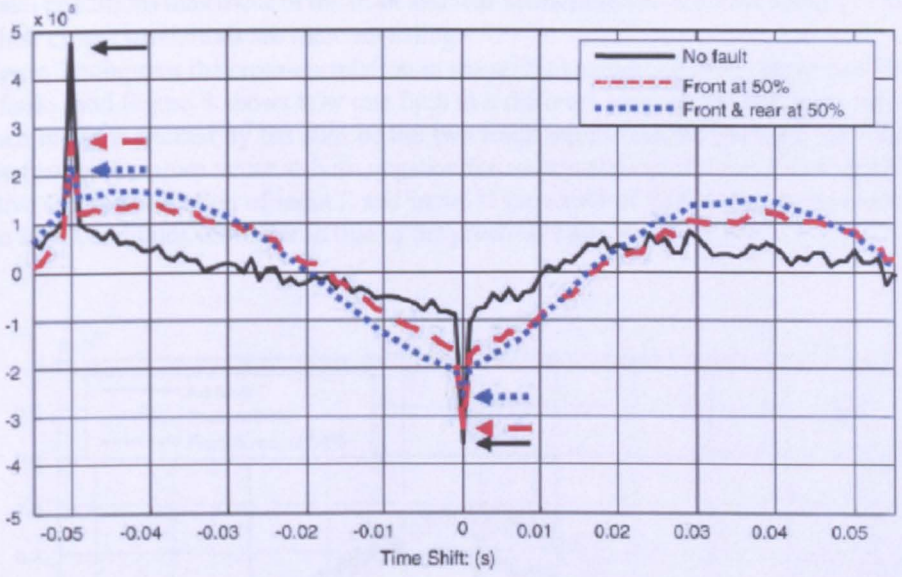

Figure 5. Cross-correlation of accelerations at the front and rear suspensions.

obvious) at the zero time shift, which is caused by additional interactions from the non-uniform distribution of the bogie mass ($m_b \neq I_b/L_{bx}^2$, see Equations 5 and 6) and effect of the vehicle body and secondary suspension.

Different degree of a damper failure is also clearly reflected in the cross-correlations as demonstrated in Figure 6. The peak value at the time shift of -0.05 is reduced from 100% to about 56% and 30% as the damping coefficient is reduced to 50% and 25%, respectively. In both Figures 5 and 6, the effect of reduced damping on the bogie modes in the fault conditions is evident which appears as a sinusoidal waveform of around 12 Hz.

Alternatively, the bounce and pitch accelerations may be considered for the computation of the cross-correlations. The rms values of those two measurements are even less sensitive to

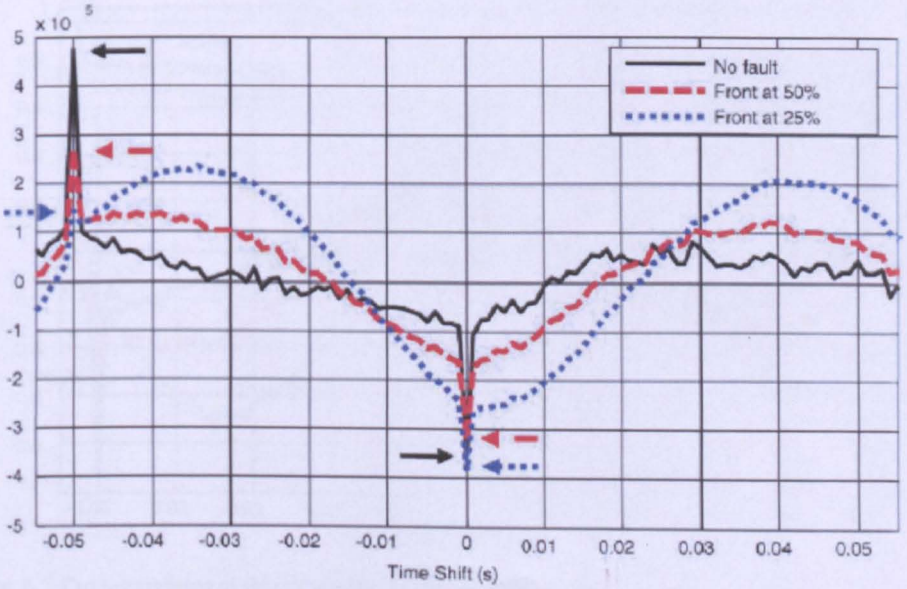

Figure 6. Cross-correlation of accelerations at the front and rear suspensions.

the fault conditions than those of the front and rear accelerations – see rows 4 and 5 of Table 1, but their cross-correlations are more revealing.

Figure 7 compares the cross-correlation in the no fault condition with that in one fault and two faults, and Figure 8 shows how one fault at a different level affects the outcome. As the bounce mode is excited by the sum of the two track inputs and the pitch by the difference of the two, peak values occur at both negative (cross-correlation of input 1 and input 2) and positive (cross-correlation of input 2 and input 1) time shift of 0.05 s. The pattern of change to the fault conditions is similar to that in the previous case.

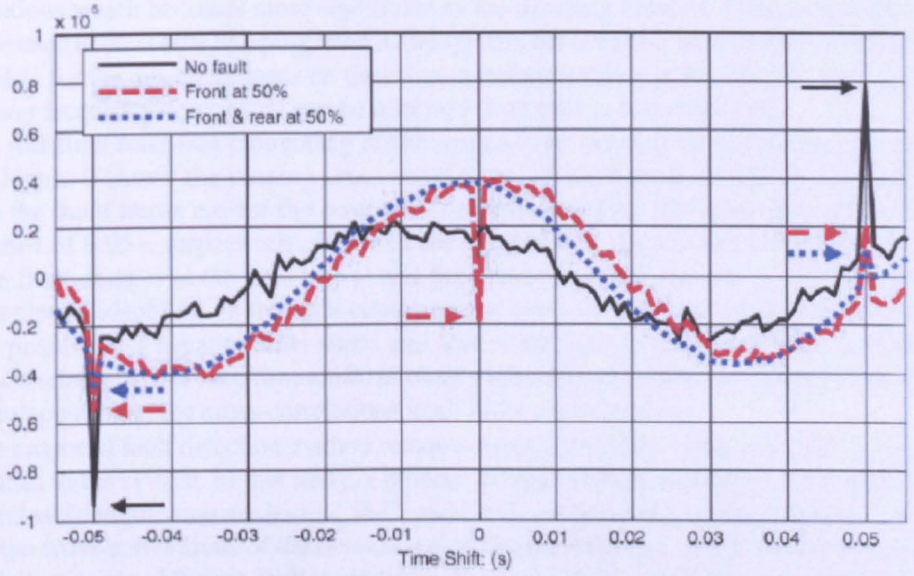

Figure 7. Cross-correlation of the bogie bounce and pitch accelerations.

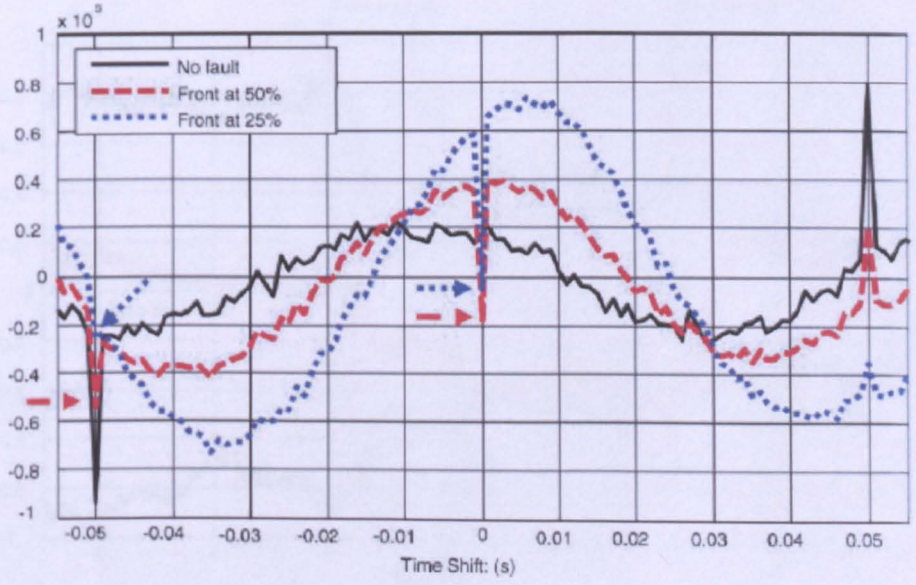

Figure 8. Cross-correlation of the bogie bounce and pitch accelerations

However, the cross-correlation at the zero time shift shows a large (negative) pulse only when there is an asymmetry between the two suspensions. In the normal condition or with the same fault in the two suspensions, there is no spike at the zero time shift at all. This is because the cross-correlation of the bounce and pitch motions due to the track input 1 (at the front suspension) cancels that due to the track input 2 (at the rear suspension) in the balanced conditions, whereas interactions between the two motions due to asymmetry in the suspensions causes a bias. The change at the point of zero time shift is far more sensitive than those at the time shift of $+/-0.05$ s, and therefore can potentially provide a far more useful means for fault detection.

Similar to the previous case, there is a sinusoidal component of around 12 Hz in the cross-correlations which becomes more significant as the damping reduces. This component itself may be used to detect the damping level in the system, but it would improve the sensitivity and reliability for the detection based on the cross-correlation values at the specific time shifts, if the lower frequency component can be removed from the cross-correlations.

For real time condition monitoring of the suspensions, running cross-correlations may be used. Figure 9 shows the running cross-correlations of the bounce and pitch accelerations, where the three traces are for the positive time shift of 0.05 s, zero time shift and negative time shift of 0.05 s, respectively. Between the three traces, the normal condition, one fault (of the front damper at the time of 6 s) and the second fault (of the rear suspension at 12 s) can be clearly identified. In the fault condition, the cross-correlations are of high magnitude at the positive and negative time shifts and low at the zero time shift. With one fault, the cross-correlation at the zero time shift becomes high while the other two become low. In the two fault condition, the cross-correlations in all three traces are low.

The proposed fault detection method remains equally effective when there are severe non-linearities in the system. In this study, a bilinear damper with the damping coefficients in the rebound and compression modes of 2.56 C_s and 0.8 C_s, respectively, is used. Figures 10 and 11 show the cross-correlations of the bounce and pitch accelerations, which indicate even better sensitivities to the different fault conditions. At the point of zero time shift, the difference between the symmetrical and asymmetrical suspensions is more than 50 times. No additional

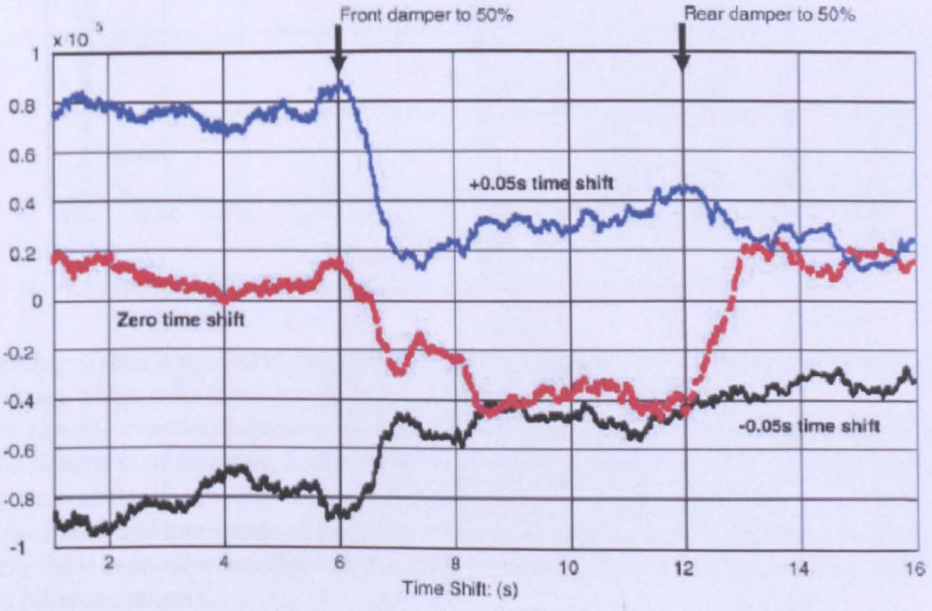

Figure 9. Running cross-correlation of the bounce and pitch accelerations.

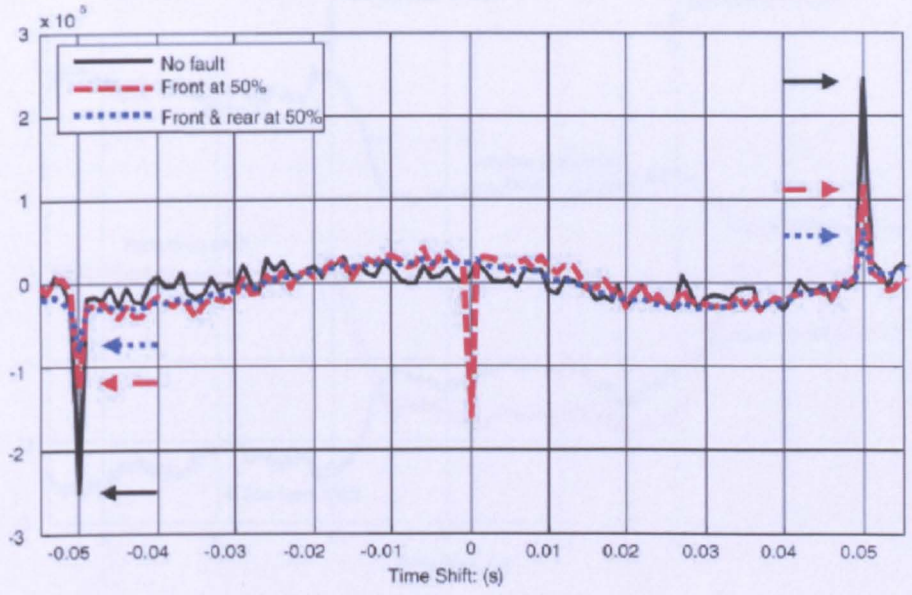

Figure 10. Cross-correlation of bounce and pitch accelerations, with bilinear dampers.

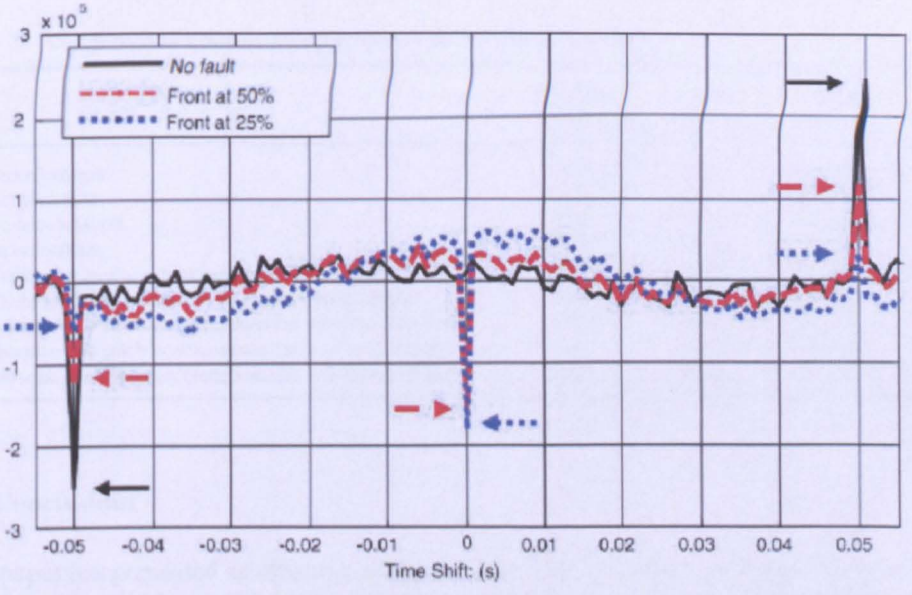

Figure 11. Cross-correlation of bounce and pitch accelerations, with bilinear dampers.

processing of data is needed in this study, which is an advantage compared to the model-based techniques where a far more complex solution would normally be needed.

The running cross-correlations in Figure 12 also demonstrate a high level of consistency for the detection of different faults in the suspensions, indicating no fault (high magnitude at the time shifts of +/−0.05 s and low at zero time shift), one fault (high magnitude at the zero time shift and low values at the other two) and two faults (low values in all three traces). Clearly there is no adverse effect on the effectiveness of the detection methods from the use of the bilinear dampers.

Detailed numerical comparisons are provided in Table 1 (for the linear damper) and Table 2 (for the nonlinear damper).

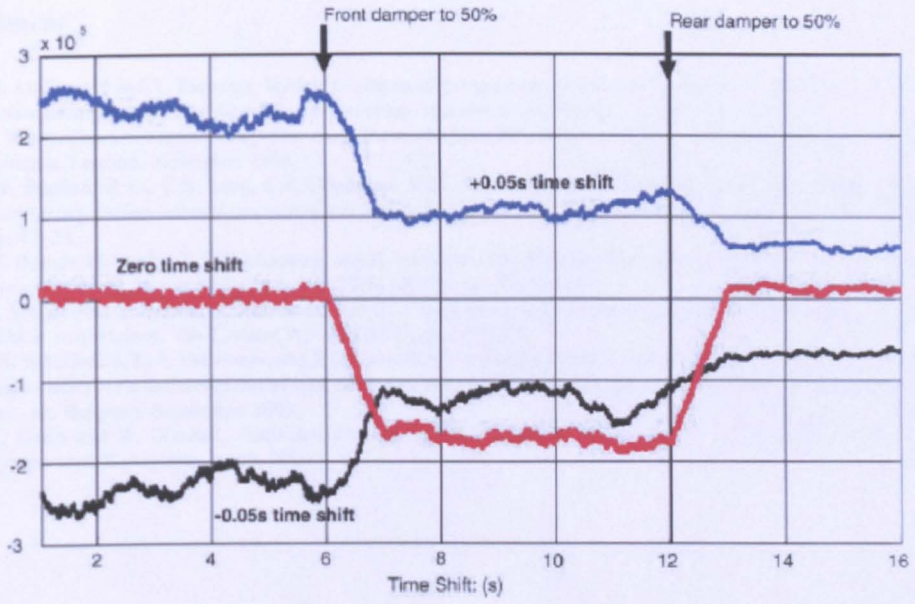

Figure 12. Running cross-correlation, with bilinear dampers.

Table 2. Comparison of different detection options, in % (bilinear dampers).

	No fault (%)	1 fault (50%)	1 fault (25%)	2 fault (50%)
Front acceleration	100	60.91	51.29	55.06
Rear acceleration	100	96.30	95.81	52.19
Bounce acceleration	100	79.54	75.07	52.17
Pitch acceleration	100	80.68	77.12	54.04
CCF, front and rear accelerations (at −0.05 s time shift)	100	49.71	23.87	28.04
CCF, front and rear accelerations (at zero time shift)	100	65.78	60.71	29.90
CCF, bounce and pitch accelerations (at −0.05 s time shift)	100	49.96	25.31	28.82
CCF, bounce and pitch accelerations (at zero time shift)	100	−8378	−9900	323
CCF, bounce and pitch accelerations (at +0.05 s time shift)	100	48.56	17.75	26.80

4. Conclusions

This paper has presented an effective method for the fault detection and condition monitoring of railway suspensions using cross-correlations between the measurements from two bogie mounted accelerometers.

The proposed method has been shown to be very sensitive and reliable in distinguishing different fault conditions. It is robust and advantageous in dealing with complex dynamic and non-linear systems, as there is no need to model (and use in the detection) those difficult characteristics. The measurements required for the detection technique are simple and inexpensive to obtain. The scheme is simple and largely independent of vehicle configuration/parameters, and hence easy to implement/tune in practice.

Although the vertical suspensions are the subject of the study in this paper, the technique may be equally applied to monitor conditions of other suspensions where the interactions may be introduced by the component failures including primary, secondary, vertical, and lateral suspensions.

References

[1] M. McDonald and A. Richards, *Vehicle health monitoring on the Docklands Light Railway*, IEE Power Division Colloquium on Advanced Condition Monitoring Systems for Railways, London, October 1995.

[2] S. Nicks, *Condition monitoring of the track/train interface*, IEE Seminar Condition Monitoring for Rail Transport Systems, London, November 1998.

[3] P.F. Weston, P. Li, C.S. Ling, C.J. Goodman, R.M. Goodall, and C. Roberts, *Track and vehicle condition monitoring during normal operation using reduced sensor sets*, Trans. Hong Kong Inst. Eng. 13(1) (2006), pp. 47–53.

[4] M. Borner, H. Straky, T. Weispfenning, and R. Isermann, *Model based fault detection of vehicle suspension and hydraulic brake systems*, Mechatronics 12(8) (2002), pp. 999–1010.

[5] P. Metallidis, G. Verros, S. Natsiavas, and C. Papadimitriou, *Fault detection and optimal sensor location in vehicle suspensions*, Vib. Control 9(3–4) (2003), pp. 337–359.

[6] J.S. Sakellariou, K.A. Petsounis, and S.D. Fassois, *On board fault detection and identification in railway vehicle suspensions via a functional model based method*, International Conference on Noise and Vibration Engineering, Leuven, Belgium, September 2002.

[7] K. Goda and R. Goodall, *Fault-detection-and-isolation system for a railway vehicle bogie*, 18th IAVSD Symposium, Kanagawa, Japan, 2003.

Condition Monitoring of Vehicle Suspensions using Relative Variances

X. J. Ding* and T. X. Mei**

* *The University of Leeds, School of Electronic and Electrical Engineering, Leeds, LS2 9JT, UK*
** *Salford University, School of Computing, Science and Engineering, Greater Manchester, M5 4WT, UK*
(corresponding author: Prof. T X Mei, e-mail: t.x.mei@theiet.org)

Abstract: This paper studies a new approach for the condition monitoring of railway vehicle suspensions based on the comparison of dynamic behaviours between the suspensions where same components are normally used. The techniques requires the use of a sensor box mounted on the bogie to measure the bounce, pitch and roll accelerations which can be used to derive the accelerations at the four corners above the suspensions. The derived data are then processed using relative variance algorithms. The study will show that there is a close relationship between the relative variances and component faults (and location of the component faults) and that the detection and isolation are sensitive to faults, but do not require detailed knowledge of the vehicle/bogie and external conditions (e.g. track inputs).

Keywords: damper, fault, detection and isolation, relative variance.

1. INTRODUCTION

Components of the suspension systems have significant influence to the performance of a railway vehicle. The unexpected component fault may deteriorate the ride comfort, increase the wheel and rail wear and endanger the passenger safety (Gillespie, 1992). This study is focussed on the detection of damper failures which occur due to the wear of the seals and the loss of oil etc (Weisppenning, 1997). Rapid and effective supervision system in detecting and locating the fault(s) is therefore highly desirable to improve the vehicle reliability and reduce the maintenance cost.

There have been recent studies of condition monitoring techniques for vehicle dynamics, most of which are targeted for automotive applications. A lot of research has been focussed on the model-based methods which include the parameter estimation, state estimation and parity equation checks etc (Bruni *et al.*, 2007; Charles, *et al.*, 2006; Goda, *et al.*, 2004; Goodall, 2006; Isermann, 2006; Li, *et al.*, 2004; Willsky, 1976). There are also more empirical approaches using direct processing techniques to subtract particular signatures or frequency features in the measured signals (Sunder, *et al.*, 2001).

However, this paper proposes a new approach focused on the comparison of different performance from the bogie corner accelerations, which can be easily derived from the measurable bounce, pitch and roll accelerations. The idea is based on the observation that the dynamic symmetry is removed if any one of the four suspensions (at the four corners of a bogie) becomes faulty, leading to increased dynamic interactions between different bogie modes and in particular changes of dynamic behaviour of the suspension concerned. Computation and comparison of relative variances of the bogie accelerations at all four suspensions reveal a close link of the variances to different fault conditions which are exploited in this study in the fault detection and isolation for the vehicle suspension systems.

2. MATHEMATICAL MODELLING

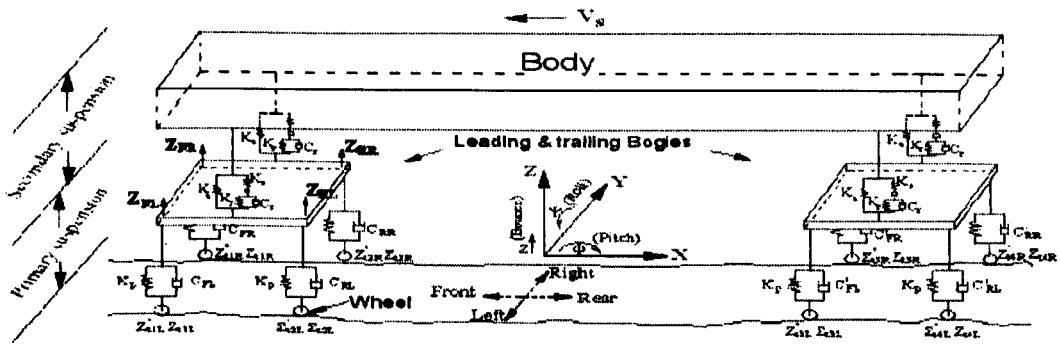

Fig 1. A comprehensive conventional vehicle in vertical dynamics

Figure 1 gives a simplified diagram of a conventional railway bogie vehicle used in the study, which consists of a vehicle body, two bogies, two sets of airsprings for the secondary suspensions (between the bogies and the body frame) and four sets of primary suspensions on each of the two bogies connected the bogie to four wheelsets. Only vertical springs/airsprings and dampers are shown and studied, although in practice there are also longitudinal, lateral and yaw dynamics. Because the study is aimed at monitoring of the vertical suspensions, only motions affected by the suspensions are considered, i.e. three degrees of freedom in bounce, pitch and roll directions for the body and the bogies. The mathematical models of the leading bogie are given in equations 1-4, where bounce, pitch and roll motions are converted to the vertical movements at the four suspensions. Models for the other bogie and for the body frame have also been developed and used in the simulation.

In general, the bogie modes have a relatively high frequency range of around 10 Hz (or higher) whereas the body modes tend to have a lower frequency of around 1 Hz, as indicated in Table 1. The lower frequency of the body modes also is a factor that the transmitted force from the bogies to the body via the secondary suspension be much lower than that via the primary suspensions. Consequently the effect of the secondary suspension forces F_d or F_e will be negligible compared to that of the primary suspension forces in the development of the proposed condition monitoring method.

Table 1. Natural frequency and damping of a bogie vehicle

		Freq. (Hz)	Damping
Bogie Mode	Bounce	10.57	0.23
	Pitch	14.07	0.32
	Roll	14.79	0.31
Body Mode	Bounce	0.68	0.16
	Pitch	0.84	0.19
	Roll	0.84	0.19

$$
\begin{aligned}
&(I_{bx}/L_x^2+m_b)/2\cdot\ddot{z}_{FL}+(3C_{FL}+C_{FR}+C_{RL}-C_{RR})\cdot\dot{z}_{FL}+4K_p\cdot z_{FL}\\
&-(C_{FL}-C_{FR}+C_{RL}-C_{RR})/2\cdot\dot{z}_{FR}\\
&+(I_{by}/L_y^2-I_{bx}/L_x^2)/2\cdot\ddot{z}_{RL}-(C_{FL}+C_{FR}-C_{RL}-C_{RR})/2\cdot\dot{z}_{RL}\\
&-(I_{by}/L_y^2-m_b)/2\cdot\ddot{z}_{RR}+(C_{FL}-C_{RR})\cdot\dot{z}_{RR}\\
&=(3C_{FL}\cdot\dot{z}_{r1L}+C_{FR}\cdot\dot{z}_{r1R}+C_{RL}\cdot\dot{z}_{r2L}-C_{RR}\cdot\dot{z}_{r2R})\\
&+K_p(3z_{r1L}+z_{r1R}+z_{r2L}-z_{r2R})+F_d+F_e
\end{aligned}
\tag{1}
$$

$$
\begin{aligned}
&I_{by}/L_y^2\cdot\ddot{z}_{FR}+(C_{FL}+3C_{FR}+C_{RL}+C_{RR})/2\cdot\dot{z}_{FR}+4K_p\cdot z_{FR}\\
&-[I_{by}/L_y^2-(I_{bx}/L_x^2+m_b)/2]\cdot\ddot{z}_{FL}+(C_{FL}+C_{FR}-C_{RL}-C_{RR})\cdot\dot{z}_{FL}\\
&+(I_{by}/L_y^2-I_{bx}/L_x^2)/2\cdot\ddot{z}_{RL}-(C_{FL}+C_{FR}-C_{RL}-C_{RR})/2\cdot\dot{z}_{RL}\\
&-(I_{by}/L_y^2-m_b)/2\cdot\ddot{z}_{RR}+(C_{FR}-C_{RL})\cdot\dot{z}_{RR}\\
&=(C_{FL}\cdot\dot{z}_{r1L}+3C_{FR}\cdot\dot{z}_{r1R}-C_{RL}\cdot\dot{z}_{r2L}+C_{RR}\cdot\dot{z}_{r2R})\\
&+K_p(z_{r1L}+3z_{r1R}-z_{r2L}+z_{r2R})+F_d-F_e
\end{aligned}
\tag{2}
$$

$$
\begin{aligned}
&(I_{by}/L_y^2+I_{bx}/L_x^2)\cdot\ddot{z}_{RL}+(C_{FL}+C_{FR}+3C_{RL}+C_{RR})/2\cdot\dot{z}_{RL}+4K_p\cdot z_{RL}\\
&-(I_{bx}/L_x^2-m_b)/2\cdot\ddot{z}_{FL}+(C_{FL}-C_{FR}+C_{RL}-C_{RR})\cdot\dot{z}_{FL}\\
&-(C_{FL}-C_{FR}+C_{RL}-C_{RR})/2\cdot\dot{z}_{FR}\\
&-[(I_{by}/L_y^2-m_b)-(C_{FL}-C_{FR}+C_{RL}-C_{RR})]/2\cdot\ddot{z}_{RR}\\
&-(C_{FL}+C_{FR}-C_{RL}-C_{RR})/2\cdot\dot{z}_{RR}\\
&=(C_{FL}\cdot\dot{z}_{r1L}-C_{FR}\cdot\dot{z}_{r1R}+3C_{RL}\cdot\dot{z}_{r2L}+C_{RR}\cdot\dot{z}_{r2R})\\
&+K_p(z_{r1L}-z_{r1R}+3z_{r2L}+z_{r2R})+F_d+F_e
\end{aligned}
\tag{3}
$$

$$
\begin{aligned}
&m_b/2\cdot\ddot{z}_{RR}+(C_{FR}+C_{RL}+2C_{RR})\cdot\dot{z}_{RR}+4K_p\cdot z_{RR}\\
&-(I_{bx}/L_x^2-m_b)/2\cdot\ddot{z}_{FL}\\
&-(C_{FL}-C_{FR}+C_{RL}-C_{RR})/2\cdot\dot{z}_{FR}\\
&-(I_{by}/L_y^2-I_{bx}/L_x^2)/2\cdot\ddot{z}_{RL}-(C_{FL}+C_{FR}-C_{RL}-C_{RR})/2\cdot\dot{z}_{RL}\\
&=(-C_{FL}\cdot\dot{z}_{r1L}+C_{FR}\cdot\dot{z}_{r1R}+C_{RL}\cdot\dot{z}_{r2L}+3C_{RR}\cdot\dot{z}_{r2R})\\
&+K_p(-z_{r1L}+z_{r1R}+z_{r2L}+3z_{r2R})+F_d-F_e
\end{aligned}
\tag{4}
$$

where

C_{FL}, C_{FR}, C_{RL}, C_{RR} – Front left, front right, rear left, rear right dampings of leading bogie

F_d,F_e – Additional forces from the secondary suspension

I_{bx}, I_{by} – Pitch and Roll inertia of bogie

K_p – One spring stiffness of primary suspensions

L_x,L_y - Half wheel space of the vehicle bogie in pitch and roll directions

m_b - Mass of bogie

z_{r1L}, z_{r1R}, z_{r2L}, z_{r2R} - Front left, front right, rear left, rear right track inputs of leading bogie.

In practice, the basic movements of bounce, pitch and roll can be measured from a solid sensor box (with accelerometers and gyros) mounted onto the bogie frame (Charles, *et al.*, 2006). The accelerations of the bogie above the four suspensions may be easily derived using the output signals from the three sensors and bogie geometrical parameters as given in equations 5-8.

$$\ddot{z}_{FL} = \ddot{z}_b + L_x\cdot\ddot{\phi}_b + L_y\cdot\ddot{\psi}_b \tag{5}$$

$$\ddot{z}_{FR} = \ddot{z}_b + L_x\cdot\ddot{\phi}_b - L_y\cdot\ddot{\psi}_b \tag{6}$$

$$\ddot{z}_{RL} = \ddot{z}_b - L_x\cdot\ddot{\phi}_b + L_y\cdot\ddot{\psi}_b \tag{7}$$

$$\ddot{z}_{RR} = \ddot{z}_b - L_x\cdot\ddot{\phi}_b - L_y\cdot\ddot{\psi}_b \tag{8}$$

where z_b, ϕ_b, ψ_b- bounce, pitch and roll motions of a bogie

3. SCHEME OF THE PROPOSAL METHOD

Figure 2 shows a block diagram of the proposed technique for detecting and isolating damper faults in the primary suspensions, which may be implemented in three stages. The first stage will be to derive the bogie accelerations at the positions above the four primary suspensions from bounce, pitch and roll motions using equations 5-8.

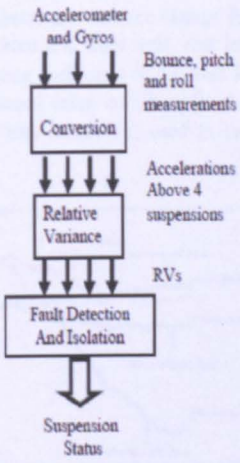

Fig 2. Proposed Condition Monitoring Scheme

Variances of the four accelerations can then be calculated with a fixed number of samples (i.e. fixed time window) as shown in equations 9-12, which may be implemented online with a running (i.e. sliding) time window.

$$V_{FL}(k) = \sum_{i=k}^{k+n-1} (\ddot{z}_{FL}(i) - \overline{\ddot{z}_{FL}})^2 \Big/ n \tag{9}$$

$$V_{FR}(k) = \sum_{i=k}^{k+n-1} (\ddot{z}_{FR}(i) - \overline{\ddot{z}_{FR}})^2 \Big/ n \tag{10}$$

$$V_{RL}(k) = \sum_{i=k}^{k+n-1} (\ddot{z}_{RL}(i) - \overline{\ddot{z}_{RL}})^2 \Big/ n \tag{11}$$

$$V_{RR}(k) = \sum_{i=k}^{k+n-1} (\ddot{z}_{RR}(i) - \overline{\ddot{z}_{RR}})^2 \Big/ n \tag{12}$$

It is possible to use the variance values for fault detection, as any change in suspension conditions will have a direct effect on the bogie accelerations especially at the location of the corresponding suspension. However, there are other factors which may also affect the variances, most noticeably the vehicle speed as input (vibration) excitations from the track irregularities differ significantly at different speeds.

This may be overcome by comparing the four outputs of the variance calculations presents using the concept of majority 'voting', as the variance values should be similar in nominal (no fault) condition but differ if there are faults at some of the suspensions - as far as all four suspensions do not fail at the same time in the same manner the probability of which would be very low. This is based on the fact that same components are typically used on the railway suspensions and the bogies are symmetrical in configuration in the normal condition and only become unbalanced when some of suspensions start to fail. To make the comparison easier, relative variance is introduced which is normalised between the four variances as shown in equations 13-16.

$$RV_{FL}(k) = \frac{4 \times V_{FL}(k)}{V_{FL}(k) + V_{FR}(k) + V_{RL}(k+m) + V_{RR}(k+m)} \tag{13}$$

$$RV_{FR}(k) = \frac{4 \times V_{FR}(k)}{V_{FL}(k) + V_{FR}(k) + V_{RL}(k+m) + V_{RR}(k+m)} \tag{14}$$

$$RV_{RL}(k) = \frac{4 \times V_{RL}(k)}{V_{FL}(k-m) + V_{FR}(k-m) + V_{RL}(k) + V_{RR}(k)} \tag{15}$$

$$RV_{RR}(k) = \frac{4 \times V_{RR}(k)}{V_{FL}(k-m) + V_{FR}(k-m) + V_{RL}(k) + V_{RR}(k)} \tag{16}$$

Where k is the step for each set of the sampling acceleration. m is the number of delayed sampling interval which is decided by the wheel space and the vehicle speed.

The relative variance calculations at the two rear suspensions (Equation 15 and 16) are almost the identical in structure with those for the front suspensions (Equations 13 and 14) except the delayed time interval m, so that the comparisons are made based on the same track inputs. The relative variance for each of the four accelerations should remain largely unchanged in normal conditions even if the operation speed changes. Only a fault in a component (e.g., a damper in the suspension) can lead to changes in the relative variances. The most significant change of a relative variance is expected to correspond with the fault at the particular suspension and therefore fault isolation is also possible.

4. PERFORMANCE ASSESSMENTS

In this section, the simulation results are given to assess the performance of the proposed fault detection scheme. Both the variances and the relative variance (i.e. normalised) for the four accelerations are presented.

Figure 3 compares the acceleration at the front left corner in the cases of no fault and the damper with 50% of the nominal damping coefficient. The overall acceleration is slightly reduced, as the (partial) damper fault reduces the damping of the bogie modes and increases the corresponding resonances even though the responses at higher frequencies are lowered. This faulty damper also affects the accelerations at the other three corners, although these changes are much smaller. Although there is a link between the bogie vibrations and the suspension conditions, the sensitivity is relatively low for practical applications.

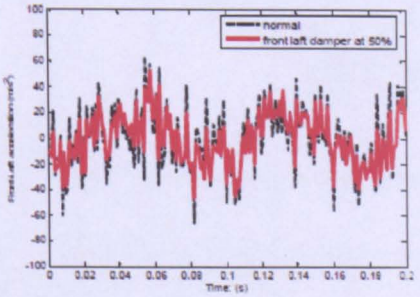

Fig 3. Front left acceleration change with front left damper fault

Clear improvements may be obtained with the variance approach. Figure 4 shows the variance change for the four corner accelerations front left, front right, rear left and rear right – with the damping coefficient of the front left damper reduced from the nominal value to 50% at 8s. A 5 seconds moving (i.e. sliding) time window is used to calculate the running variances.

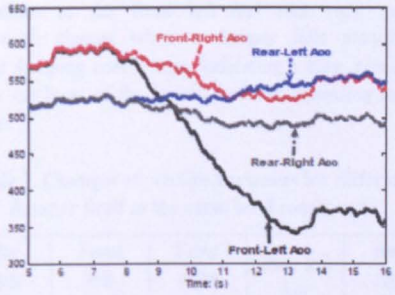

Fig 4. Running variance of corner acceleration with front left damper faulty

The variance of the front left acceleration is the most sensitive to the fault for obvious reasons. There are also changes in the other three variances, but those are much smaller. A potential issue with the direct use of the variance values is that there are some noticeable fluctuations in both normal and fault conditions, which makes setting/tuning of threshold difficult. The fluctuations are caused by the changes of bogie responses to varying track input excitation which is inevitable as track misalignment is of random feature.

The proposed use of the relative variance overcomes the problem, as all calculations are normalised which removes the effect of the input variations. Figure 5 show the relative variance changes of the four corner accelerations when the front left damper has a 50% fault, where only the relative variance of the front right acceleration is significantly lower. Figure 6 shows the results with front right damper at 50% of the nominal damping coefficients and again only the relative variance of the acceleration at the corresponding suspension becomes much lower in the fault condition. More significantly, it is clear from the figures that the (running) relative variances give much smooth results and the variations due to different inputs are considerably smaller compared to the variance values because of the normalisation. The advantage of the normalisation is also clear when the input excitations are varied due to different vehicle speed. Figures 7 and 8 compare the variance and relative variance of the front left acceleration at the speeds of 25m/s and 50m/s. The variance value of the acceleration is nearly twice at 50m/s as that at 25m/s, in both the normal and damper fault situations. However, the relative variance change is more consistent which has similar magnitude and reduction for either normal or faulty circumstance. With a proper threshold, the fault could be detected effectively when relative variance approach is applied.

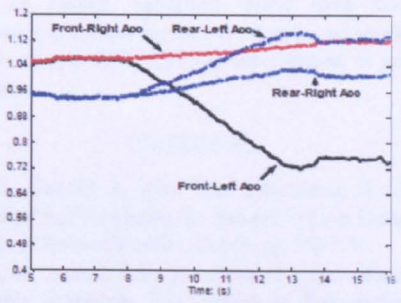

Fig 5. Relative variance change with front left damper fault

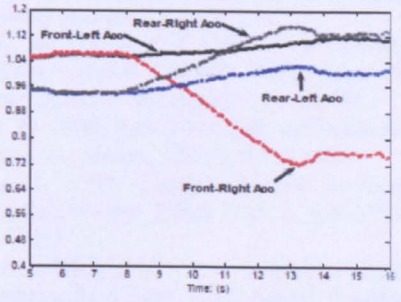

Fig 6. Relative variance change with front right damper fault

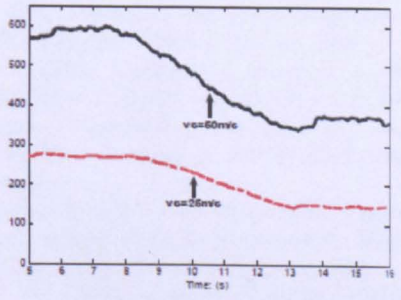

Fig 7. Variance change with different vehicle velocities

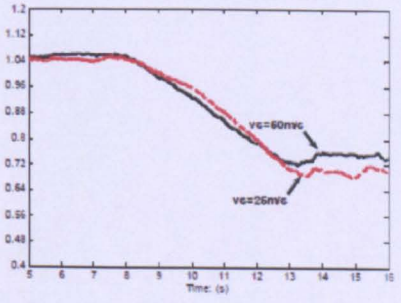

Fig 8. Relative Variance change with different vehicle velocities

4.3 Fault Identification

The proposed relative variance approach is not only valid for detecting faults in the suspensions, but also useful to their

identification. because of the strong link between the relative variance of any particular acceleration and the corresponding suspension. Table 2 confirms how each of the damper faults (at 50%) affect the relative variances and it is clear that only significant change to the relative variance of the acceleration corresponds to the damper fault at the same position whereas the effect on the three other relative variances is limited. Table 3 and 4 present how the relative variances (of the bogie accelerations at the front left and rear right damper respectively) change when a damper fails partially to different damping coefficients, indicating a clear correlation between the level of the fault(s) and corresponding relative variances.

Table 2. Changes of relative variances for different damper fault at the same level conditions

Faulty damper at 50%	Front left Acc	Front right Acc	Rear left Acc	Rear right Acc
No fault	106	106	94	94
Front left	74.3	111.5	112.8	101.4
Front right	110.0	74.6	101.1	113.2
Rear left	134.8	113.7	53.4	98.1
Rear right	113.0	135.7	97.8	53.5

Table 3. Changes of relative variances for front left damper faults at different level conditions

Front left damping remains	Front left Acc	Front right Acc	Rear left Acc	Rear right Acc
75%	85.4	109.0	106.4	99.2
50%	74.3	111.5	112.8	101.4
25%	68.0	109.1	117.3	105.7
0%	63.6	101.0	122.0	113.4

Table 4. Changes of relative variances for rear right damper faults at different level conditions

Rear right damping remains	Front left Acc	Front right Acc	Rear left Acc	Rear right Acc
75%	108.6	120.0	98.3	73.0
50%	113.0	135.7	97.8	53.5
25%	116.7	147.8	95.3	40.2
0%	121.6	154.8	90.2	33.4

5. CONCLUSIONS

A novel condition monitoring technique for faulty components detection in railway suspension is developed in this paper. Based on the dynamics study of a comprehensive conventional vehicle, it is verified that the suspension accelerations have the same structure and their interactions may change due to damper fault. The reliable fault monitoring technique using relative variance is developed to detect the change. Simulation results show that the performance of relative variance is effective and acceptable, for both damper fault detection and isolation in primary suspension.

REFERENCES

Bruni, S., Goodall, R., Mei, T.X., Tsunashima, H. (2007), Control and Monitoring for Railway Vehicle Dynamics, *Vehicle System Dynamics*. Vol 45, pp. 743-779

Charles, G., Goodall, R.M., and Dixon, R. (2006), Wheel-rail Profile Estimation, *The Institute of Engineering and Technology International Conference on Railway Condition Monitoring*, pp. 32-37

Gillespie, T.D. (1992), Fundamentals of Vehicle Dynamics, *Society of Automotive Engineers, Inc.*

Goda, K. and Goodall, R.M. (2004), Fault Detection and Isolation System to a Railway Vehicle Bogie, *Vehicle System Dynamics*, Supplement 41, pp. 468-476

Goodall, R. (2006), Advanced Control and Monitoring for Railway Suspensions, *KRRI Seminar*, London

Isermann, R. (2001), Diagnosis Methods for Electronic Controlled Vehicles, *Vehicle System Dynamics*, Vol. 36, pp. 77-117

Li, P and Goodall, R.M. (2004), Model-based Condition Monitoring for Railway Vehicle System, *Procedings of the UKACC International Conference on Control*, University of Bath, UK

Mei, T.X. and Ding, X.J. (2007), A Model-less Technique for the Fault Detection of Rail Vehicle Suspension, *20th IAVSD Symposium*, Berkeley, California, USA

Sunder, R. (2001), Kolbasseff, A., Kieninger, A., Rohm, A.and Walter, J., Operational Experience with Onboard Diagnosis System for High Speed Trains, *In Processings of the World Congress on Rail Research*, Cologne, Germany

Weisppenning, T. (1997), Fault Detection and Diagnosis of Components of Vehicle Vertical Dynamics, Meccanica 32, Kluwer Academic Publishers, pp. 459-472

Willsky, A.S. (1976), a Survey of Design Methods for Failure Detection in Dynamic System, *Automation*, Vol 12, pp. 601-611

Fault Detection for Vehicle Suspensions Based on System Dynamic Interactions

X J Ding* and T X Mei**

School of Electronic and Electrical Engineering,
The University of Leeds, Leeds LS2 9JT, UK
** eenxd@leeds.ac.uk and ** t.x.mei@leeds.ac.uk*

Abstract: This paper presents a novel method for the fault detection and isolation for rail vehicle suspensions that explores the additional dynamic interactions between different motions of a bogie or body caused by the failure of suspension components by taking advantage of symmetrical mechanical configurations of railway bogies. The study is focused on the monitoring of the vertical primary suspensions of a conventional bogie vehicle to demonstrate the general principle and effectiveness of the proposed method in detecting damper faults, although the technique is equally applicable for suspensions in other directions.

Keywords: fault detection, isolation, vehicle dynamics, suspension, damper

1. INTRODUCTION

Condition monitoring is considered as a novel area of Fault Detection and Isolation (FDI) in railway suspension systems, which is starting to show great potentials (Bruni *et al.*, 2007). A failure to the suspension component may not only increase the wear of wheel and rail, but also affect system stability, deteriorate ride comfort and even endanger passenger safety in extreme cases (Gillespie, 1992). The monitoring of the suspension condition changes in an early stage can prevent further damages, and rapid and effective monitoring techniques are essential to increase vehicle reliability and reduce maintenance cost.

The condition monitoring for vehicle system has drawn increased attention in academic research and some techniques have been recommended in automobile industry. There have been a number of theoretical studies and experimental investigations on different approaches for FDI (Willsky, 1976; Isermann, 2001; Fisher *et al.*, 2003), and in railway applications (Goda *et al.*, 2004, Li *et al.*, 2004; Goodall, 2006; Mei *et al.*, 2007). Most of the studies are concerned with model based techniques which use mathematical models to generate additional output signals and compare with the original measurable parameters. Those methods rely on a well-developed model to estimate the prior and posterior difference of the parameter or the residual between them. Therefore the detection quality is clearly affected by the accuracy and the complexity of the mathematical model (Isermann, 2001).

This paper studies a different and potentially very powerful technique for detecting and isolating suspension faults. The configuration and modelling of a typical bogie vehicle is firstly presented. The principle and development of the proposed fault detection technique are introduced and applied to the bogie vehicle. Only faults in dampers are considered which are much more common than springs failures in practice. Different fault conditions are assessed and computer simulations are used to show how those suspension faults may be detected and identified. The sensitivity to faults and robustness against external condition changes are demonstrated.

2. SYSTEM DESCRIPTION

2.1 Vehicle Configuration

Figure 1 shows the configuration of a conventional bogie vehicle. The vehicle consists of a vehicle body, two bogie frames and four solid axle wheelsets. The main external excitations are track geometries (deterministic input of gradients and curves) and irregularities (random input) transmitted to a vehicle through the wheelsets, but attenuated through the use of suspensions. The primary suspensions are located between the wheelsets and bogie frame, which normally includes coil springs and hydraulic damper in longitudinal, lateral and vertical directions. Normally, same suspension components are used for all suspensions at the four corners of each of the two bogies and therefore the bogie configurations are mostly symmetrical. The secondary suspensions are mounted between the bogie and the vehicle body, which are often comprised of rubber airsprings. The primary suspensions are mainly used to control the running behaviour, whereas the secondary suspensions are designed to ensure good ride comfort of passengers. Similar to the primary suspensions, same airbags tend to be used for the secondary suspensions on both sides (referred to as left and right sides) of each of the two bogies.

Because this paper deals with vertical suspensions, only motions related to vertical dynamics are included in the models which are the bounce, pitch and roll movements of the vehicle body and two bogie frames. Motions in other directions (and corresponding suspensions) are largely decoupled and excluded from the study. The vertical movements of the wheelsets are considered to be constrained to the track surface, which is a normal practice in the study of railway vehicle dynamics.

The natural frequencies and damping ratios of the modes derived from a typical railway vehicle are given in Table 1, where the first

three rows show those for the bounce, pitch and roll movements of the bogies and the last three rows those for the bounce, pitch and roll motions of the car body. It is clear that the frequencies of the bogies are above 10Hz and much higher than those of the body modes.

Table 1.Natural frequency and damping of a bogie vehicle

		Freq. (Hz)	Damping
Bogie Mode	Bounce	10.57	0.23
	Pitch	14.07	0.32
	Roll	14.79	0.31
Body Mode	Bounce	0.68	0.16
	Pitch	0.84	0.19
	Roll	0.84	0.19

2.2 The Characteristic of Track Inputs

Apart from intended track features such as gradients, there are considerable random excitations due to track misalignments which may be somewhat different on two sides of a track. In the vertical direction, the random track input is usually described in terms of a power spectrum for the track vertical displacement, which is an approximate function of frequency given by A_r/f_t^2 (Mei, *et al.*, 2001). In this paper, two random inputs that conform to the power spectrum distribution are used in the simulations for the left and right sides of the track, where the difference between the two sides is typically 10% (also in a random manner) of the inputs. The inputs to all the wheelsets are the same, but there are time shifts between them, which are determined by $\tau=2\cdot L_b/V_s$ between the leading and trailing wheelsets of each bogie and $\tau=2\cdot(L_c-L_b)/V_s$ between the trailing wheelset of the leading bogie and leading wheelset of the trailing bogie, where L_b is the half wheel space, L_c is the half distance between the centre positions of the two bogies, and V_s is the vehicle operating velocity.

3. FAULT DETECTION METHOD

Railway vehicles tend to use identical suspension components which result in symmetrical arrangements in the primary or secondary suspensions. A previous study based on the analysis of a simple side view model of a railway bogie shows that the bounce and pitch motions of the bogie are decoupled in normal conditions, but dynamic interactions are introduced once an asymmetry occurs due to a fault at one of the suspensions which may be readily explored for fault detection (Mei *et al.*, 2007). The study in this paper is extended much further than the initial investigation. A detailed and practical scheme for both fault detection and isolation for all vertical primary suspensions is developed to demonstrate a clear link between the level/nature of the interactions and different fault conditions.

Equations 1 – 3 give the equations of motion for the bounce (z_{b1}), pitch (ϕ_{b1}) and roll (ψ_{b1}) movements of the leading bogie in no fault conditions. Clearly the three motions are independent from one another and the primary suspensions do not introduce any interactions. The forces from the secondary suspension affect the bogie bounce (from the total secondary suspension force, or ΣF_s) and roll (from the difference in force between the left and right sides, or ΔF_s), which turn out to be trivial.

$$m_b\cdot\ddot{z}_{b1}+4c_p\cdot\dot{z}_{b1}+4k_p\cdot z_{b1} = c_p(\dot{z}_{t1l}+\dot{z}_{t1r}+\dot{z}_{t2l}+\dot{z}_{t2r})+k_p(z_{t1l}+z_{t1r}+z_{t2l}+z_{t2r})+\Sigma F_s \quad (1)$$

$$(I_{by}/L_b^2)L_b\cdot\ddot{\phi}_{b1}+4c_pL_b\cdot\dot{\phi}_{b1}+4k_pL_b\cdot\phi_{b1} = c_p(\dot{z}_{t1l}+\dot{z}_{t1r}-\dot{z}_{t2l}-\dot{z}_{t2r})+k_p(z_{t1l}+z_{t1r}-z_{t2l}-z_{t2r}) \quad (2)$$

$$(I_{bx}/B_b^2)B_b\cdot\ddot{\psi}_{b1}+4c_pB_b\cdot\dot{\psi}_{b1}+4k_pB_b\cdot\psi_{b1} = c_p(\dot{z}_{t1l}-\dot{z}_{t1r}+\dot{z}_{t2l}-\dot{z}_{t2r})+k_p(z_{t1l}-z_{t1r}+z_{t2l}-z_{t2r})+\Delta F_s \quad (3)$$

The main connections between the three motions are the track inputs from the four wheels, where the bounce is excited by the sum of the four, the pitch by the difference of the front and rear two, and the roll by the difference between the two sides of the wheelsets. This balanced condition will no longer be true, if any one of the suspension components becomes faulty which in most

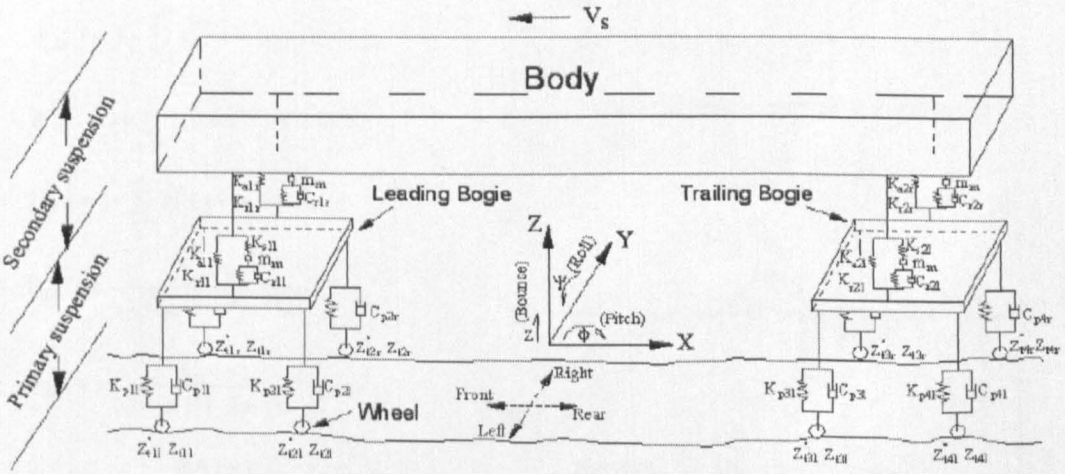

Fig 1. Illustration of a conventional vehicle

cases reduces the damping coefficient. Therefore the cross correlations between the three motions of a bogie will vary with the level as well the location of unbalances, especially at no time shift (due to excitations of the input at the same wheel) and to time shift $\tau=2L_b/V_x$ (due to the time delay between the leading and trailing wheelsets of the same bogie, which is fixed for any given speed).

Figure 2 shows the overall scheme of the proposed fault detection and isolation method.

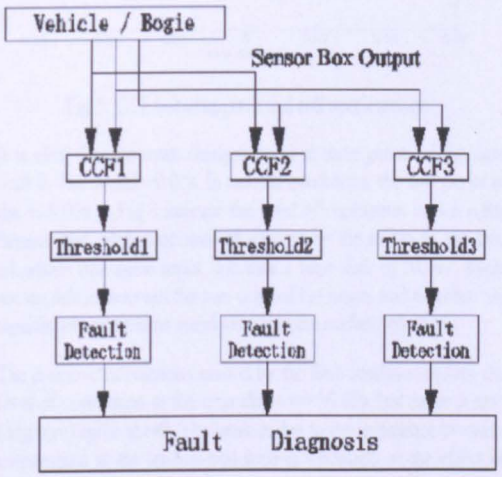

Fig 2. Proposed Fault Detection and Diagnosis Scheme

A single sensor box may be mounted onto the bogie frame to provide the measurements of the bounce, pitch and roll accelerations (Charles, *et al.*, 2006). This type of the sensor box often consists of one accelerometer (for bounce) and two gyros (for pitch/roll velocities), so the pitch and roll accelerations be derived from the rate of change in pitch and roll gyros. The cross correlation (CCF1, CCF2, CCF3) between any two of the three signals are computed using equations 4-6. There are additional benefits to compute cross correlation coefficients as given in equations 7-9 instead of the cross correlations which will be further explained in the performance assessments.

$$R_{BP}(m)=\sum_{n=1}^{N}\ddot{z}_b^2(n+m)\cdot\ddot{\phi}_b^2(n) \tag{4}$$

$$R_{BR}(m)=\sum_{n=1}^{N}\ddot{z}_b^2(n+m)\cdot\ddot{\psi}_b^2(n) \tag{5}$$

$$R_{PR}(m)=\sum_{n=1}^{N}\ddot{\phi}_b^2(n+m)\cdot\ddot{\psi}_b^2(n) \tag{6}$$

$$C_{BP}(m)=\frac{R_{BP}(m)}{\sqrt{R_{BB}(0)\cdot R_{PP}(0)}} \tag{7}$$

$$C_{BR}(m)=\frac{R_{BR}(m)}{\sqrt{R_{BB}(0)\cdot R_{RR}(0)}} \tag{8}$$

$$C_{PR}(m)=\frac{R_{PR}(m)}{\sqrt{R_{PP}(0)\cdot R_{RR}(0)}} \tag{9}$$

For a fixed step size Δt, the time window $T=N\cdot\Delta t$ should be selected far greater than Δt so that there is sufficient amount of data to produce consistent results. In this paper, a step size Δt for simulation is set to *1ms* and the time window is chosen to *2s*.

The output of each of the cross correlation (or cross correlation coefficient) calculations is compared to a pre-defined threshold for fault detection, and the outcome of the all three channels will then be used to identify which one of the dampers has failed. On-line real time detection is possible by computing running cross correlations or coefficients with a moving time window of data.

One important basis for the new method is that the probability of two or more identical components (used at different locations) failing at the exactly same time, in the same manner and to the same degree may be considered extremely low.

4. PERFORMANCE ASSESSMENTS

4.1 Use of Cross-Correlations (CCF) in Fault Detection

Figure 3 compares cross correlation between the bounce and pitch accelerations in no fault and when the damping coefficient of the front-left damper is reduced to 50% of its nominal value. Figure 4 shows a comparison of bounce/roll correlations between the two conditions and Figure 5 give that of pitch/roll correlations. The vehicle speed is 50m/s, and the time delay between the track inputs at the leading and trailing wheelsets of a bogie is calculated as 0.05s.

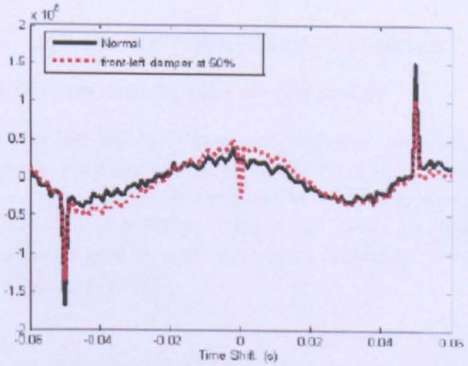

Fig 3. CCF between bounce and pitch accelerations

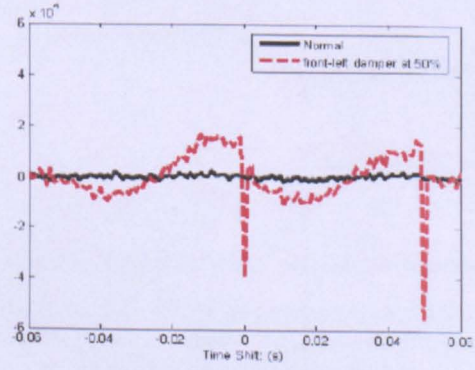

Fig 4. CCF between bounce and roll accelerations

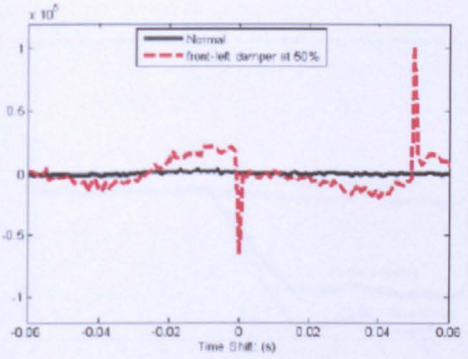

Fig 5. CCF between pitch and roll accelerations

It is clear that the main changes occur at three points of the time shift 0, -0.05s and +0.05s. In normal conditions, the two peaks at the +/-0.05s in Fig 3 indicate the level of correlation between the bounce and pitch accelerations caused by the inputs to the two wheelsets (the same input, but with a time shift of 0.05s). There are no delays between the two sides of the bogie, and therefore no significant correlations are observed in the no fault condition.

The dynamic interactions caused by the fault condition reduce the level of correlation at the time shifts t=+/-0.05s, but cause a new (negative) spike at t=0. The latter is due to the imbalance between suspensions at the leading and trailing wheelsets as the effect of input at the leading suspensions can no longer cancel out that at the trailing suspensions. Similar spikes are observed at t=0 (negative) and t=0.05s (negative) in Fig 4, and at t=0 (negative) and t=0.05s (positive) in Fig 5 due to the same reasons.

When the damper fault occurs at a different position, e.g. the rear-right on, the effect of the dynamic interactions on the cross-correlations is equally obvious, but the pattern of the changes is different as shown in Figs 6-8. In this case the peak at t=0 becomes positve for the bounce/pitch and bounce/roll cross correlations. The bounce/roll CCF also results in a positive peak at t=-0.05s (rather than a negative one at t=0.05s as in the previous case). The pitch/roll CCF gives a positive peak at t=-0.05s (rather than t=0.05s).

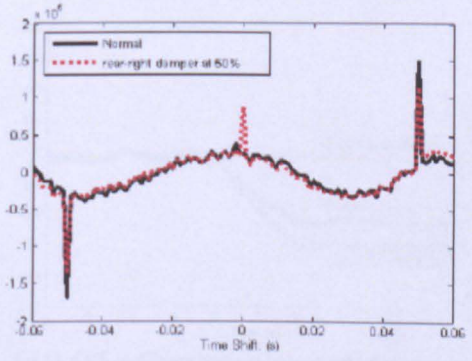

Fig 6. CCF value between bounce and pitch accelerations

The detection of the spikes and their level of changes provide an essential indication of the suspensions conditions, but the differences between the different faults can be used to help and locate where a fault has occurred.

There is a sinusoidal component in some of the cross correlations which is caused by one of the bogie modes. The oscillations tend to become larger when the level of a fault becomes worse due to reduced damping to the bogie.

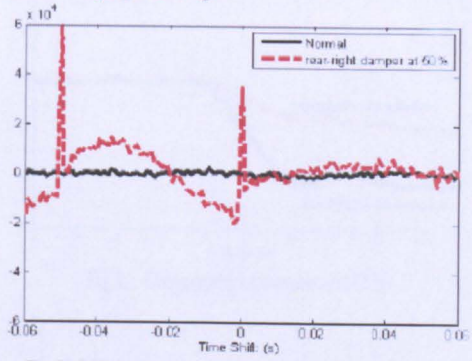

Fig 7. CCF value between bounce and roll accelerations

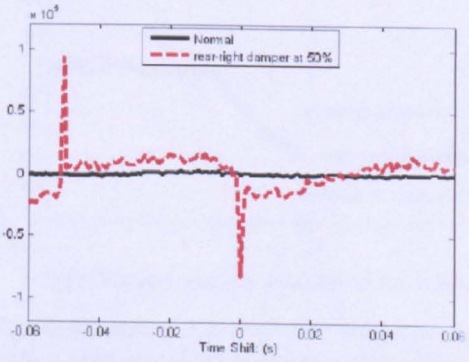

Fig 8. CCF value between pitch and roll accelerations

4.2 On Line Fault Detection with Running CCF

For on line (real time) detection, running cross correlations will have to be used to find changes at the three specific time shifts. Figs 9 and 10 show the running CCFs of the bounce/pitch and bounce/roll accelerations respectively, where the damping coefficient of the front left suspension is reduced by 50% at the simulation time t=6s.

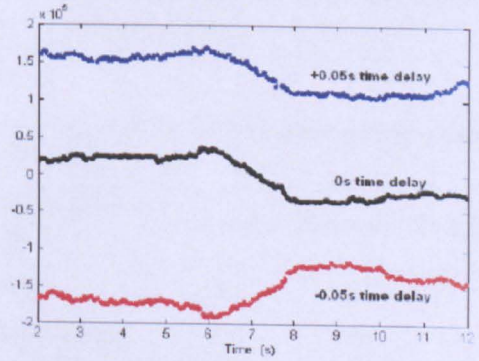

Fig 9. Running CCF value with bounce and pitch accelerations

The changes in CCFs at the relevant time shifts are clearly linked to the assumed fault condition, but the bounce/roll CCF appear to be more sensitive to the fault than the bounce/pitch one.

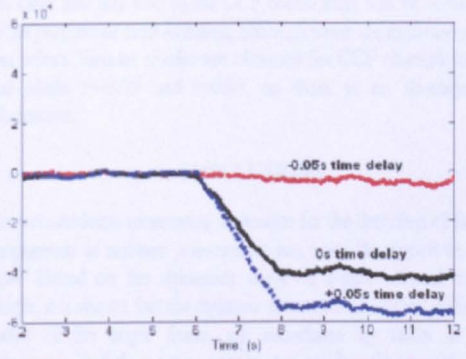

Fig. 10. Running CCF value with bounce and roll accelerations

4.3 Use of CCF Coefficients

There are two robustness issues in practical implementation of the proposed technique using cross correlation calculations – both are related to the level of input excitations but in different ways. One is that the actual geometry of the track may vary from one section of a track to another. Although track irregularities may be considered as random noises, real measured data suggest that there are sometimes variations in the magnitude. Also there are other types of changes such as joints and switches. Those variations will cause certain fluctuations in the input excitations and consequently in the output of the CCF calculations – some of the effect may be observed in Figs 9 and 10. The other is that the travelling speed of rail vehicles is not necessary constant. Changes in speed will change the level of excitations for the same track, which can affect the cross correlations more than fault conditions. Threshold levels for fault detection may be adjusted according to speed, but tuning would be difficult and track specific.

The effect of the variations can be removed by using cross correlation coefficients, which are relative quantities as illustrated in equations 7-9. Fig 11 shows the CCF coefficient of the bounce/roll accelerations. The changes at the time shifts of t=0 and t=0.05s are similarly sensitive to the fault (the coefficient of the front left damper is reduced by 50% at t=6s), but are more consistent (or smoother) compared to the CCFs in Fig 10.

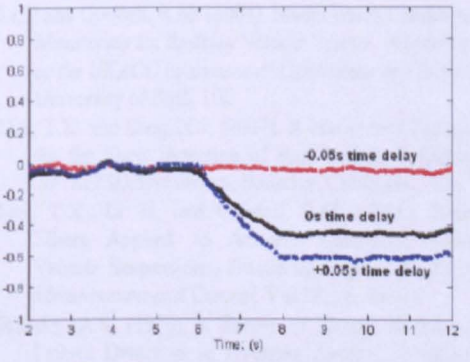

Fig 11. CCF coefficient between bounce and roll accelerations

Fig 12 compares the bounce/roll cross correlations at the speeds of 25m/s and 50m/s, where the difference is self-evident even though the fault condition is the same. In Fig 13, however, the effect of the fault on the cross correlation coefficients at the different speeds is virtually the same.

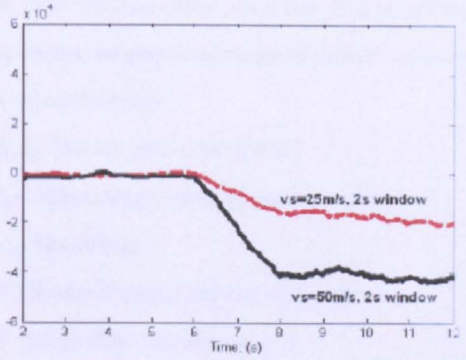

Fig 12. Comparison of bounce/roll CCFs

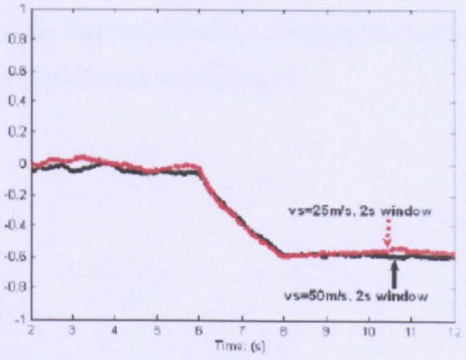

Fig 13. Comparison of bounce and roll CCF coefficients

To study the robustness of the proposed technique against sensing errors, a sensor noise of 1% of the measurement range is also included in the analysis which showed little adverse effect. This is because the noises from different sensors are in general uncorrelated and their effects at the specific time shifts of the cross correlation calculations are expected to be small.

4.4 Fault Isolation

CCF coefficient results of different suspension faults at four corners of the bogie show that the any individual fault may be readily isolated by exploring different ways the CCF coefficients are altered by the different faults. Table 2 shows each fault affects the CCF coefficients of bounce/pitch, bounce/roll and pitch/roll accelerations at the time shift of 0s, where the vehicle speed is set to 50m/s.

Table 2. Changes of CCF coefficients in different fault conditions (at the time shift of 0s only).

CCF coefficient to 50%	Bounce/pitch	Bounce/roll	Pitch/roll
No fault	0	0	0
Front left damper	-0.30	-0.58	-0.56
Front right damper	-0.30	0.57	0.57
Rear left damper	0.31	-0.58	0.56
Rear right damper	0.31	0.57	-0.57

It is clear that any two of the CCF coefficients will be sufficient for the purpose of fault isolation, although some are more sensitive than others. Similar results are obtained for CCF changes at the time shifts t=-0.05 and t=0.05, so there is no shortage of information.

5. CONCLUSIONS

A novel condition monitoring technique for the detection of faulty components in railway suspensions has been developed in this paper. Based on the dynamics study of a conventional bogie vehicle, it is shown that the dynamic interactions between different modes of the bogie frame are introduced by faults in the suspensions and their cross correlations can be used to not only detect but also isolate damper faults. The effectiveness as well as robustness against external disturbances has been demonstrated using computer simulations.

REFERENCES

Bruni, S., Goodall, R., Mei, T.X., Tsunashima, H. (2007), Control and Monitoring for Railway Vehicle Dynamics, *Vehicle System Dynamics*, **Vol 45**, pp. 743-779

Charles, G., Goodall, R.M., and Dixon, R. (2006), Wheel-rail Profile Estimation, *The Institute of Engineering and Technology International Conference on Railway Condition Monitoring*, pp. 32-37

Fisher, D., Kaus, E. and Isermann, R. (2003), Fault Detection for an Active Vehicle Suspension, *Proceeding of the American Control Conference*, Denver, Colorado

Gillespie, T.D. (1992), Fundamentals of Vehicle Dynamics, *Society of Automotive Engineers, Inc.*

Goda, K. and Goodall, R.M. (2004), Fault Detection and Isolation System to a Railway Vehicle Bogie, *Vehicle System Dynamics*, **Supplement 41**, pp. 468-476

Goodall, R. (2006), Advanced Control and Monitoring for Railway Suspensions, *KRRI Seminar*, London

Isermann, R. (2001), Diagnosis Methods for Electronic Controlled Vehicles, *Vehicle System Dynamics*, **Vol. 36**, pp. 77-117

Li, P and Goodall, R.M. (2004), Model-based Condition Monitoring for Railway Vehicle System, *Procedings of the UKACC International Conference on Control*, University of Bath, UK

Mei, T.X. and Ding, X.J. (2007), A Model-less Technique for the Fault Detection of Rail Vehicle Suspension, *20th IAVSD Symposium*, Berkeley, California, USA

Mei, T.X., Li, H. and Goodall, R.M. (2001), Kalman Filters Applied to Actively Controlled Railway Vehicle Suspensions, *Transactions of the Institute of Measurement and Control*, **Vol 23**, pp. 163-181

Willsky, A.S. (1976), a Survey of Design Methods for Failure Detection in Dynamic System, *Automation*, **Vol 12**, pp. 601-611

LIST OF PARAMETERS

A_v – Track roughness factor in vertical direction

B_b - Half wheel space of the vehicle bogie in lateral direction

c_p – Normal damping of each damper in primary suspensions

f_t – Spatial frequency

I_{bx}, I_{by} - Roll and pitch inertia of bogie

k_p – Stiffness of each coil spring in primary suspensions

m_b - Mass of bogie

N – Number of sampled data in each time window

T – Length of the chosen time window

z_{tfl}, z_{trl} - Left vertical track inputs for front and rear wheels

z_{tfr}, z_{trr} - Right vertical track inputs for front and rear wheels

Δt – Time step between each sampling

NEW CONDITION MONITORING TECHNIQUES FOR VEHICLE SUSPENSIONS

T.X. Mei*, X.J. Ding †

The University of Leeds, Leeds, LS2 9JT, UK
Emails *t.x.mei@leeds.ac.uk; †eenxd@leeds.ac.uk
Fax: 44 (0) 113 3432032

Keywords: Suspensions, fault detection, dynamic interactions, cross correlation, relative variance.

Abstract

This paper presents two simple and potentially powerful approaches for the condition monitoring of rail vehicle suspensions, which explore the relative changes between different dynamic motions caused by suspension faults. Damper failures in vertical (primary) suspensions of a conventional bogie are detected based on the measurements of the bounce, pitch and roll accelerations of the bogie frame. The effectiveness of the proposed fault detection methods is demonstrated

1 Introduction

On line fault detection and condition monitoring for railway applications have attracted much interest in research and development [1]. Conventional approaches are mainly based on the direct measurement of relevant signals which are analysed using sophisticated time and/or frequency domain signal processing, e.g. to find features or signatures related to particular faults [5, 9]. More recently, there have been a number of developments that investigate the use of model-based techniques to either identify the parameters of the components required monitoring or estimate the system states and their residuals [2, 3, 4, 10]. The model based techniques compare a real system with a mathematical model of the system, and the performances are therefore affected by the appropriateness and complexity of the models. There are potential difficulties related non-linear properties in some suspension components such as the dampers and the 'normal' variations in the system, which may lead to very complex solutions.

This paper presents two different approaches that takes advantage of the vehicle (suspension) configurations and explores the additional dynamic interactions between different motions of a bogie or body caused by the failure of suspension components. The detection methods require very little prior knowledge of the system (i.e. the bogie), apart from some basic parameters such as vehicle travelling speed and distance between suspensions. Instead, it is focussed on the comparison of dynamic behaviours between the suspensions at different positions of a bogie where identical components are normally used.

The proposed techniques are simple but very effective for the detection of suspension faults. There is no need for complex modelling and detailed knowledge of external conditions (e.g. track inputs), therefore it offers extra benefits of robustness against nonlinearities and uncertainties as well as that of easy tuning.

The paper is organised as follows. Detail of the vehicle configuration used in the study is given in section 2. The two fault detection techniques are explained in section 3. The effectiveness of the methods is assessed using computer simulations in section 4, and conclusions are given in section 5.

2 System Configuration

A conventional railway vehicle consisting of a body frame and two bogies is used in the study, a schematic diagram of which is given in Figure 1. The fault detection of the vertical primary suspensions is studied in the paper to demonstrate the principle and effectiveness of the proposed methods, although the techniques may be extended for the condition monitoring of the suspensions in other directions or positions. Therefore only motions directly related to the vertical suspensions are modelled, including the bounce, pitch and roll movements of the body and those of the two bogie frames resulting in a 9 DoF model. The dynamics of the air-springs in the secondary suspensions are approximated using a linearised model.

In the normal condition where there is no fault in any suspensions, the four primary suspensions and two secondary suspensions of each bogie are typically symmetrical in structure and in parameters. The effect of the suspensions on the bogie dynamics is expected to be similar and interactions between the different motions will be minimal. The dedicated balances between the suspensions and between the motions would be broken up if one (or more) of the suspensions develop a fault, leading to asymmetrical behaviours and additional interactions. The manner of the changes is closely related to the type and location of a fault and therefore may be explored for fault detection and isolation, by using cross correlations [6, 7] and/or variance comparisons [8].

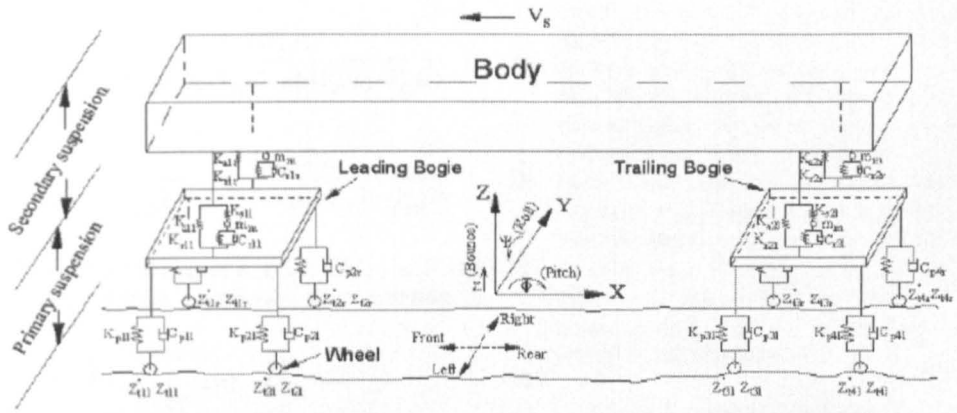

Figure 1. Vehicle Configuration

3 Fault Detection Methods

The general principles of the proposed fault detection techniques are introduced in [6-8], but this paper is to focus on relative comparisons using normalised cross correlations and normalised variances which offers additional advantages in terms of easy tuning and improved detection reliability in different operation conditions.

The detection of either scheme involves the use of a single sensor box mounted on the bogie frame in a centre position to measure the bounce, pitch and roll accelerations of the bogie. Those measurements can also be used to derive the bogie accelerations above the four primary suspensions.

3.1 Cross Correlation

This method computes cross correlations between any two of the bounce, pitch and roll accelerations, and compares the results at three specific time shifts – 0 time delay for correlations due to the same input excitations, +/- time delays due to the time difference between the track inputs at the leading and trailing wheelsets.

Equations 1-3 give the cross correlation coefficients between the bounce and pitch accelerations, between the bounce and roll accelerations, and between the pitch and roll accelerations. The cross correlation coefficients reflect the normalised correlations between two signals, and therefore are much less affected by the changes in operation conditions due to a vehicle travelling at different speeds and/or on different tracks where the vibrations experienced on the bogie frame would vary even when the vehicle condition remains the same.

$$SC_{BP}(k) = \frac{S_{BP}(k)}{S_{BB}(0) \cdot S_{PP}(0)} \quad (1)$$

$$SC_{BR}(k) = \frac{S_{BR}(k)}{S_{BB}(0) \cdot S_{RR}(0)} \quad (2)$$

$$SC_{PR}(k) = \frac{S_{PR}(k)}{S_{PP}(0) \cdot S_{RR}(0)} \quad (3)$$

The auto correlation S_{xx} of a signal (x) and the cross correlation S_{xy} of any two signals (x, y) may be calculated using equations 4 and 5 respectively.

$$S_{xx}(0) = \sum_{i=1}^{N} x(i) \cdot x(i) \quad (4)$$

$$S_{xy}(k) = \sum_{i=N-k}^{N+k} x(i+k) \cdot y(i) \quad (5)$$

For any chosen sampling interval of T_s, the time window for each cross correlation calculation is $T_w = N*T_s$ from a total of N number of sampling intervals. The number of shifted intervals k may be varied from $-N$ to N for a complete set of cross correlation calculations, although in practice only values at and near k=0 and ± time delay between the two wheelsets / sampling interval T_s are of particular interest for the proposed fault detection scheme.

3.2 Relative Variance

This method detects changes in variance of the accelerations of the bogie frame above the four primary suspensions caused by suspension component failures. Normalisation of the variances as defined in equations 6-9 provides a means for relative comparisons to overcome the problems related to variations in operation conditions or external inputs which may appear to be similar to a fault condition.

$$RV_{FL}(k) = \frac{4 \times V_{FL}(k)}{V_{FL}(k) + V_{FR}(k) + V_{RL}(k+m) + V_{RR}(k+m)} \quad (6)$$

$$RV_{FR}(k) = \frac{4 \times V_{FR}(k)}{V_{FL}(k) + V_{FR}(k) + V_{RL}(k+m) + V_{RR}(k+m)} \quad (7)$$

$$RV_{RL}(k)=\frac{4\times V_{RL}(k)}{V_{FL}(k-m)+V_{FR}(k-m)+V_{RL}(k)+V_{RR}(k)} \quad (8)$$

$$RV_{RR}(k)=\frac{4\times V_{RR}(k)}{V_{FL}(k-m)+V_{FR}(k-m)+V_{RL}(k)+V_{RR}(k)} \quad (9)$$

The variance of a signal in a time window of N number of sampling intervals is calculated as shown in equation 10.

$$V_X(k)=\frac{1}{n}\sum_{i=k}^{N+k-1}(x(i)-\bar{x})^2 \quad (10)$$

4 Simulations and Performance Assessments

Computer simulations based on the models for the bogie vehicle described in section 2 are used to study the performance of the proposed fault detection schemes. Unless otherwise specified, a damper fault where the damping cofficient is reduced by 50% at the front left suspension is assumed for fault detection – similar results can be obtained for faults at different suspensions. The track irregularities used in the study are generated in the simulation to represent the roughness of a typical main line with evenly distributed power spectrum density in the derivative of the vertical displacement.

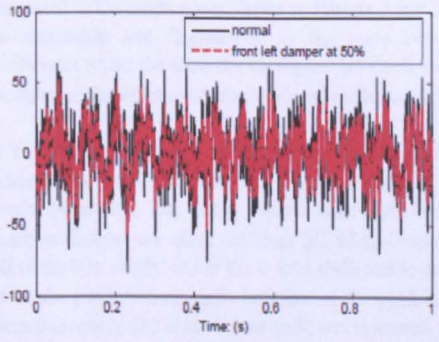

Figure 2. Acceleration above the front left suspension (m/s^2), V_t=50m/s

Figure 2 compares the accelerations at the front left suspension in the normal and half-fault conditions. The reduced damping ratio increases resonances at the bogie modes, but suppresses higher frequency components more – leading to a reduced overall acceleration for the track input. The accelerations above the other three suspensions remain largely unchanged, which is expected because of the location of the only fault assumed in the study.

It is possible to use the changes in magnitude as an indicator of component condition, but there are certain limitations. Figures 3 and 4 show the running rms values of the acceleration (over a 3s moving time window) at the speeds of 50m/s and 25m/s respectively. The difference between the normal and fault conditions is fairly obvious. However there are relatively large fluctuations even at a constant speed, as the bogie accelerations are very sensitive to changes in the input irregularities which may vary from one section of a track to another. It may not always be possible to make a clear distinction between a lower rms value in the normal condition and a higher one in a fault condition. Furthermore, any changes in the operation speed or rail tracks will result in large corresponding changes in the vibrations detected from the bogie frame. Therefore the use of thresholds for fault detection will have to be highly adaptive to both vehicle speed and track conditions which would not be straight forward to achieve in practice.

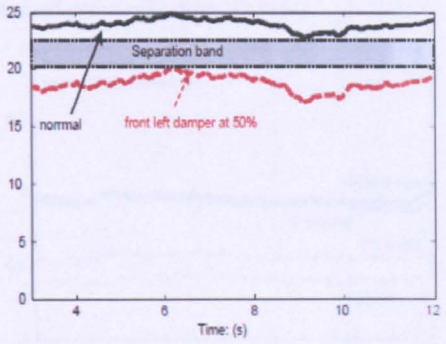

Figure 3. Running rms of the acceleration above the front left suspension (m/s^2), V_t=50m/s

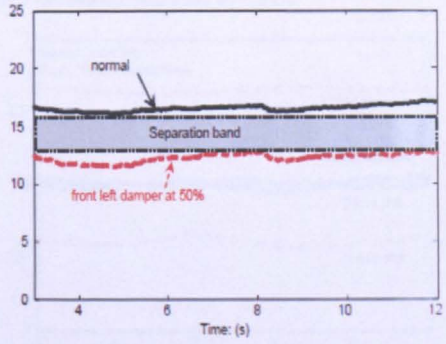

Figure 4. Running rms of the acceleration above the front left suspension (m/s^2), V_t=25m/s

4.1 Fault Detection with Cross Correlation Coefficient

Cross correlations (CCF) between different bogie motions are more sensitive to condition changes in the suspensions. Figure 5 compares the CCF of the bounce and pitch accelerations in the nominal condition with that in a half-fault condition where the damper coefficient of the front left suspension is reduced by half.

The peak values at the zero time shift and at the +/-0.05s (the delays between the two wheelsets) are clearly related to the changes in the dynamic interactions caused by the fault. For real time detection, running CCF coefficients with a moving

time window of fixed duration are proposed to be used to monitor the changes at the specific time shifts.

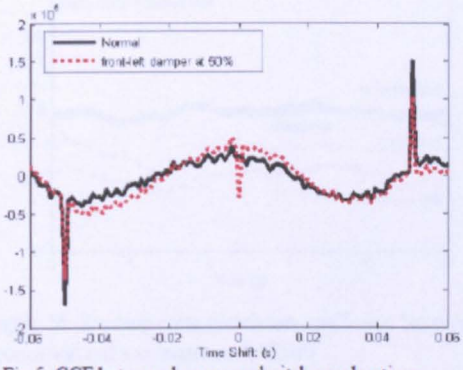

Fig 5. CCF between bounce and pitch accelerations

Figures 6-8 give the running cross correlation coefficients (SC) between two of the measured bogie accelerations of the bounce, yaw and roll motions. The moving time window for the computations is set to 2s and the vehicle speed is 50m/s.

The reduction of the damping coefficient by 50% causes changes in the cross correlations at the 0 and +0.05s time shifts, but almost no change at the -0.05s time shift because the failure occurs at the leading wheelset. The latter is only shown in Figure 5 and not in other two figures as there are no significant changes.

Compared to the running rms shown in Figures 3 and 4, there are noticeably less fluctuations in the cross correlation coefficients where the same track irregularities (with the same variations in the input excitation) are used in the simulation.

In Figure 6, the change in SC of the bounce and pitch accelerations for the 0 time shift from 0 to around -0.2 is clearly larger than that at the positive time shift, but more sensitive changes are observed from SC of the bounce and roll (from 0 to nearly -0.5 at the 0 time shift, and to around -0.6 at the positive time shift) and that of the pitch and roll (from 0 to nearly -0.5 at the 0 time shift, and to around +0.7 at the positive time shift) as indicated in Figures 7 and 8.

The manner of the changes such as at what time shifts and signs of the SC values helps to identify the specific position of a failed damper, e.g. a damper failure at the trailing wheelset will lead to SC changes in the negative time shift.

Because of the normalisation, the cross correlation coefficients are insensitive to changes in the vehicle speed. Figures 9-11 show the same SC results as in Figures 6-8, but at half of the speed (25m/s). Only minor differences may be observed between the two sets of results, which make the use and tuning of thresholds for fault detection much easier.

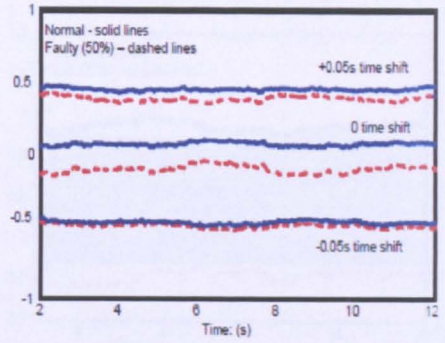

Figure 6. Running cross correlation coefficient between the bounce and pitch accelerations, V_s=50m/s

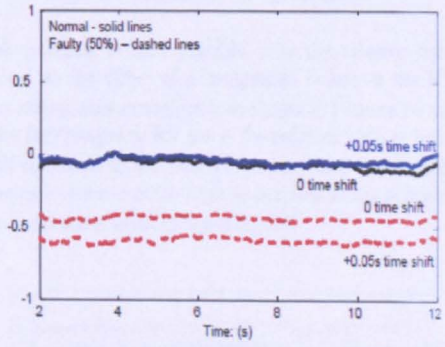

Figure 7. Running cross correlation coefficient between the bounce and roll accelerations, V_s=50m/s

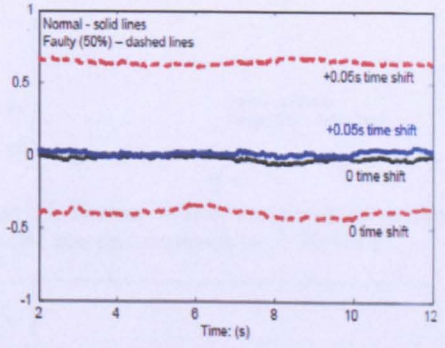

Figure 8. Running cross correlation coefficient between the pitch and roll accelerations, V_s=50m/s

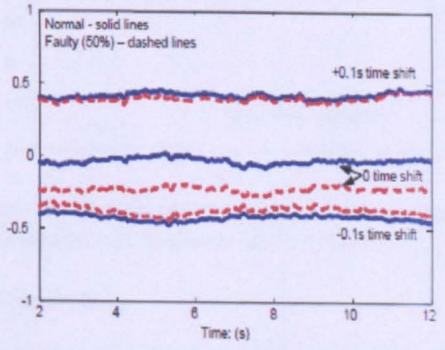

Figure 9. Running cross correlation coefficient between the bounce and pitch accelerations, V_s=25m/s

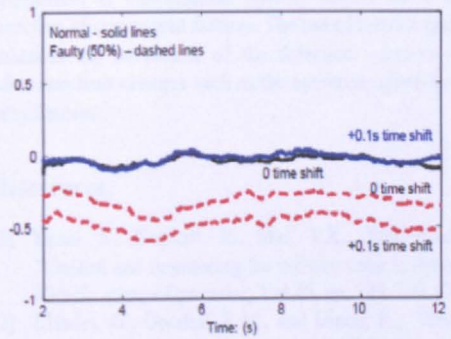

Figure 10. Running cross correlation coefficient between the bounce and roll accelerations, V_s=25m/s

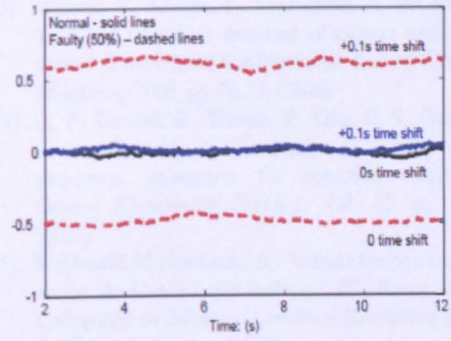

Figure 11. Running cross correlation coefficient between the pitch and roll accelerations, V_s=25m/s

4.2 Fault Detection with Relative Variance

The use of relative variance is also effective in overcoming the difficulties associated with the (normal) variations in the track input and in the vehicle travel speed. Figures 12 and 13 show the running relative variances (over a moving time window of 3s) of the bogie acceleration above the front left suspension at the speeds of 50m/s and 25m/s respectively. The change in RV due to the component failure is from 1 to around 0.6/0.7 (or 30-40%) in both cases, demonstrating excellent robustness against the (non-fault) condition variations.

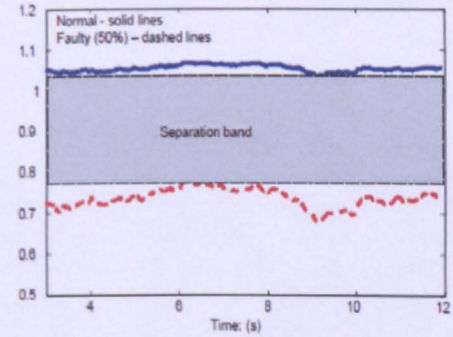

Figure 12. Running relative variance of the acceleration above the front left suspension (m/s^2), V_s=50m/s

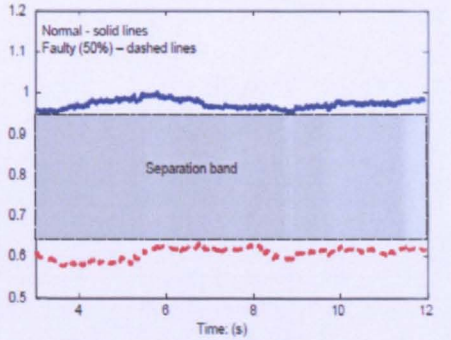

Figure 13. Running relative variance of the acceleration above the front left suspension (m/s^2), V_s=25m/s

Fault isolation is also possible with the relative variance method, as the effect of a component failure in the RVs at other suspensions is negligible as shown in Figures 14 and 15, where the changes in RV are in the order of 10% or less. The small increases in the relative variance are due to reduced (absolute) variance at the fault suspension which is one of the four denominate terms in equations 6-9.

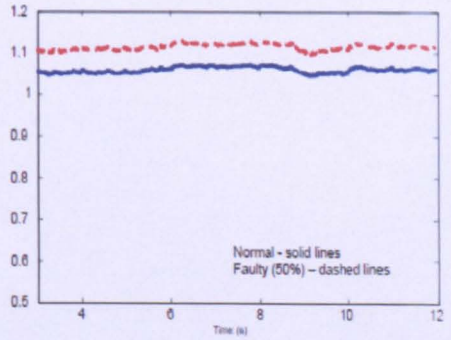

Figure 14. Running relative variance of the acceleration above the front right suspension (m/s^2), V_s=50m/s

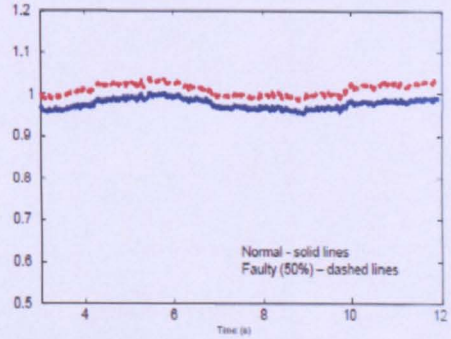

Figure 15. Running relative variance of the acceleration above the front right suspension (m/s^2), V_s=25m/s

5 Conclusions

Effective fault detection and condition monitoring of vehicle suspensions do not necessarily require sophisticated and/or difficult to implement techniques. This paper has presented

two relatively simple approaches which explore the structure symmetries in conventional railway bogies for a reliable detection of component failures. The use of relative quantities enhances the robustness of the detection schemes against other non-fault changes such as the operation speed and track irregularities.

References

[1] Bruni, S., Goodall, R., Mei, T.X., Tsunashima, H., "Control and monitoring for railway vehicle dynamics", *Vehicle System Dynamics*, **Vol 45**, pp. 743-779, (2007)

[2] Charles, G., Goodall, R.M., and Dixon, R., "Wheel-rail Profile Estimation", *The Institute of Engineering and Technology International Conference on Railway Condition Monitoring*, pp. 32-37, (2006).

[3] Hayashi, Y., Kojima, T., Tsunashima, H. and Marumo, Y., "Real time fault detection of railway vehicle and tracks", *International Conference on Railway Condition Monitoring 2006*, pp. 20-25, (2006)

[4] Li, P., Goodall, R., Weston, P., Ling, C. S., Goodman, C. and Roberts, C., "Estimation of railway vehicle suspension parameters for condition monitoring", *Control Engineering Practice*, **Vol. 15**, pp. 43-55, (2006)

[5] McDonald, M.; Richards, A, "Vehicle health monitoring on the Docklands Light Railway", *IEE Power Division Colloquium on Advanced Condition Monitoring Systems for Railways*, London, (1995)

[6] Mei, T.X. and Ding, X.J., "A model-less technique for the fault detection of rail vehicle suspension", *20th IAVSD Symposium*, Berkeley, California, USA, (2007).

[7] Mei, T.X. and Ding, X.J., "Fault detection for vehicle suspensions based on system dynamic interactions", *UKACC 2008*, (2008).

[8] Mei, T.X. and Ding, X.J., "Condition monitoring of primary suspensions using relative variance", *CompRail 2008*, (2008).

[9] Nicks S, "Condition monitoring of the track/train interface", *IEE Seminar Condition Monitoring for Rail Transport Systems*, London, (1998)

[10] Xia, F., Cole, C. and Wolfs, P., "A method for setting wagon speed restrictions based on wagon responses", *Vehicle System Dynamics* Supplement 44, pp. 424-432, (2006)